AD-A077 370 NATIONAL AEROSPACE LAB AMSTERDAM (NETHERLANDS) F/G 20/4
TRANSONIC WIND TUNNEL TESTS ON AN OSCILLATING WING WITH EXTERNA--ETC(U)
SEP 79 H TIJDEMAN , J W VAN NUNEN AFOSR-77-3233
UNCLASSIFIED NLR-TR-78106-U-PT-4 AFFDL-TR-78-194-PT-4 NL

1 OF 2
AD
A077370

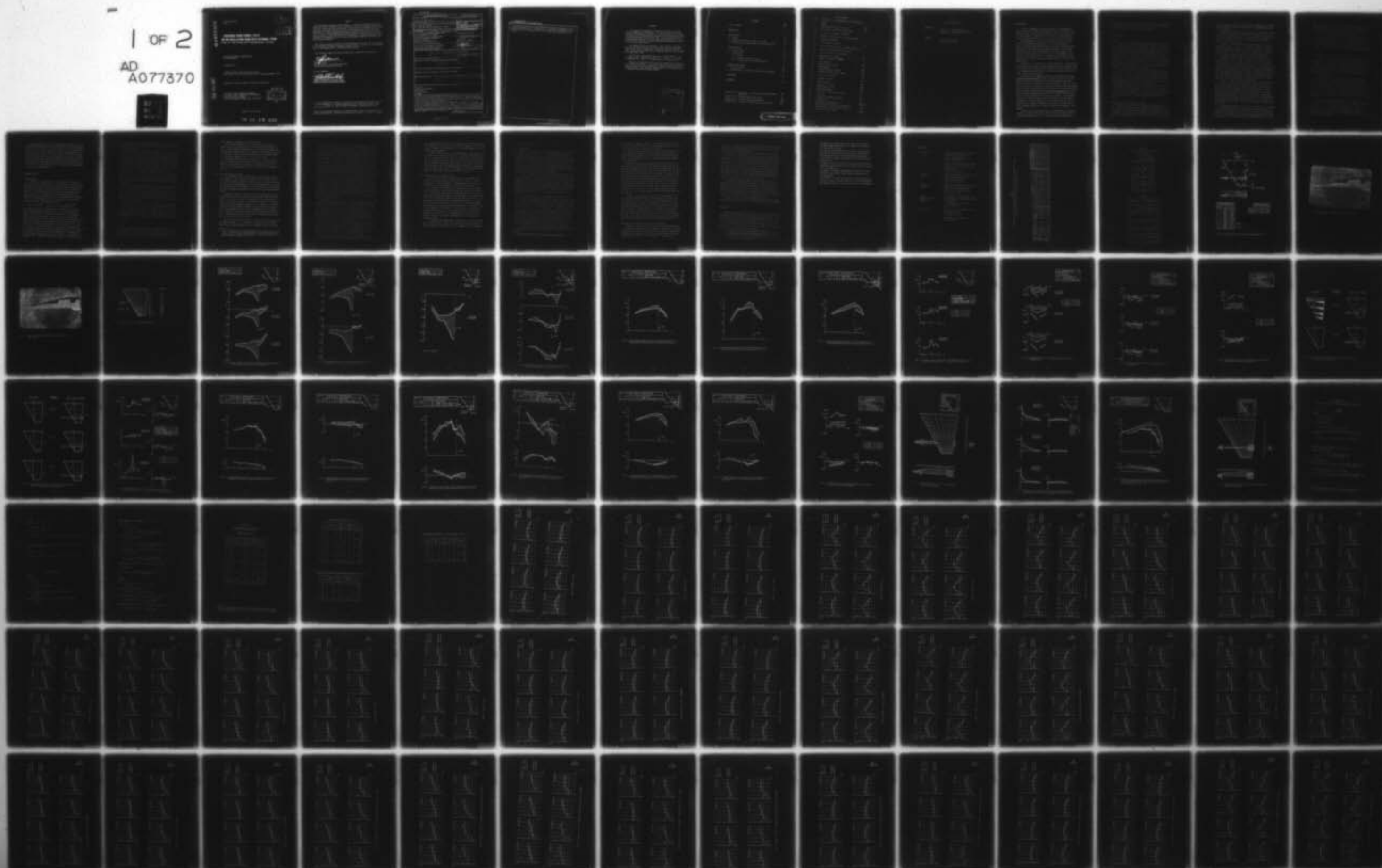

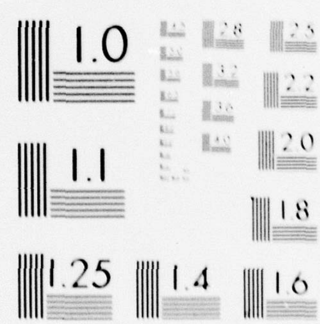

MICROCOPY RESOLUTION TEST CHART

AFFDL-TR-78-194,
Part IV

TRANSONIC WIND-TUNNEL TESTS ON AN OSCILLATING WING WITH EXTERNAL STORE

PART IV: THE WING WITH UNDERWING - STORE

A074910
Part
III

NATIONAL AEROSPACE LABORATORY NLR
THE NETHERLANDS

SEPTEMBER 1979

TECHNICAL REPORT AFFDL-TR-78-194, PART IV
Final Report for the Period February 1977 through September 1979

Approved for public release; distribution unlimited

AIR FORCE FLIGHT DYNAMICS LABORATORY
AIR FORCE WRIGHT AERONAUTICAL LABORATORIES
AIR FORCE SYSTEMS COMMAND
WRIGHT-PATTERSON AIR FORCE BASE, OHIO 45433

Report IV of IV Parts

NOTICE

When Government drawings, specifications, or other data are used for any purpose other than in connection with a definitely related Government procurement operation, the United States Government thereby incurs no responsibility nor any obligation whatsoever; and the fact that the government may have formulated, furnished, or in any way supplied the said drawings, specifications, or other data, is not to be regarded by implication or otherwise as in any manner licensing the holder or any other person or corporation, or conveying any rights or permission to manufacture, use, or sell any patented invention that may in any way be related thereto.

This report has been reviewed by the Information Office (OI) and is releasable to the National Technical Information Service (NTIS). At NTIS, it will be available to the general public, including foreign nations.

This technical report has been reviewed and is approved for publication.

JAMES J. OLSEN
Actg Ch, Analysis & Optimization Branch
Structures and Dynamics Division

FOR THE COMMANDER

RALPH L. KUSTER, JR., Colonel, USAF
Chief, Structures & Dynamics Division

"If your address has changed, if you wish to be removed from our mailing list, or if the addressee is no longer employed by your organization please notify ___________,W-PAFB, OH 45433 to help us maintain a current mailing list".

Copies of this report should not be returned unless return is required by security considerations, contractual obligations, or notice on a specific document.

UNCLASSIFIED

SECURITY CLASSIFICATION OF THIS PAGE (When Data Entered)

REPORT DOCUMENTATION PAGE		READ INSTRUCTIONS BEFORE COMPLETING FORM
1. REPORT NUMBER AFFDL-TR-78-194, Part IV	2. GOVT ACCESSION NO.	3. RECIPIENT'S CATALOG NUMBER 9
4. TITLE (and Subtitle) 6 Transonic Wind Tunnel Tests on an Oscillating Wing with External Store. Part IV. The Wing with Underwing - Store.		5. TYPE OF REPORT & PERIOD COVERED Final Report. February 1977 — September 1979
		6. PERFORMING ORG. REPORT NUMBER NLR-TR-78106-U - PT-4
7. AUTHOR(s) 10 H./Tijdeman, J.W.G./van Nunen, A. N./Draan, A. J./Persoon, R./Poestkoke, R. Roos, P. Schnippers, C. M. Siebert		8. CONTRACT OR GRANT NUMBER(s) 14 AFOSR Grant 77-3233
9. PERFORMING ORGANIZATION NAME AND ADDRESS National Aerospace Laboratory Anthony Fokkerweg 2 Amsterdam, The Netherlands		10. PROGRAM ELEMENT, PROJECT, TASK AREA & WORK UNIT NUMBERS PE 61101F Work Unit 2307N503
11. CONTROLLING OFFICE NAME AND ADDRESS Air Force Flight Dynamics Laboratory Structures and Dynamics Division Wright-Patterson AFB OH 45433		12. REPORT DATE 11 September 1979
		13. NUMBER OF PAGES 170 12 179
14. MONITORING AGENCY NAME & ADDRESS (if different from Controlling Office) 15 AFOSR-77-3233		15. SECURITY CLASS. (of this report) Unclassified
		15a. DECLASSIFICATION/DOWNGRADING SCHEDULE

16. DISTRIBUTION STATEMENT (of this Report)

Approved for Public Release: Distribution Unlimited

16 2307   17 N5

17. DISTRIBUTION STATEMENT (of the abstract entered in Block 20, if different from Report)

Approved for Public Release: Distribution Unlimited

18. SUPPLEMENTARY NOTES

18 AFFDL   19 TR-78-194-PT-4

19. KEY WORDS (Continue on reverse side if necessary and identify by block number)

Transonic
Unsteady Aerodynamics
Experiments
External Stores
Flutter

20. ABSTRACT (Continue on reverse side if necessary and identify by block number)

A wind-tunnel investigation was carried out on an oscillating model of the F-5 wing with and without an external store (AIM-9J missile). Detailed steady and unsteady pressure distributions were obtained over the wing, while on the store total aerodynamic loads were measured.
The tests covered the Mach number range between Ma = 0.6 and Ma = 1.35, and reduced frequencies ranging up to k = 0.4 at Ma = 0.6 and to k = 0.2 at Ma = 1.35. This report (Part IV) gives an analysis of the results of the configuration with the store mounted at a pylon under the wing. Emphasis is put on the influence

DD FORM 1 JAN 73 1473 EDITION OF 1 NOV 65 IS OBSOLETE

UNCLASSIFIED

SECURITY CLASSIFICATION OF THIS PAGE (When Data Entered)

402 964

JOB

of the pylon and store on the wing loading and further on the loads acting on the pylon and store itself. A comparison is presented of experimental data and theoretical results obtained with the unsteady NLRI and Doublet Lattice methods.

FOREWORD

This report was prepared by the National Aerospace Laboratory (NLR of Amsterdam, the Netherlands. The sponsors were the Air Force Armament Test Laboratory (AFATL/DLJ) of Eglin Air Force Base, Florida and the Air Force Flight Dynamics Laboratory (AFFDL/FBR and AFFDL/FBE) of Wright-Patterson Air Force Base, Ohio. The sponsorship was performed through AFOSR Grant 77-3233, administered by Captain D. Wilkins of the Air Force Office of Scientific Research (AFOSR/TKN) of Bolling Air Force Base, Washington D.C.

The report consists of four parts. Part I contains the general description; Part II discusses the steady and unsteady aerodynamic tests of the clean F-5 wing; Part III discusses the tests for the wing with tip-mounted stores; and Part IV discusses the tests for the wing with under-wing stores.

The principal investigators were Dr. H. Tijdeman and Mr. J. W. G van Nunen of NLR. They were assisted by A. N. Kraan, A. J. Persoon, R. Poestkoke, Dr R. Roos, P. Schippers and C. M. Siebert of NLR.

Within the United States Air Force, this program was initiated by Lovic Thomas of the AFATL. It would not have been possible without the expert assistance of Richard Wallace (Lt Colonel, USAF, Retired), and Lt Colonel Daniel Seger and Major Robert Powell of the European Office of Aerospace Research Development (EOARD).

CONTENTS

PRECEDING PAGE BLANK

LIST OF SYMBOLS

a_{mn}	coefficient in the approximation of the vibration modes	
C	chord	(m)
$\bar{C}$	mean geometric chord; $\bar{C} = 0.4183$	(m)
C_M	pitch moment coefficient for the store	
C_m	sectional pitch moment coefficient	
C_N	yaw moment coefficient for the pylon or store	
C_p	pressure coefficient	
C_r	root chord; $C_r = 0.6396$	(m)
C_Y	side force coefficient for the pylon or store	
C_Z	normal force coefficient for the store	
C_z	sectional normal force coefficient	
F	frequency of oscillation	(Hz)
K	reduced frequency; $K = \frac{\pi F C_r}{V}$	
M	pitching moment	(Nm)
Ma	free-stream Mach number	
N	yawing moment	(Nm)
P	free-stream static pressure	(Pa)
P_i	unsteady pressure at model surface	(Pa)
P_{loc}	local static pressure	(Pa)
P_o	stagnation pressure	(Pa)
Q	dynamic pressure	(Pa)
S	semi span; $S = 0.6226$	(m)
V	free-stream velocity	(m/s)
w	modal displacement	(m)
x	coordinate in free-stream direction	(m)
Y	side force	(N)
y	coordinate in spanwise direction	(m)
Z	normal force	(N)
α	incidence; positive nose up	(degrees)
θ	amplitude of oscillation in the section of accelerometers 1 and 2; positive nose up	(rad)
ω	angular velocity; $\omega = 2\pi F$	(rad/s)

LIST OF SYMBOLS (Cont.)

SUBSCRIPTS

i	referring to unsteady quantities
q	referring to quasi-steady quantities

SUFFICES

+	denotes upper surface
-	denotes lower surface

1 INTRODUCTION

In order to determine the unsteady airloads on a representative fighter-type wing at transonic and supersonic speeds, wind-tunnel tests were carried out on an oscillating model of the F-5 wing with and without external store. If present, this external store (AIM-9J missile + launcher) was mounted either at the tip or at a pylon under the wing.

The wing model was oscillated in pitch about a 50 per cent root-chord axis at frequencies varying up to 40 Hz (for dimensions see Fig. 1a). The Mach number ranged between 0.6 and 1.35. Detailed pressure distributions, both steady and unsteady, were measured over the wing, while on the store the total aerodynamic loads were obtained. A description of the experimental test set-up and the test program is given in part I of this report (Ref. 1). The results are published in a data report (Ref. 2), while for easy data handling they are available also on magnetic tape.

To assist in the evaluation of the data, reference 1 is supplemented by three additional parts, covering successively the clean wing, the wing with tipstore and the wing with underwing-store. Each part contains plots of the steady and unsteady pressure distributions and gives a brief analysis of some selected results.

The present report (part IV) focusses on the configuration of the wing with the underwing-store (figure 1b shows the model of this configuration mounted on the side wall of the NLR High Speed Tunnel (HST), while the location of the pressure orifices is given in figure 1c). The report considers the influence of the pylon and store on the wing loading and on the loads experienced by the store itself. For the wing this analysis concerns a comparison with the clean wing configuration, results of which are taken from part II (Ref. 3). For the loads on the pylon and store the contributions due to the pylon, the launcher, and the missile body with aft wings and canard fins are considered. This last part of the analysis is slightly hampered of the fact that during one of the testruns on the complete configuration the canard fins broke from the model, causing the omission of supersonic data for the complete configuration.

For Ma = 0.6 the experimental data are supplemented with theoretical results obtained with the NLRI-method, an unsteady panel method for wing-body configurations (Ref. 5). Further, since the NLRI-method is

rather costly in terms of computer costs, a successful attempt has been made to devise a panel distribution, which will lead to comparative results when applied in a Doublet Lattice calculation.

2 STEADY RESULTS

2.1 General

During the wind-tunnel experiment steady pressures were measured over the wing at incidences of -0.5, 0 and 0.5 degrees. A listing of the test variables as well as a complete set of plots of the resulting steady pressure distributions in the eight measuring sections is gathered in Appendix IV.B. In addition to the pressures on the wing also the normal load, the side load, the pitching moment and the yawing moment, experienced by the store, as well as the side load and yawing moment felt by the pylon, were measured. These loads were measured by two independent strain gage balances located at the interfaces of wing and pylon as well as pylon and store. The exact locations are given in figure 1a. The results are given in Appendix IV.D.

For the limiting case of zero frequency so-called "quasi-steady" results can be obtained by considering the steady results for small incidences around a certain mid-position. In the present investigation "quasi-steady" loads for a mid-position of zero degrees were obtained from the steady data taken at incidences of -0.5 and 0.5 degrees. The corresponding definitions are given in Appendix IV.A.

The steady and quasi-steady load distributions on the wing were obtained form the measured pressure distributions. In this respect, it is noted that for the integration in section 3 and 5 the faulty value, found on the upperside near the leading edge, was replaced by a new value obtained by spanwise interpolation between the sections 2, 4 and 6.

2.2 Steady and quasi-steady loads on the wing

In order to better understand the influence the underwing-store has on the quasi-steady and unsteady spanwise load sidtributions, first its effect on the steady load distribution will be considered. Figures 2a through 2c show these distributions for subsonic (Ma = 0.6), transonic (Ma = 0.9) and supersonic (Ma = 1.35) flow conditions. For incidences

of -0.5, 0 and 0.5 degrees, each figure gives a comparison of the steady load distributions for the configuration with the underwing-store and for the clean wing.

In general, attaching a pylon and store under a wing has a considerable effect on the flow field. The flow has to diverge, which locally results in increased flow velocities, causing a further lowering of the pressure, especially on the lower side of the wing (e.g. see Figs. IV.B. 33 - 35 of Appendix IV.B.).

In figure 2a it is shown how this effect influences the spanwise normal load distribution at Ma = 0.6. Besides a decrease of the load, which is maximal just inboard of the pylon one observes also a discontinuity across the pylon. This jump in the loading, which corresponds to a side load on the pylon, reduces with increasing incidence.

At transonic conditions (Ma = 0.9; Fig. 2b) the addition of the pylon and store introduces a region of supersonic flow over the lower surface of the wing on both sides of the pylon. This supersonic region is responsible for the relatively large decrease of the steady normal load on the inboard part of the wing. With the load on the outboard section remaining almost unaffected by the presence of the pylon/store combination, the jump over the pylon has increased with respect to the Ma = 0.6 case. The dependence on incidence is similar to the subsonic case, be it that for $\alpha = -0.5$ the normal force near the tip reaches even a larger value than found for the clean wing configuration.

For Ma = 1.35 (Fig. 2c) the interference effect from the pylon and store is smaller and also less regular over the span. Just inboard of the pylon the normal load is decreased, but around 50 per cent of the span the load for the configuration with store grows above the value for the clean wing. In section 2, just outside the zone of influence originating from the front of the pylon, the difference becomes negligible again. Between the pylon and the wing tip the interference effects vary strongly with the spanwise position. The jump in the normal force over the pylon remains small. The trend with incidence is similar to the other cases.

The quasi-steady spanwise load distributions derived from the steady distributions, are presented in figures 3a to 3c. Qualitatively, the effect of the pylon and store is the same for the three flow conditions considered: an increase of the quasi-steady loading inboard of the pylon and a decrease on the outboard part of the wing, together resulting in a

jump of the quasi-steady normal force across the pylon. This jump is maximal for transonic conditions, for which the pylon and store have introduced a region of supersonic flow and thus a shockwave over the lower surface of the wing on both sides of the pylon.

To show the effect of Mach number on the sectional loads, figure 4 gives the quasi-steady normal loads in the sections 2, 5 and 8 as a function of Mach number. However, due to the sparcity of data points for the configurations with underwing-store a clear development is not found. It can be concluded only that far away from the pylon (sections 2 and 8) the interference effects are negligible for all Mach numbers considered.

2.3 Steady and quasi-steady loads on the pylon and store

The present tests were carried out with the underwing-store in various stages of completeness, making it possible to investigate the aerodynamic contribution of the pylon and of specific parts of the store. The behaviour of the individual forces and moments with Mach number is given in Appendix IV.D. In figures 5a and 5b the total steady side force and yawing moment experienced by the combination of pylon and store, if present, are plotted versus Mach number for the three test incidences -0.5 , 0 and 0.5 degrees.

For all configurations the side force (Fig. 5a) points inward, while the magnitude decreases with increasing incidence. Of course, both observations are in accordance with the behaviour of the jump in the steady spanwise normal load distributions described in section 2.2. Further, for all incidences the addition of the launcher doubles the total side force. The missile body with aft wings and the canard fins has a similar effect, although due to the mishap with the canard fins no differentiation can be made for the effect of either one of these control surfaces.

The total steady yawing moment (Fig. 5b) is relatively small for all configurations, and no clear variations with incidence are apparent. The contribution of the pylon is virtually nil for all cases tested (see als Fig. IV.D.6). For subsonic Mach numbers the launcher does not contribute to the yawing moment, while for supersonic conditions the contribution remains small. Most of the yawing moment is produced by the aft wings and the canard fins.

The quasi-steady side force and yawing moment coefficients for the combination of the pylon and store are presented in figure 6. The quasi-steady side force is positive (pointing outward) for all configurations, which is in line with the behaviour of the quasi-steady spanwise load distributions on the wing near the pylon (Fig. 3). With only the pylon present, the side load is very small. Addition of the launcher increases the side load uniformly over the Mach number range considered. Next, adding the missile body together with the aft wings and canard fins more than doubles the quasi-steady side load. The quasi-steady yawing moment is small for all configurations.

3 UNSTEADY RESULTS

3.1 Vibration modes

To monitor the vibration modes of the wing and store during the tests, the model was equipped with 12 accelerometers, eight in the wing and four in the launcher, of which two were measuring in vertical direction and the other two in lateral direction (for exact loacations see figure 1a). In the same way as for the clean wing configurations (see Ref. 3) also for the configurations with the underwing-store, the readings of these accelerometers were used to make analytical approximations of the vibration modes for the 20 Hz testruns. The polynomial expression used for these approximations is:

$$w(x,y) = \sum a_{mn} x^n y^m \quad \begin{array}{l}(m = 0,\ 1,\ 2;\ n = 0,1 \text{ for the wing})\\ (m = 0;\ n = 0,1 \text{ for the store})\end{array}$$

This expression assumes no deformation in chordwise direction and a parabolic deformation in spanwise direction. In using the measured values, for testrun 48 the reading of accelerometer 5 was weighted to ensure a realistic development of the torsion angle along the span. Further, for testrun 43 the accelerometers in the store measuring in vertical direction gave erroneous readings. Therefore, the vertical displacement of the store was taken equal to the displacement of the wing at the location of the pylon attachment, which was in accordance with the findings for the other testruns. Taking these two points into account, the difference between the analytically approximated displacements and the experimental readings remains within 2 per cent of the maximal displacement. Table 1 presents the numerical values of the coefficients a_{mn}

for the analyzed vibration modes. The normalization is carried out such that at the wing section of accelerometer 2 the tangent of the angle of oscillation equals one.

To obtain insight into the effect of the pylon and store on the vibration modes of the wing, the nodal lines as found for the clean wing (see reference 3) and the wing with underwing-store are presented in figures 7a and 7b. For Ma = 0.6 and 0.9 the comparison concerns the store with the canard fins (Fig. 7a), while for Ma = 0.9, 1.10 and 1.35 the store without the canard fins (Fig. 7b) is considered. The figures show that for 20 Hz the addition of the pylon store hardly influences the position of the nodal line. The difference found for Ma = 1.10 (Fig. 7b) most probably is caused by the change in stagnation pressure from 1.0×10^5 Pa for the clean wing to 0.7×10^5 Pa for the wing with underwing-store. In part III of this report (Ref. 4) it was found that for the wing with tipstore such a change in stagnation pressure makes the nodal line move forward, which corresponds with the behaviour for the present configuration.

The development with Mach number is similar to that of the clean wing i.e.: in the subsonic and transonic regime the nodal line bends to the rear, while in the supersonic range the nodal line tends to return to its original position. The local torsion angle was found to remain almost constant over the wing. As mentioned before, in vertical direction the store follows the motion of the wing. In lateral direction the motion is negligibly small.

No approximations were made for the 40 Hz testruns of the configuration with underwing-store. However, a preliminary analysis was made to check the validity of the results. Contrary to what was found for the wing with complete tipstore (Ref. 4) all runs except no. 44 show a stable vibration mode. In testrun 44 a complex mode was encountered, which casts doubts on the unsteady store loads measured by the balances.

3.2 Unsteady loads

3.2.1 General

For all pylon/store configurations the unsteady pressure distributions measured over the wing are tabulated in reference 2 and plotted in the present raport. These plots and a listing of the relevant test variables are given in Appendix IV.C. For a better comparison the values

on the upperside are shown with a reversed sign.

In the present experiment the unsteady side force and yawing moment acting on the pylon, as well as the unsteady normal force, side force, pitching moment and yawing moment on the store were measured by the same strain gage balances used to obtain the steady data (for details see references 1 and 6). Plots of these quantities versus Mach number are presented in Appendix IV.D for all 20 Hz test cases.

The problems with the vibration modes in the test runs 43 and 44 are the cause for the incorrectness of the values for the forces and moments on pylon and store as given in the tabulated results (Ref. 2). For run 43 the correct values could be retrieved. They are presented in table 2.

3.2.2 Unsteady loads on the wing

The development of the unsteady normal force*) with Mach number in the sections 2, 5 and 8 is given in figure 8. For a frequency of 20 Hz this figure presents a comparison between the results of the clean wing and the wing with underwing-store. For the lower Mach numbers the store is complete, while for the higher ones the data represent the configuration with the canard fins missing. At Ma = 0.9 both configurations were tested.

Comparison of figures 4 and 8 show that the character of the interference found for 20 Hz is similar to that for quasi-steady conditions except in section 8. In section 2 the presence of the pylon and store is not felt, while in section 5 the difference between the two configurations at 20 Hz is slightly less than for 0 Hz. However, in section 8, contrary to the quasi-steady findings, the pylon and store do influence the unsteady normal load at 20 Hz. As explained below, the reason for this is different for each Mach number. The large differences found for Ma = 1.1 may be caused partly by the change in stagnation pressure from $P_o = 1.0 \times 10^5$ Pa to $P_o = 0.7 \times 10^5$ Pa.

To find out how the interference of the pylon and store spreads over the wing, in figures 9 to 11 the spanwise distribution of the unsteady normal force and pitching moment for the configuration with and without

---

*) For the integration of the unsteady pressure distributions in sections 3 and 5 the zero value, wrongly measured on the upperside near the leading edge, was replaced by a new value, obtained by spanwise interpolation between sections 2, 4 and 6.

store are compared for Ma = 0.6, 0.9 and 1.35 and a frequency of 20 Hz.

At Ma = 0.6 the pylon and store introduce the expected jump in the real part of the normal force distribution (Fig. 9a). However, contrary to the quasi-steady case (Fig. 3a), this interference remains localized around the attachment position of the pylon. The inboard 70 per cent of the span apparently is not affected by the presence of the store. The reason is found by comparing the unsteady pressure distributions for the two configurations. This shows that for the wing with store the unsteady pressures at the leading edge on the lower side are significant lower than for the clean wing, thus resulting in a lower unsteady normal force. The relatively large difference found in section 8 can be explained by the fact that the bulge found in the unsteady pressure distribution on the lower side of the clean wing (see part II of the present report, Ref. 3), does not show up for the present configuration (see Fig. IV.C.32 of Appendix IV.C). The imaginary part of the unsteady normal force is not influenced at all by the pylon and store. As far as the pitching moment distribution is concerned (Fig. 9b), the real part shows an interference more spread out over the wing; however, it must be realized that the values remain very small. The difference between the two configurations corresponds to a shift of the normal force of about 5 per cent of the local chord. As with the normal force, the imaginary part is free of interference effects.

At transonic flow conditions (Ma = 0.9) the pylon/store interference extends over the whole wing. Inboard of the pylon the normal force distribution (Fig. 10a) shows an irregular interference pattern. The shape of the real part of the unsteady spanwise distribution for the wing with store corresponds very well with the quasi-steady one (see Fig. 3b). The dip at section 3 is caused by the shock which for this configuration exists on the lower wing surface. The sharp decrease at section 5 was explained in part II (Ref. 3) as partly due to an insufficient resolution necessary to integrate over the peaks, generated by the shock moving over the upper surface of the wing. Outboard of the pylon, the presence of the store results in a significant decrease. The imaginary part of the normal load is affected most near the wing-tip. As can be expected the pitching moment is influenced also rather irregularly (Fig. 10b). The maximum interference is found in the vicinity of the pylon.

In the unsteady measurements for Ma = 0.9 the configuration with underwing-store was tested with and without canard fins in order to have

an overlap between the subsonic and supersonic case, of which the latter was tested with only the aft wings present. The figures 10a and 10b show that the influence of the canard fins on the unsteady spanwise load distributions is negligible.

At Ma = 1.35 the effect of the underwing-store is very regular. The real part of the normal force (Fig. 11a) is increased over the inboard part of the wing and decreased over the outboard part, as was observed also for the quasi-steady case (Fig. 3c). In section 2, just outside the zone of influence originating from the front of the pylon, the influence has become almost zero. The imaginary part, being smaller in magnitude, is affected only near the pylon. The behaviour of the unsteady pitching moment is similar apart from a dip in section 4 (Fig. 11b).

3.2.3 Unsteady loads on the pylon and store

The sum of the unsteady lateral loads at 20 Hz measured by the balances in the pylon and the store is plotted in figure 12 versus Mach number. As the configuration is gradually made more complex, the influence of the different parts of the store can be studied.

The behaviour of the real part of the side force and the yawing moment coefficients is very similar to what was found for 0 Hz (Fig. 6). This is valid for the development with Mach number as well as for the variations resulting from changes in the configuration. The main contribution to the side force comes from the aft wings. For Ma = 0.9 it is shown that the canard fins give a negligible contribution. The reason for this is clear. Their location far in front of the main wing makes any interference originating from this wing minimal. Therefore the only way the canard fins can contribute to the side force is by means of a lateral motion of the store itself, and this motion was found to be negligible (see section 3.1). The imaginary part of the side force is almost zero, with only a small contribution of the aft wings in the supersonic range.

The total unsteady yawing moment remains small. As fas as the real part is concerned, the launcher and missile body contribute most, while the aft wings give a small reduction. The imaginary part is negligible.

4 COMPARISON WITH THEORY

4.1 The NLRI-method

Next to the Doublet Lattice method the NLR possesses a theoretical method for the calculation of the unsteady aerodynamic forces on a wing-body configuration oscillating in subsonic flow. This so-called "NLRI-method" is a panel-type method based on the potential flow approximation. For the bodies, such as fuselage and stores, use is made of a representation in terms of unsteady source panels distributed over the contour of the body, while for the lifting surfaces, which are taken to be infinitely thin, the Doublet Lattice approach is used. A detailed description of the method is given in reference 5.

As part of the present investigation the NLRI-method was applied to the configuration with the complete underwing-store at Ma = 0.6 and a frequency of 20 Hz. The panel distribution used in this calculation is shown in figure 13. The wing, the pylon, the canard fins and the aft wings are represented as thin lifting surfaces, while the launcher and missile body are combined to one long body with an open rear end. Apart from the pylon, the panel distribution is similar to the one used in the NLRI-calculations made for the wing with tipstore (see Part III, Ref. 4).

The theoretical pressure distributions in three sections of the wing are compared with experimental data*) in figure 14. The theorecical lines represent the calculated pressure jump across the wing divided by two. In the sections 2 and 8 the agreement between theory and experiment is good. In section 5, just inboard of the pylon the agreement looks not so good. However, it should be noted that for this section because of the local asymmetry of the configuration the comparison would be better if the experimental data would represent also the jump across the wing surface. In fact, the theoretical line quite closely averages the experimental values. The remaining differences may be explained by the fact that the flow stagnates against the pylon (see Fig. IV.B.34 of Appendix IV.B), an effect which cannot be accounted for in the theory.

A comparison of the corresponding theoretical and experimental unsteady spanwise normal load distributions for the wing with and without

---

*) Note that for the purpose of comparison the unsteady pressures measured on the upperside are plotted with a reversed sign.

underwing-store is given in figure 15. The theoretical results for the wing with store were computed with the NLRI-method, while for the clean wing the Doublet Lattice method was used (Ref. 3).

As found for the clean wing, also for the wing with pylon and store, the real part of the calculated unsteady normal force, as normal, is larger than the experimental value. Since the differences are similar for both configurations, conclusions concerning interference effects should remain valid.

The theoretical calculations predict an interference due to the presence of the pylon and store, which agrees reasonably with the experimental findings. In the real part of the unsteady loading the calculated and measured jump over the pylon are of the same order. The predicted reduction of the load on the outboard part of the wing is larger than found experimentally. The reason for this is the relatively low experimental values for the clean wing, which as explained in part II (Ref. 3) are caused by unexpected peaks and bulges in the measured unsteady pressure distributions and which tend to lower the integrated values. The small increase of the normal load inboard of the pylon is not observed in the tests for 20 Hz for reasons explained above in section 3.2.2, but a similar increase is found in the quasi-steady case (see Fig. 3a).

In table 3 the experimental normal force, pitching moment, side force and yawing moment acting on the combination of pylon and store are compared with the values obtained with the NLRI-method. For the unsteady normal and side forces the agreement is good, while for the pitching and yawing moment the theoretical values are off by a factor of two. However, in evaluating this, it should be realized that the normal force as well as both moments are very small. For example, the real part of the normal force is only 7 per cent of the force acting on a strip of the wing on both sides of the pylon having the same width as the store. For the side force this value is about 30 per cent.

4.2 Schematization in terms of the Doublet Lattice Method

Compared to the Doublet Lattice (DL) method, the NLRI-method uses 2 to 3 times more computer time. This makes the computation of unsteady aerodynamic force coefficients for flutter certification very expensive and impractical if carried out solely with the NLRI-method. Therefore, as proposed in reference 5, it is worthwhile to investigate the

possibility to carry out such calculations solely with a cheaper method, such as the DL-method, after the panel distribution has been checked against results of a NLRI-computation.

In the present investigation it is tried to devise such a panel distribution for the DL-method, in which the store is represented by additional thin lifting surface parts. These additional lifting surfaces have to fulfil two roles. They should lead to a good prediction of the interference on the wing and at the same time give reliable values for the store loads. In part III (Ref. 4) a panel distribution is shown which satisfies these criteria reasonably well for the configuration with complete tipstore. The same panelling scheme, with an additional horizontal row of panels to model normal force and pitching moment on the launcher and missile body, is used for the wing with underwing-store. This panel distribution is given in figure 16.

The unsteady pressure and normal load distributions on the wing, obtained with this DL panel-layout for Ma = 0.6 and F = 20 Hz, are identical to the ones found with the NLRI-method. The unsteady loads on pylon and store are given in table 3. Although the panel-layout was adopted from the configuration with tipstore and no special tuning for the present configuration was made, the agreement with experimental store loads is very good. Even the moments are predicted well.

Clearly, the type of panel schematization presented above for the Doublet Lattice method may be of use in practical flutter investigations.

5 CONCLUSIONS

A wind-tunnel investigation was carried out on a harmonically oscillating model of the F-5 wing with and without external store. As part of the test program steady and unsteady measurements were performed on the configuration with a pylon and store mounted under the wing. These measurements concerned pressures on the wing and aerodynamic loads on the pylon and store. The present report gives a brief analysis of the results for this configuration. This analysis concerns:

- the interference of the tipstore on the steady, quasi-steady and unsteady wing loadings, indicating that pylon and store are responsible for an increase of the loading inboard of the pylon and a decrease on the outboard side

- the behaviour with Mach number, which shows that at Ma = 0.9 the wing loading is dominated by the formation of a shock on the lower side of the wing
- the influence of the complexity of the store, which indicates that the side force grows consistently as the store becomes more complex, while the yawing moment remains very small
- a description in terms of polynomials of the in-wind vibration modes for 20 Hz
- a comparison of these vibration modes with those of the clean wing, showing that the pylon and store hardly influence the position of the nodal line
- a comparison of unsteady experimental data for Ma = 0.6 with the results obtained with the NLRI-method, showing a satisfactory agreement
- the definition of a panel distribution for Doublet Lattice calculations of which the results agree well with the experimental data and which may be of use in practical flutter investigations.

6 REFERENCES

1	Tijdeman, H. et al.	Transonic wind-tunnel tests on an oscillating wing with external store. Part I: General description NLR TR 78106 U (1978)
2		Results of transonic wind-tunnel measurements on an oscillating wing with external store. NLR TR 78030 U (1978)
3	Tijdeman, H. et al.	Transonic wind-tunnel tests on an oscillating wing with external store. Part II: The clean wing NLR TR 78106 U (1978)
4	Tijdeman, H. et al.	Transonic wind-tunnel tests on an oscillating wing with external store. Part III: The wing with tipstore NLR TR 78106 U (1979)
5	Roos, R. Bennekers, B. and Zwaan, R.J.	Calculation of unsteady subsonic flow about harmonically oscillating wing/body configurations. J. of Aircraft, Vol. 14, No. 5, pp 447 - 454, 1977
6	Persoon, A.J.	Measuring unsteady aerodynamic loads on wing-mounted stores. NLR TR 79013 U (1979)
7		AGARD manual on Aeroelasticity Vol. VI (1968)

TABLE 1

Coefficients a_{mn} for the approximation of the in-wind vibration modes of the wing with pylon and store at an oscillation frequency of 20 Hz

Conf.	Run	Ma	$P_o \times 10^{-5}$	F (Hz)	K	WING a_{00}	WING a_{01}	WING a_{10}	WING a_{11}	WING a_{20}	a_{21}	STORE Vertical a_{00}	STORE Vertical a_{01}	STORE Lateral a_{00}	STORE Lateral a_{01}
Store + CF	43	0.6	1.0	20	0.201	-0.302	0.891	-0.362	1.371	0.681	-2.606	-0.320	0.952	0.017	-0.047
	48	0.9	1.0		0.138	-0.346	1.007	0.053	-0.084	-0.246	0.155	-0.376	0.994	0.021	-0.072
Store - CF	88	0.9	1.0		0.141	-0.353	1.020	0.129	-0.253	-0.386	0.502	-0.361	0.980	0.017	-0.067
	92	1.10	0.7		0.118	-0.348	1.014	0.103	-0.182	-0.288	0.359	-0.352	0.986	0.019	-0.067
	97	1.35	0.7	20	0.099	-0.342	1.008	0.065	-0.095	-0.192	0.178	-0.336	0.964	0.020	-0.068

TABLE 2

Modified experimental pylon and store loads for testrun 43

	Pylon Balance	Launcher Balance
Re C_Z		0.0106
Im C_Z		0.0081
Re C_M		0.0211
Im C_M		-0.0070
Re C_Y	0.0124	0.0337
Im C_Y	-0.0002	0.0015
Re C_N	-0.0036	-0.0083
Im C_N	0.0003	-0.0004

TABLE 3

Comparison of theoretical and experimental unsteady loads on the underwing-store

Conf. 301: Wing + pylon + complete store

Ma = 0.6 F = 20 Hz	Experiment	Theory NLRI	Theory DL
Re C_Z	0.011	0.010	0.010
Im C_Z	0.008	0.005	0.005
Re C_M	0.021	0.011	0.022
Im C_M	-0.007	-0.001	-0.007
Re C_Y	0.046	0.044	0.051
Im C_Y	0.001	-0.009	-0.002
Re C_N	-0.012	-0.006	-0.007
Im C_N	0	-0.002	0.001

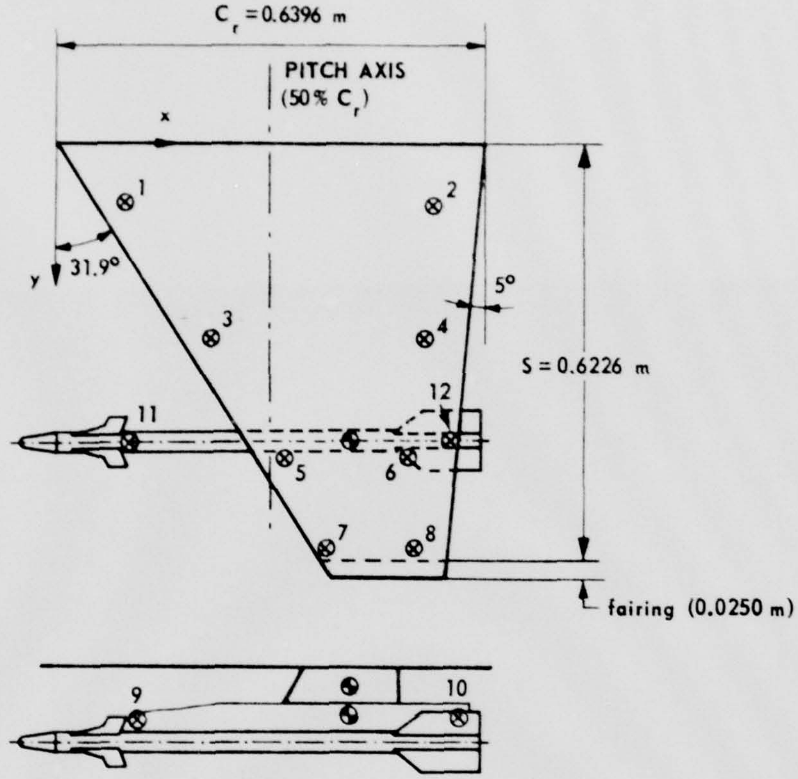

⊗ ACCELEROMETERS			
NR	x (m)	y (m)	
1	0.1087	0.0957	
2	0.5648	0.0977	
3	0.2309	0.2971	
4	0.5475	0.2991	
5	0.3422	0.4772	
6	0.5270	0.4772	
7	0.4070	0.6176	
8	0.5390	0.6176	
9	0.0869	0.477	lateral
10	0.5962	0.477	lateral
11	0.0869	0.477	vertical
12	0.5837	0.477	vertical

	BALANCE CENTRES		
	x	y	z
PYLON	0.43	0.477	−0.025
STORE	0.43	0.477	−0.066

Fig. 1a Dimensions of the wing model with underwing store

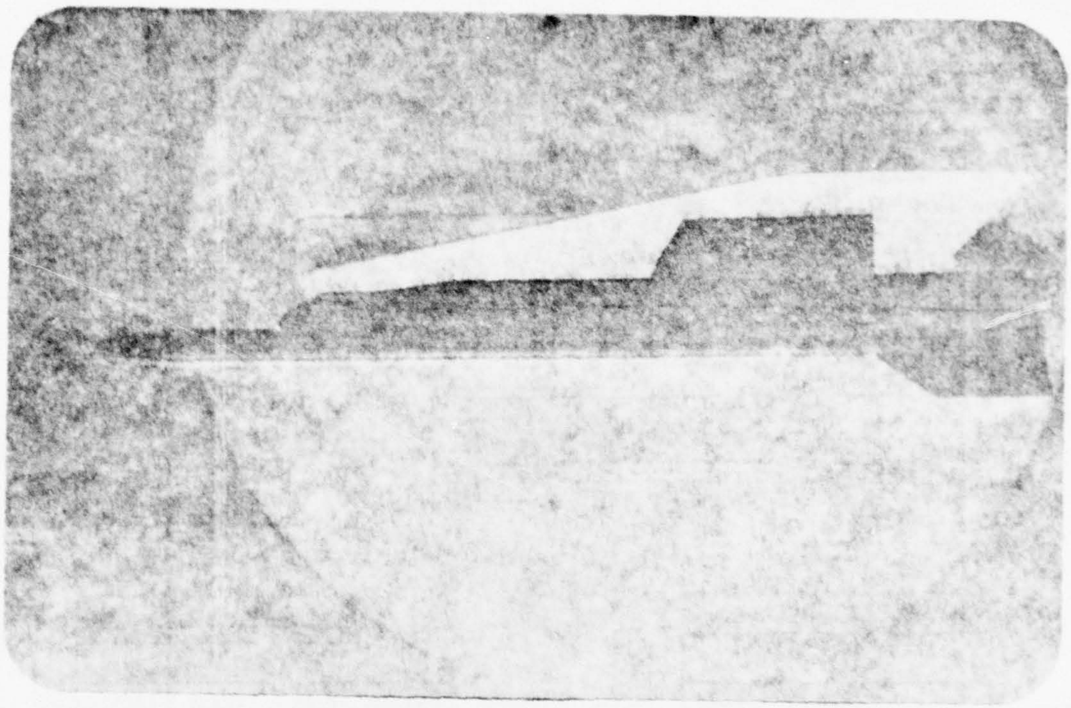

Fig. 1b Model of wing with underwing store mounted in the wind tunnel

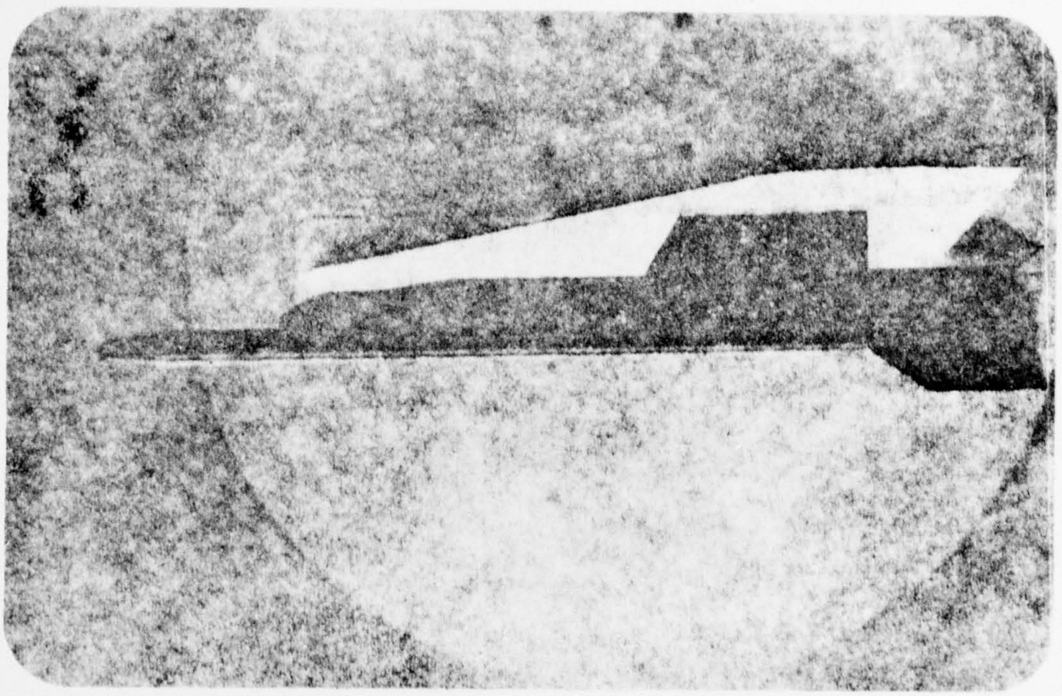

Fig. 1b Model of wing with underwing store mounted in the wind tunnel

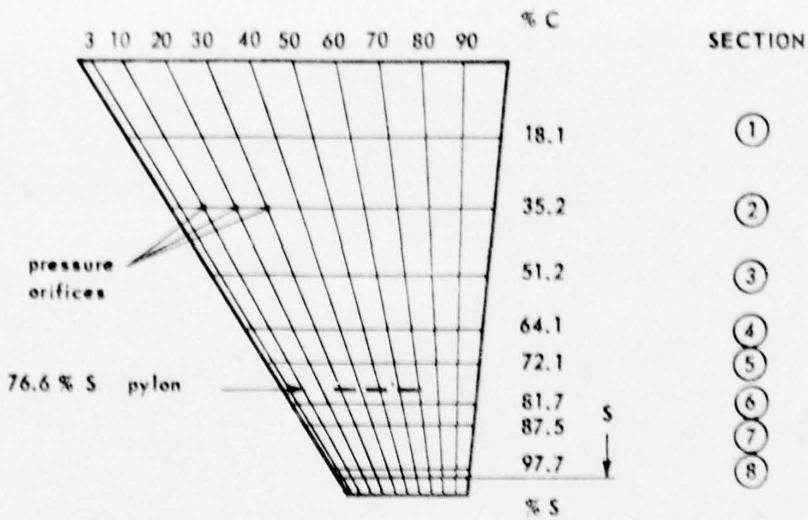

Fig. 1c Location of the pressure orifices

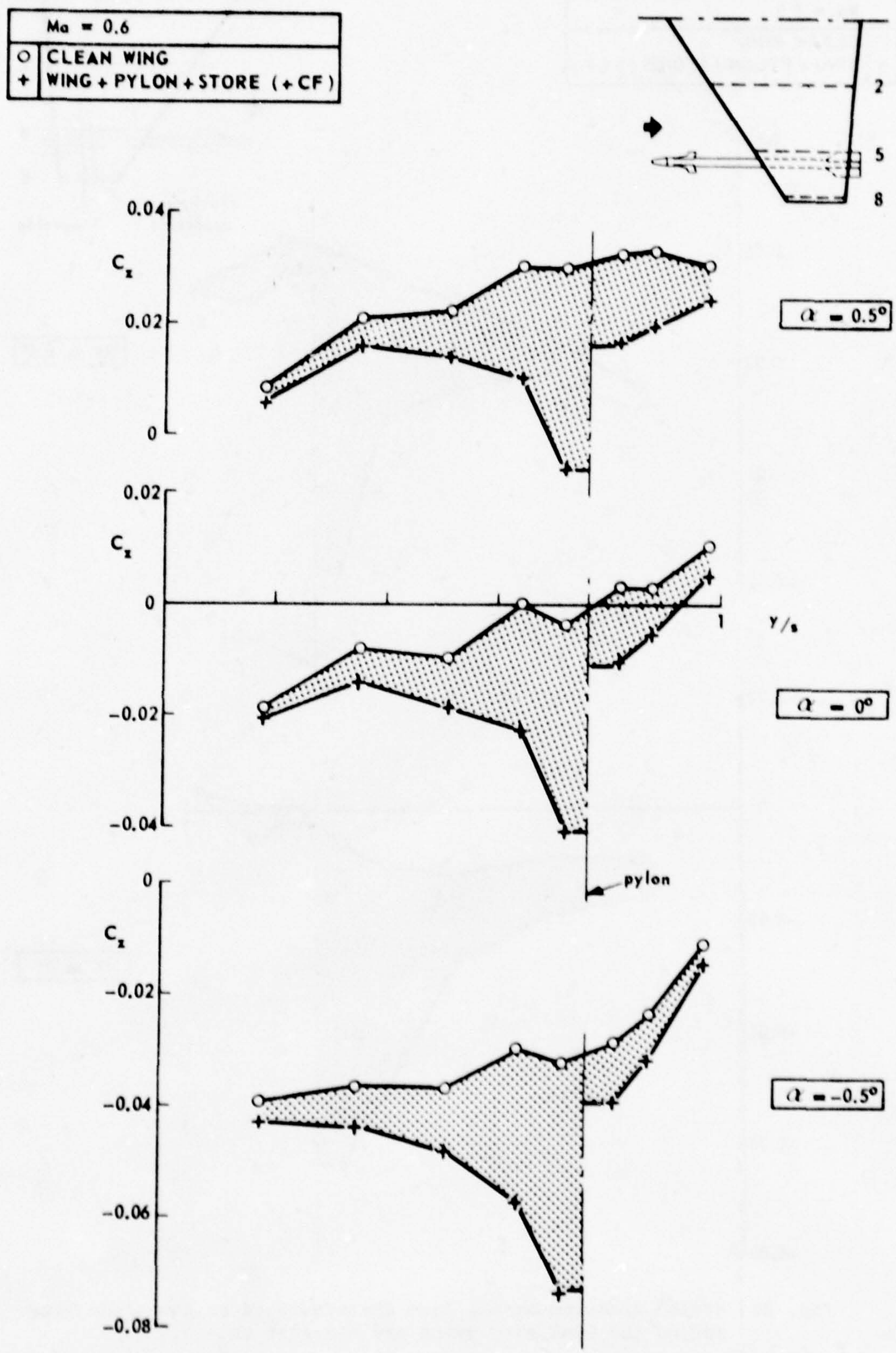

Fig. 2a Steady spanwise normal load distributions on the clean wing and on the wing with pylon and store at Ma = 0.6

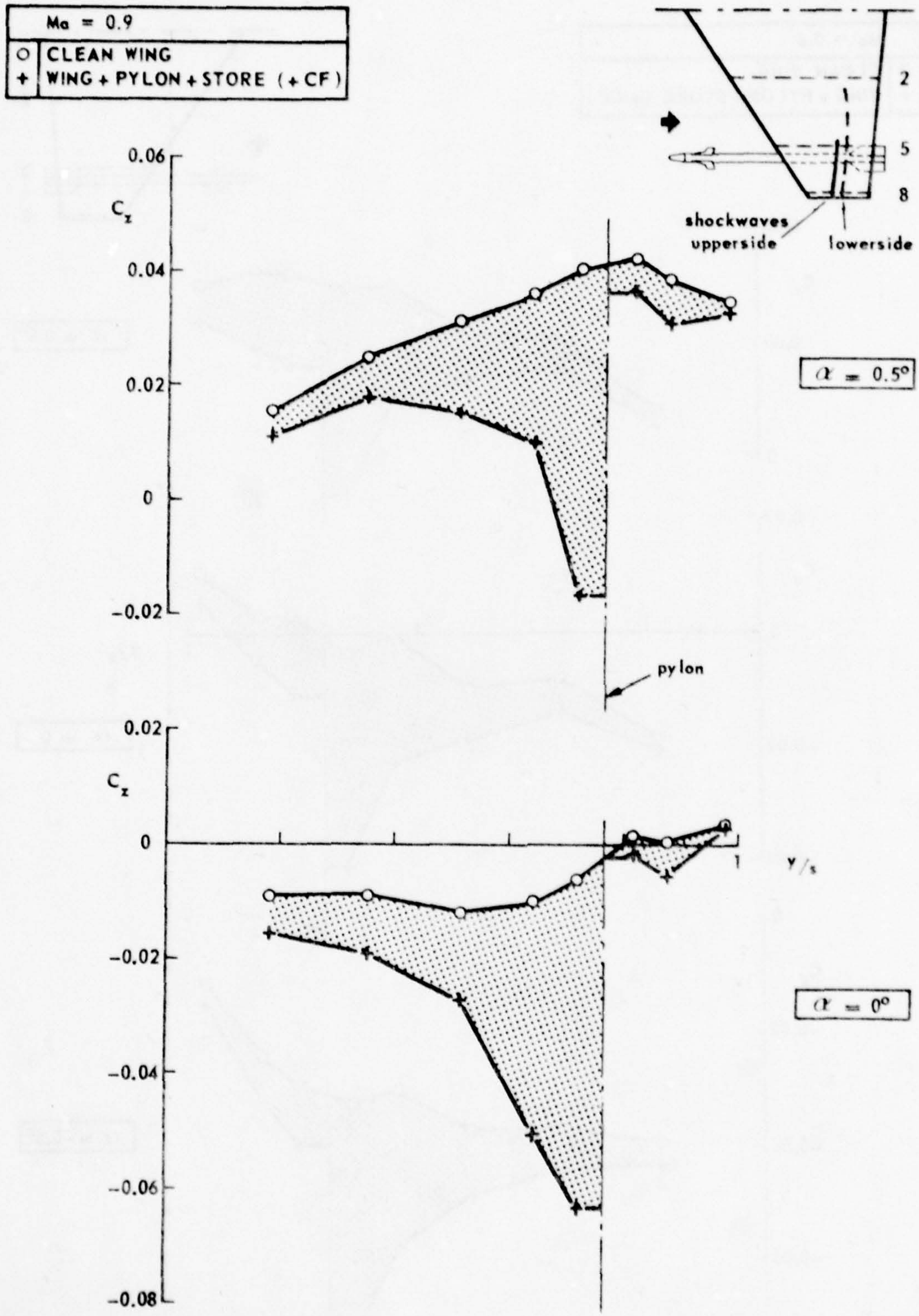

Fig. 2b Steady spanwise normal load distributions on the clean wing and on the wing with pylon and store at Ma = 0.9

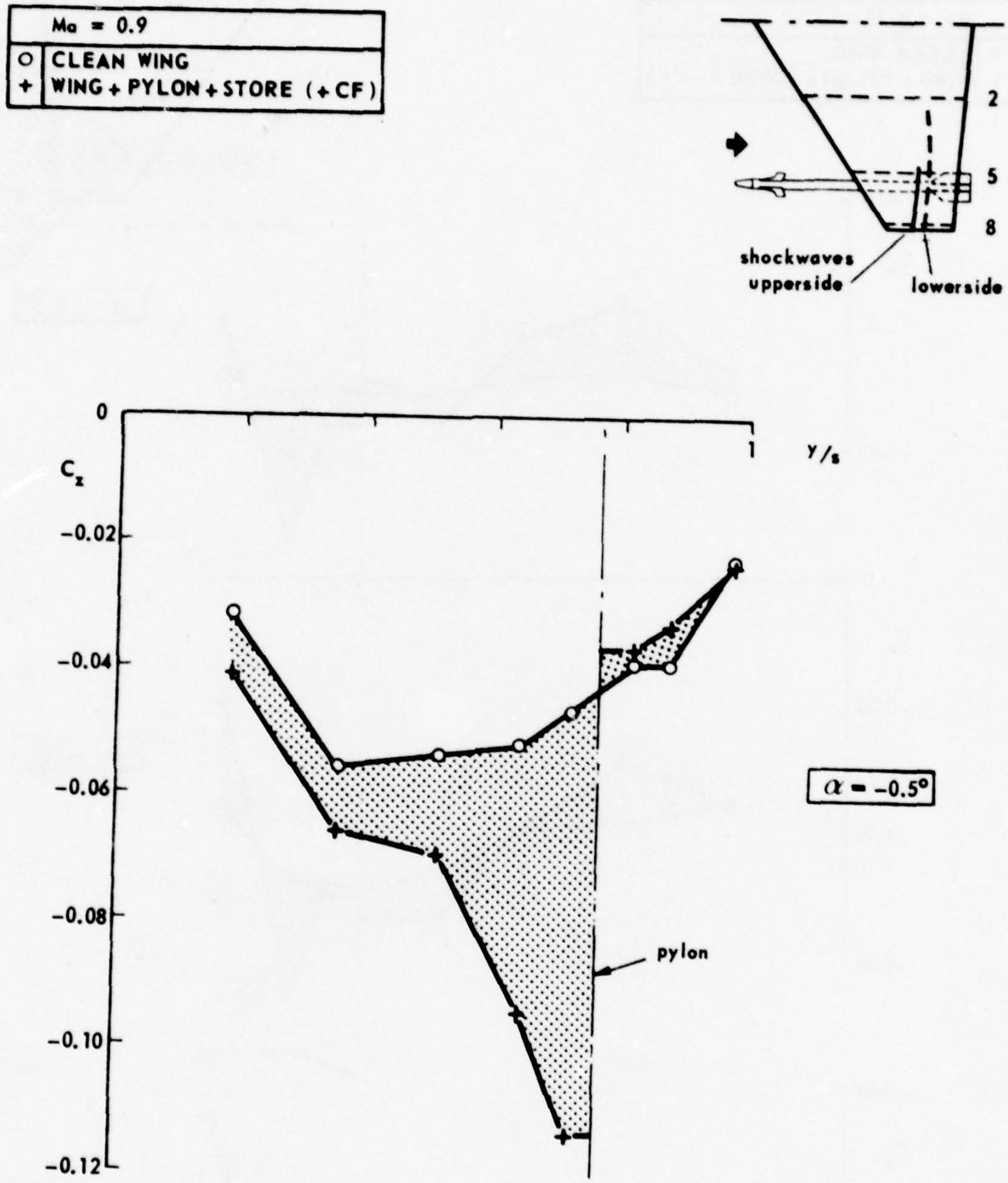

Ma = 0.9
○ CLEAN WING
+ WING + PYLON + STORE (+ CF)
2
5
8
shockwaves
upperside
lowerside
0
C_z
-0.02
-0.04
-0.06
-0.08
-0.10
-0.12
1
y/s
pylon
α = -0.5°

Fig. 2b (Cont'd)

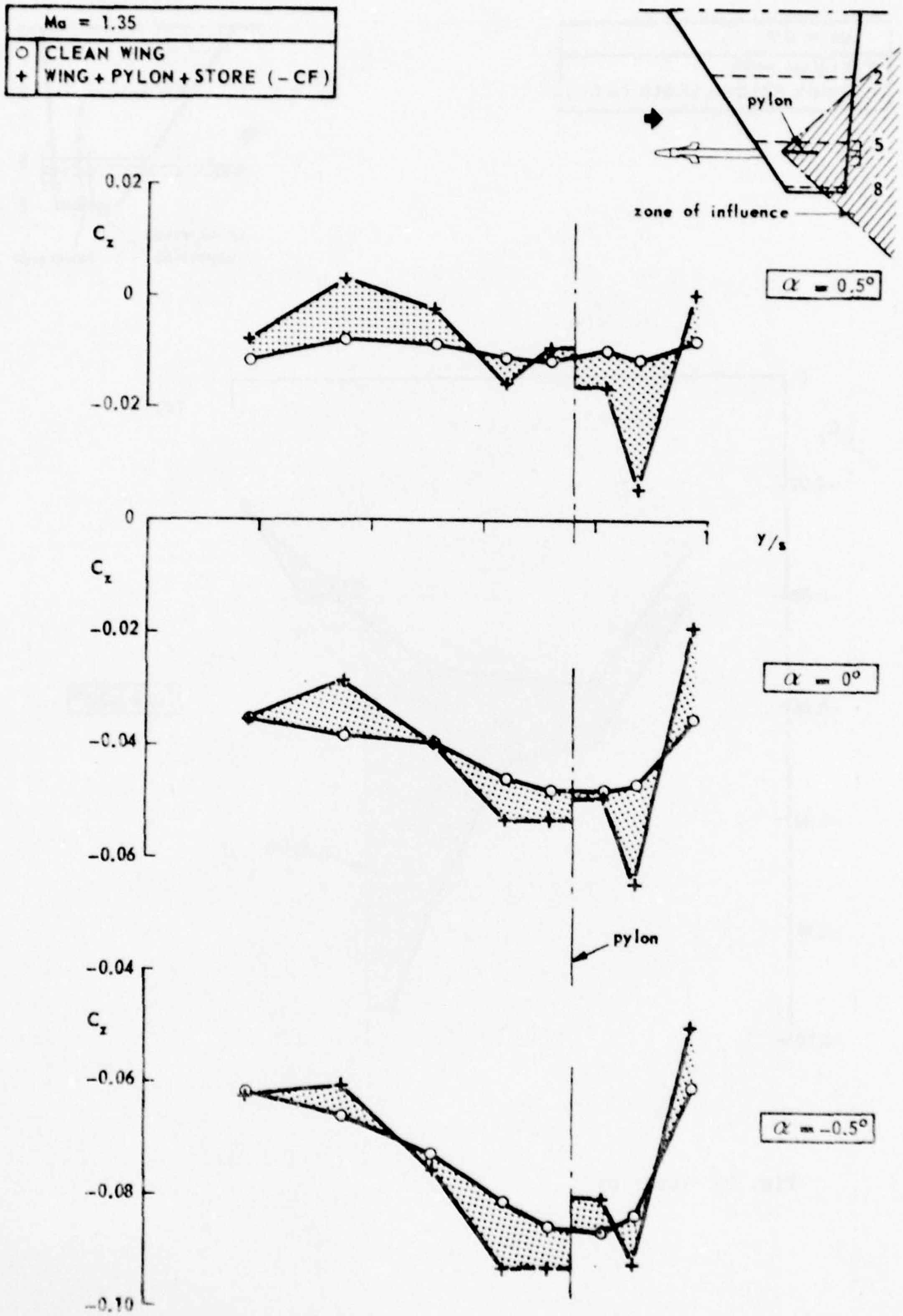

Fig. 2c Steady spanwise normal load distributions on the clean wing and on the wing with pylon and store at Ma = 1.35

Ma = 0.6	EXP.	RUN	CONFIGURATION
F = 0 Hz	O	137	CLEAN WING
	+	41	WING + PYLON + STORE (+ CF)

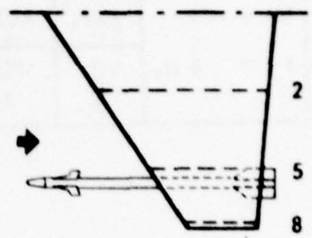

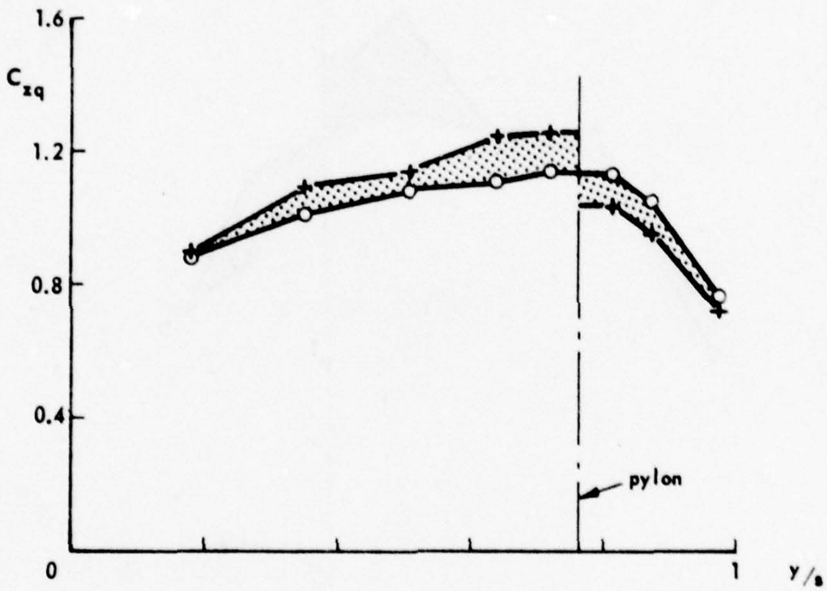

Fig. 3a Quasi-steady spanwise normal load distributions on the clean wing and the wing with pylon and store at Ma = 0.6

Ma = 0.9	EXP.	RUN	CONFIGURATION
F = 0 Hz	O	151	CLEAN WING
	+	46	WING + PYLON + STORE (+ CF)

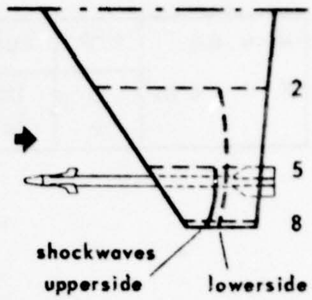

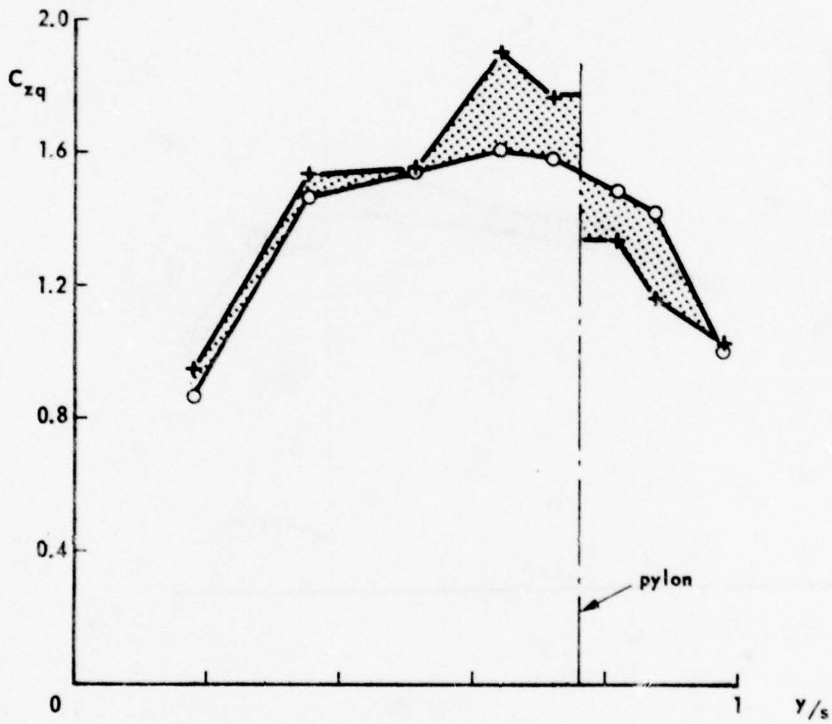

Fig. 3b Quasi-steady spanwise normal load distributions on the clean wing and the wing with pylon and store at Ma = 0.9

Ma = 1.35	EXP.	RUN	CONFIGURATION
F = 0 Hz	o	190	CLEAN WING
	+	95	WING + PYLON + STORE (- CF)

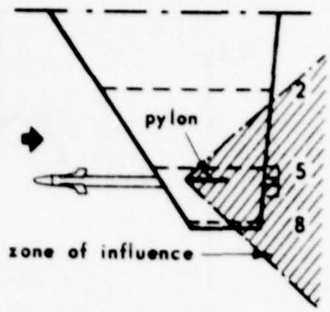

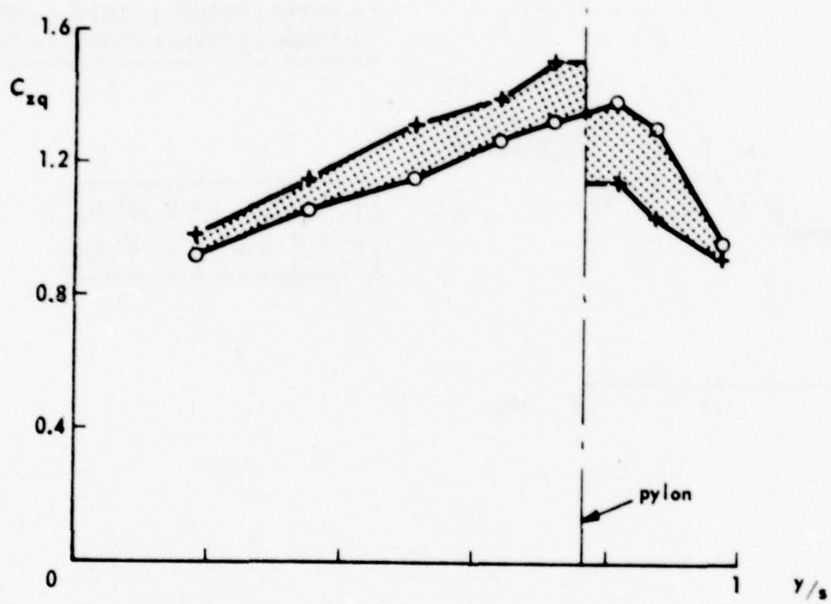

Fig. 3c Quasi-steady spanwise normal load distributions on the clean wing and the wing with pylon and store at Ma = 1.35

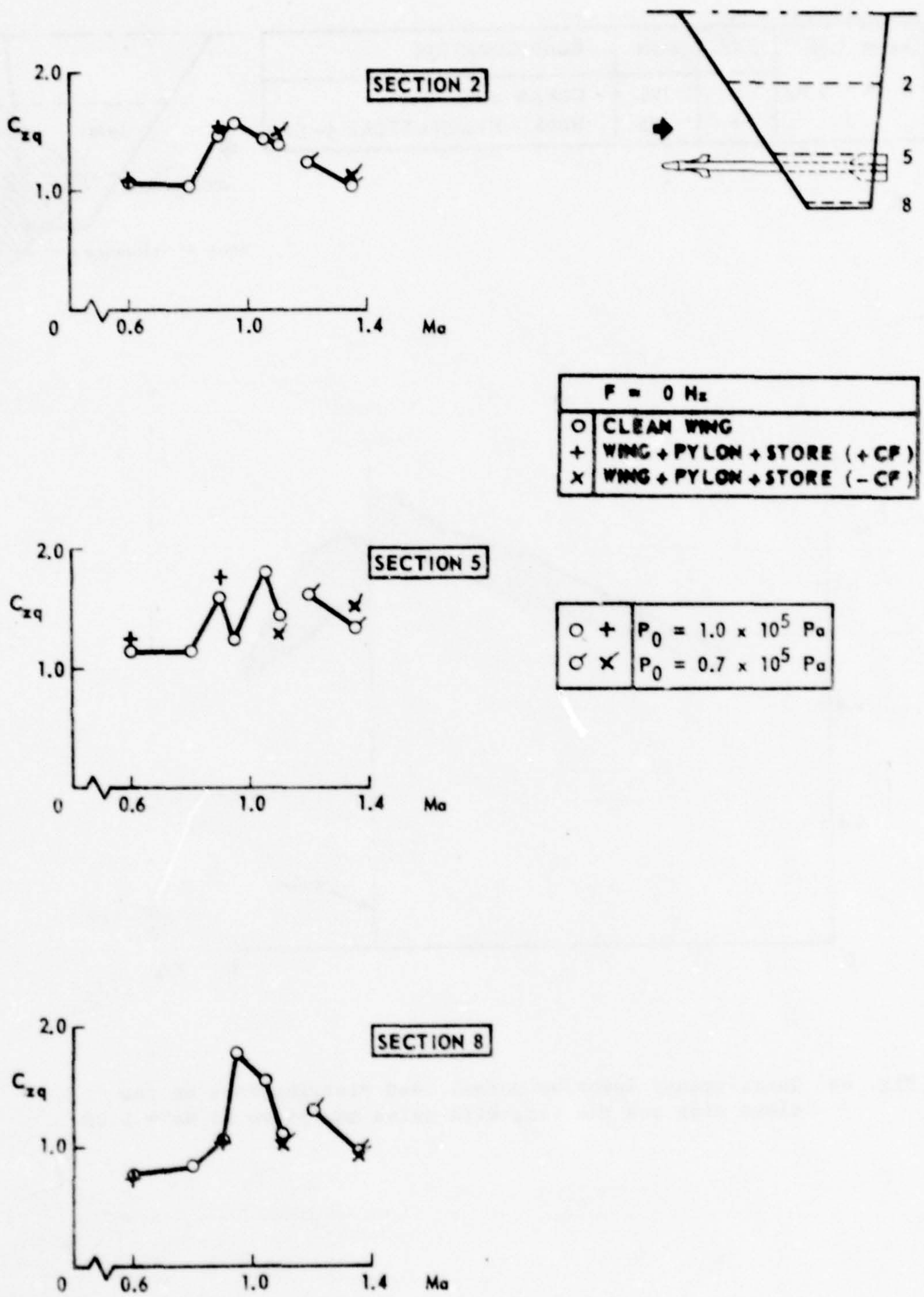

Fig. 4 Sectional quasi-steady normal load distribution on the clean wing and the wing with pylon and store versus Mach number

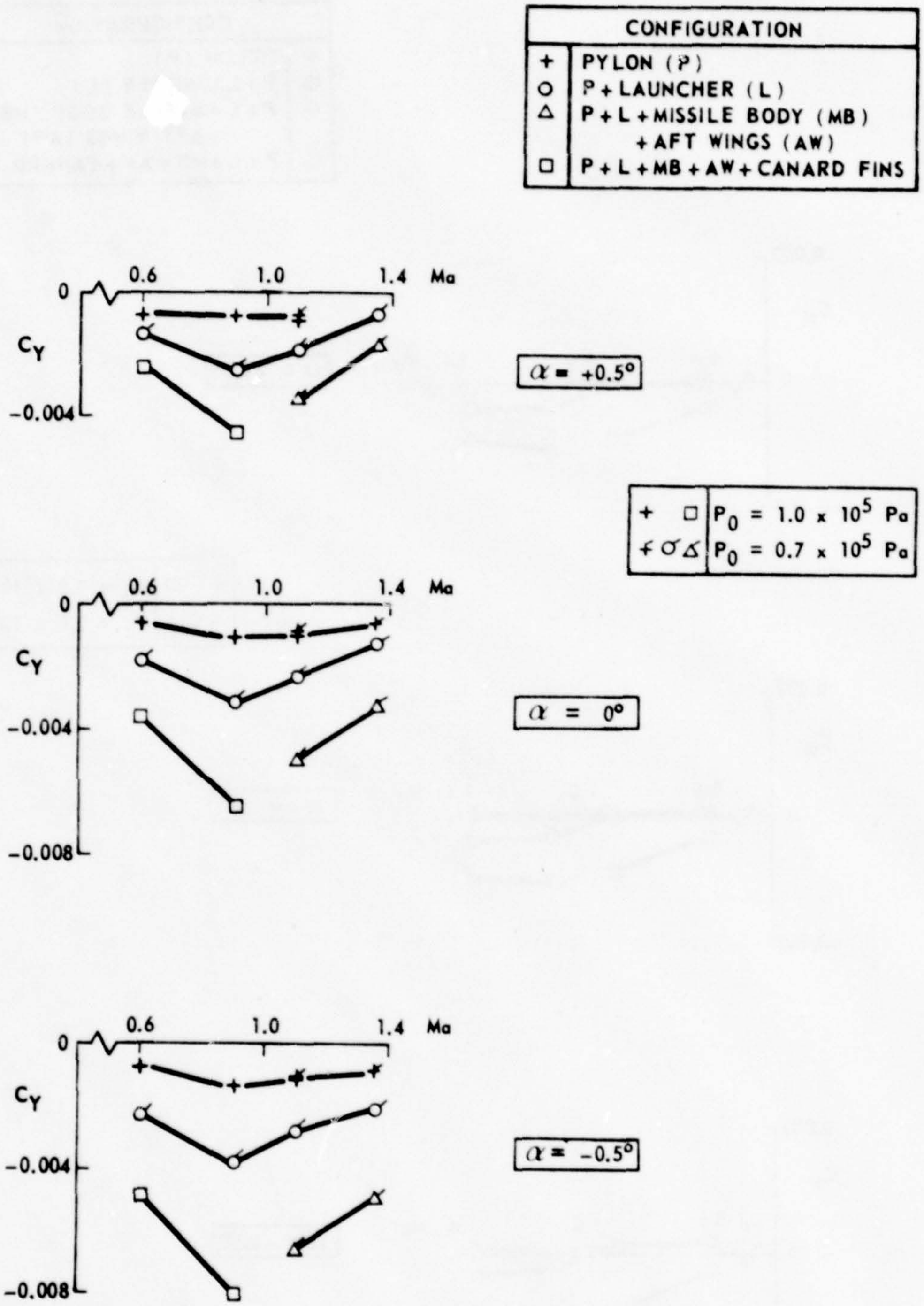

Fig. 5a Steady side force on the pylon and store for various configurations

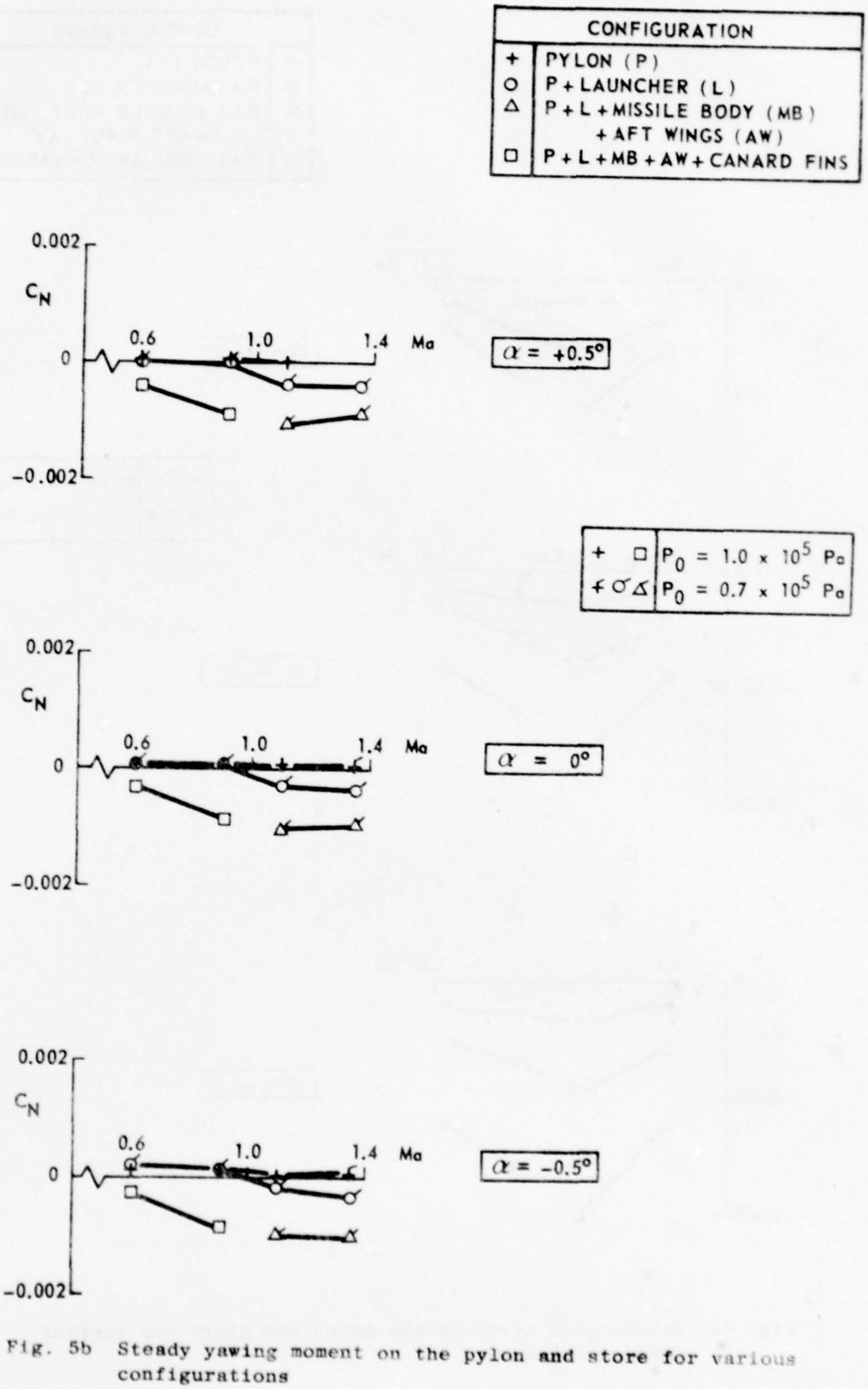

Fig. 5b Steady yawing moment on the pylon and store for various configurations

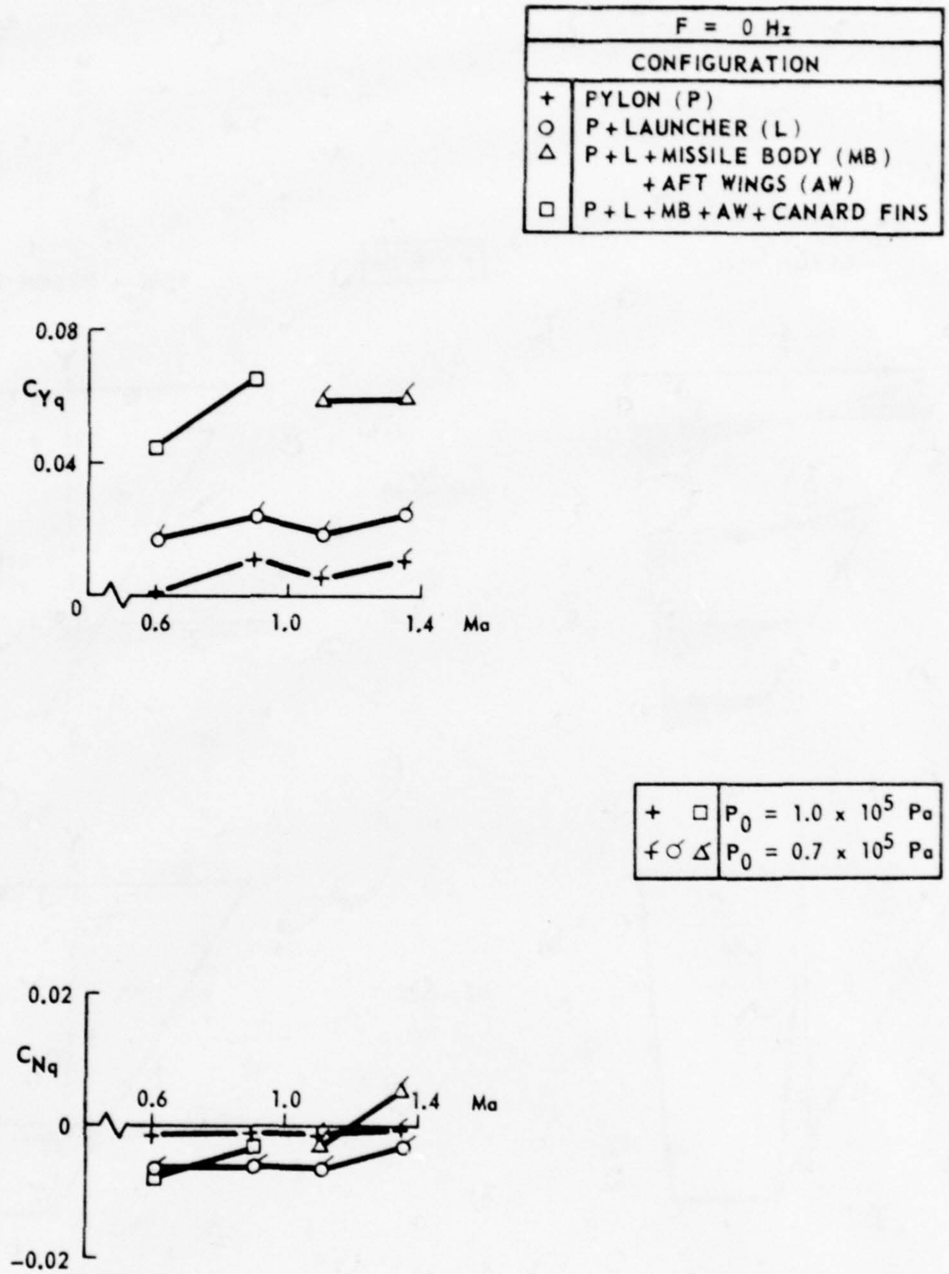

Fig. 6 Quasi-steady side force and yawing moment on the pylon and store for various configurations

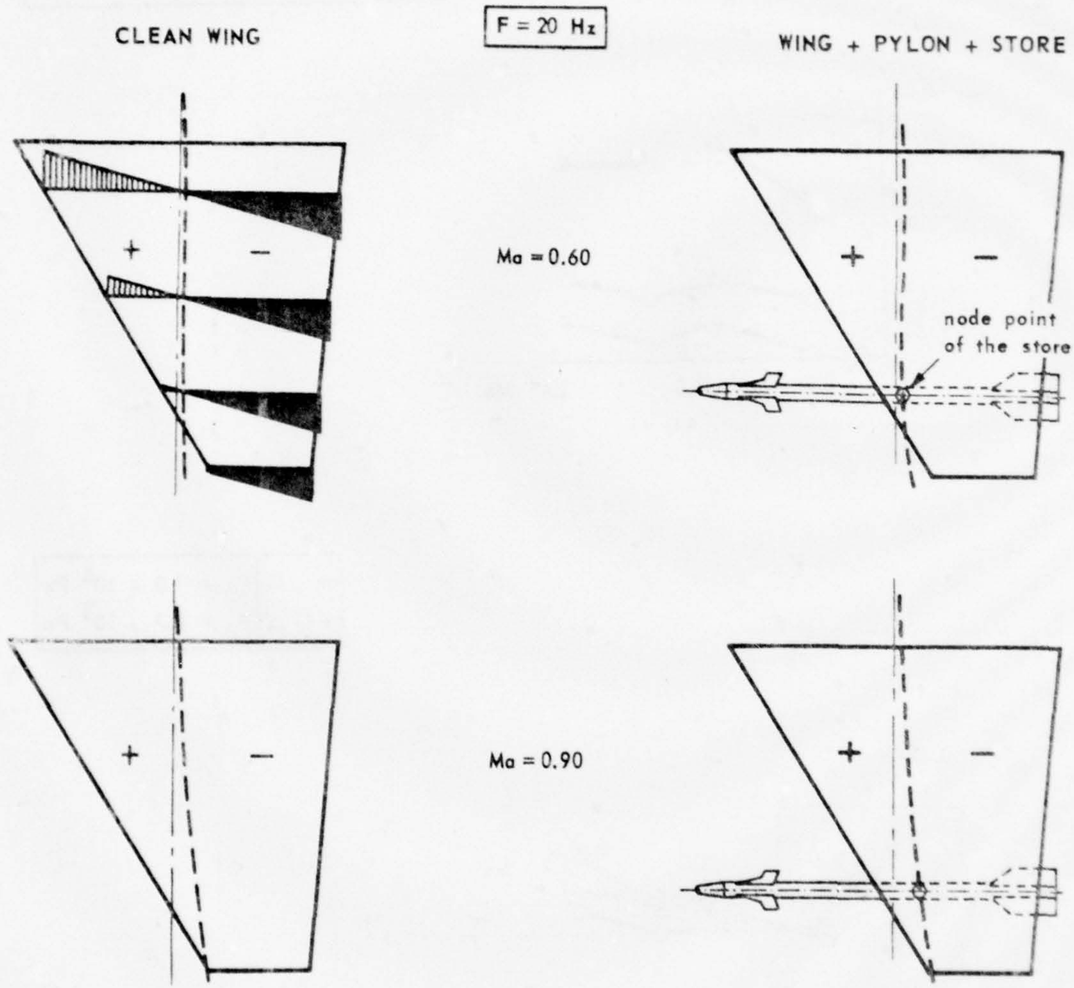

Fig. 7a In-wind vibration modes of the clean wing and the wing with pylon and complete store

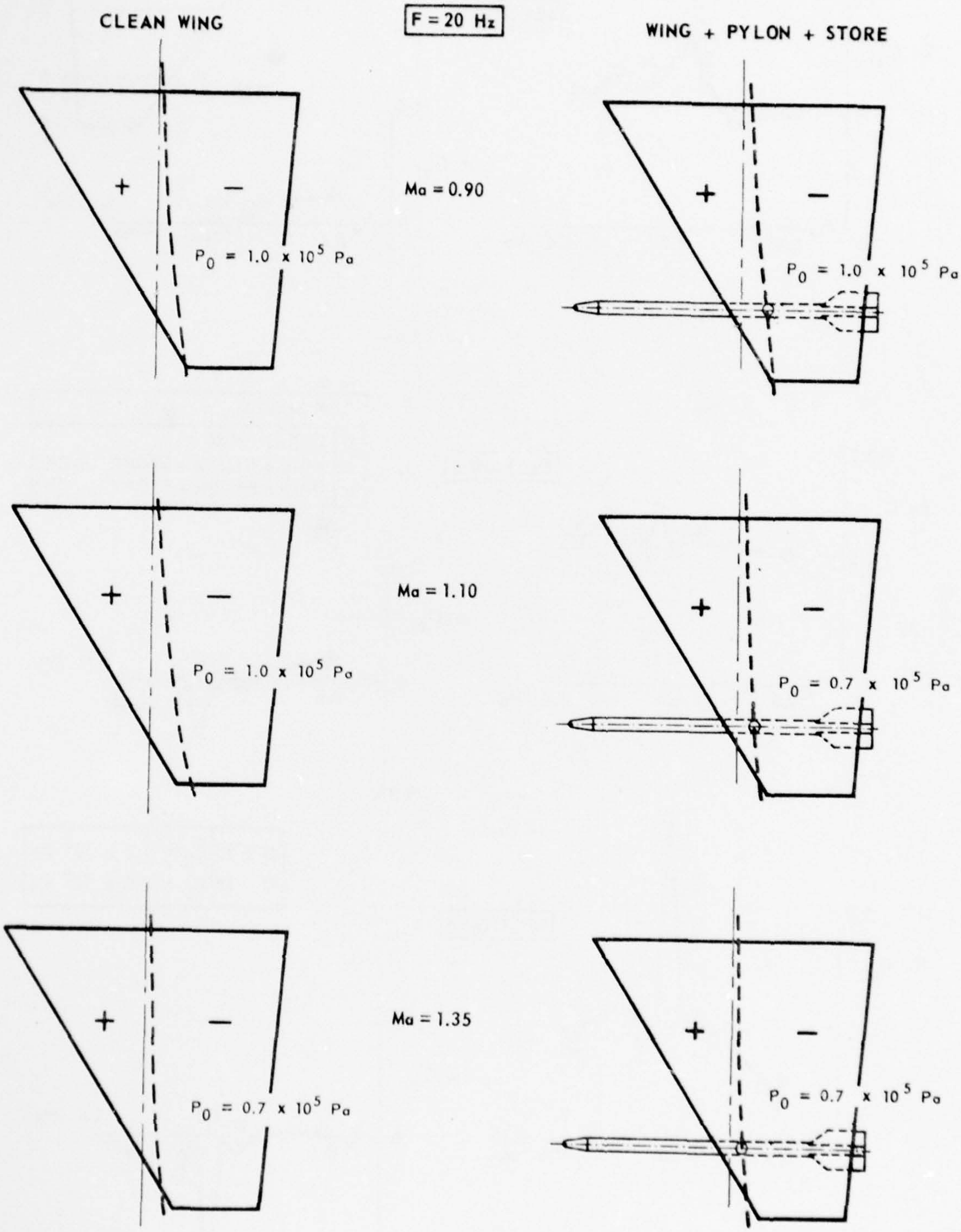

Fig. 7b In-wind vibration modes of the clean wing and the wing with pylon and store without canard fins

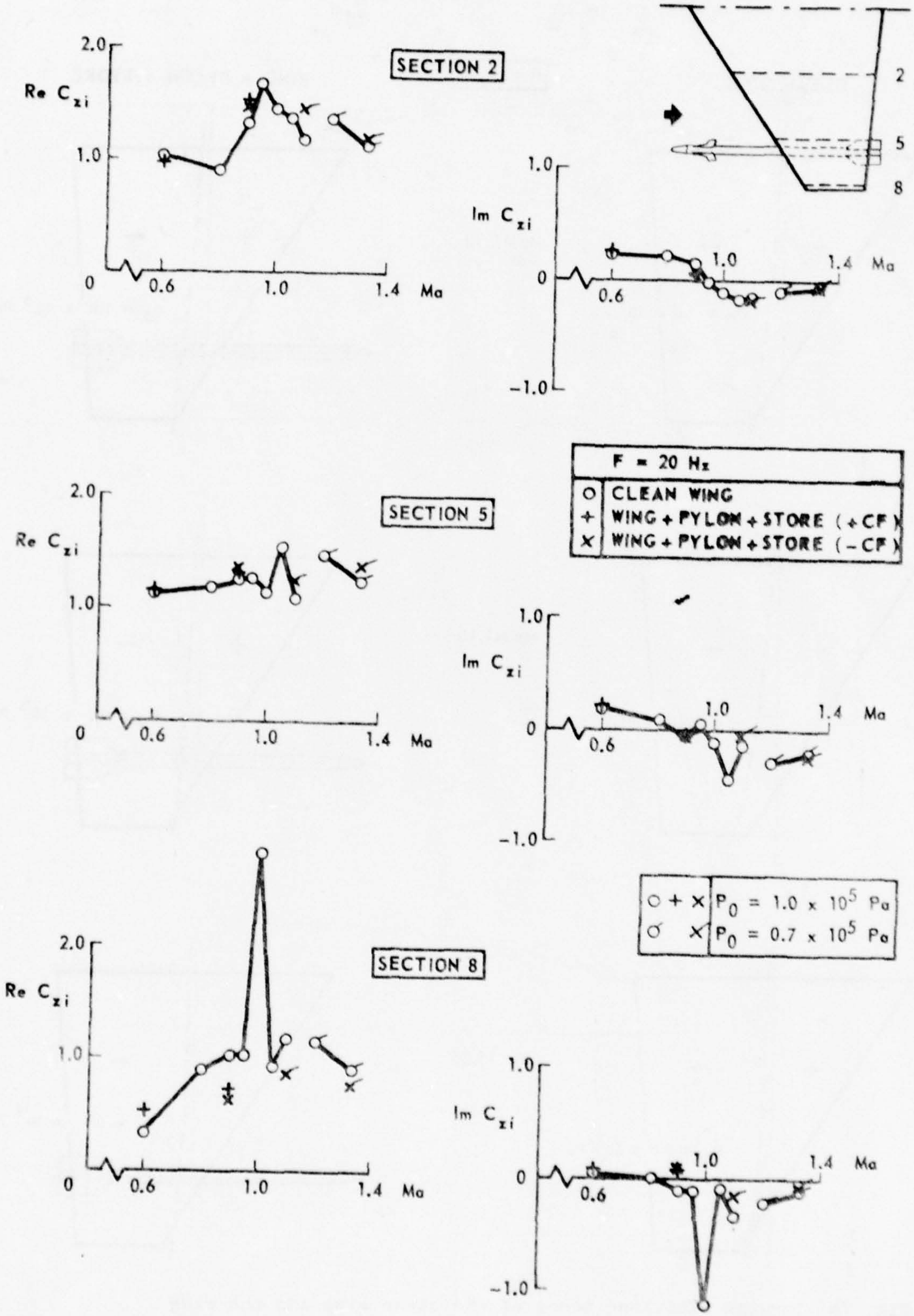

Fig. 8 Sectional unsteady normal load distribution on the clean wing and on the wing with pylon and store versus Mach number

Ma = 0.6	EXP.	RUN	CONFIGURATION
F = 20 Hz	O	382	CLEAN WING
K = 0.2	+	43	WING + PYLON + STORE (+ CF)

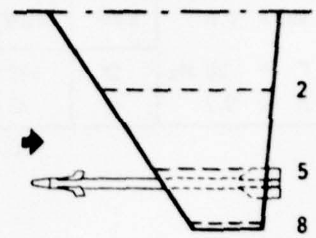

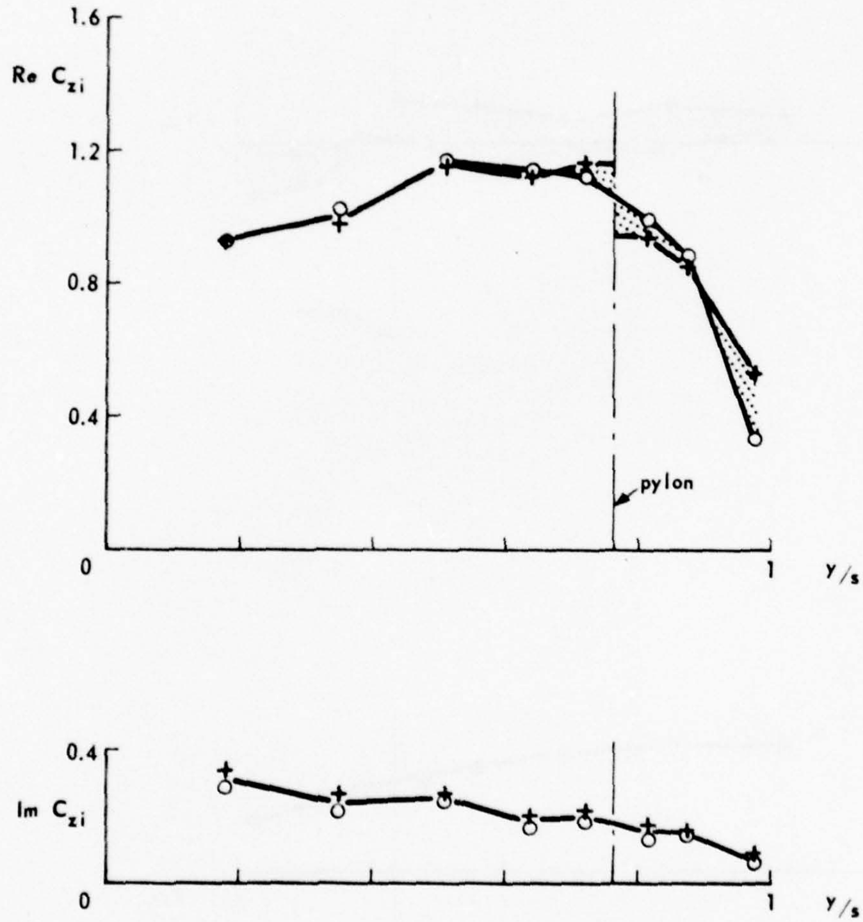

Fig. 9a Unsteady spanwise normal load distributions on the clean wing and on the wing with pylon and store at Ma = 0.6

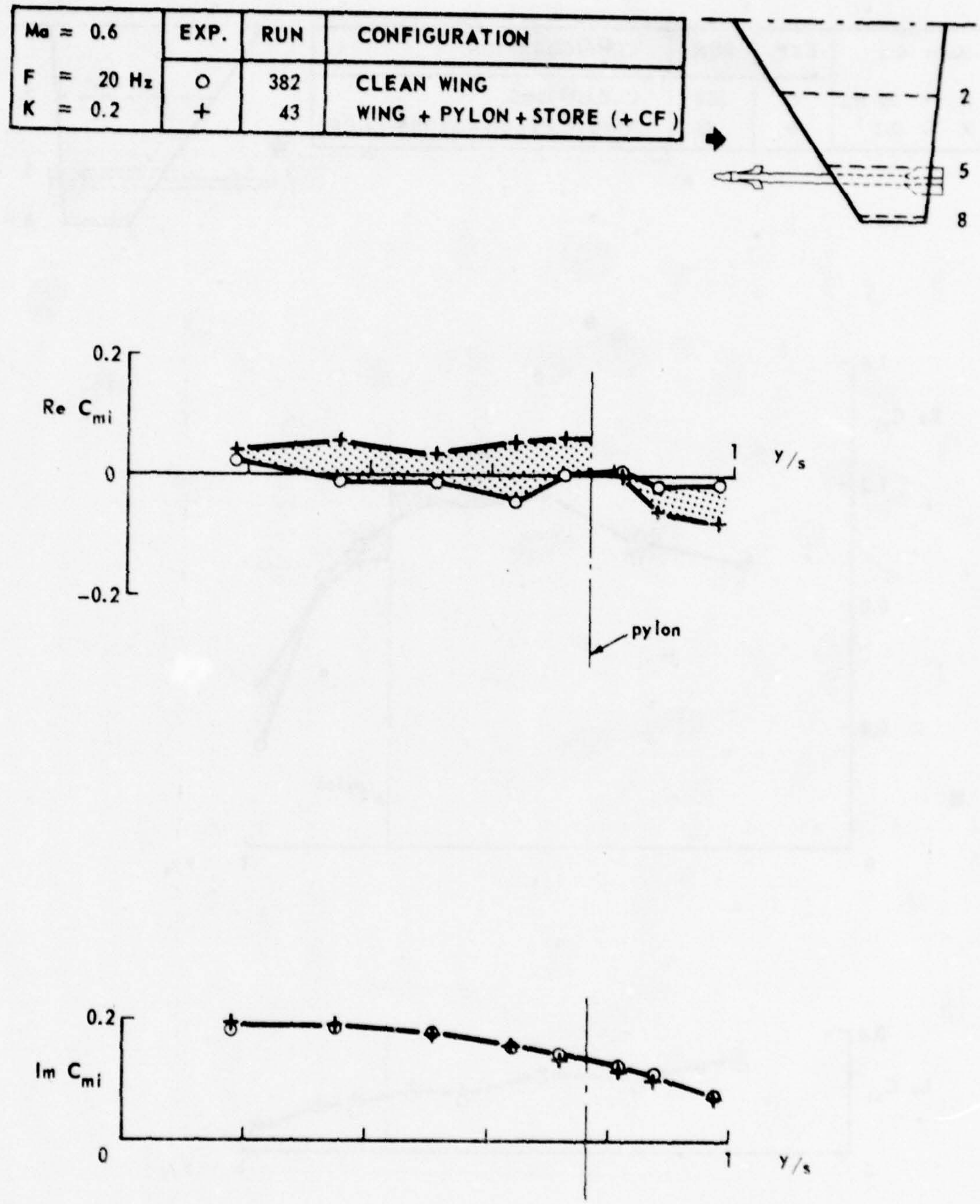

Fig. 9b Unsteady spanwise pitching moment distributions on the clean wing and on the wing with pylon and store at Ma = 0.6

Ma = 0.9	EXP.	RUN	CONFIGURATION
F = 20 Hz	o	369	CLEAN WING
K = 0.14	+	48	WING + PYLON + STORE (+ CF)
	x	88	WING + PYLON + STORE (− CF)

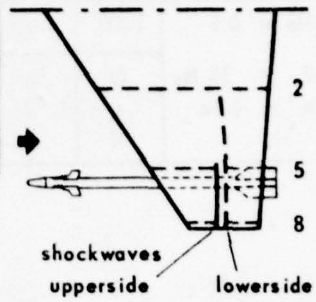

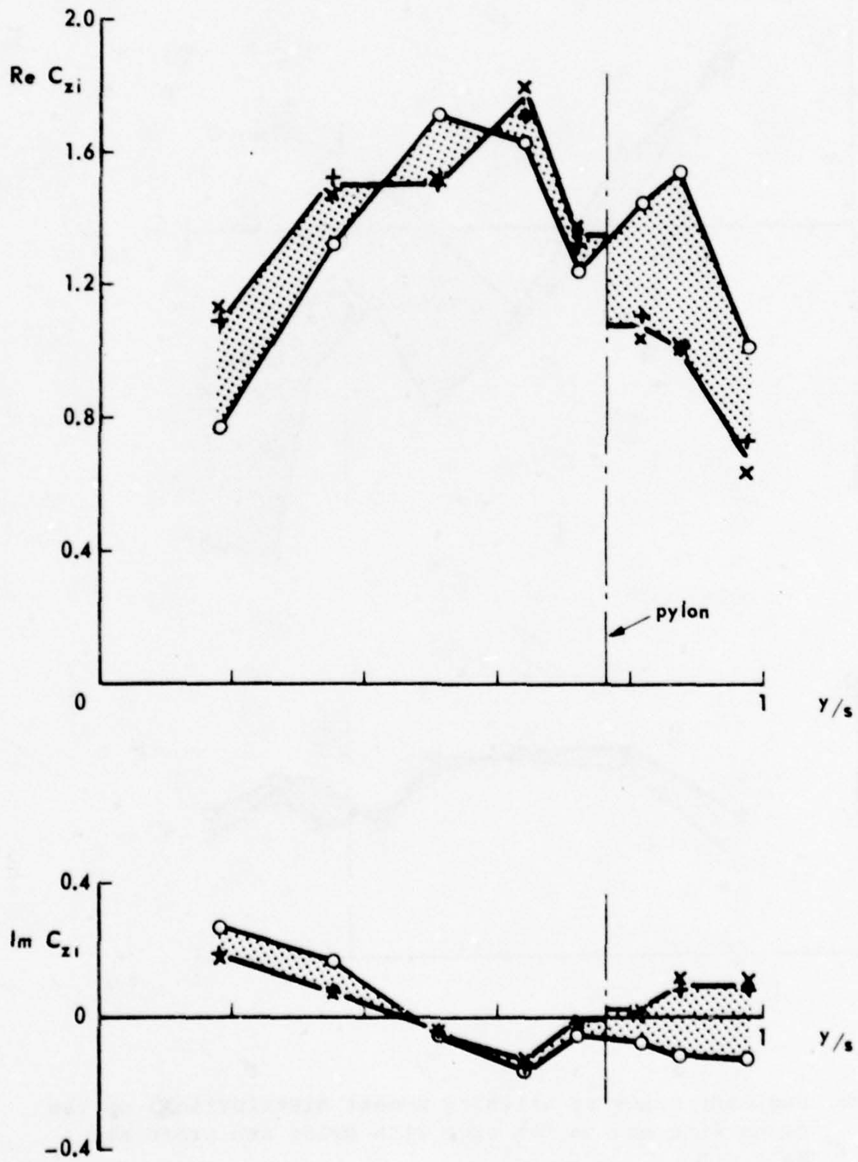

Fig. 10a Unsteady spanwise normal load distributions on the clean wing and on the wing with pylon and store at Ma = 0.9

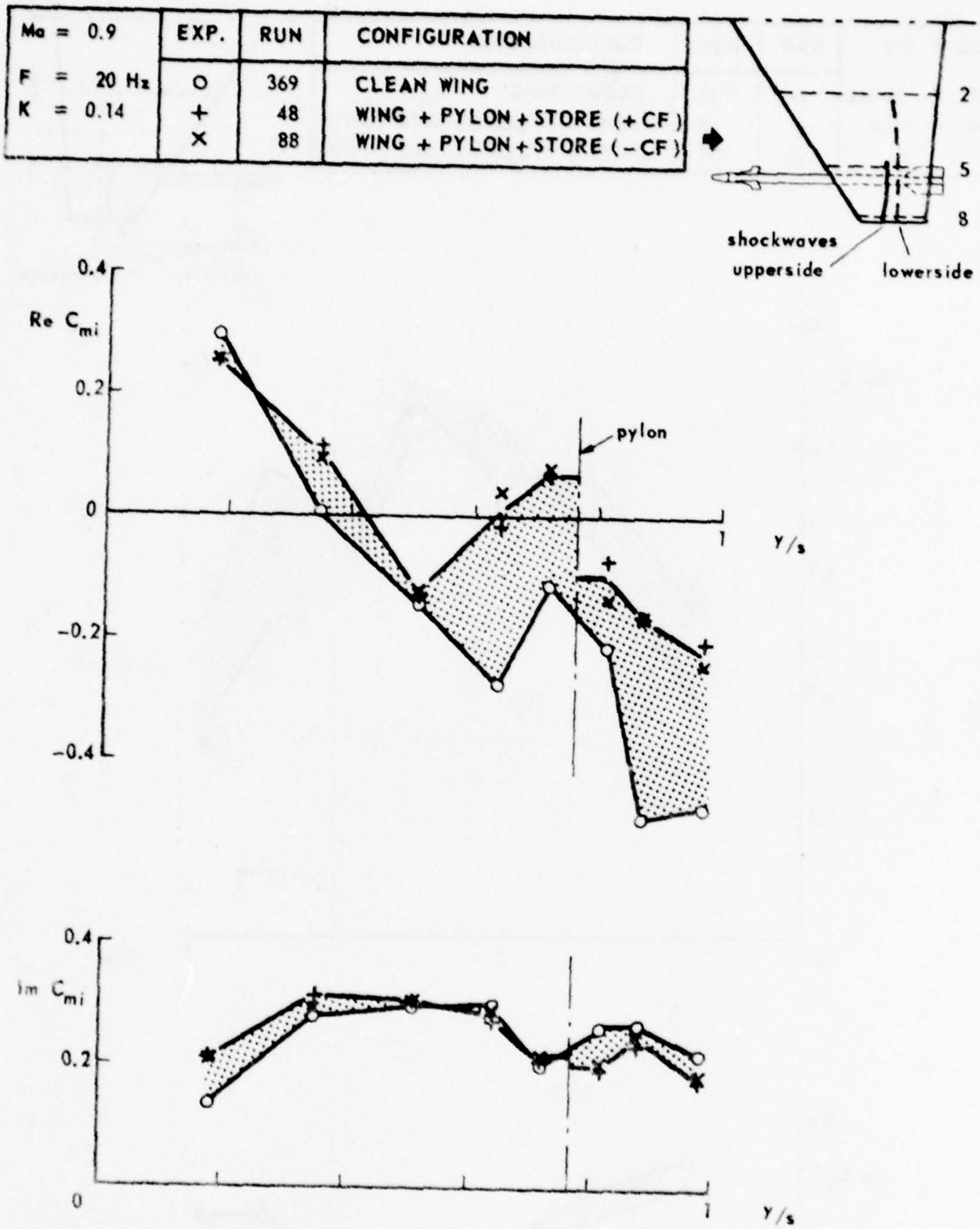

Fig. 10b Unsteady spanwise pitching moment distributions on the clean wing and on the wing with pylon and store at Ma = 0.9

Ma = 1.35	EXP.	RUN	CONFIGURATION
F = 20 Hz	O	192	CLEAN WING
K = 0.1	+	97	WING + PYLON + STORE (– CF)

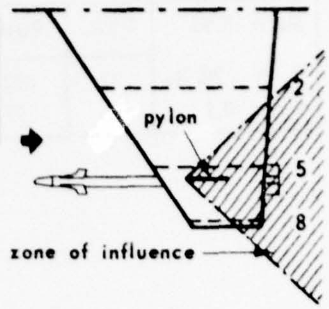

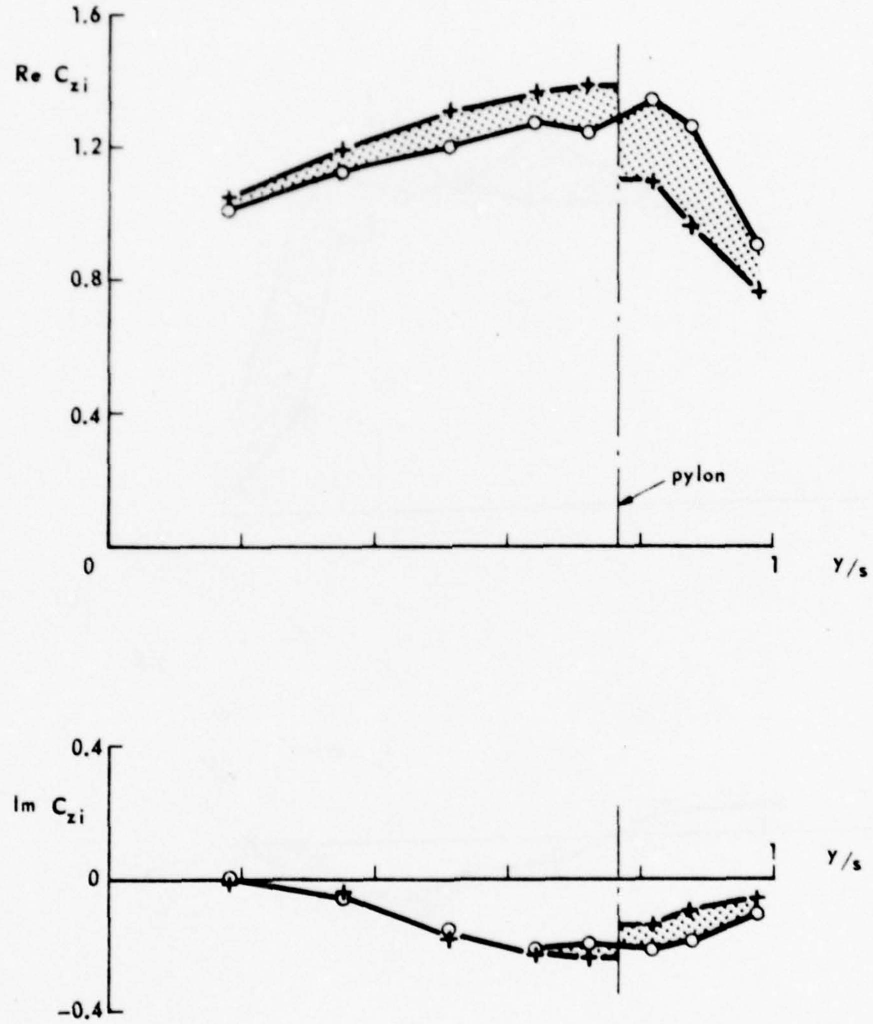

Fig. 11a Unsteady spanwise normal load distributions on the clean wing and on the wing with pylon and store at Ma = 1.35

Ma = 1.35	EXP.	RUN	CONFIGURATION
F = 20 Hz	O	192	CLEAN WING
K = 0.1	+	97	WING + PYLON + STORE (– CF)

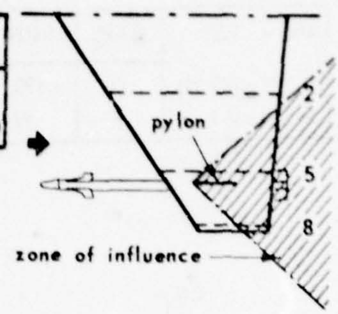

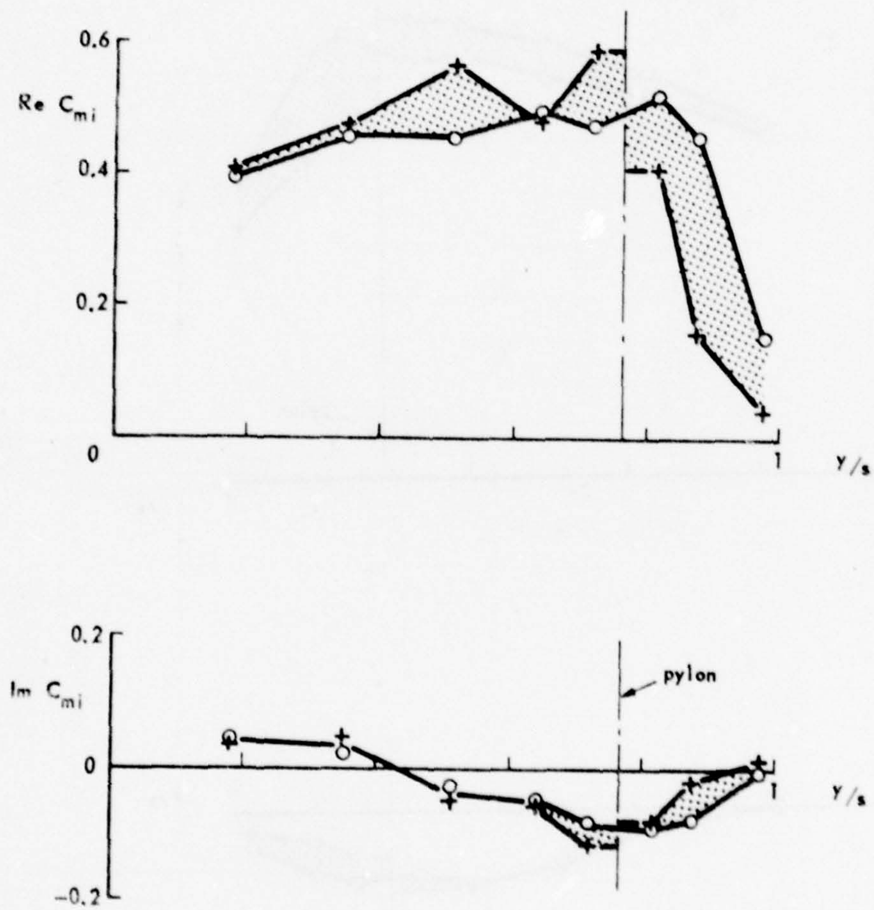

Fig. 11b Unsteady spanwise pitching moment distributions on the clean wing and on the wing with pylon and store at Ma = 1.35

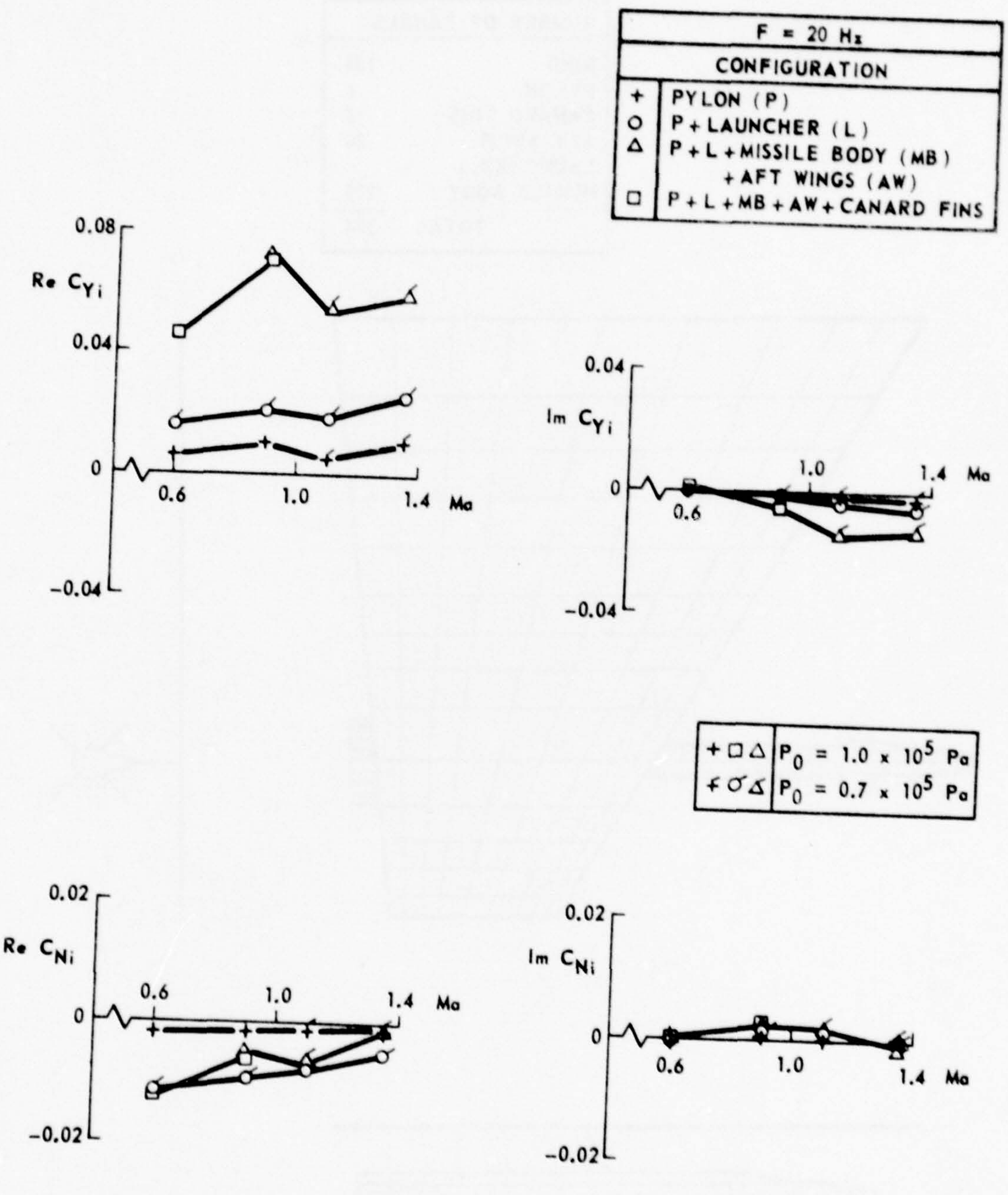

Fig. 12 Unsteady side force and yawing moment on the pylon and store for various configurations

NUMBER OF PANELS	
WING	126
PYLON	6
CANARD FINS	16
AFT WINGS	36
LAUNCHER + MISSILE BODY	210
TOTAL	394

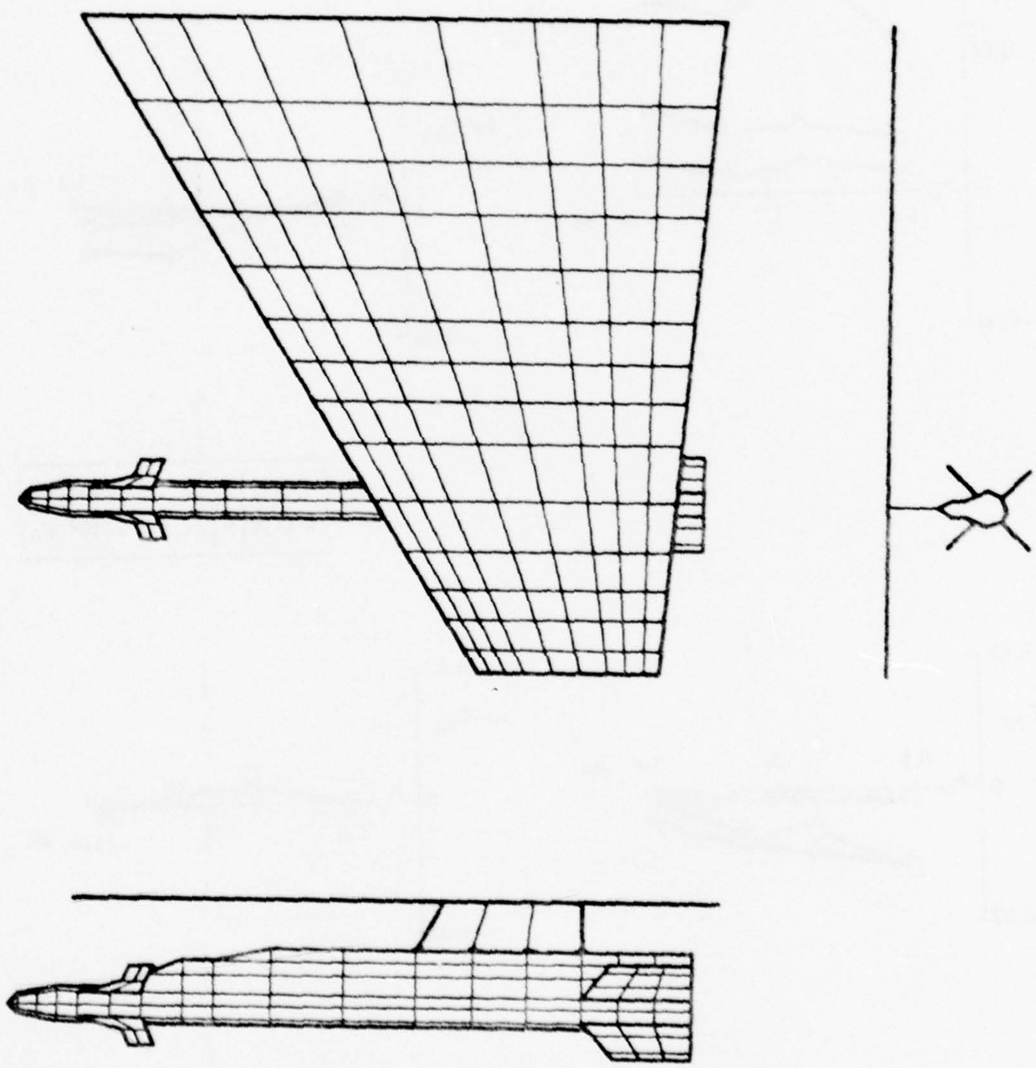

Fig. 13 Panel distribution used in the calculations with the "NLRI" method

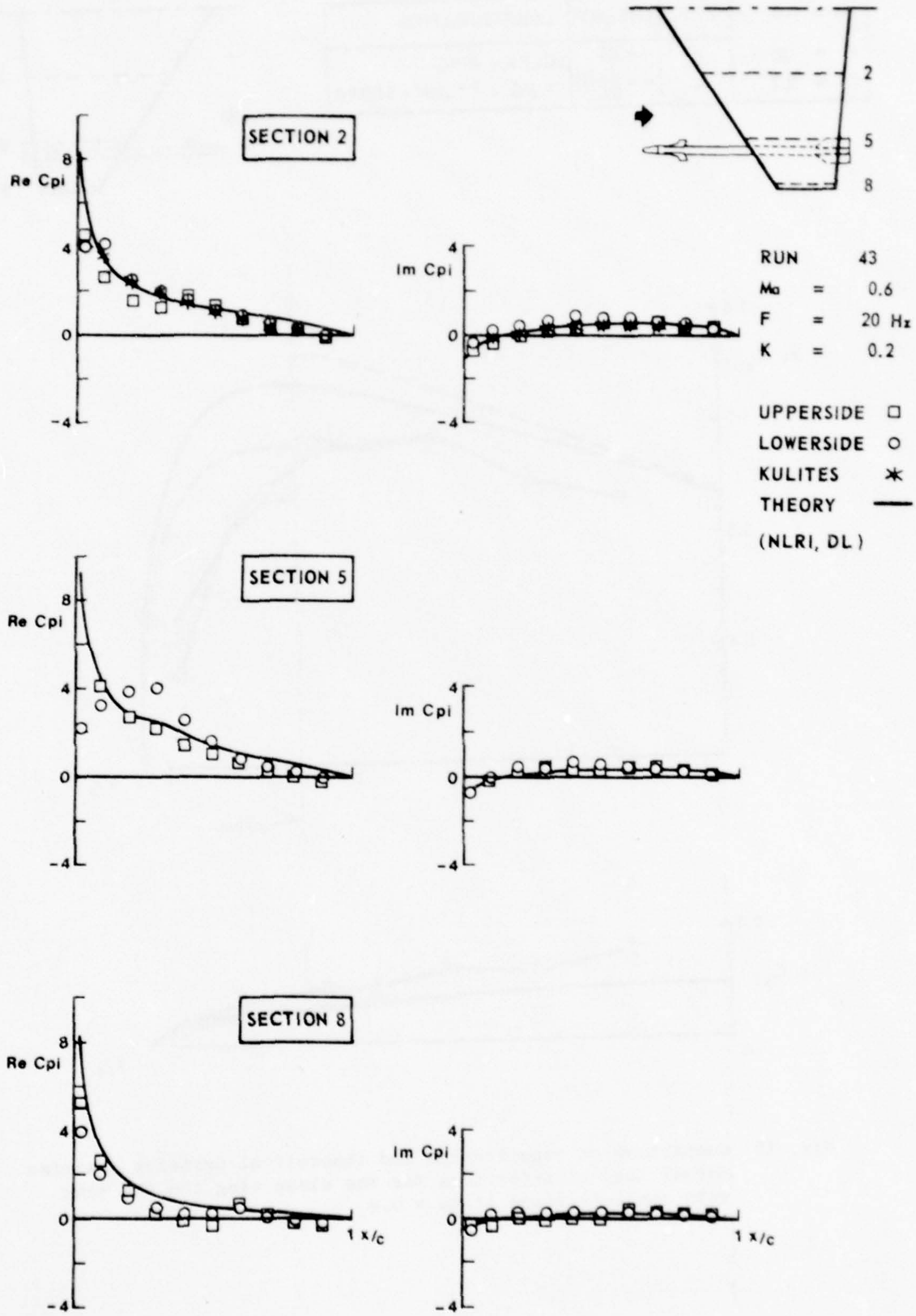

Fig. 14 Comparison of experimental and theoretical unsteady pressure distributions on the wing with complete tipstore at Ma = 0.6

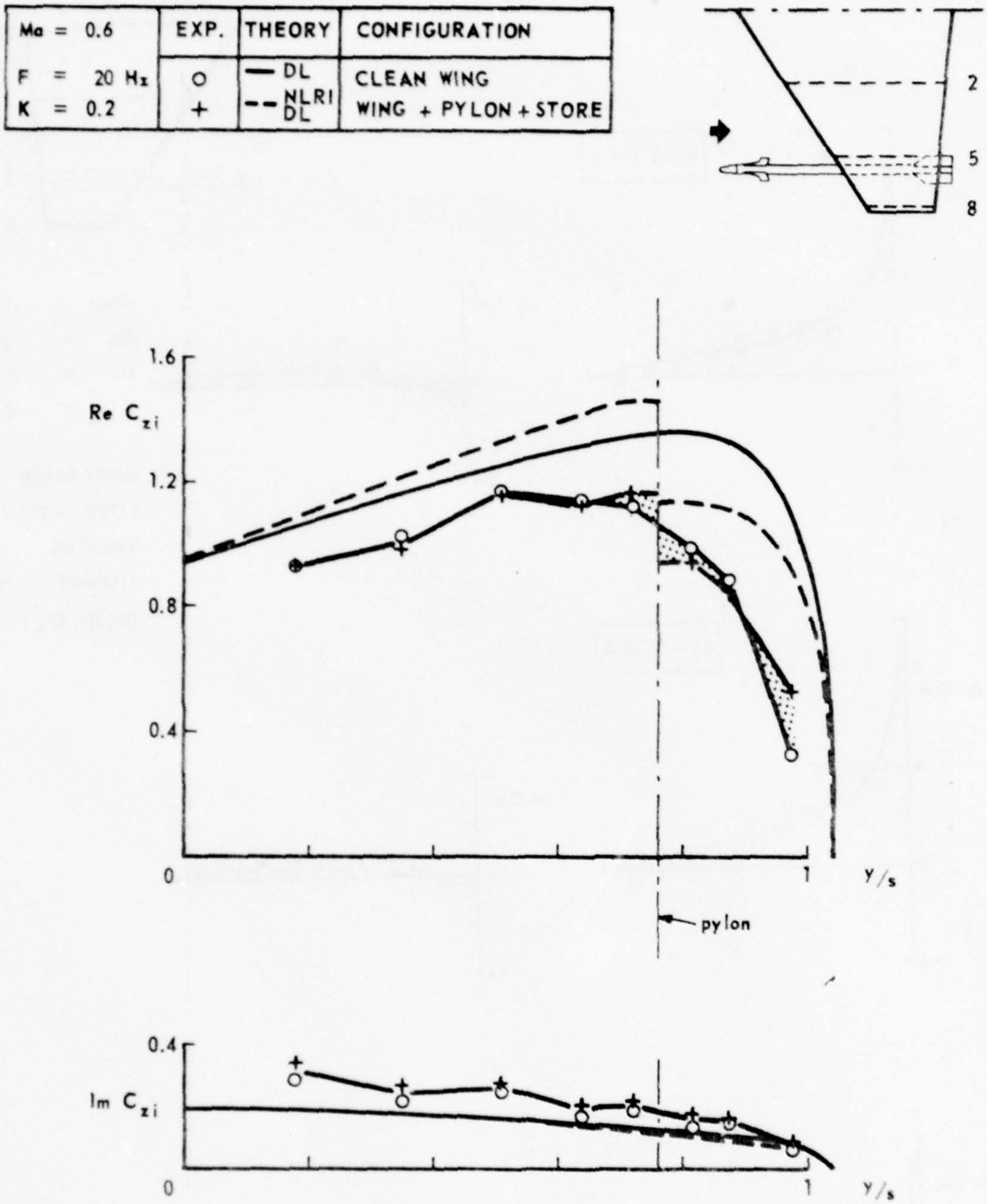

Fig. 15 Comparison of experimental and theoretical unsteady spanwise normal load distributions for the clean wing and the wing with complete store at Ma = 0.6

NUMBER OF PANELS	
WING	126
PYLON	6
CANARD FINS	24
AFT WINGS	48
LAUNCHER + MISSILE BODY	40
TOTAL	244

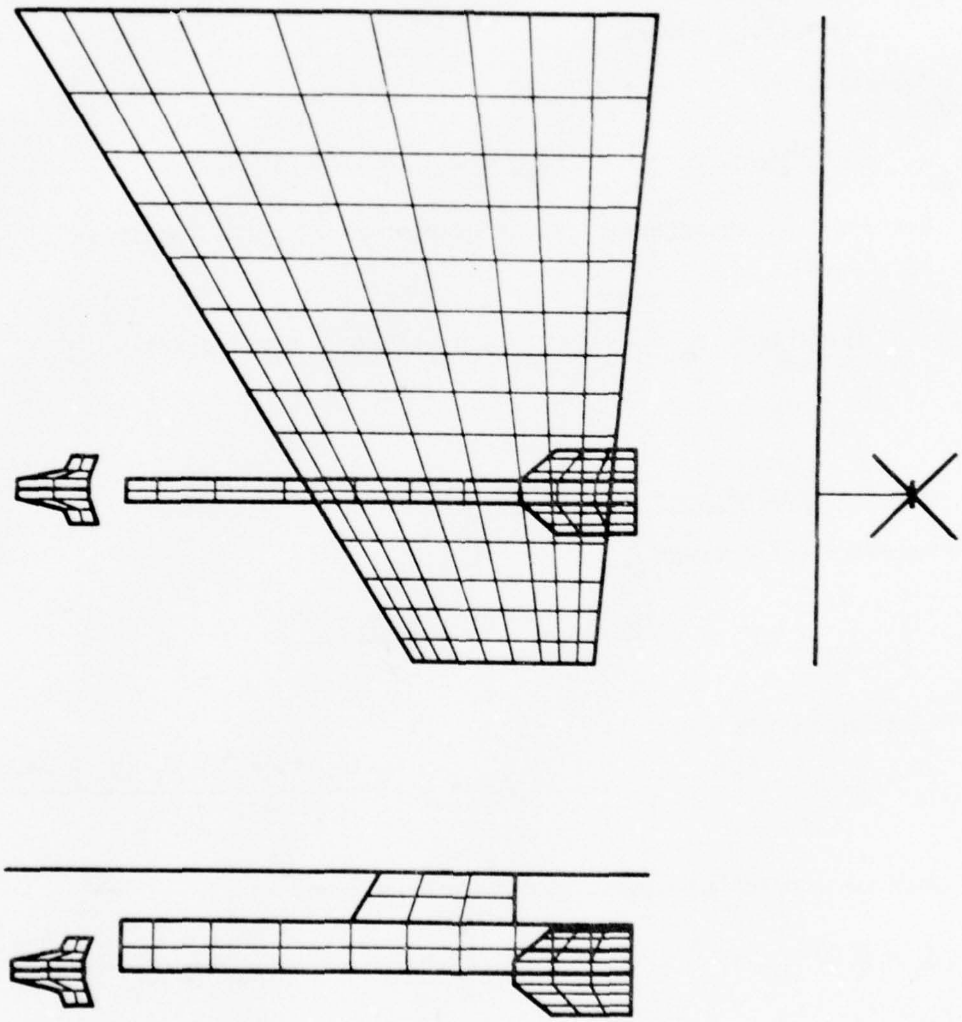

Fig. 16 Panel distribution used in the calculations with the Doublet Lattice method

APPENDIX IV.A.

Definitions of Steady and Unsteady Aerodynamic Quantities*)

THE WING

Steady

Pressure coefficient C_p :

$$C_p = (P_{loc} - P)/Q \quad .$$

Sectional normal force :

$$Z = C_z QC \ , \ C_z = - \int_o^1 (C_{p+} - C_{p-}) \ d(x/C) \quad .$$

Sectional pitching moment about quarter chord point (positive nose down) :

$$M = C_m QC^2, \ C_m = - \int_o^1 (C_{p+} - C_{p-}) \ (x/C - 0.25) \ d(x/C) \quad .$$

Quasi-steady at zero incidence $(\omega = 0; \alpha_o = 0^o)$

Pressure coefficient C_{pq} :

$$C_{pq} = \Delta C_p/\Delta\alpha = \frac{C_p(\alpha_o + \Delta\alpha_1) - C_p(\alpha_o - \Delta\alpha_2)}{\Delta\alpha_1 + \Delta\alpha_2} \quad .$$

Sectional normal force :

$$Z_q = \pi QCC_{zq}\theta e^{i\omega t} \ , \ C_{zq} = \frac{1}{\pi} \Delta C_z/\Delta\alpha = \frac{1}{\pi} \frac{C_z(\alpha_o + \Delta\alpha_1) - C_z(\alpha_o - \Delta\alpha_2)}{\Delta\alpha_1 + \Delta\alpha_2} \quad .$$

Sectional pitching moment (positive nose down) :

$$M_q = \frac{\pi}{2} QC^2 C_{mq}\theta e^{i\omega t} \ , \ C_{mq} = \frac{2}{\pi} \Delta C_m/\Delta\alpha = \frac{2}{\pi} \frac{C_m(\alpha_o + \Delta\alpha_1) - C_m(\alpha_o - \Delta\alpha_2)}{\Delta\alpha_1 + \Delta\alpha_2} \quad .$$

---

*) The definitions for the unsteady aerodynamic quantities are according to the AGARD manual on Aeroelasticity vol. VI (Ref. 6).

Unsteady

Pressure coefficient C_{pi} :

$$C_{pi} = ReC_{pi} + iImC_{pi} = P_i/Q \quad .$$

Sectional normal force :

$$Z_i = \pi QCC_{zi}\theta e^{i\omega t} \; , \; C_{zi} = ReC_{zi} + iImC_{zi} = -\frac{1}{\pi} \int_o^1 (C_{pi+} - C_{pi-}) \, d(x/C) \quad .$$

Sectional pitching moment about quarter chord point (positive nose down) :

$$M_i = \frac{\pi}{2} QC^2 \, C_{mi}\theta e^{i\omega t} \; ,$$

$$C_{mi} = ReC_{mi} + iImC_{mi} = -\frac{2}{\pi} \int_o^1 (C_{pi+} - C_{pi-}) \, (x/C - 0.25) \, d(x/C) \quad .$$

THE PYLON AND STORE

Steady

Normal force :

$$Z = C_Z Q\bar{C}S \quad .$$

Side force (positive outward) :

$$Y = C_Y Q\bar{C}S \quad .$$

Pitching moment about balance centre (positive nose up) :

$$M = C_M Q\bar{C}^2 S \quad .$$

Yawing moment about balance centre (positive nose inward) :

$$N = C_N Q\bar{C}^2 S \quad .$$

Quasi-steady at zero incidence ($\omega = 0$; $\alpha_o = 0^o$)

Normal force :

$$Z_q = \pi Q\bar{C}SC_{Zq}\theta e^{i\omega t} \ ,$$

$$C_{Zq} = \frac{1}{\pi} \Delta C_Z/\Delta\alpha = \frac{1}{\pi} \frac{C_Z(\alpha_o + \Delta\alpha_1) - C_Z(\alpha_o - \Delta\alpha_2)}{\Delta\alpha_1 + \Delta\alpha_2} \ .$$

Side force (positive outward) :

$$Y_q = \pi Q\bar{C}SC_{Yq}\theta e^{i\omega t}$$

$$C_{Yq} = \frac{1}{\pi} \Delta C_Y/\Delta\alpha = \frac{1}{\pi} \frac{C_Y(\alpha_o + \Delta\alpha_1) - C_Y(\alpha_o - \Delta\alpha_2)}{\Delta\alpha_1 + \Delta\alpha_2} \ .$$

Pitching moment about balance centre (positive nose up) :

$$M_q = \frac{\pi}{2} Q\bar{C}^2SC_{Mq}\theta e^{i\omega t}$$

$$C_{Mq} = \frac{2}{\pi} \Delta C_M/\Delta\alpha = \frac{2}{\pi} \frac{C_M(\alpha_o + \Delta\alpha_1) - C_M(\alpha_o - \Delta\alpha_2)}{\Delta\alpha_1 + \Delta\alpha_2} \ .$$

Yawing moment about balance centre (positive nose inward) :

$$N_q = \frac{\pi}{2} Q\bar{C}^2SC_{Nq}\theta e^{i\omega t}$$

$$C_{Nq} = \frac{2}{\pi} \Delta C_N/\Delta\alpha = \frac{2}{\pi} \frac{C_N(\alpha_o = \Delta\alpha_1) - C_N(\alpha_o - \Delta\alpha_2)}{\Delta\alpha_1 + \Delta\alpha_2} \ .$$

Unsteady

Normal force :

$$Z_i = \pi Q\bar{C}SC_{Zi}\theta e^{i\omega t} \ , \ C_{Zi} = ReC_{Zi} + iImC_{Zi} \ .$$

Side force (positive outward) :

$$Y_i = \pi Q\bar{C}SC_{Yi}\theta e^{i\omega t} \ , \ C_{Yi} = ReC_{Yi} + iImC_{Yi} \ .$$

Pitching moment about balance centre (positive nose up) :

$$M_i = \frac{\pi}{2} Q\bar{C}^2SC_{Mi}\theta e^{i\omega t} \ , \ C_{Mi} = ReC_{Mi} + iImC_{Mi} \ .$$

Yawing moment about balance centre (positive nose inward) :

$$N_i = \frac{\pi}{2} Q\bar{C}^2SC_{Ni}\theta e^{i\omega t} \ , \ C_{Ni} = ReC_{Ni} + iImC_{Ni} \ .$$

APPENDIX IV.B

Steady Pressure Distributions*)

Wing + Pylon (Conf. 10)

Run. No	Nominal Ma	Nominal α (degrees)	Nominal $P_o \times 10^{-5}$ (Pa)	Fig.No.
125	0.6	-0.5	1.0	IV.B. 1
126		0		2
127		+0.5		3
120	0.9	-0.5		IV.B. 4
121		0		5
122		+0.5		6
116	1.10	-0.5		IV.B. 7
117		0		8
118		+0.5	1.0	9
106	1.10	-0.5	0.7	IV.B.10
107		0		11
108		+0.5		12
101	1.35	-0.5		IV.B.13
102		0	0.7	14

*) Note that in sections 3 and 5 the first point on the upperside showing a zero value is a faulty pressure point, which should not be considered in any evaluation.

Wing + Pylon + Launcher (Conf. 20)

Run No.	Nominal Ma	Nominal α (degrees)	Nominal $P_o \times 10^{-5}$ (Pa)	Fig.No.
54	0.6	-0.5	0.7	IV.B.15
55		0		16
56		+0.5		17
61	0.9	-0.5		IV.B.18
62		0		19
63		+0.5		20
68	1.10	-0.5		IV.B.21
69		0		22
70		+0.5		23
75	1.35	-0.5		IV.B.24
76		0		25
77		+0.5	0.7	26

Wing + Pylon + Launcher + Missile Body + Aft Wings (Conf. 31)

Run No.	Nominal Ma	Nominal α (degrees)	Nominal $P_o \times 10^{-5}$ (Pa)	Fig.No.
89	1.10	-0.5	0.7	IV.B.27
90		0		28
91		+0.5		29
94	1.35	-0.5		IV.B.30
95		0		31
96		+0.5	0.7	32

Wing + Pylon + Launcher + Complete Missile (Conf. 301)

Run No.	Nominal Ma	Nominal α (degrees)	Nominal $P_o \times 10^{-5}$ (Pa)	Fig.No.
40	0.6	-0.5	1.0	IV.B.33
41		0		34
42		+0.5		35
45	0.9	-0.5		IV.B.36
46		0		37
47		+0.5	1.0	38

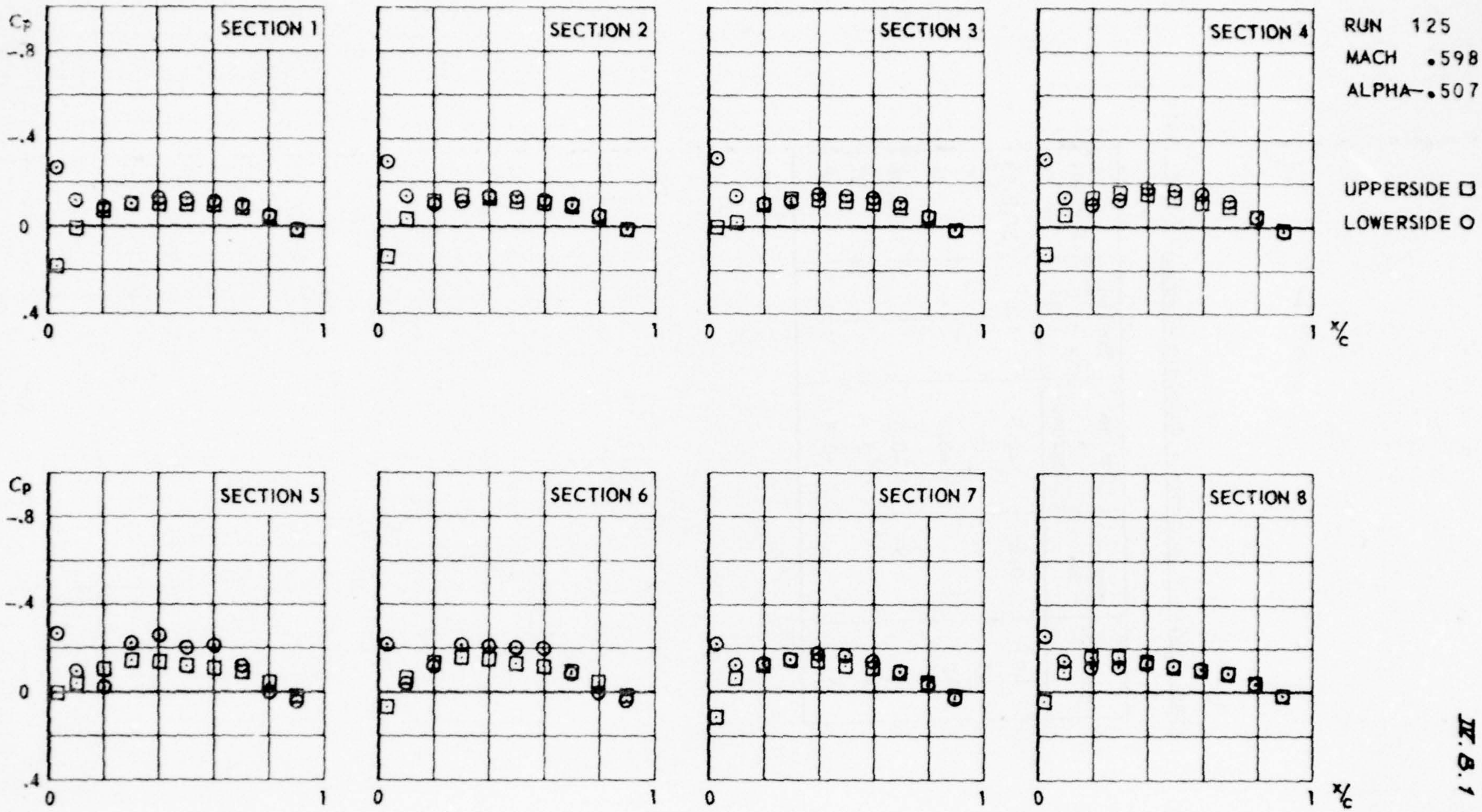

CONF.10 (WING + PYLON)

FIG.
IV.B.1

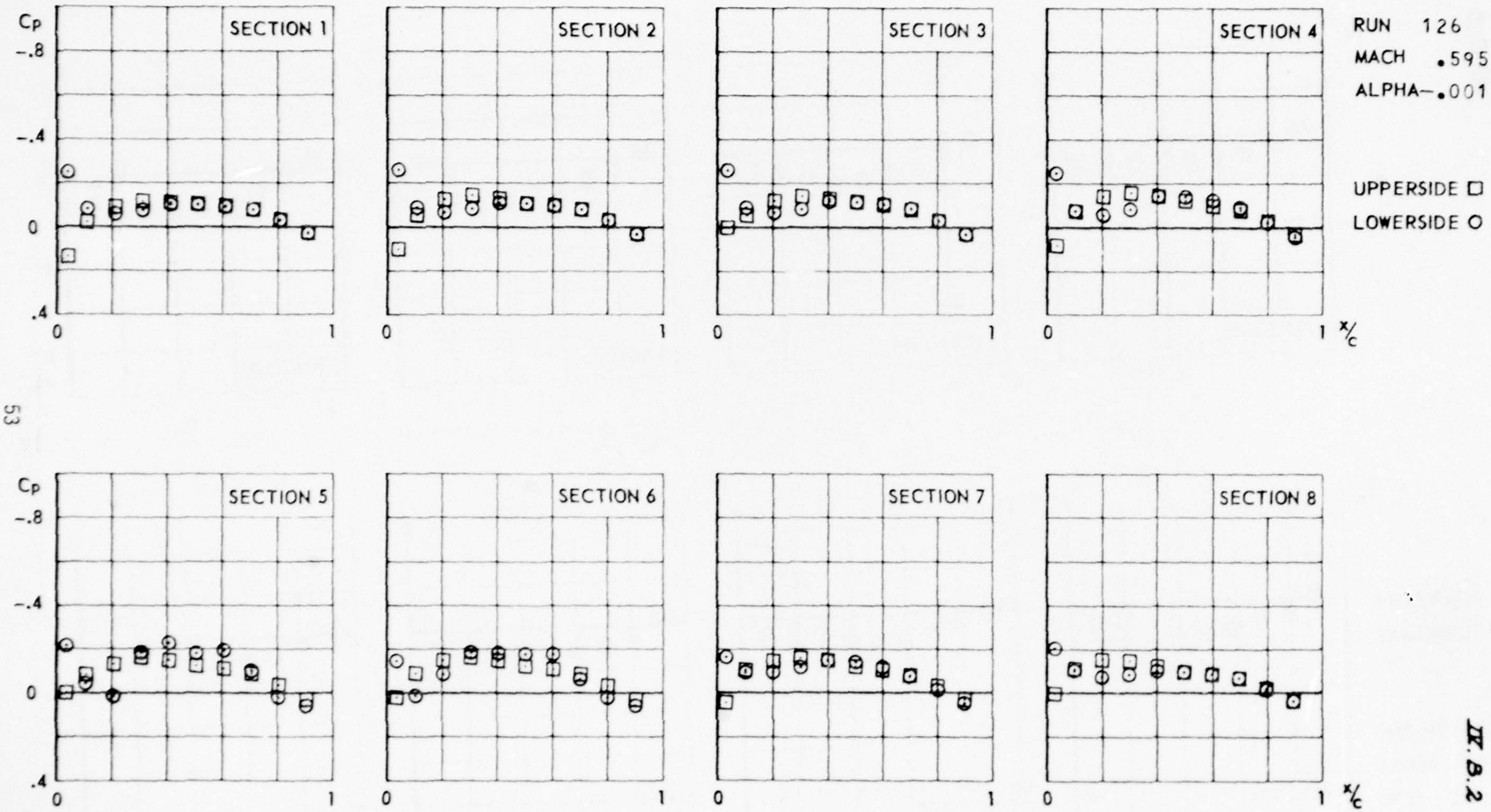

CONF.10 (WING + PYLON)

FIG. IV.B.2

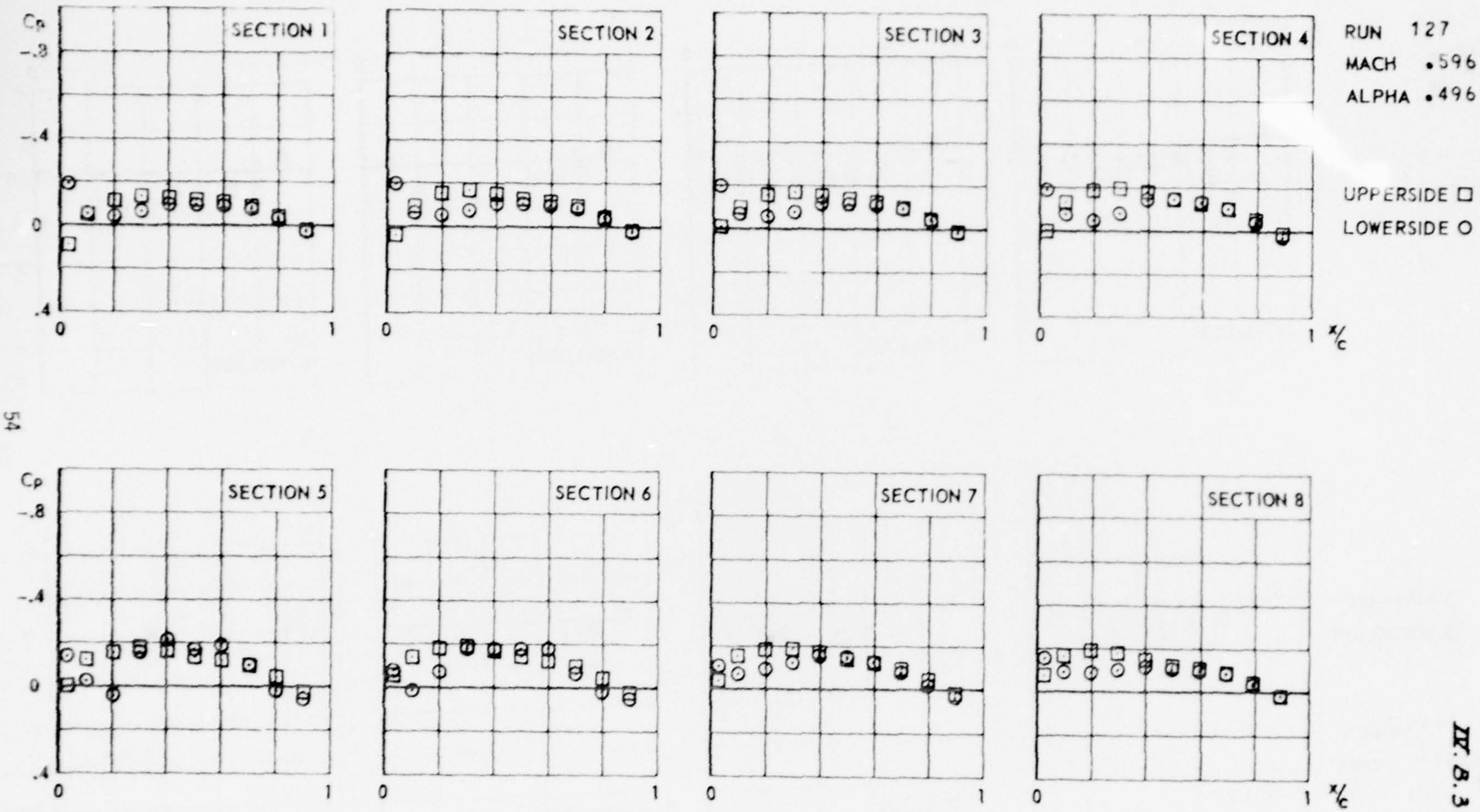

CONF.10 (WING + PYLON)

FIG. IV.B.3

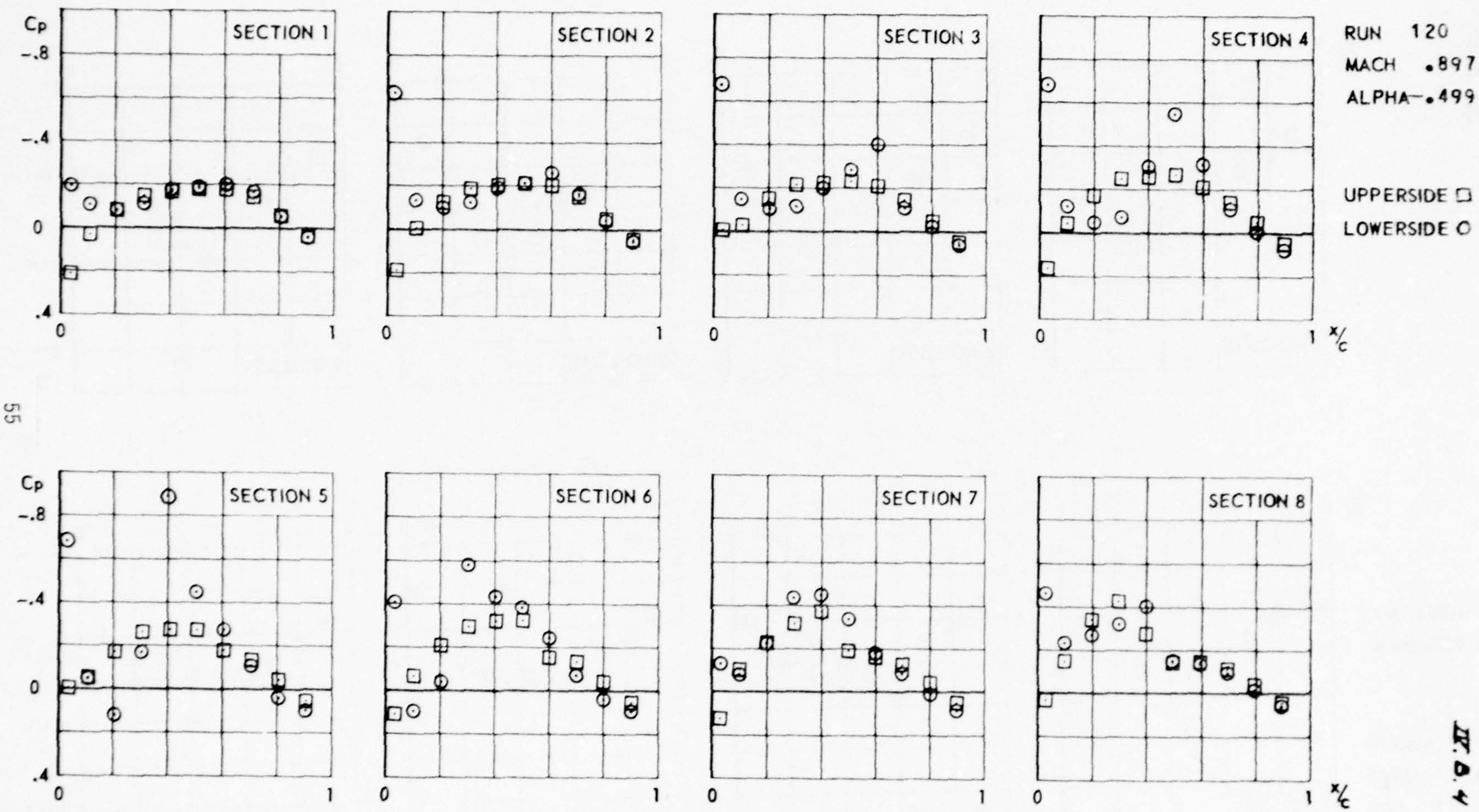

CONF.10 (WING + PYLON)

FIG. IV. B. 4

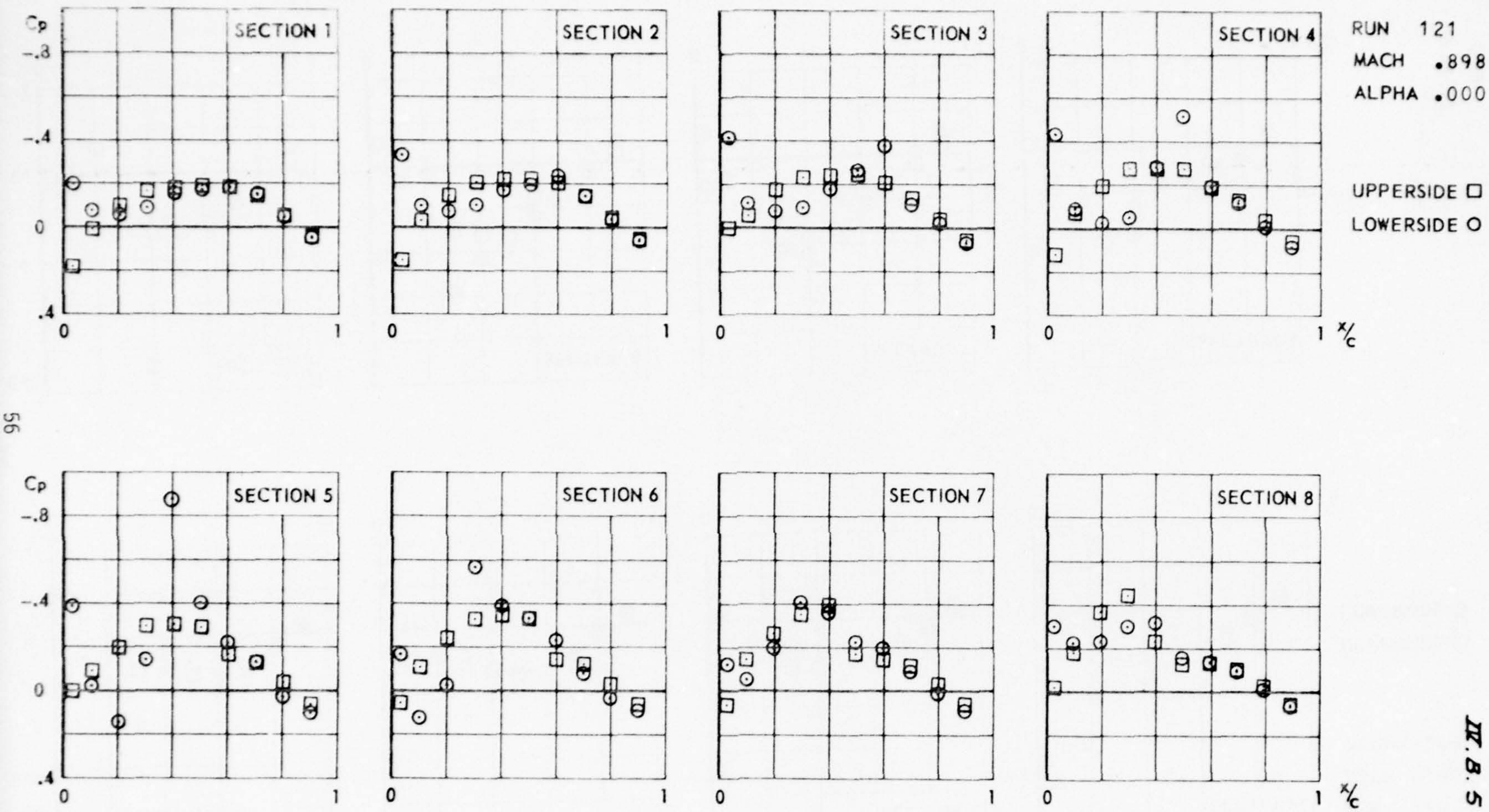

CONF.10 (WING + PYLON)

FIG. IV.B.5

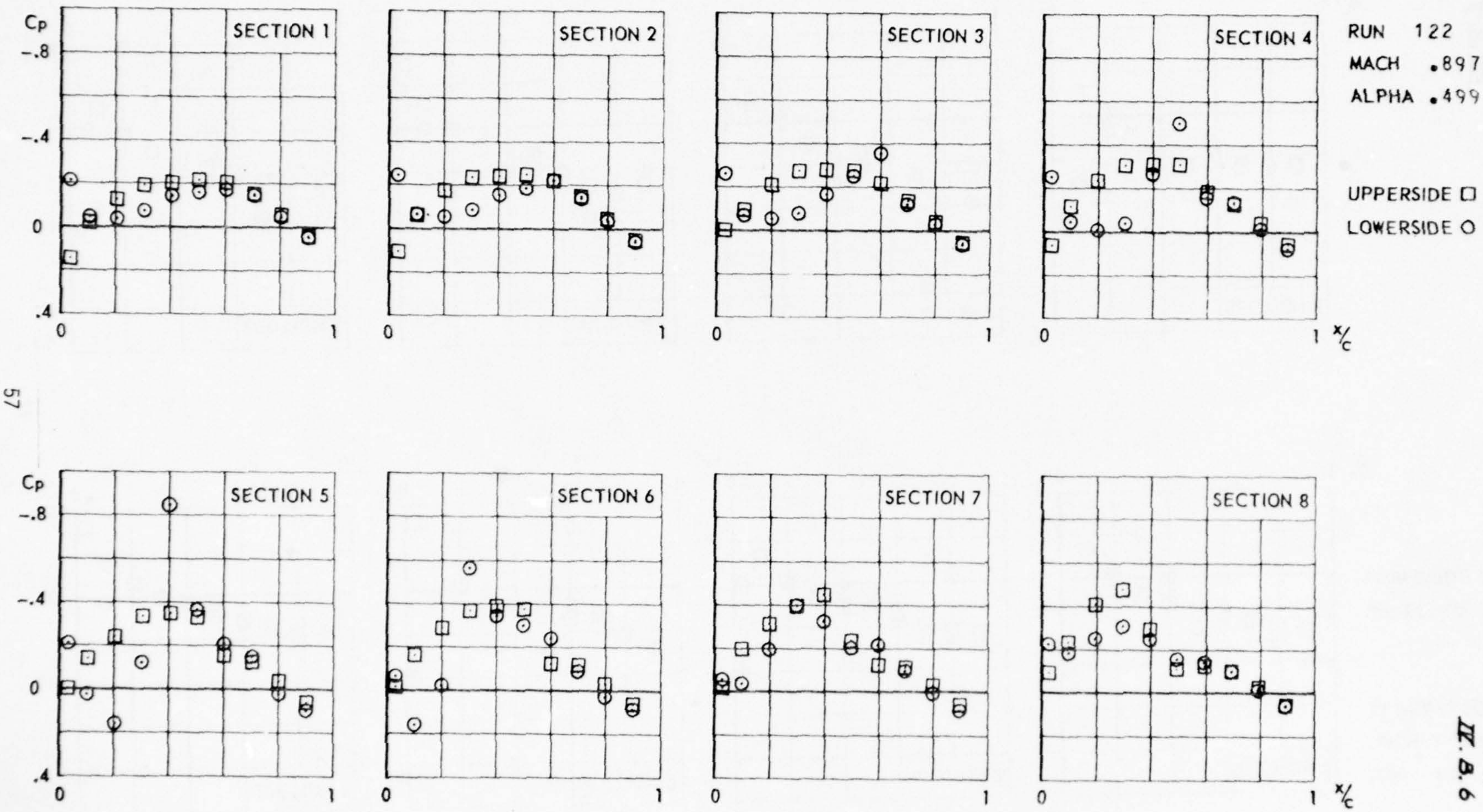

CONF.10 (WING + PYLON)

FIG.
IV.B.6

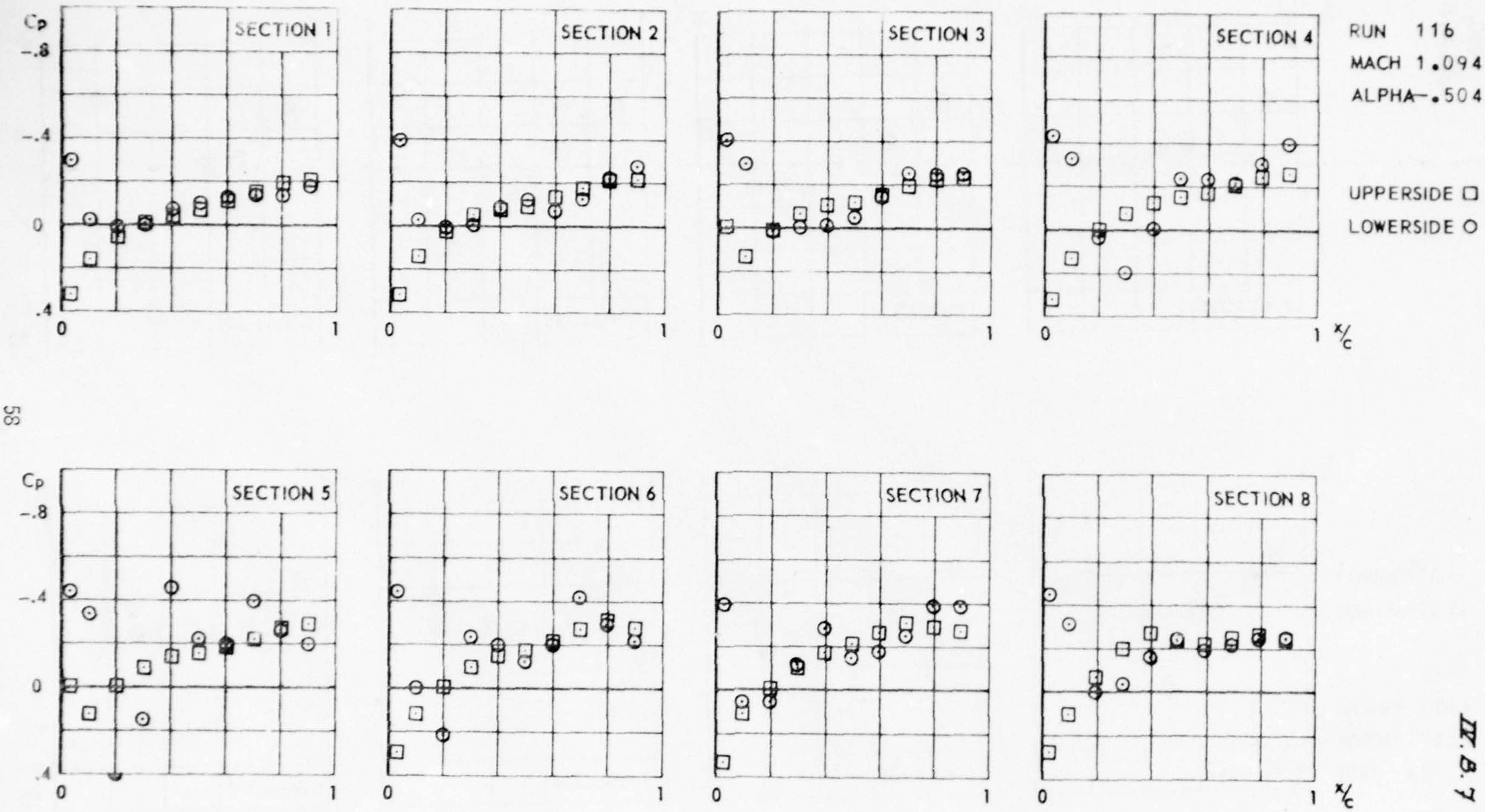

CONF.10 (WING + PYLON)

FIG. IV.B.7

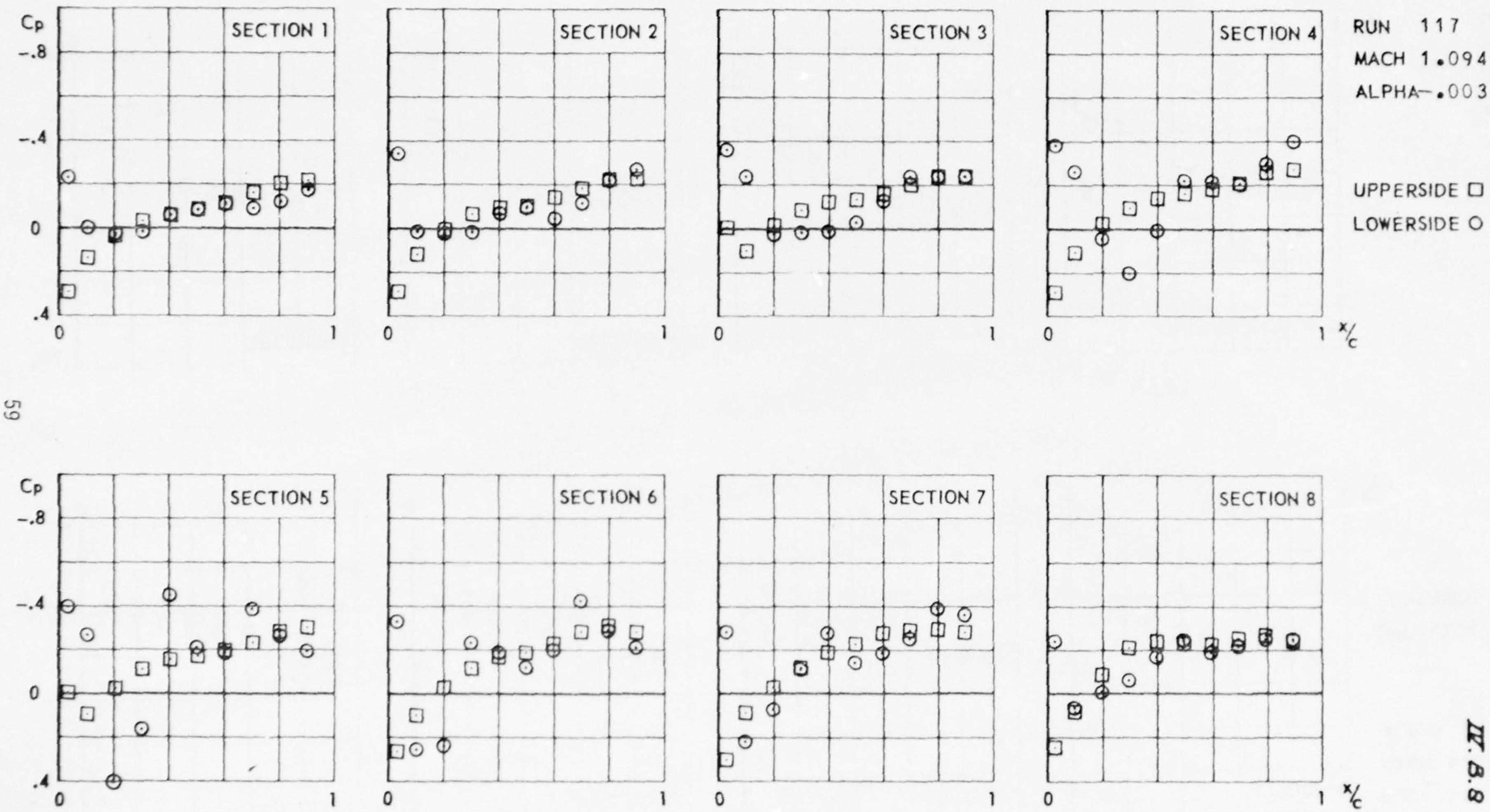

CONF.10 (WING + PYLON)

FIG. IV.B.8

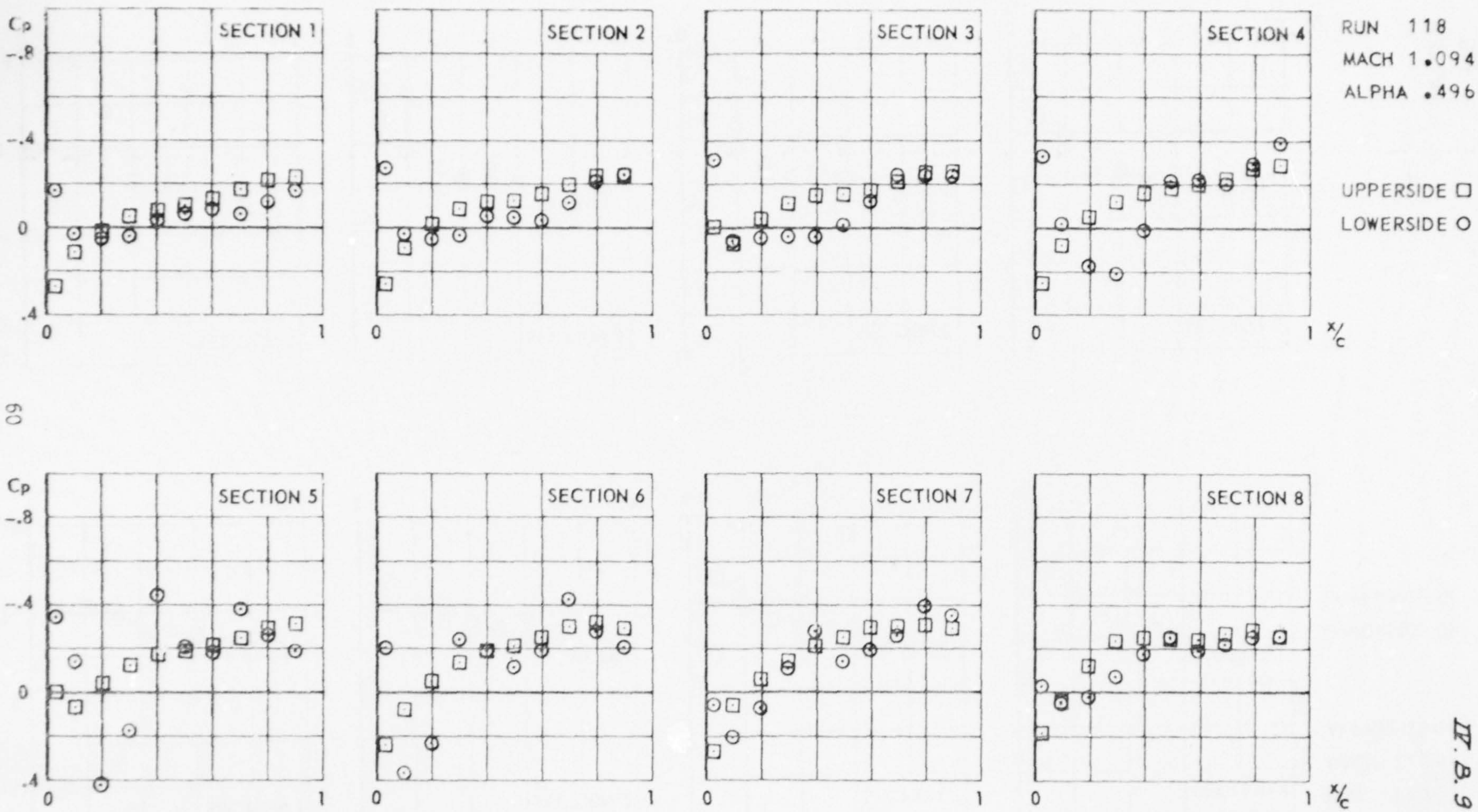

CONF.10 (WING + PYLON)

FIG. IV.B.9

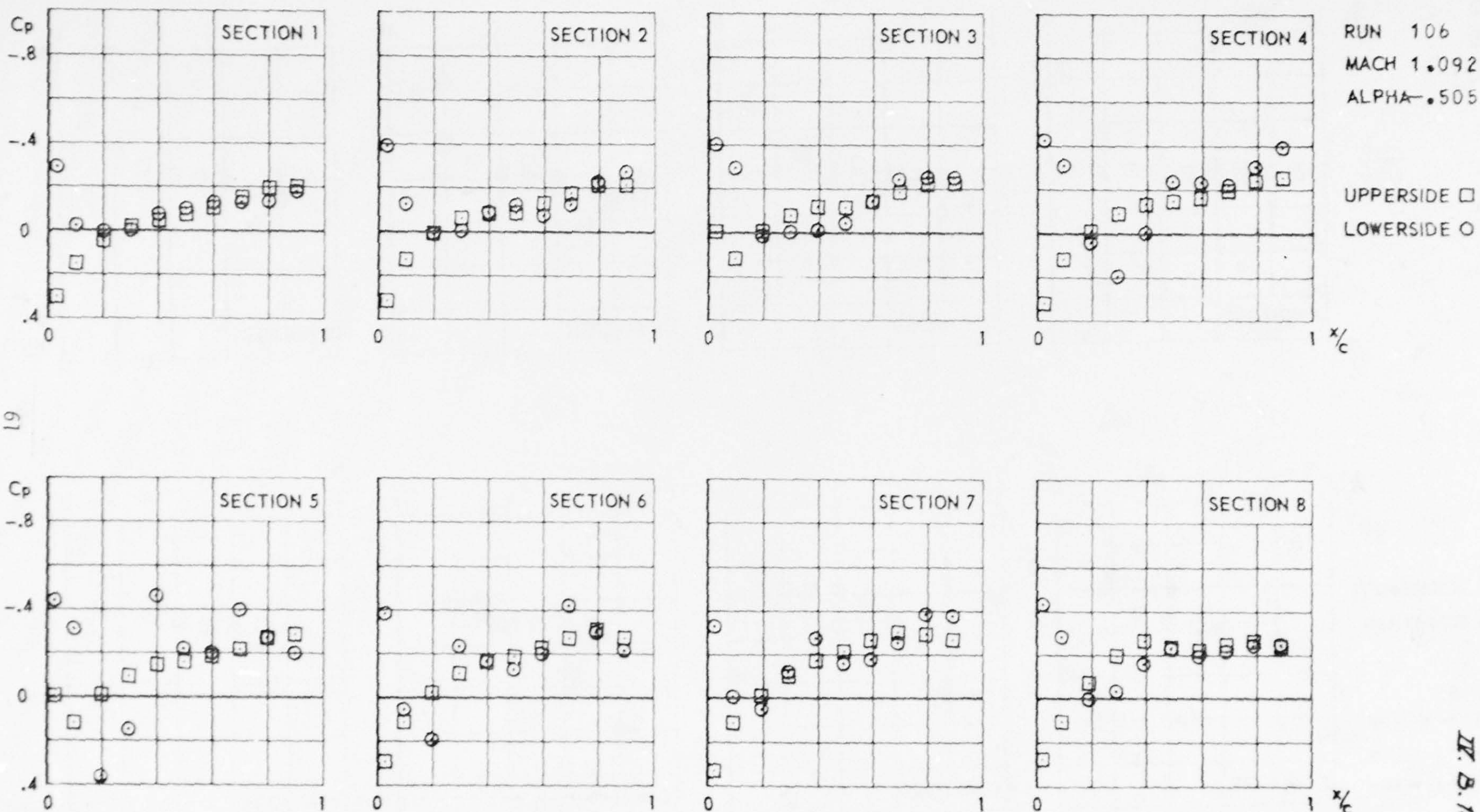

CONF.10 (WING + PYLON)

FIG. IV. B.10

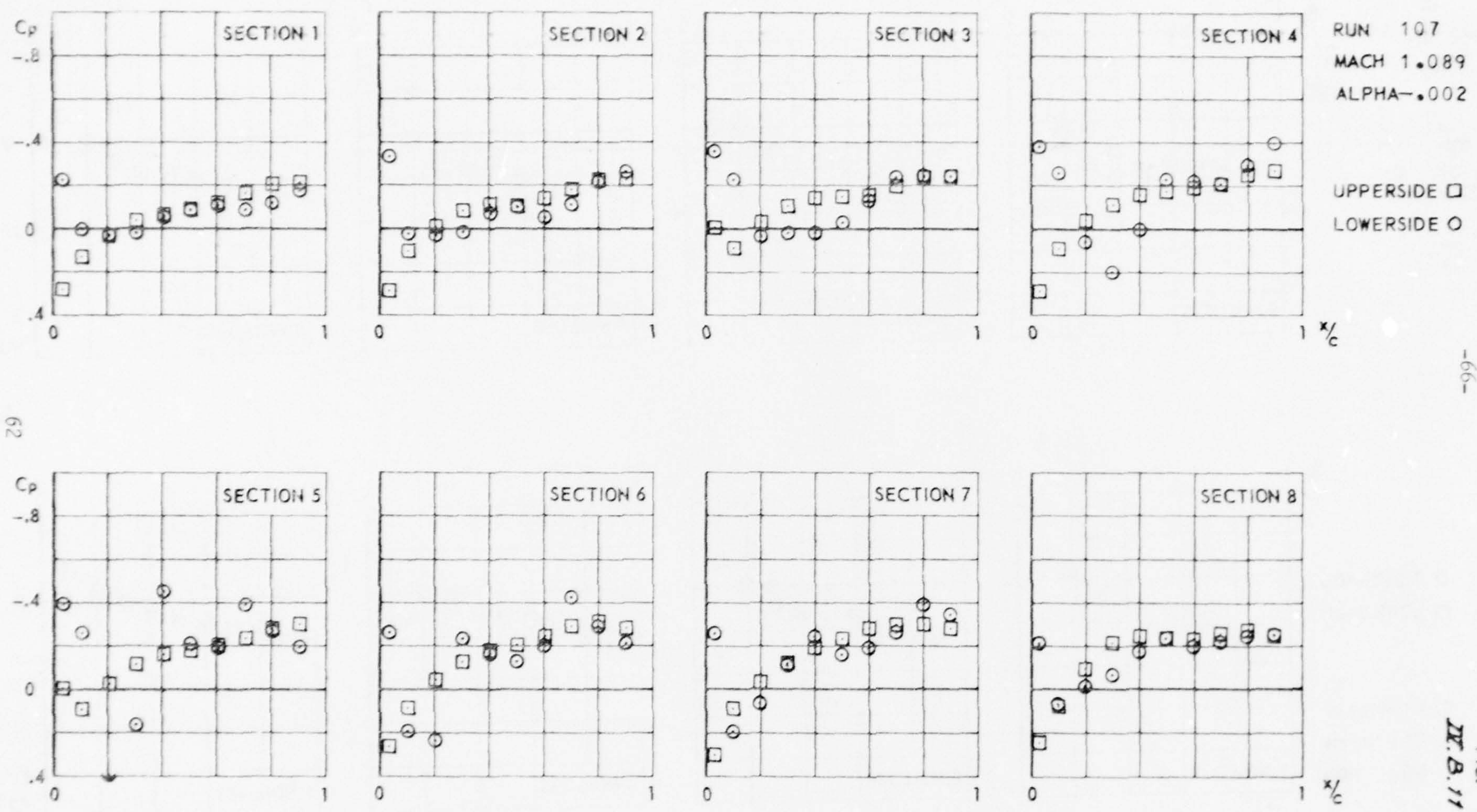

CONF.10 (WING + PYLON)

FIG. IV.B.11

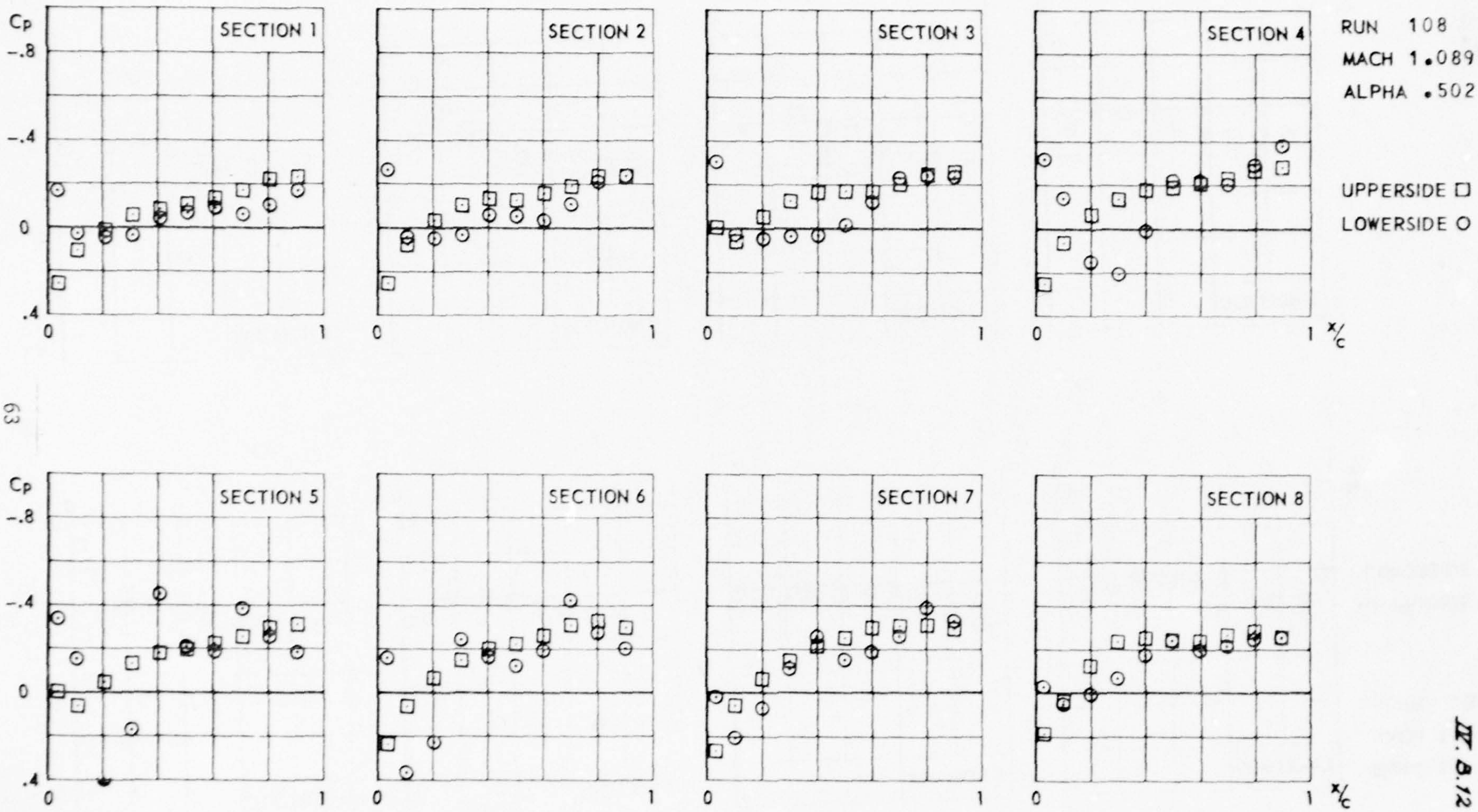

CONF.10 (WING + PYLON)

FIG. IV.B.12

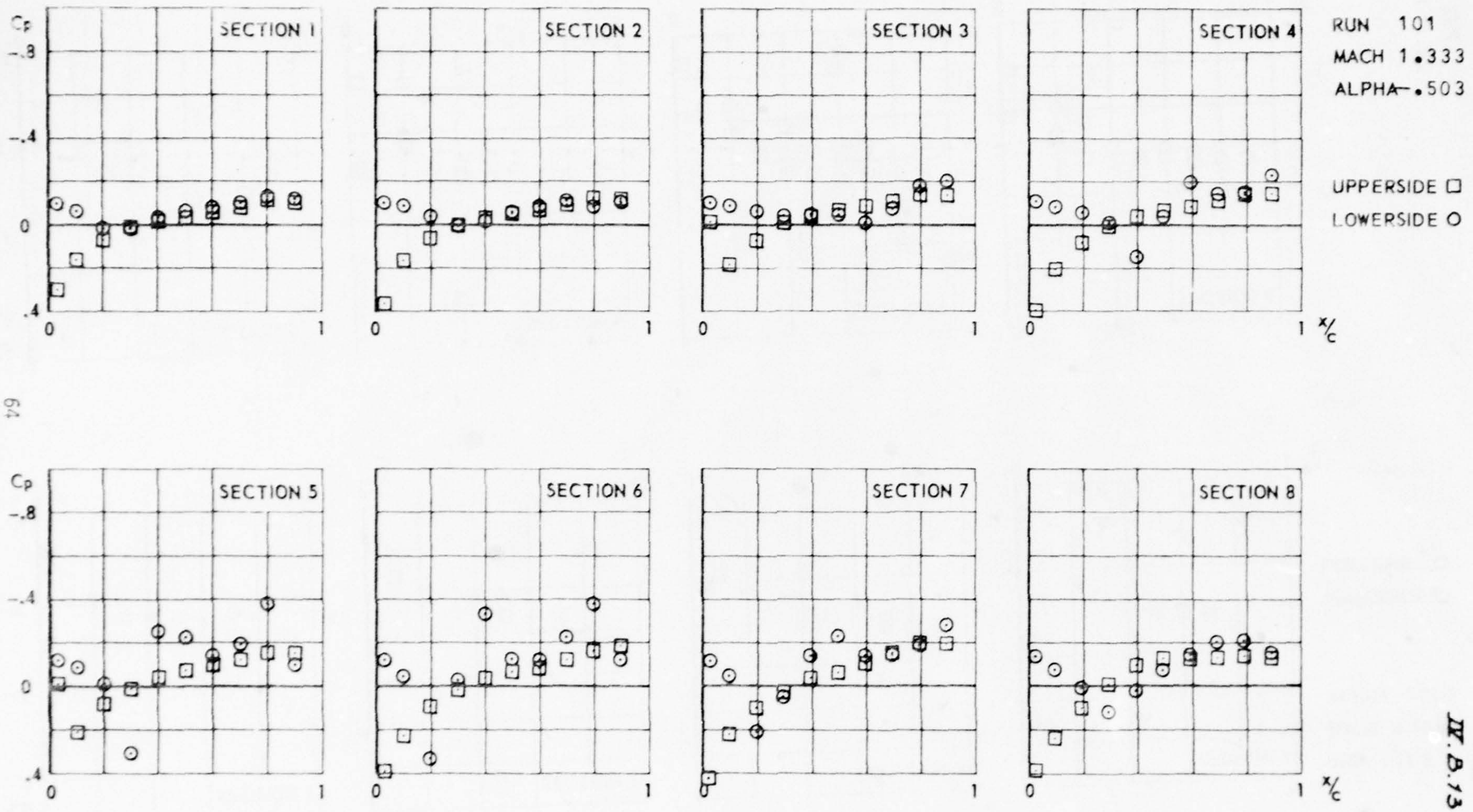

CONF.10 (WING + PYLON)

FIG. IV.B.13

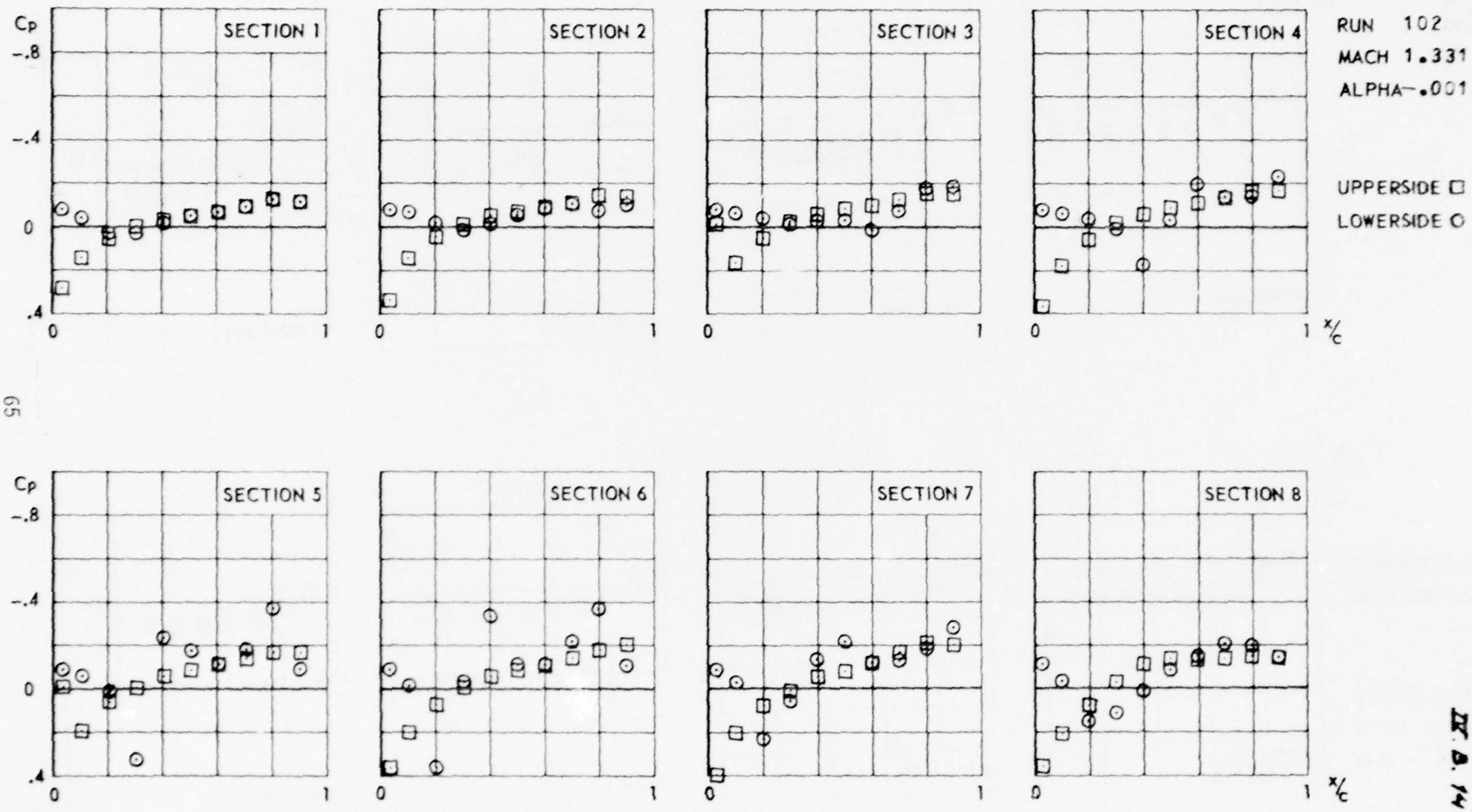

CONF.10 (WING + PYLON)

FIG. IV.B.14

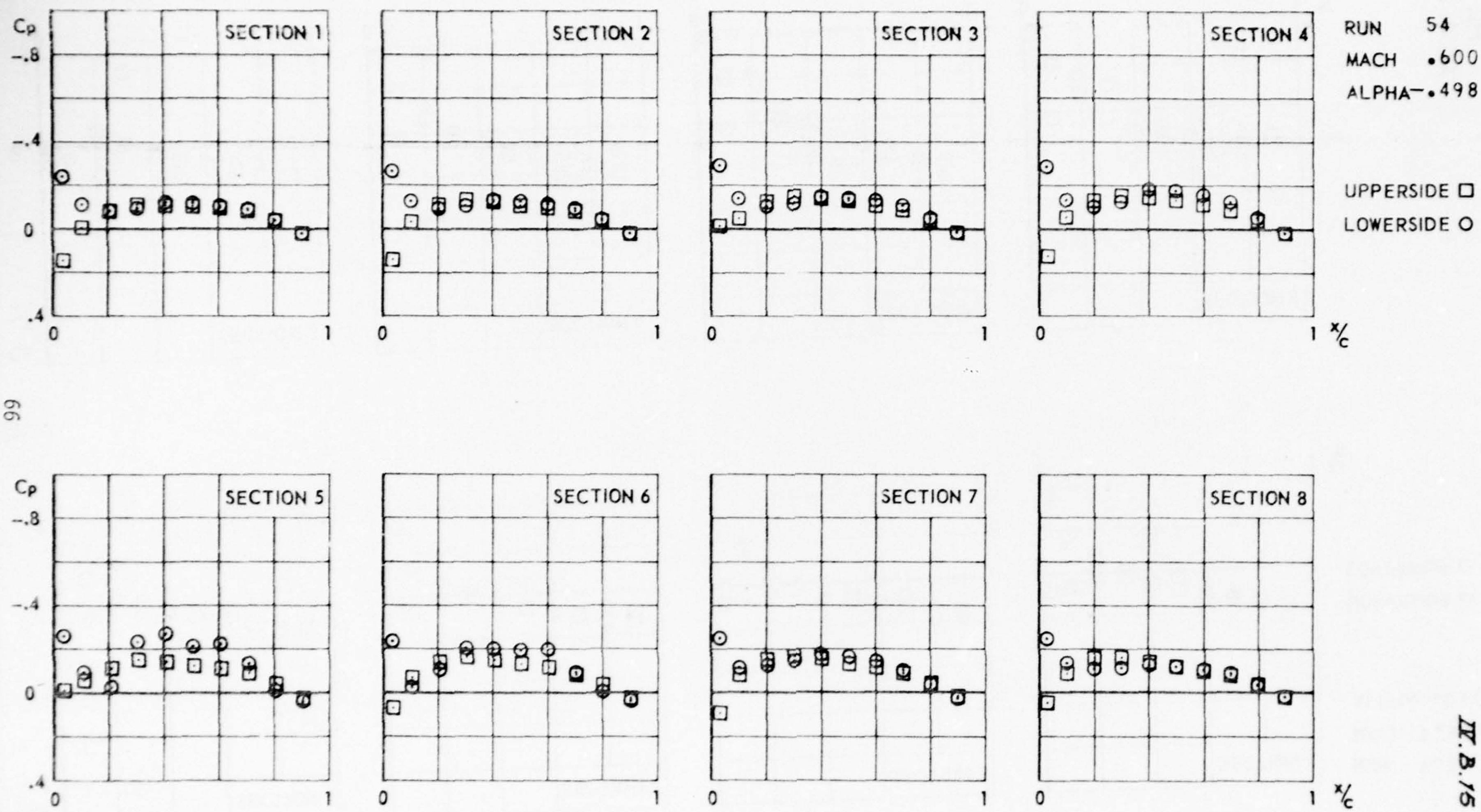

CONF.20 (WING + PYLON + LAUNCHER)

FIG.
IV.B.15

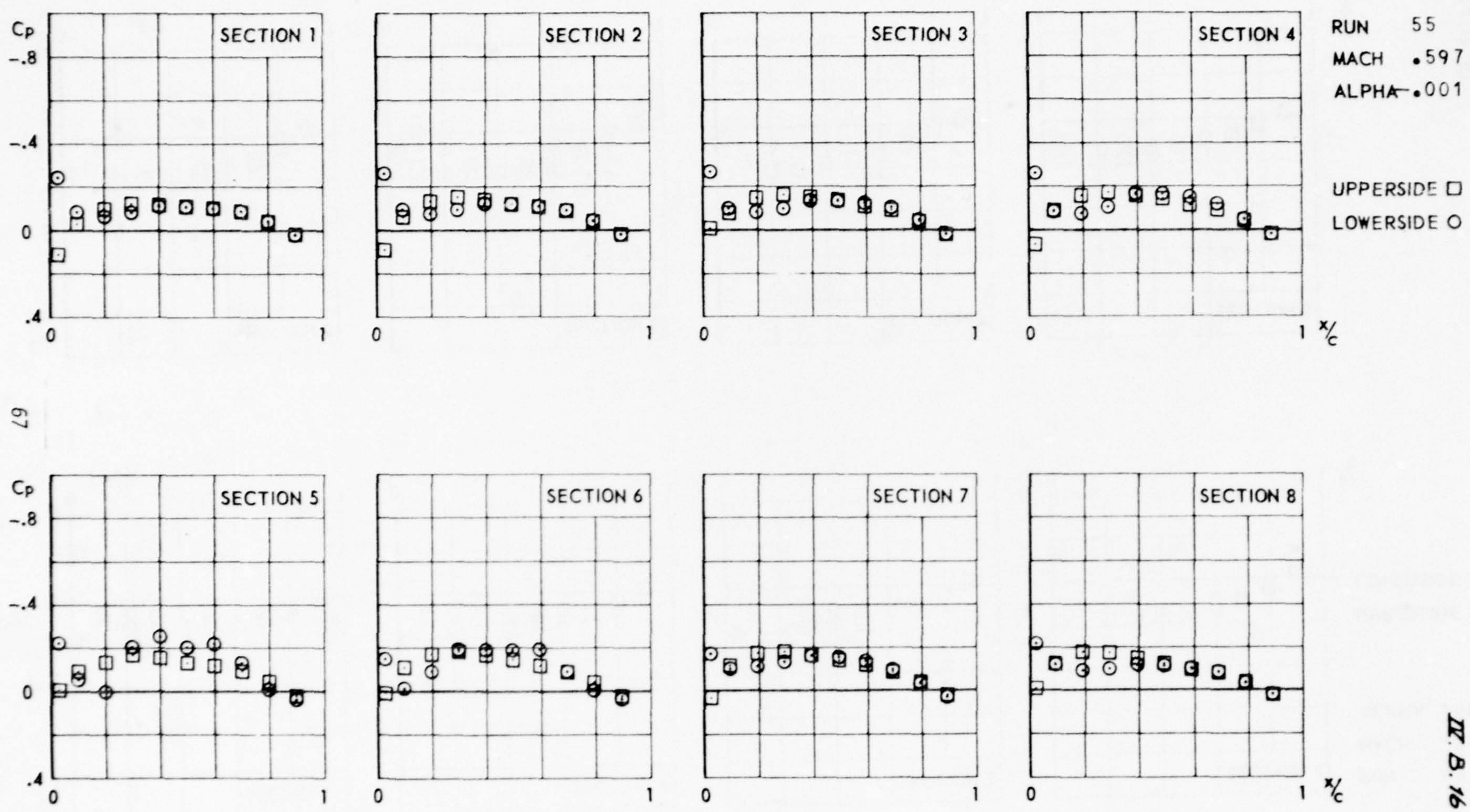

CONF.20 (WING + PYLON + LAUNCHER)

FIG.
IV. B. 16

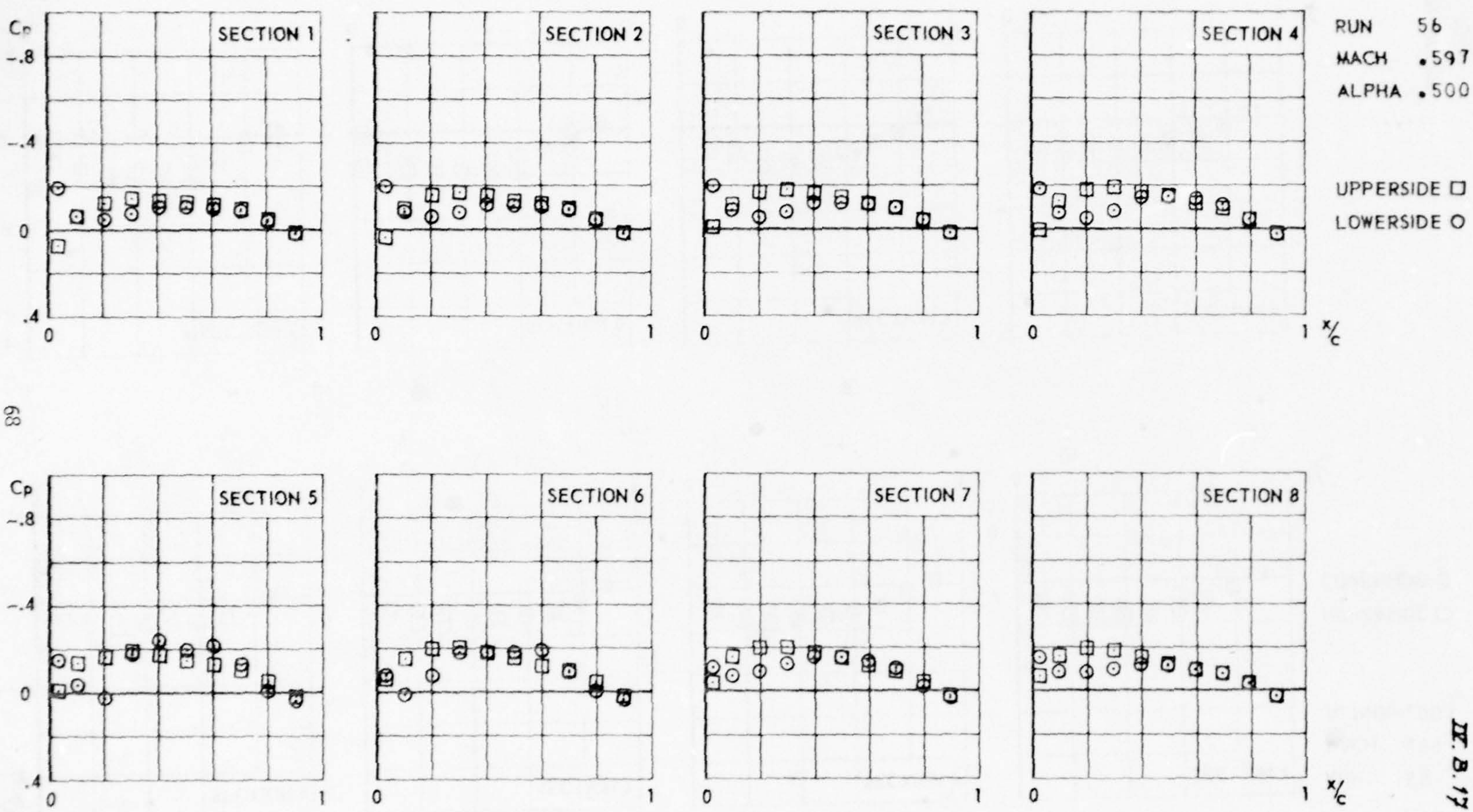

CONF.20 (WING + PYLON + LAUNCHER)

FIG.
IV.B.17

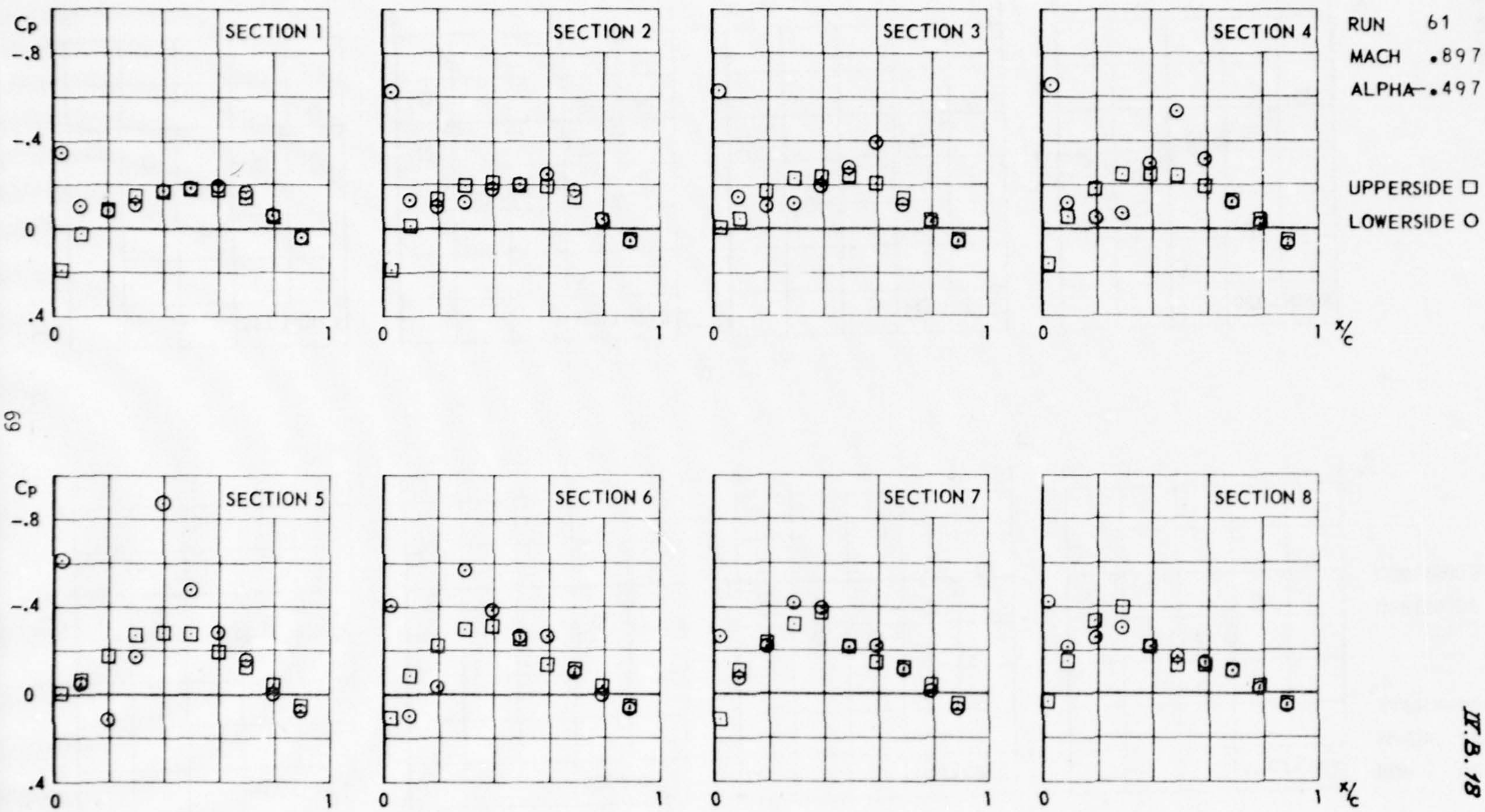

CONF.20 (WING + PYLON + LAUNCHER)

FIG.
IV.B.18

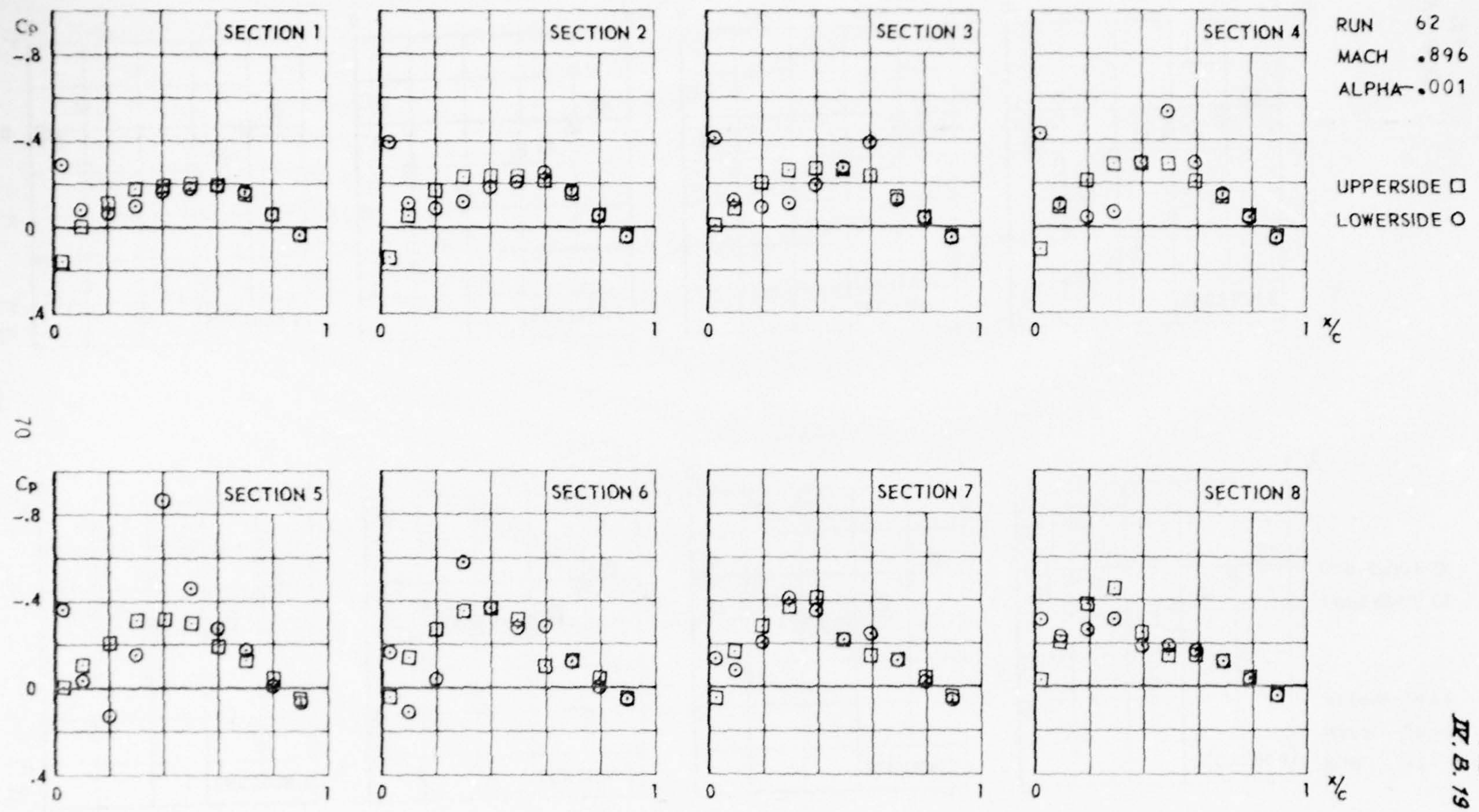

CONF. 20 (WING + PYLON + LAUNCHER)

FIG. IV. B. 19

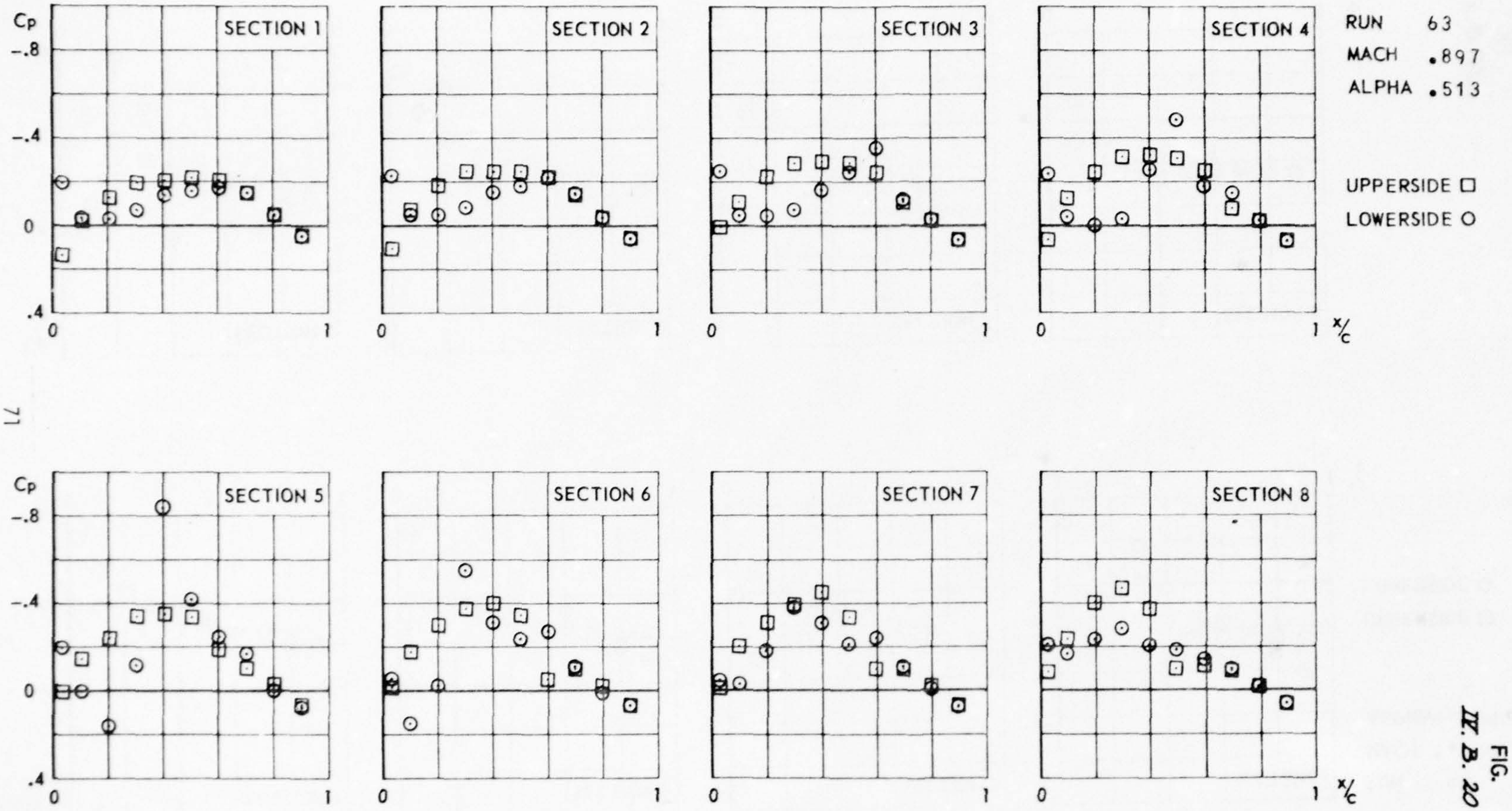

CONF.20 (WING + PYLON + LAUNCHER)

FIG. IV. B. 20

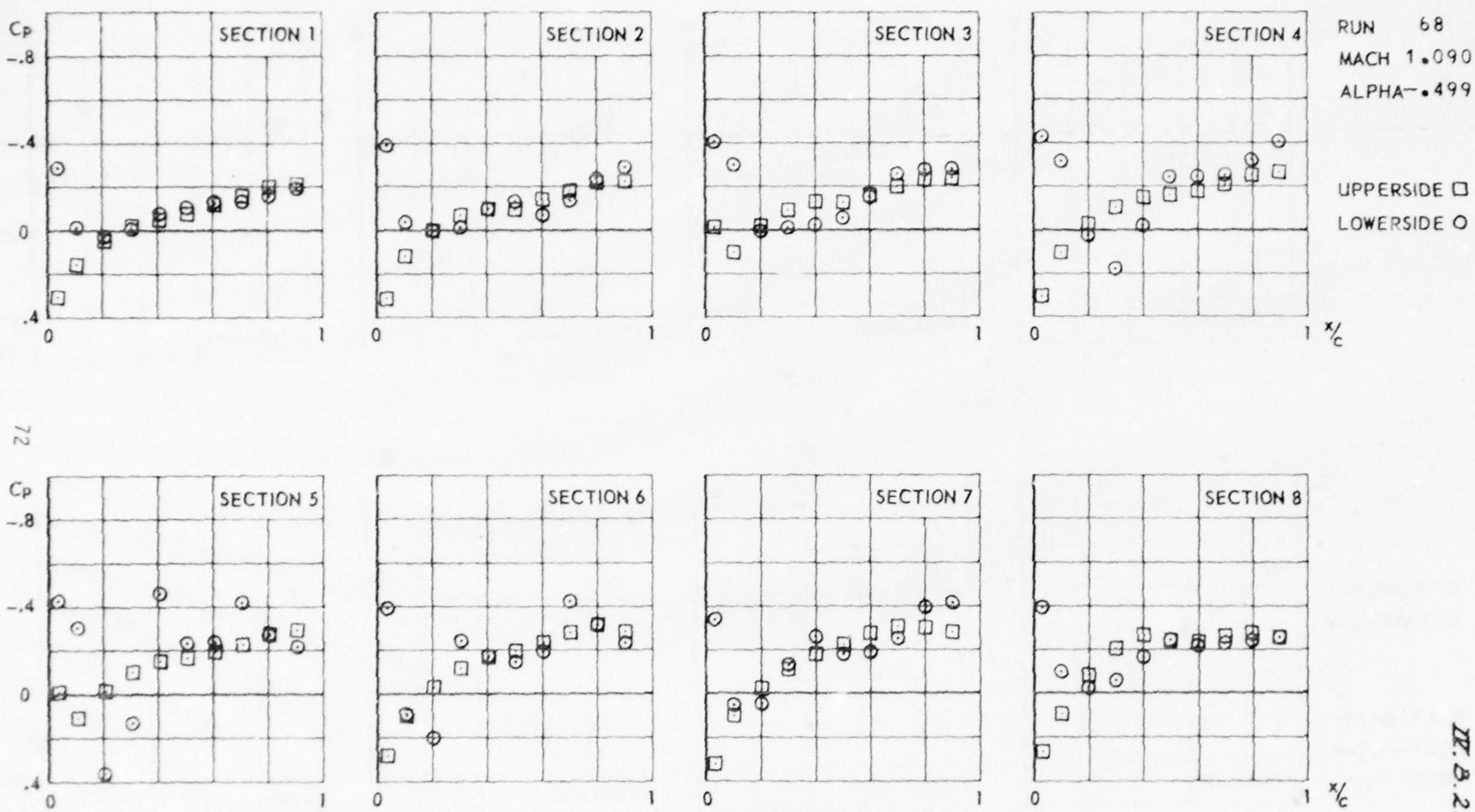

CONF.20 (WING + PYLON + LAUNCHER)

FIG. IV.B.21

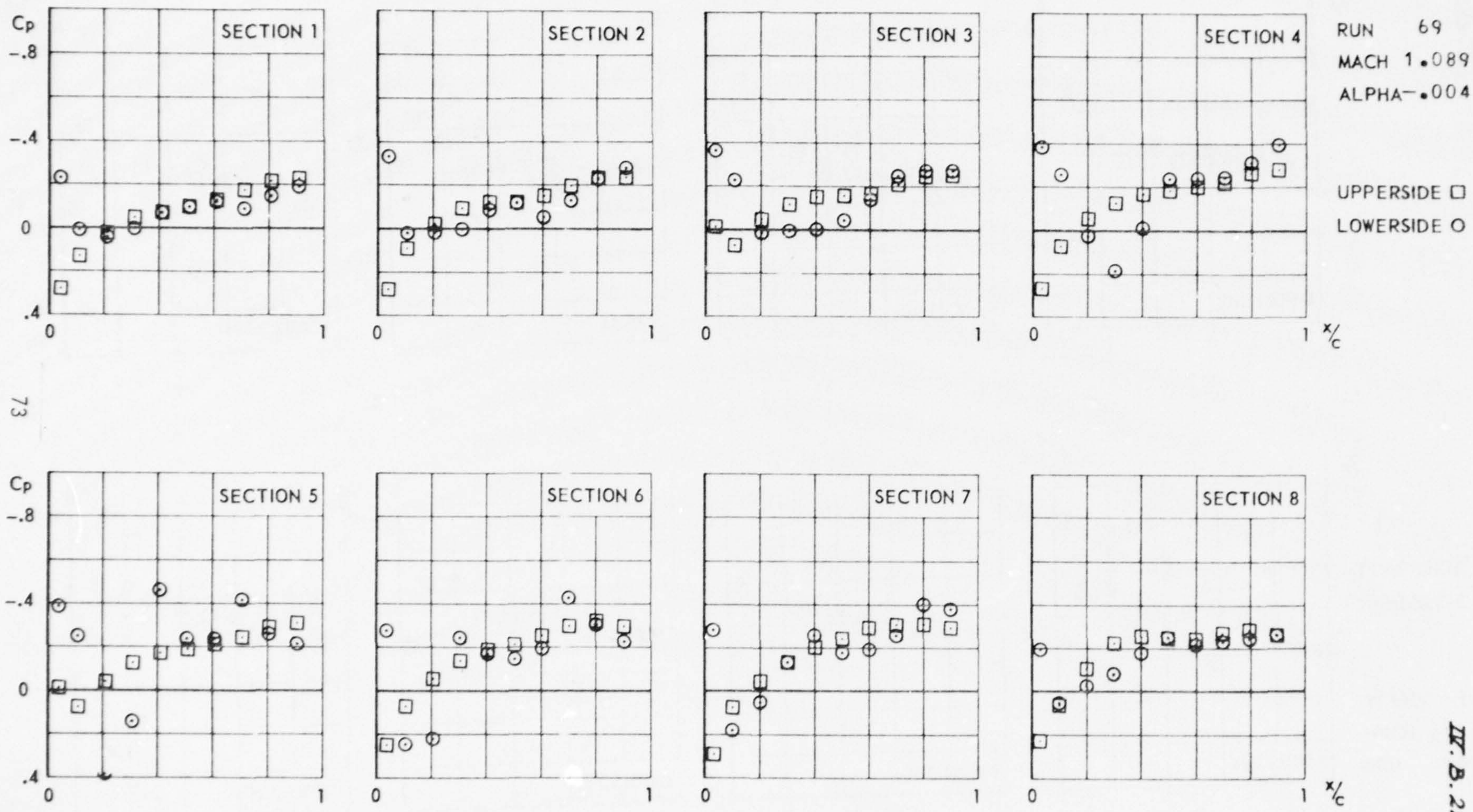

CONF.20 (WING + PYLON + LAUNCHER)

FIG. IV.B.22

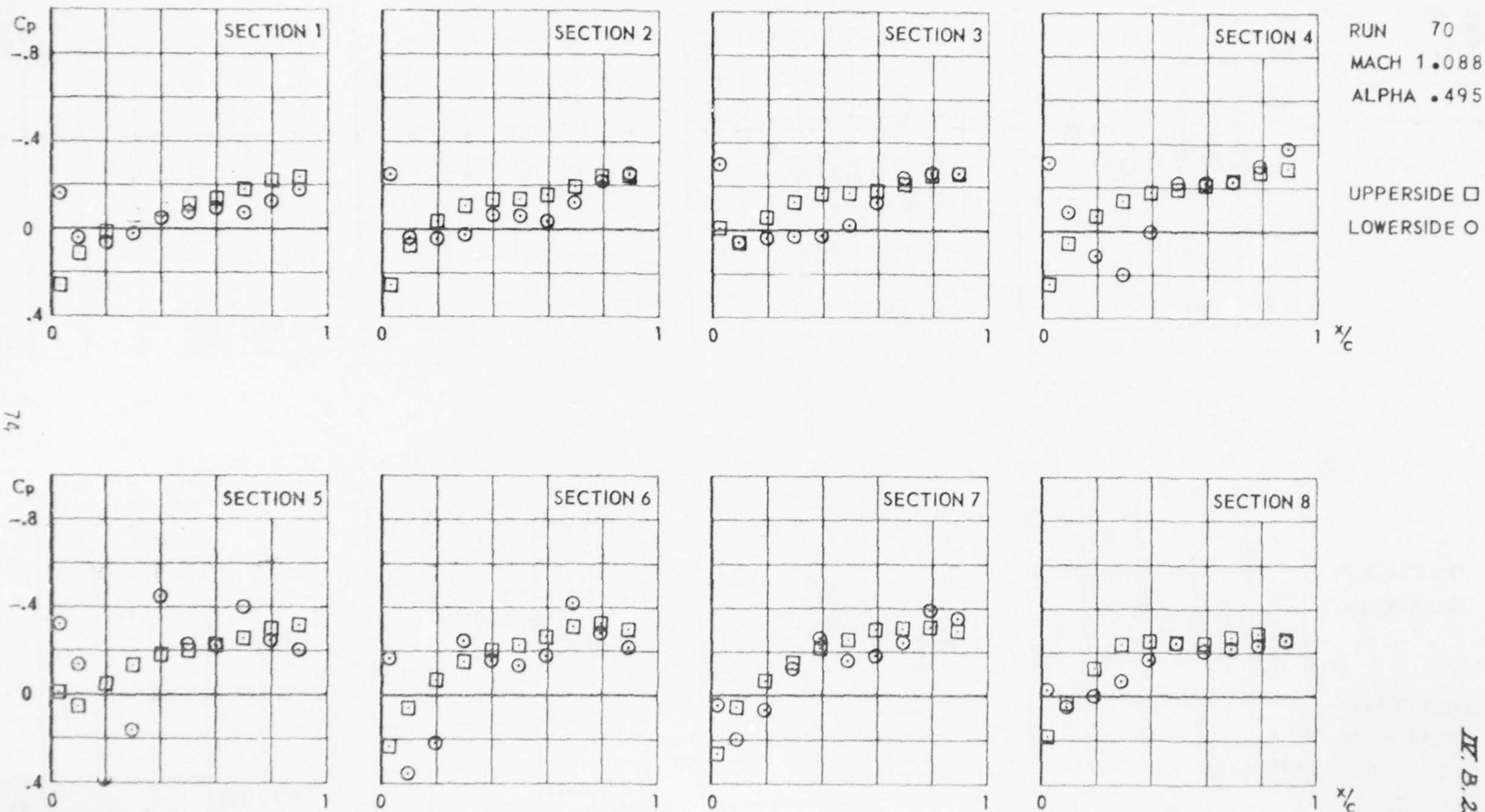

CONF.20 (WING + PYLON + LAUNCHER)

FIG.
IV. B. 23

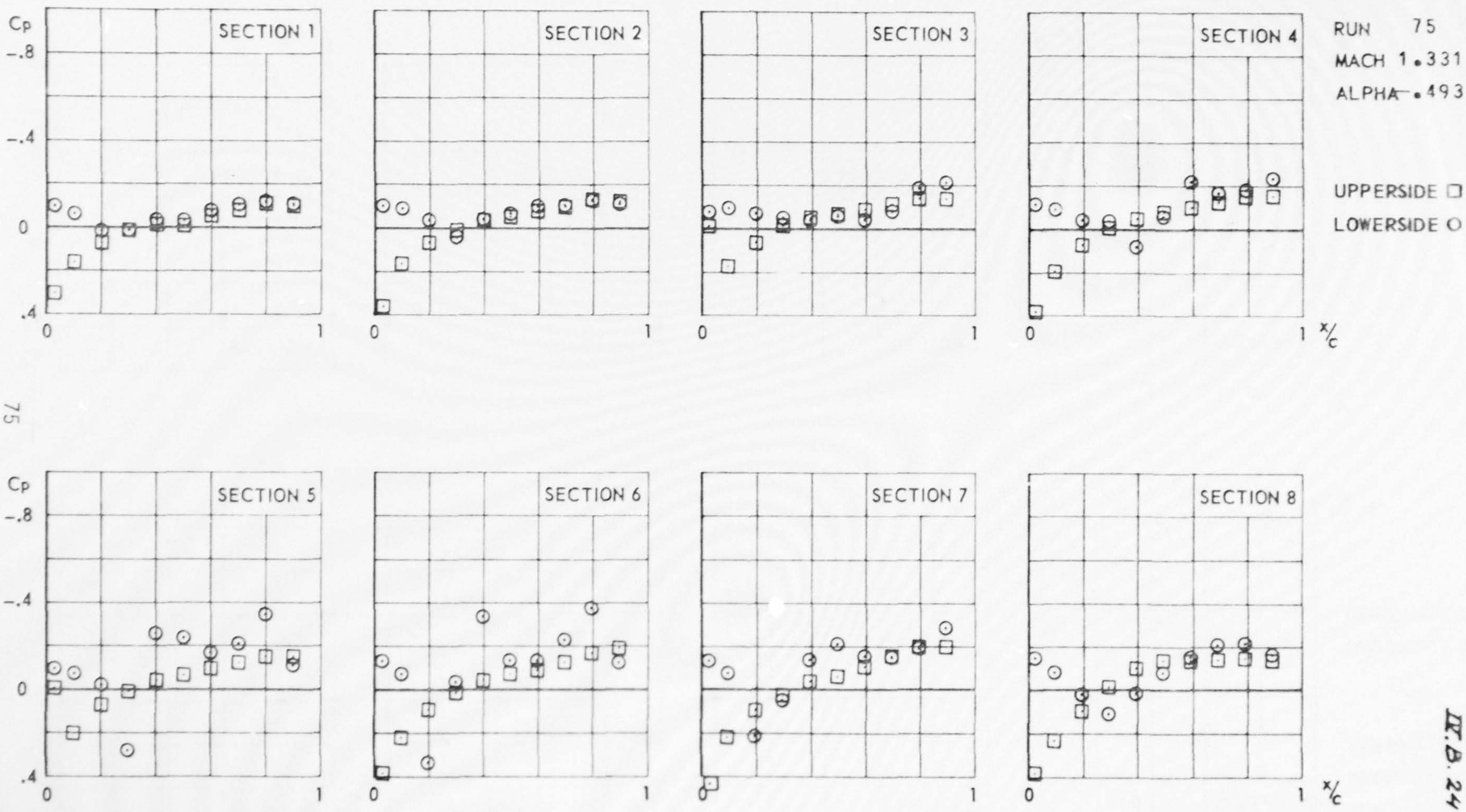

CONF.20 (WING + PYLON + LAUNCHER)

FIG. IV.B. 24

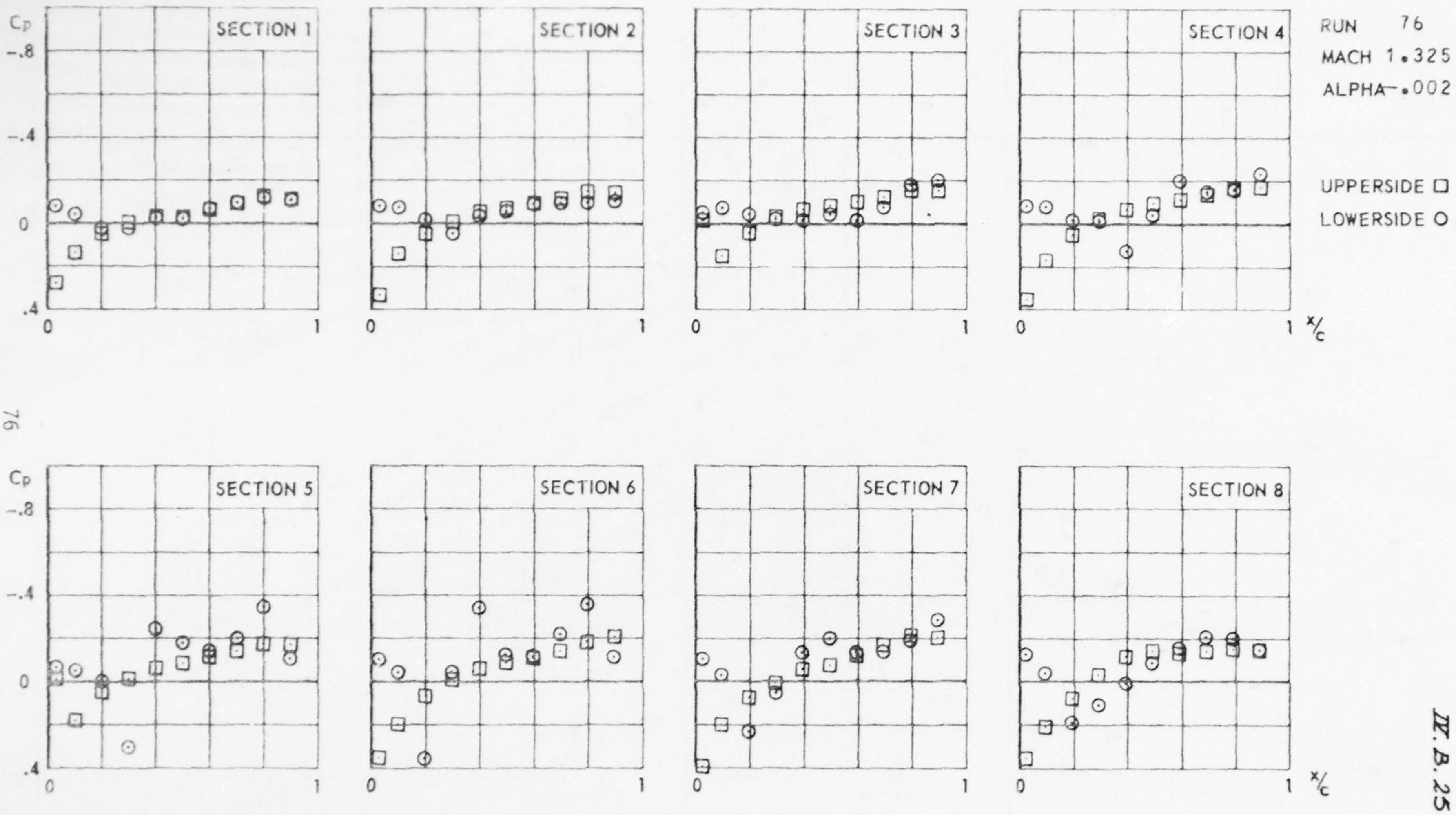

CONF.20 (WING + PYLON + LAUNCHER)

FIG. IV.B.25

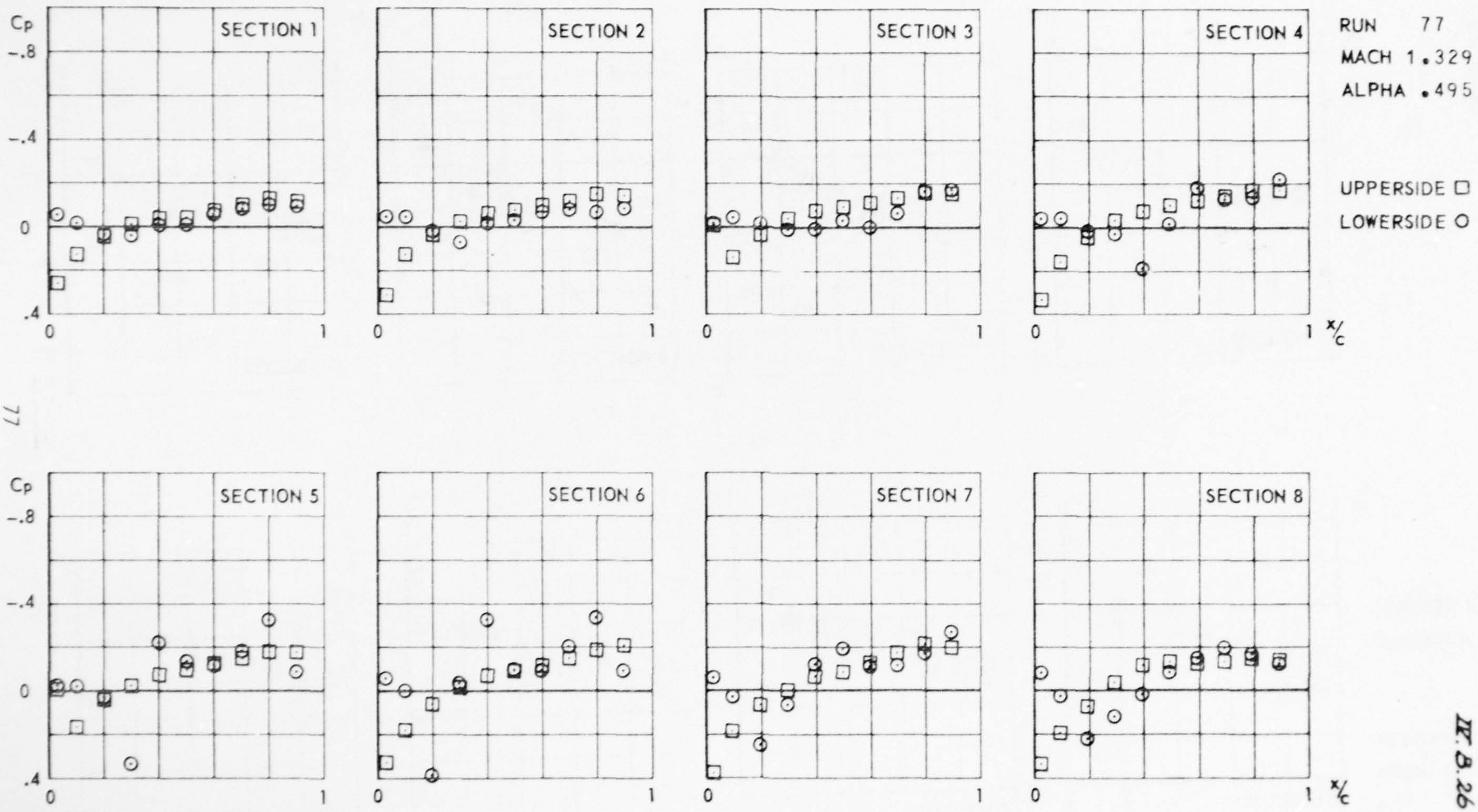

CONF.20 (WING + PYLON + LAUNCHER)

FIG. IV.B.26

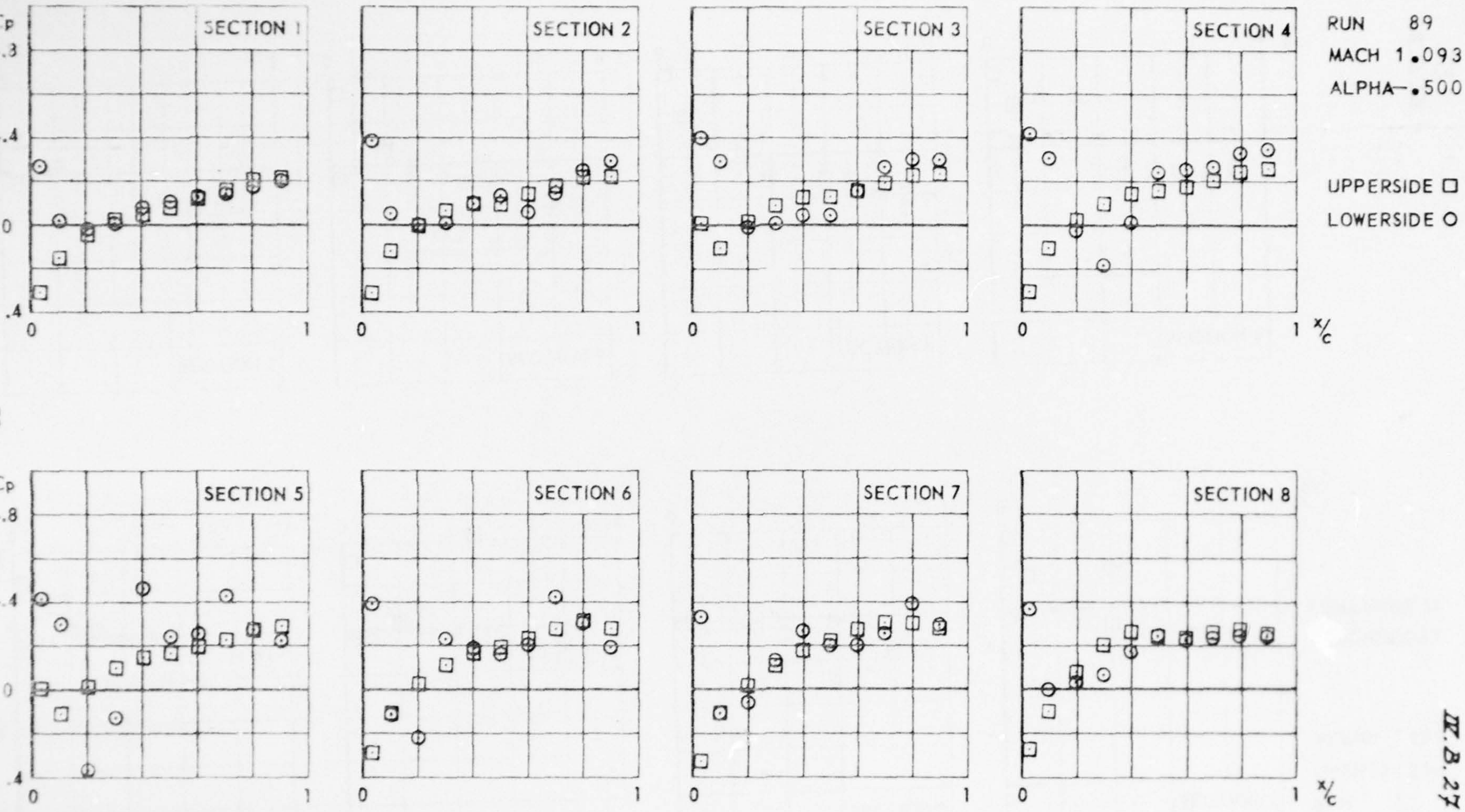

CONF.31 (WING + PYLON + LAUNCHER + MISSILEBODY WITH AFT WINGS)

FIG. IV.B.27

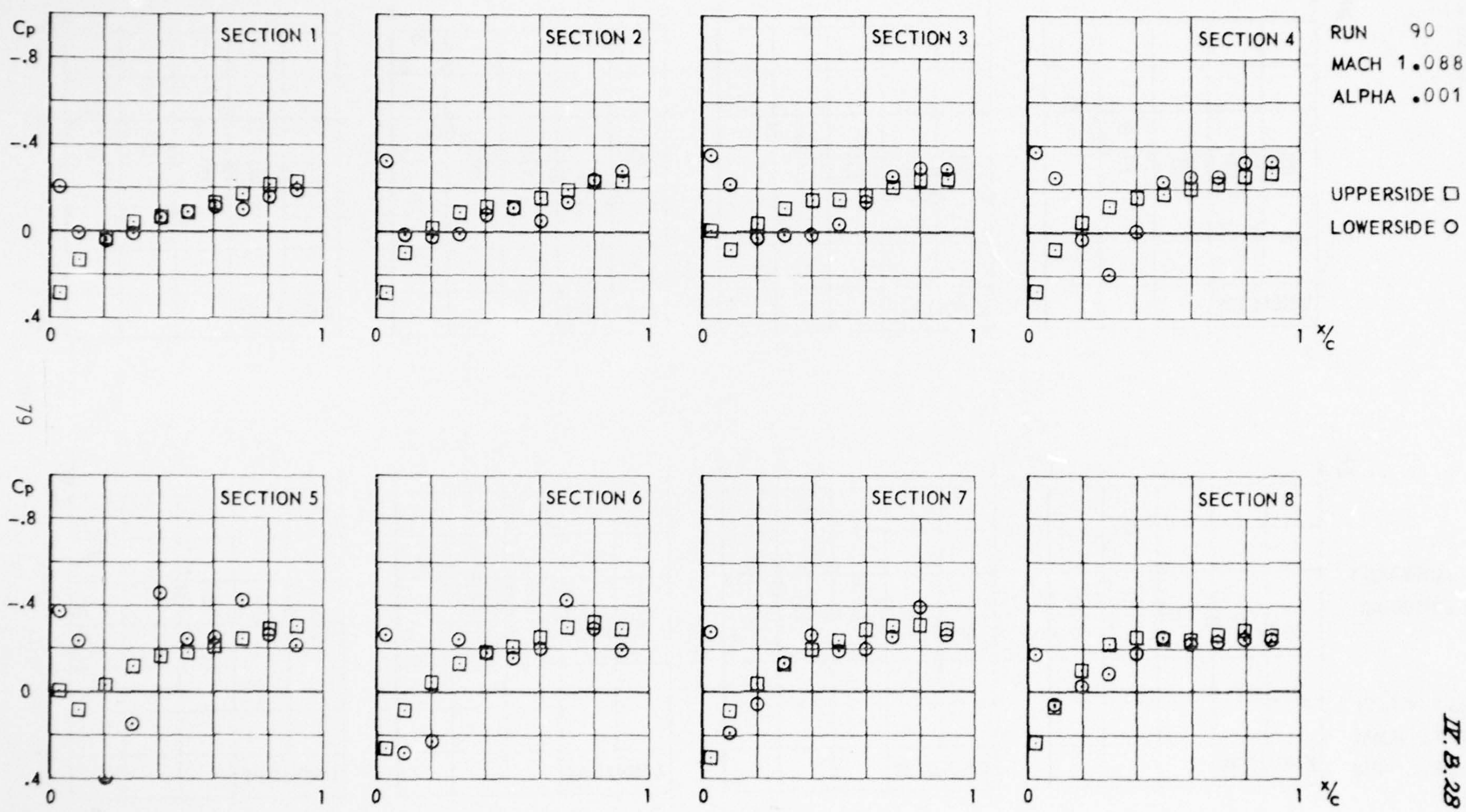

CONF.31 (WING + PYLON + LAUNCHER + MISSILEBODY WITH AFT WINGS)

FIG.
IV.B.28

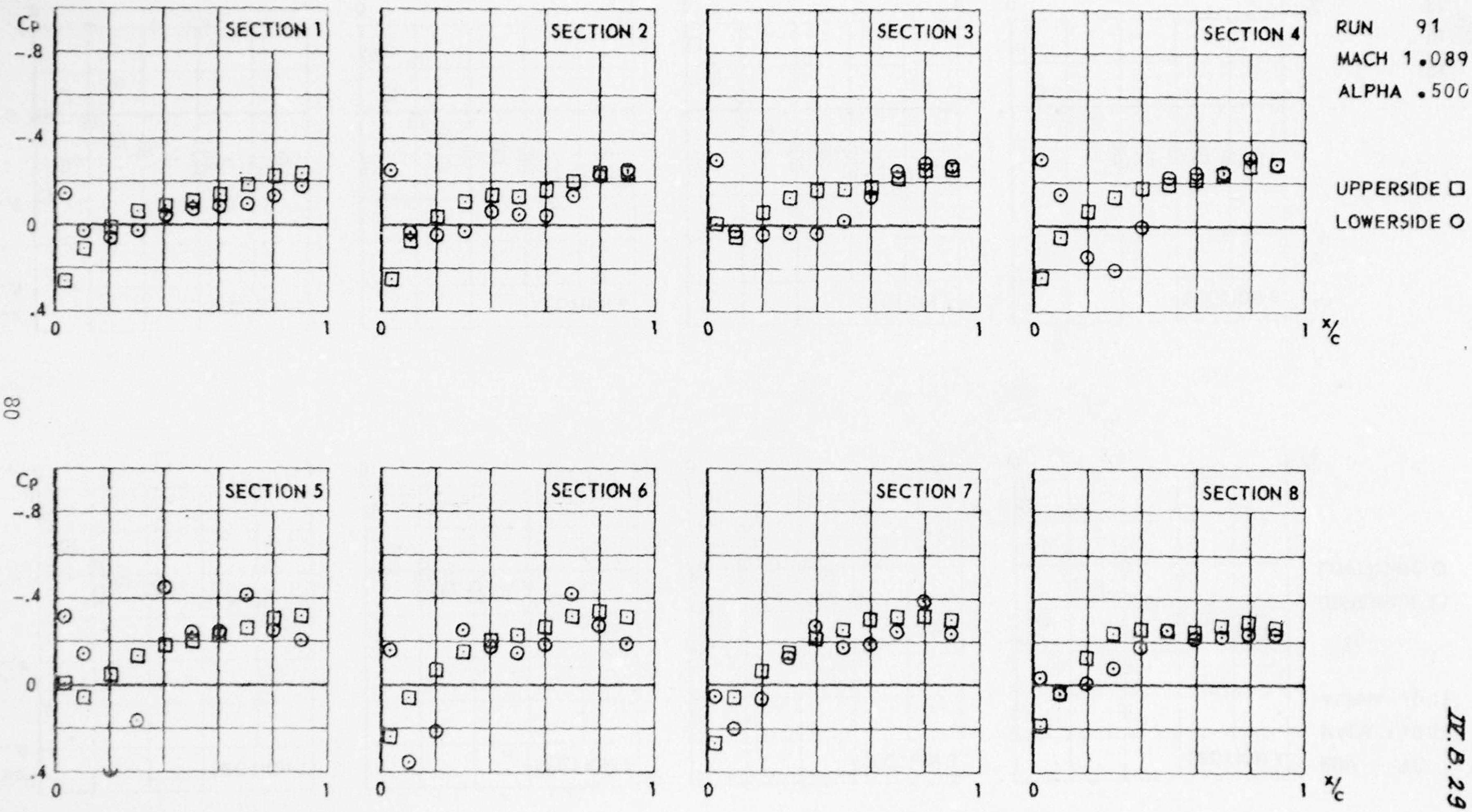

CONF. 31 (WING + PYLON + LAUNCHER + MISSILEBODY WITH AFT WINGS)

FIG. IV.B.29

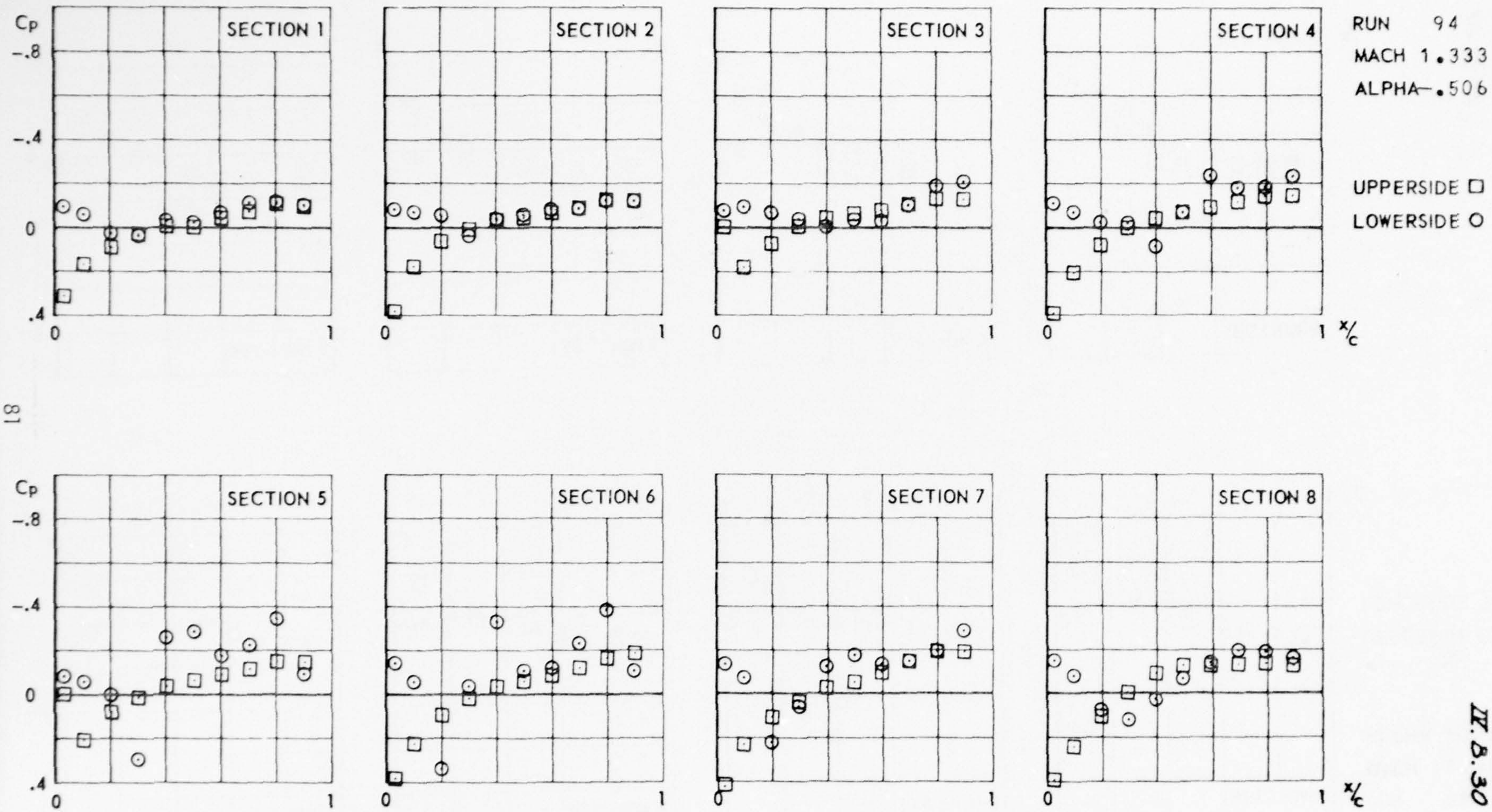

CONF.31 (WING + PYLON + LAUNCHER + MISSILEBODY WITH AFT WINGS)

FIG. IV.B.30

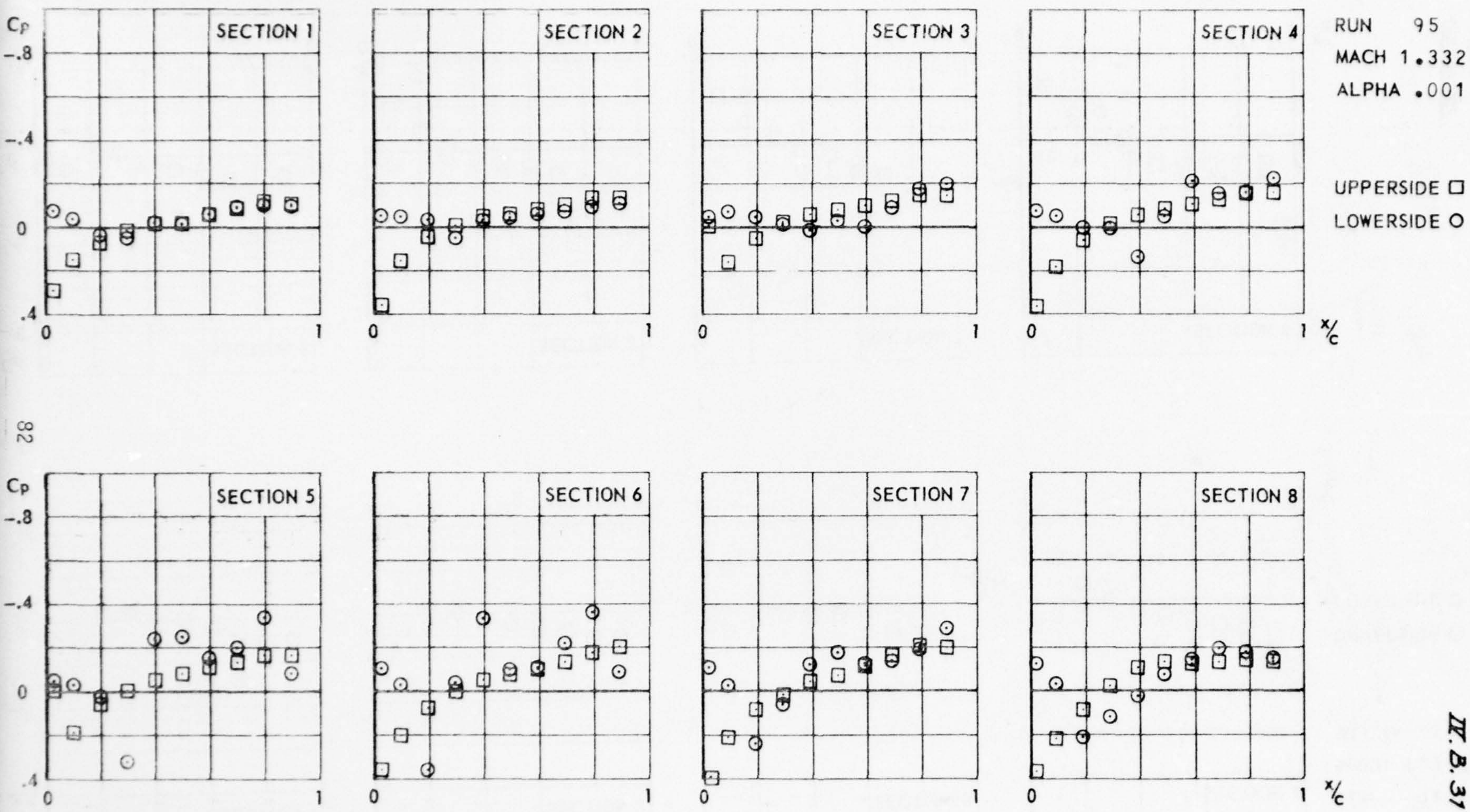

CONF.31 (WING + PYLON + LAUNCHER + MISSILEBODY WITH AFT WINGS)

FIG. IV.B.31

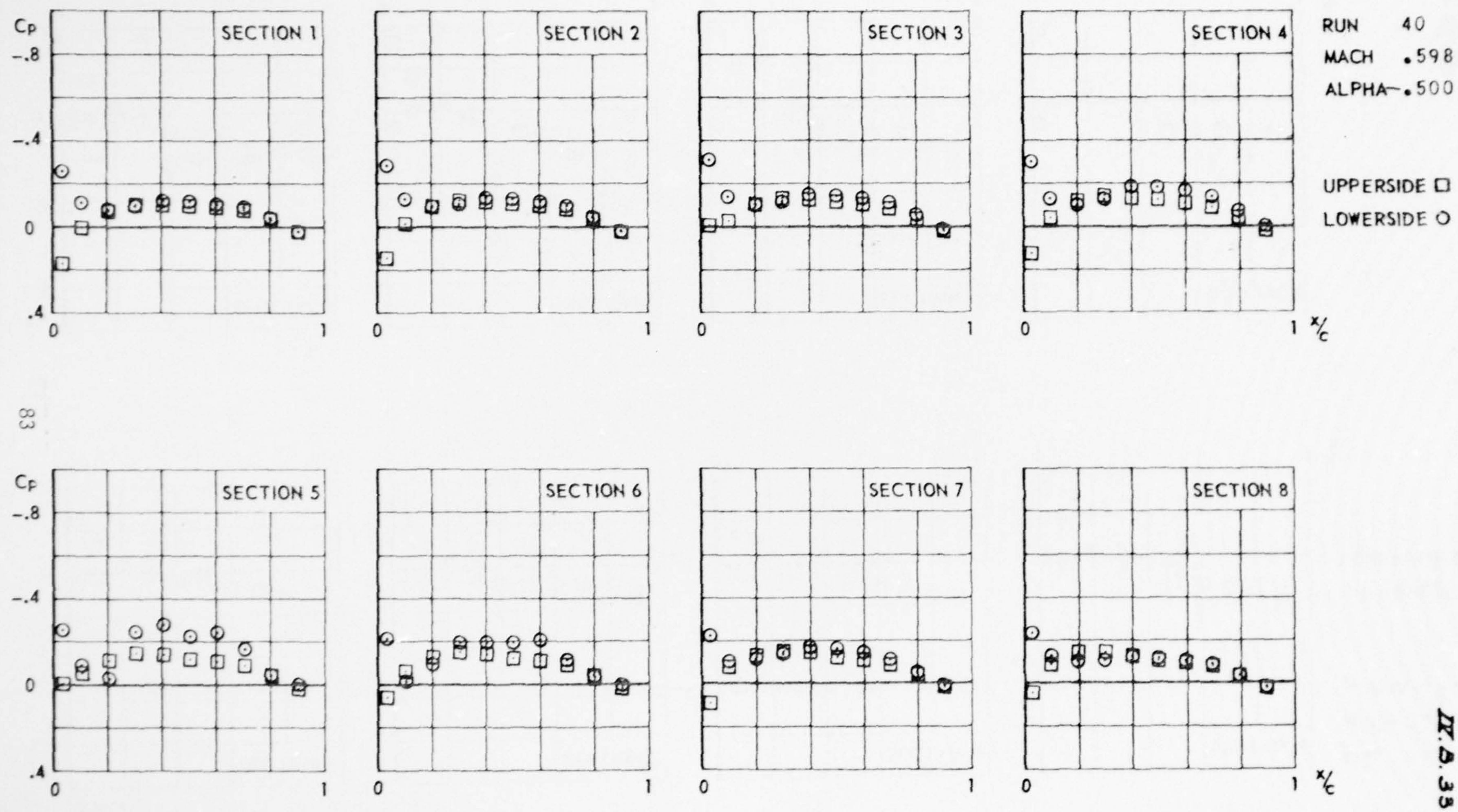

CONF.301 (WING + PYLON + LAUNCHER + COMPLETE MISSILE)

FIG. IV.B.33

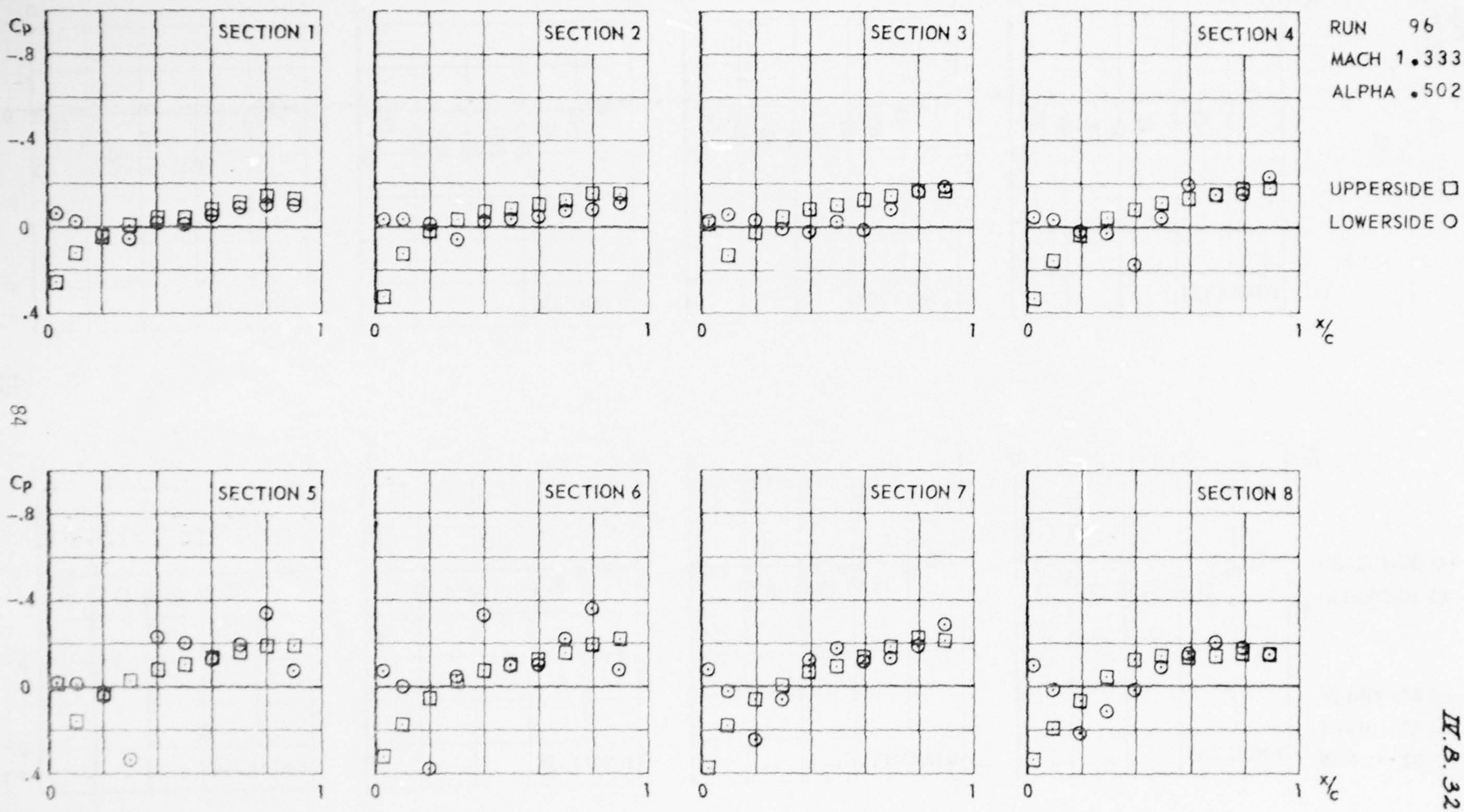

CONF.31 (WING + PYLON + LAUNCHER + MISSILEBODY WITH AFT WINGS)

FIG. IV.B.32

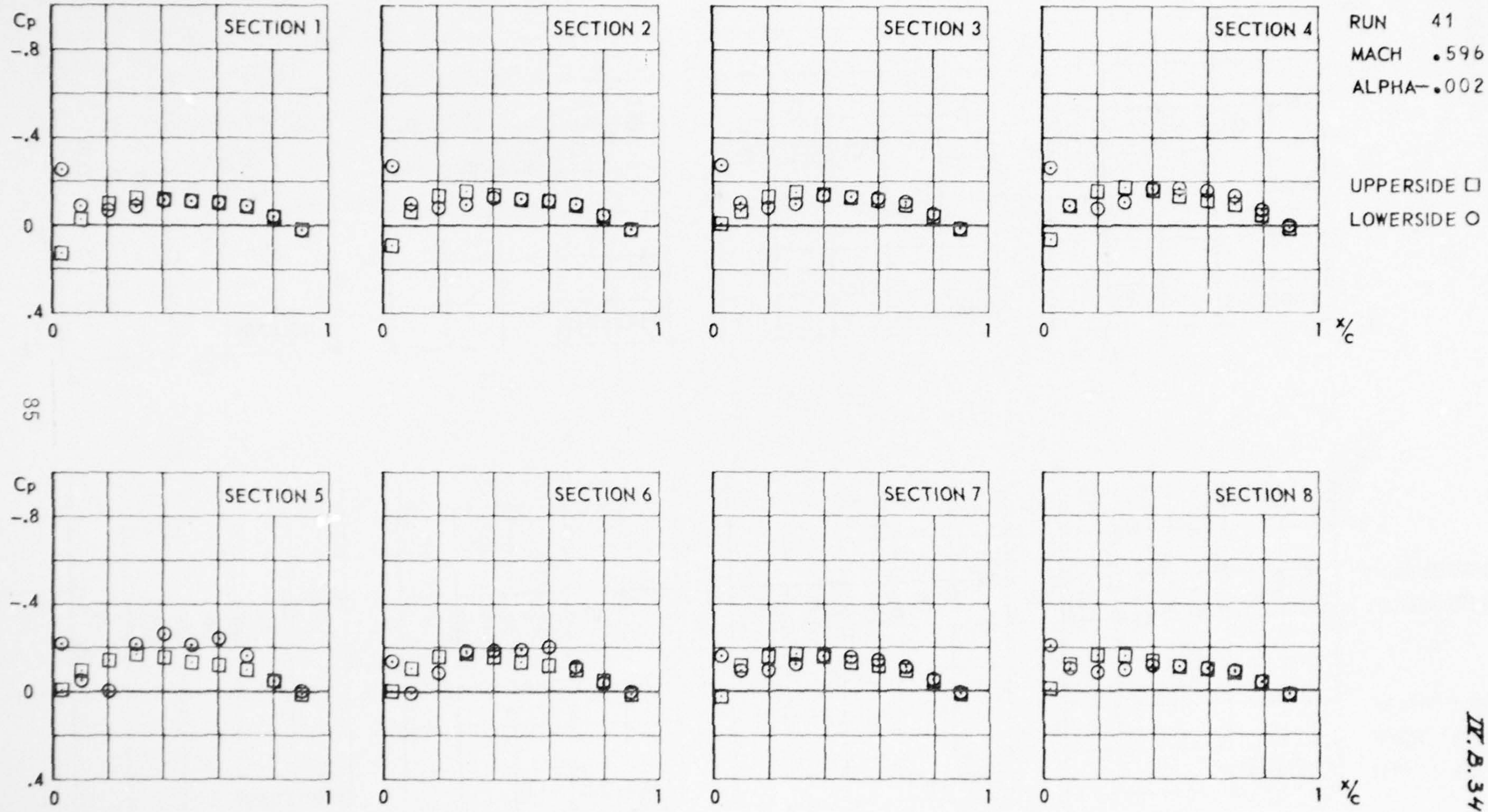

CONF.301 (WING + PYLON + LAUNCHER + COMPLETE MISSILE)

FIG.
IV.B.34

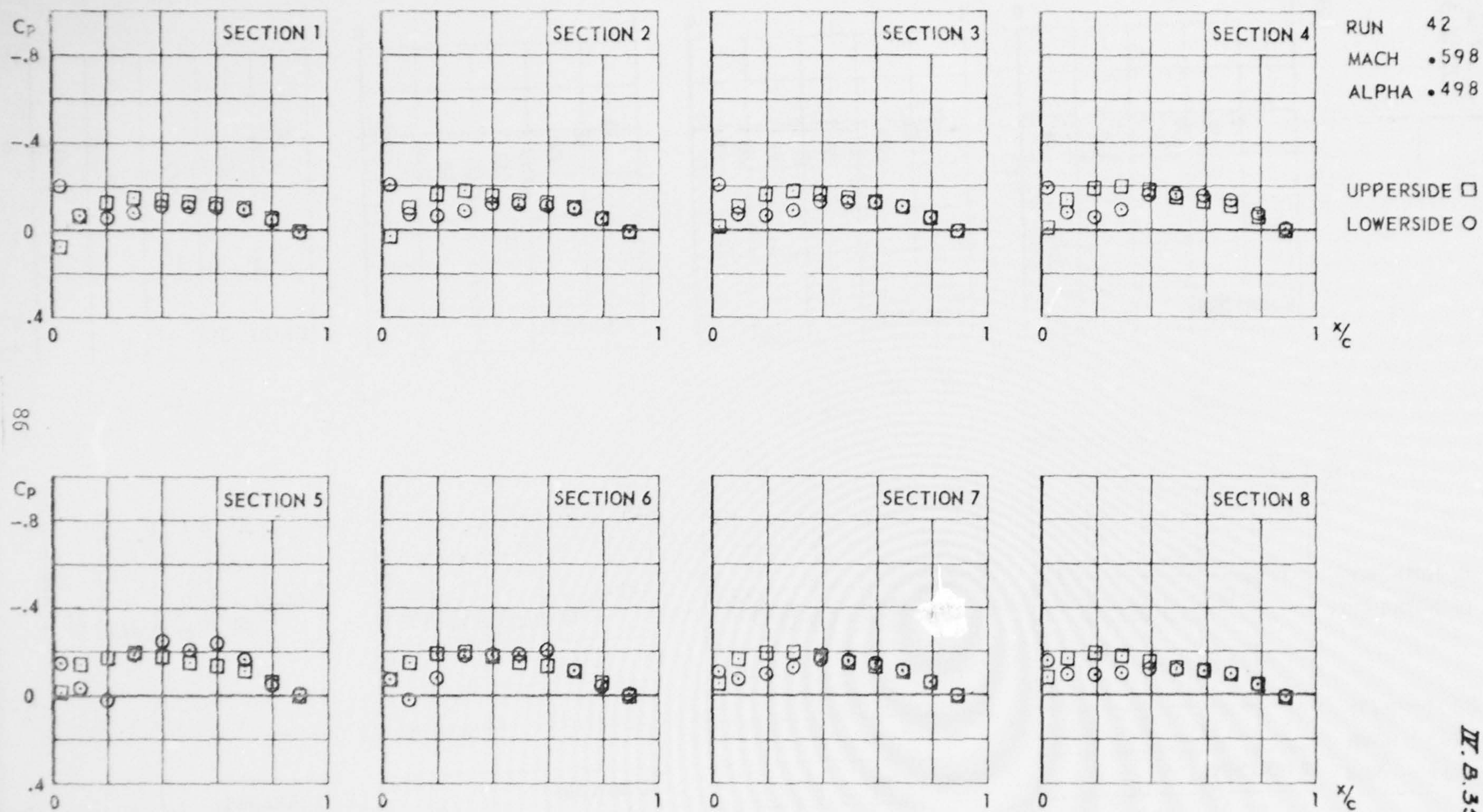

CONF.301 (WING + PYLON + LAUNCHER + COMPLETE MISSILE)

FIG. IV.B.35

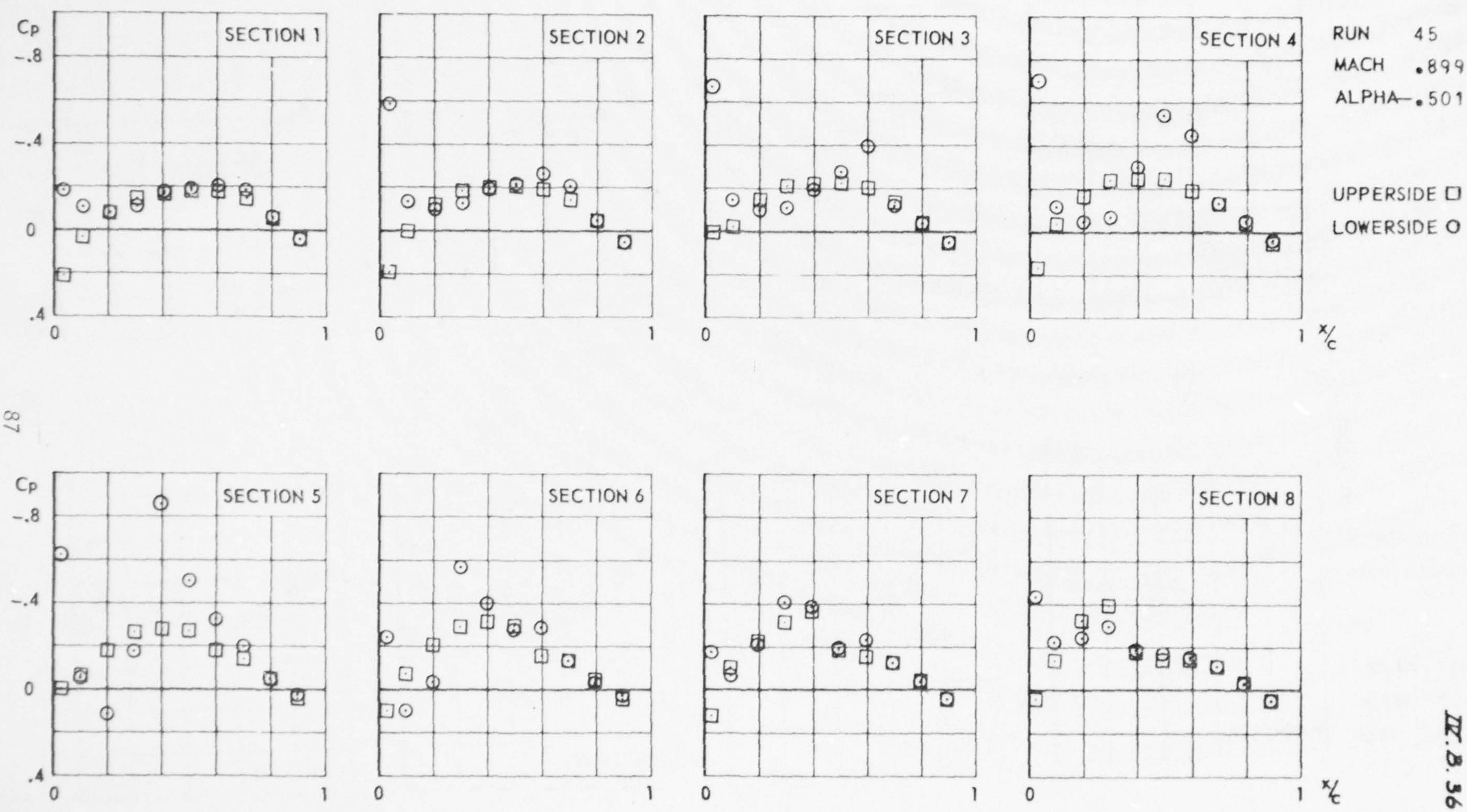

CONF.301 (WING + PYLON + LAUNCHER + COMPLETE MISSILE)

FIG. IV.B.36

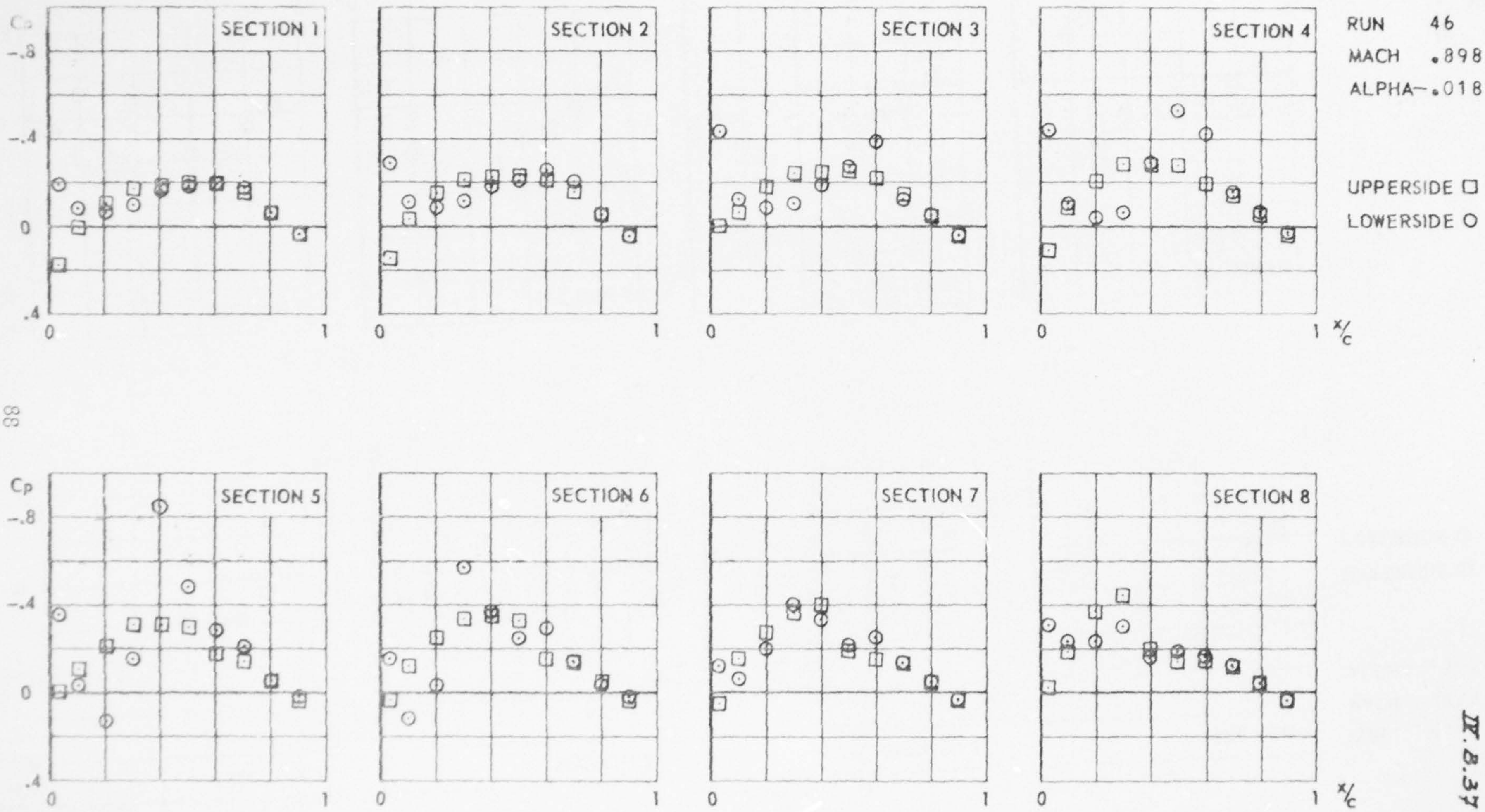

CONF.301 (WING + PYLON + LAUNCHER + COMPLETE MISSILE)

FIG. IV.B.37

AD-A077 370 NATIONAL AEROSPACE LAB AMSTERDAM (NETHERLANDS) F/G 20/4
TRANSONIC WIND TUNNEL TESTS ON AN OSCILLATING WING WITH EXTERNA--ETC(U)
SEP 79 H TIJDEMAN , J W VAN NUNEN AFOSR-77-3233
UNCLASSIFIED NLR-TR-78106-U-PT-4 AFFDL-TR-78-194-PT-4 NL

2 OF 2
AD
A077370

END
DATE
FILMED
1-80
DDC

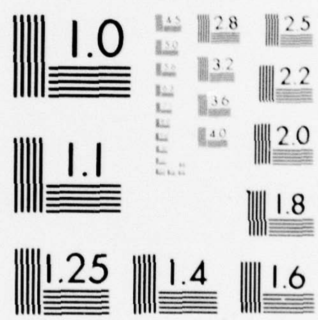

MICROCOPY RESOLUTION TEST CHART
NATIONAL BUREAU OF STANDARDS-1963-A

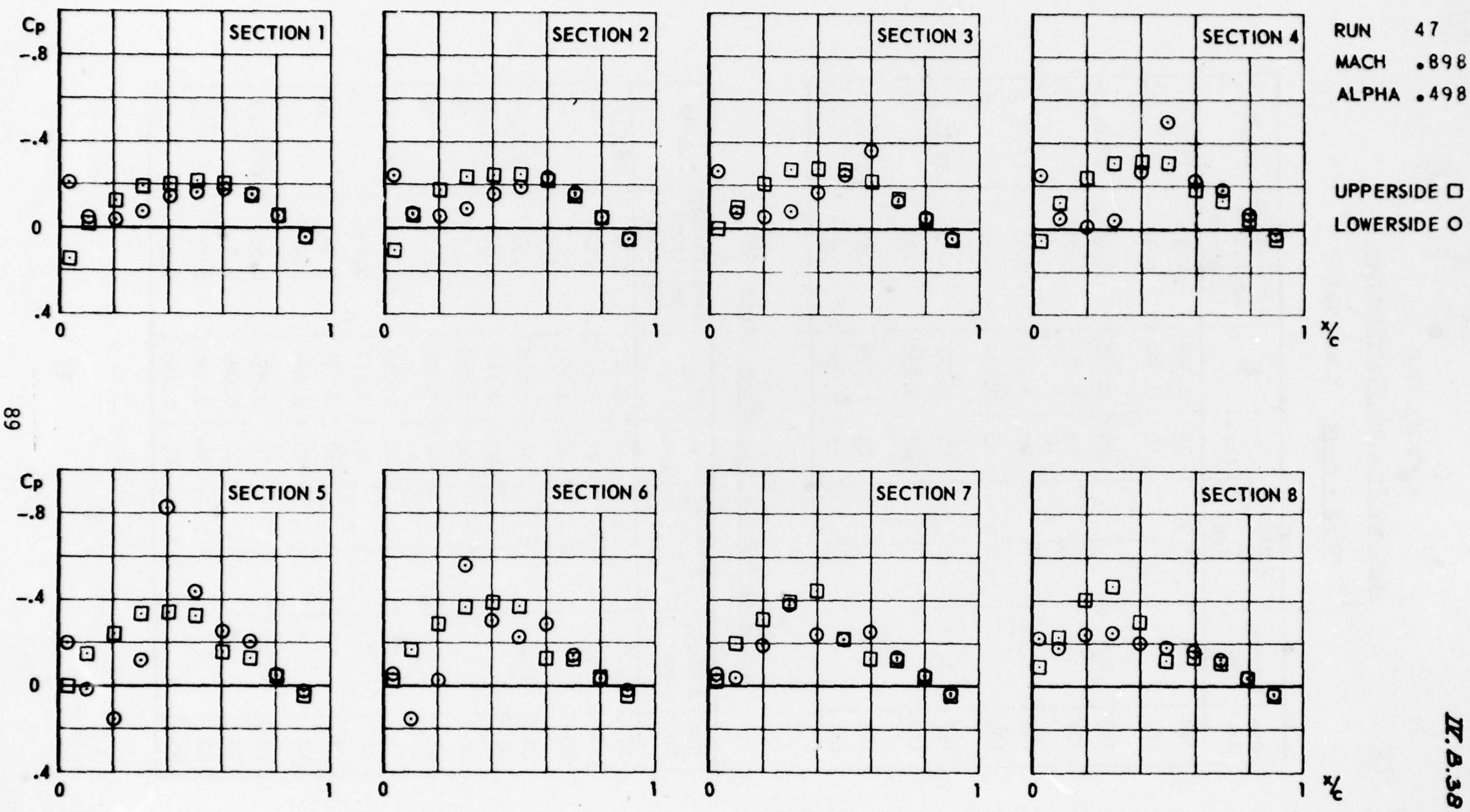

CONF. 301 (WING + PYLON + LAUNCHER + COMPLETE MISSILE)

FIG. IV.B.38

APPENDIX IV.C

Unsteady Pressure Distributions

Wing + Pylon (Conf. 10)

Run No.	Nominal Ma	Nominal $P_o \times 10^{-5}$ (Pa)	F (Hz)	K	Oscillation amplitude (degrees)	Fig.No.
128	0.6	1.0	20	0.199	0.53	IV.C. 1
129			40	0.399	0.22	2
123	0.9		20	0.137	0.53	IV.C. 3
124			40	0.273	0.22	4
114	1.10		20	0.115	0.53	IV.C. 5
115		1.0	40	0.231	0.22	6
109	1.10	0.7	20	0.117	0.52	IV.C. 7
110			40	0.233	0.22	8
104	1.35		20	0.099	0.53	IV.C. 9
105		0.7	40	0.199	0.22	10

Wing + Pylon + Launcher (Conf. 20)

Run No.	Nominal Ma	Nominal $P_o \times 10^{-5}$ (Pa)	F (Hz)	K	Oscillation amplitude (degrees)	Fig.No.
57	0.6	0.7	10	0.101	0.52	IV.C.11
58			20	0.201	0.52	12
60			40	0.403	0.23	13
64	0.9		10	0.070	0.53	IV.C.14
65			20	0.140	0.52	15
66			30	0.210	0.37	16
67			40	0.279	0.23	17
71	1.10		10	0.059	0.53	IV.C.18
72			20	0.118	0.53	19
73			30	0.176	0.37	20
74			40	0.234	0.22	21
78	1.35		10	0.050	0.53	IV.C.22
79			20	0.099	0.52	23
80			30	0.149	0.37	24
81		0.7	40	0.199	0.23	25

Wing + Pylon + Launcher + Missile Body + Aft Wings (Conf. 31)

Run No.	Nominal Ma	Nominal $P_o \times 10^{-5}$ (Pa)	F (Hz)	K	Oscillation amplitude (degrees)	Fig.No.
88	0.9	1.0	20	0.141	0.52	IV.C.26
87		1.0	40	0.281	0.23	27
92	1.10	0.7	20	0.118	0.52	IV.C.28
93			40	0.235	0.22	29
97	1.35		20	0.099	0.52	IV.C.30
98		0.7	40	0.199	0.22	31

Wing + Pylon + Launcher + Complete Missile (Conf. 301)

Run No.	Nominal Ma	Nominal $P_o \times 10^{-5}$ (Pa)	F (Hz)	K	Oscillation amplitude (degrees)	Fig.No.
43	0.6	1.0	20	0.201	0.53	IV.C.32
44			40	0.400	0.23	33
48	0.9		20	0.138	0.52	IV.C.34
49		1.0	40	0.276	0.22	35

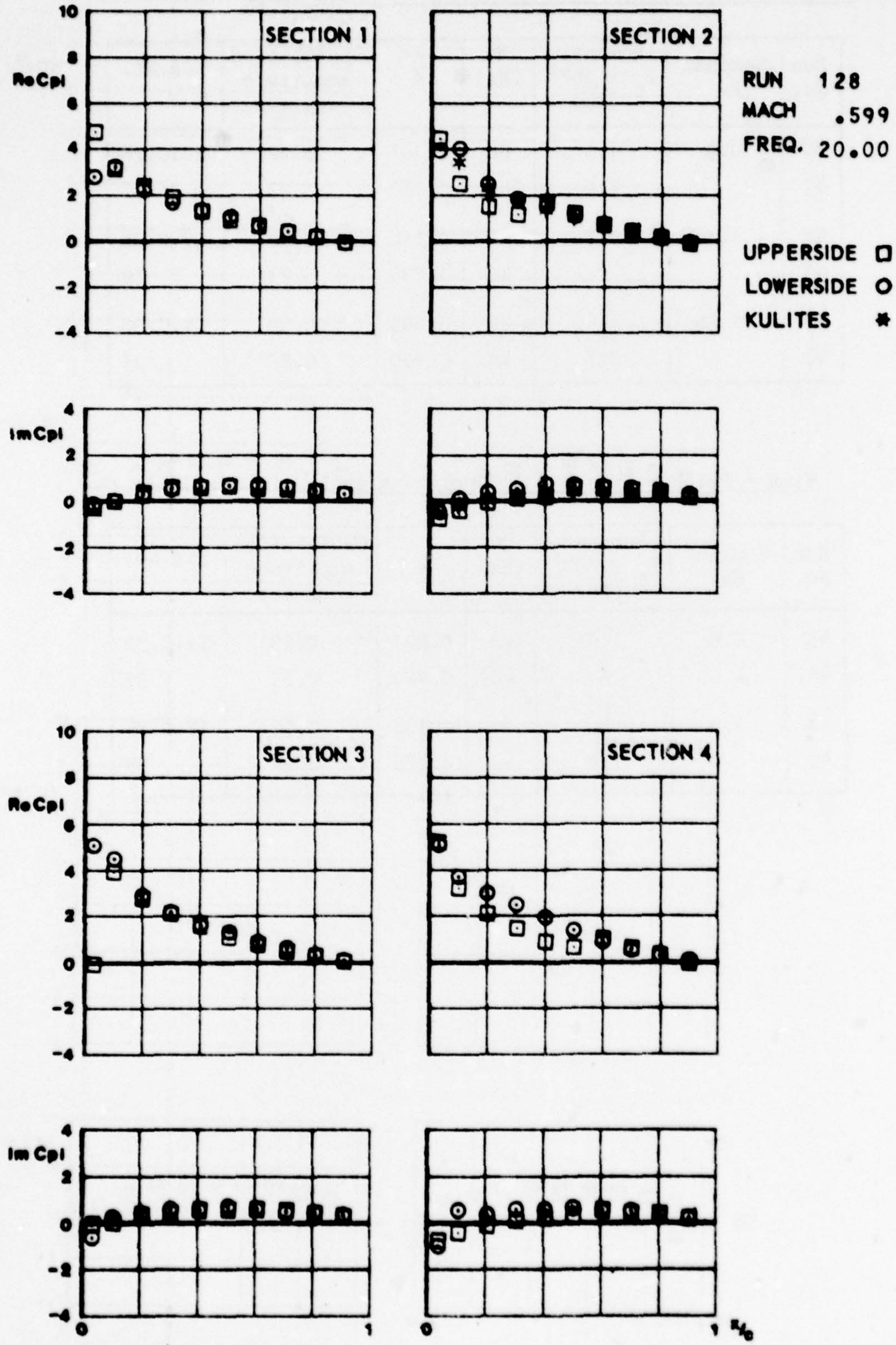

CONF.10 (WING + PYLON)

FIG. IV.C.1.6

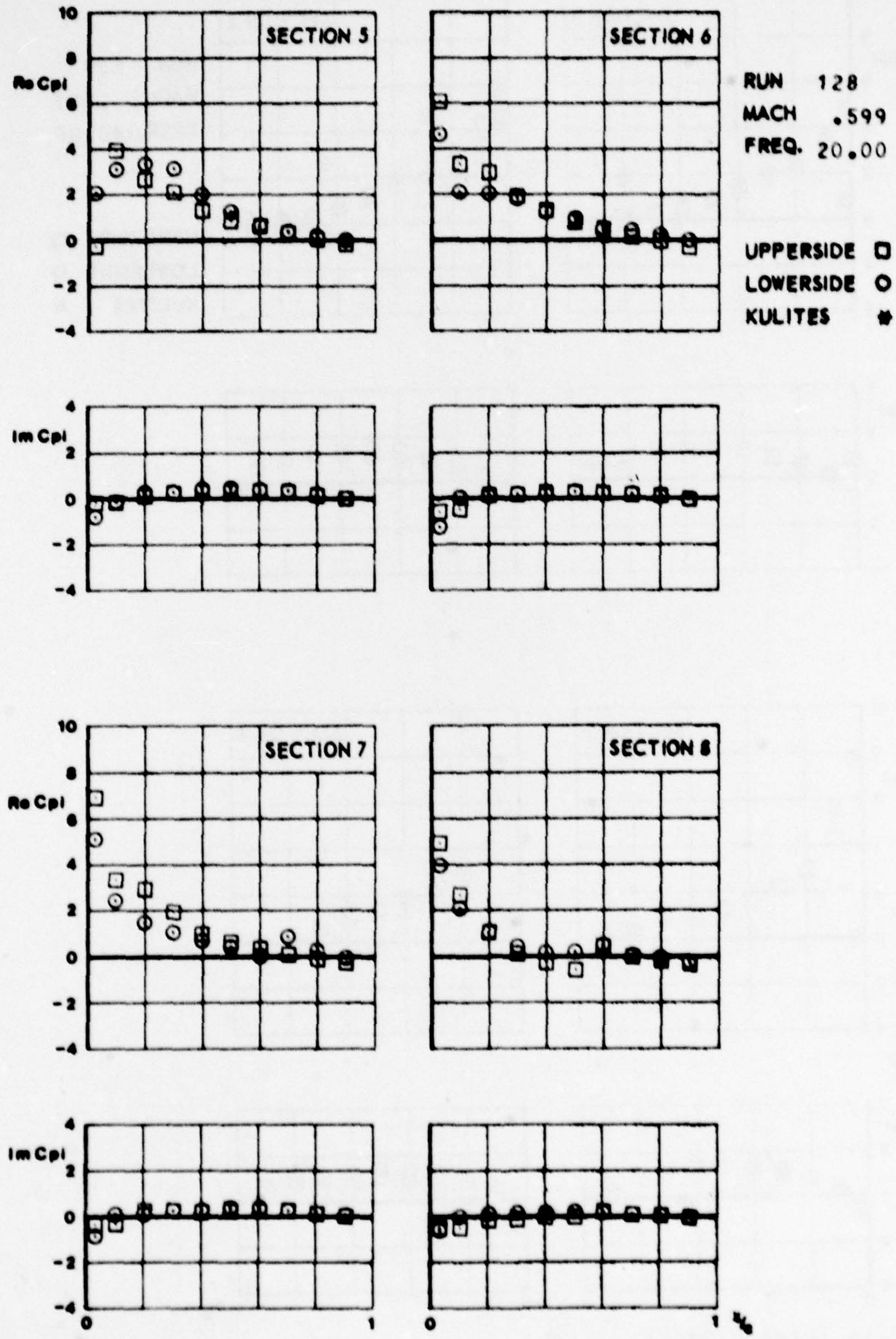

CONF. 10 (WING + PYLON)

FIG.
IV.C.2a

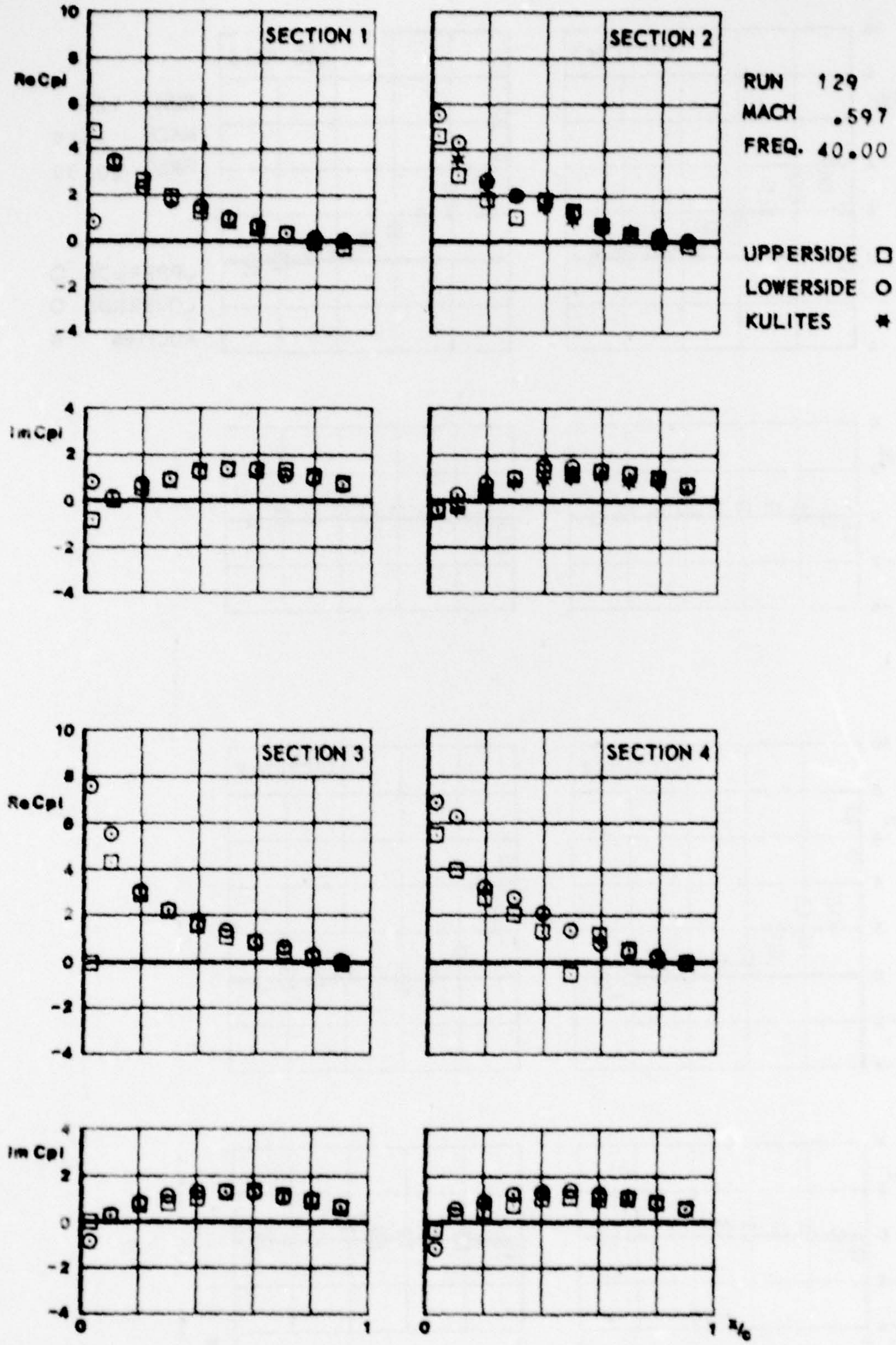

CONF.10 (WING + PYLON)

FIG. IV.C.2.b

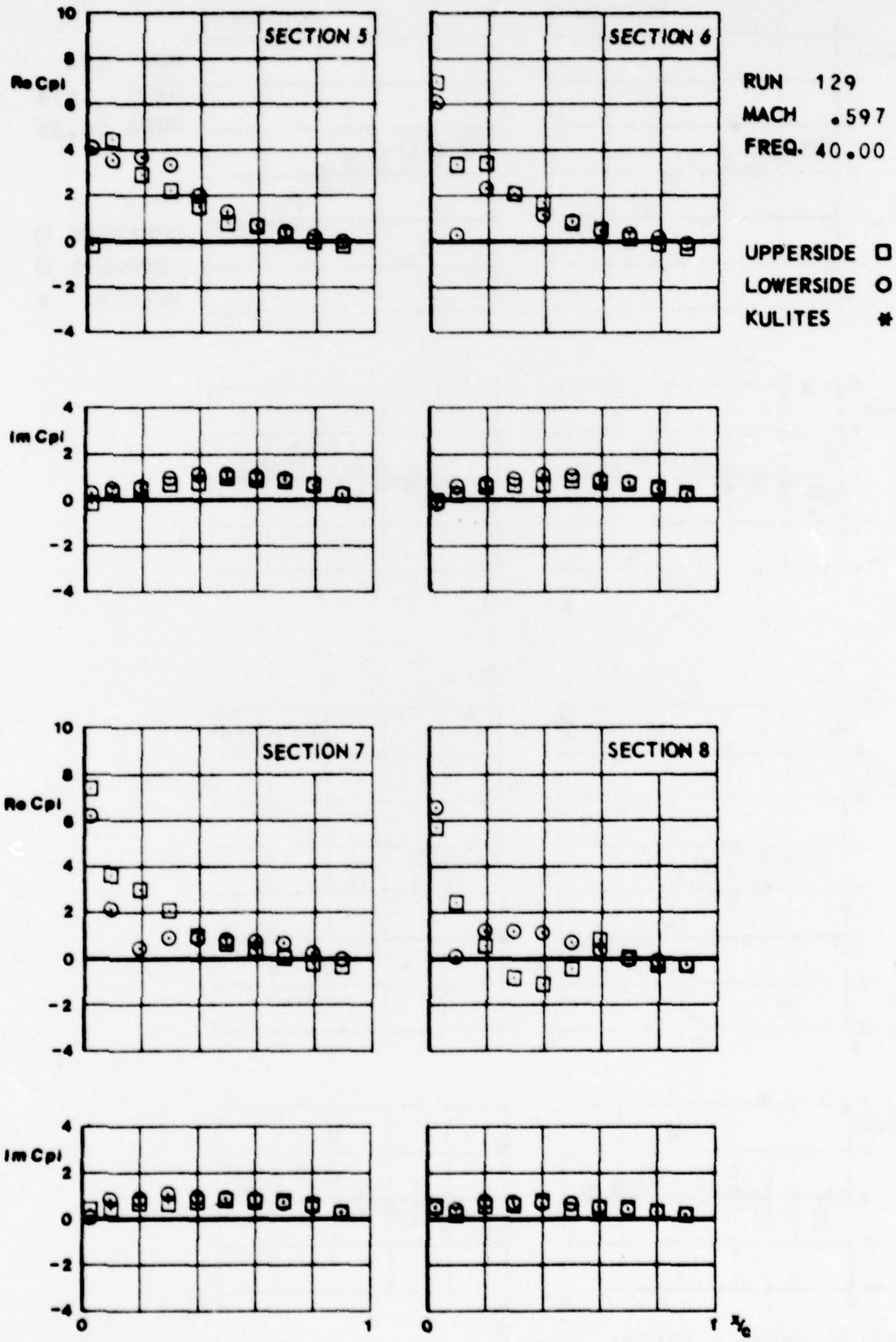

CONF. 10 (WING + PYLON)

FIG.
IV.C.3.a

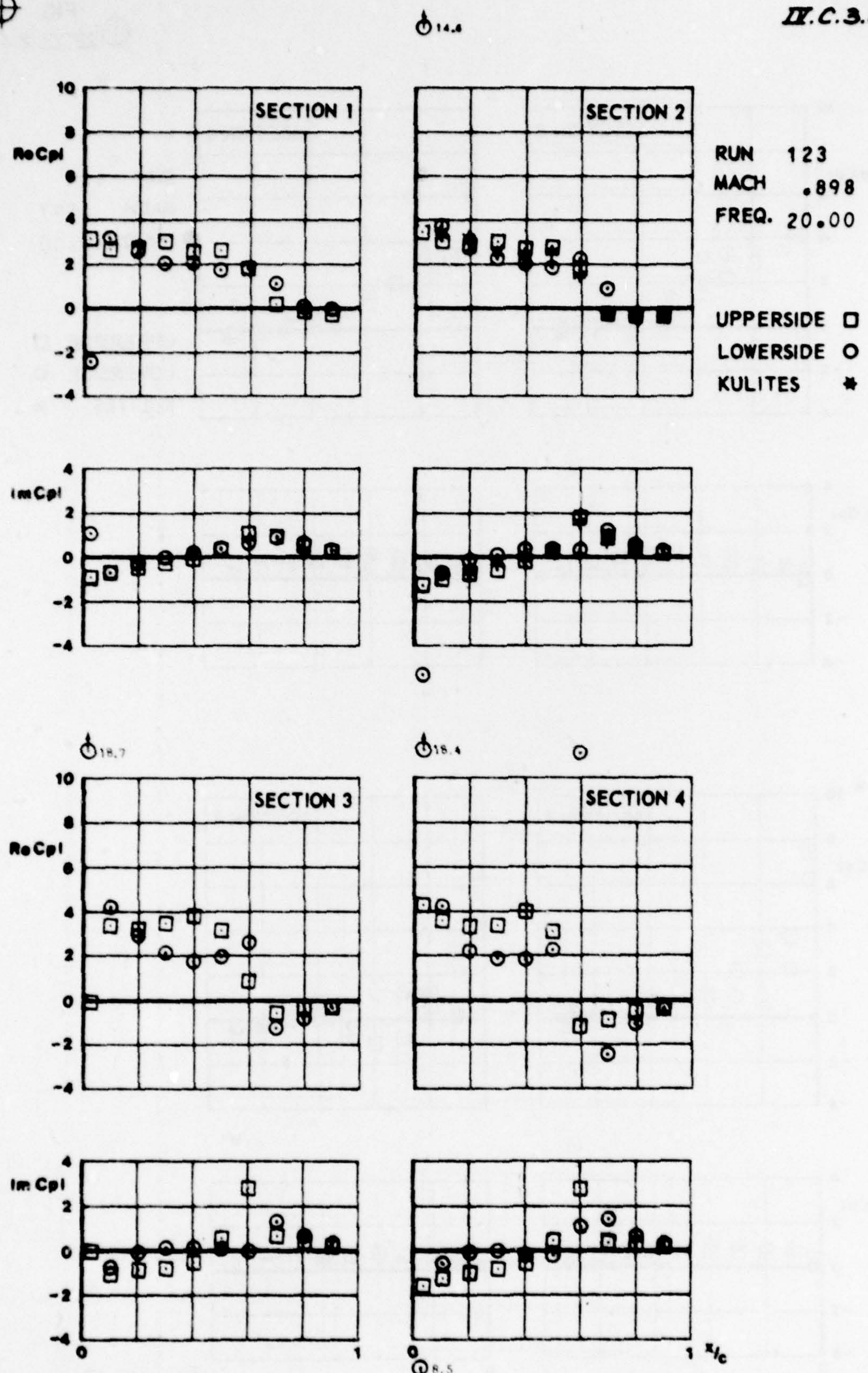

CONF. 10 (WING + PYLON)

FIG. IV.C.3.b

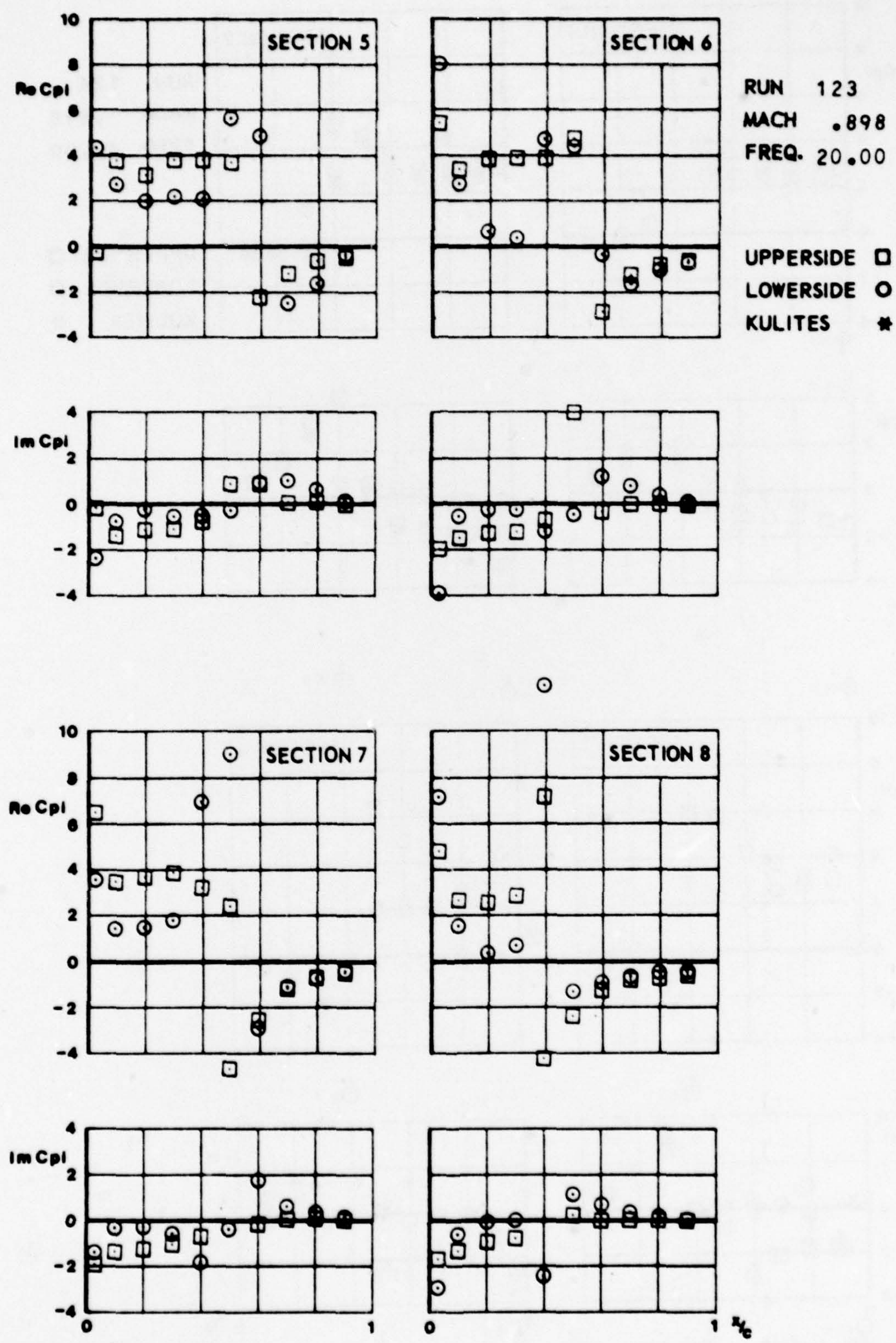

CONF. 10 (WING + PYLON)

FIG.
IV.C.4.a

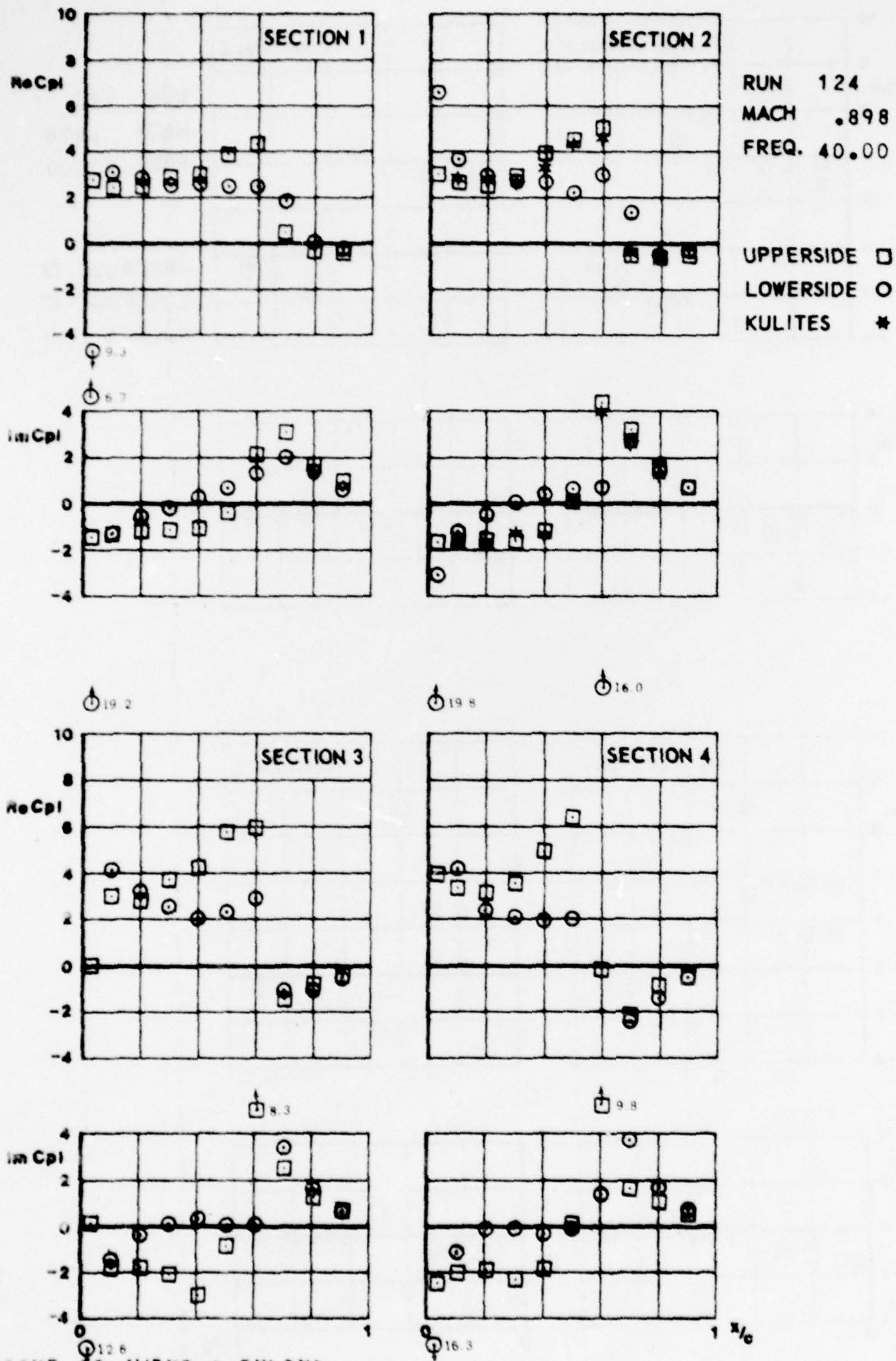

CONF. 10 (WING + PYLON)

FIG.
IV.C.4.b

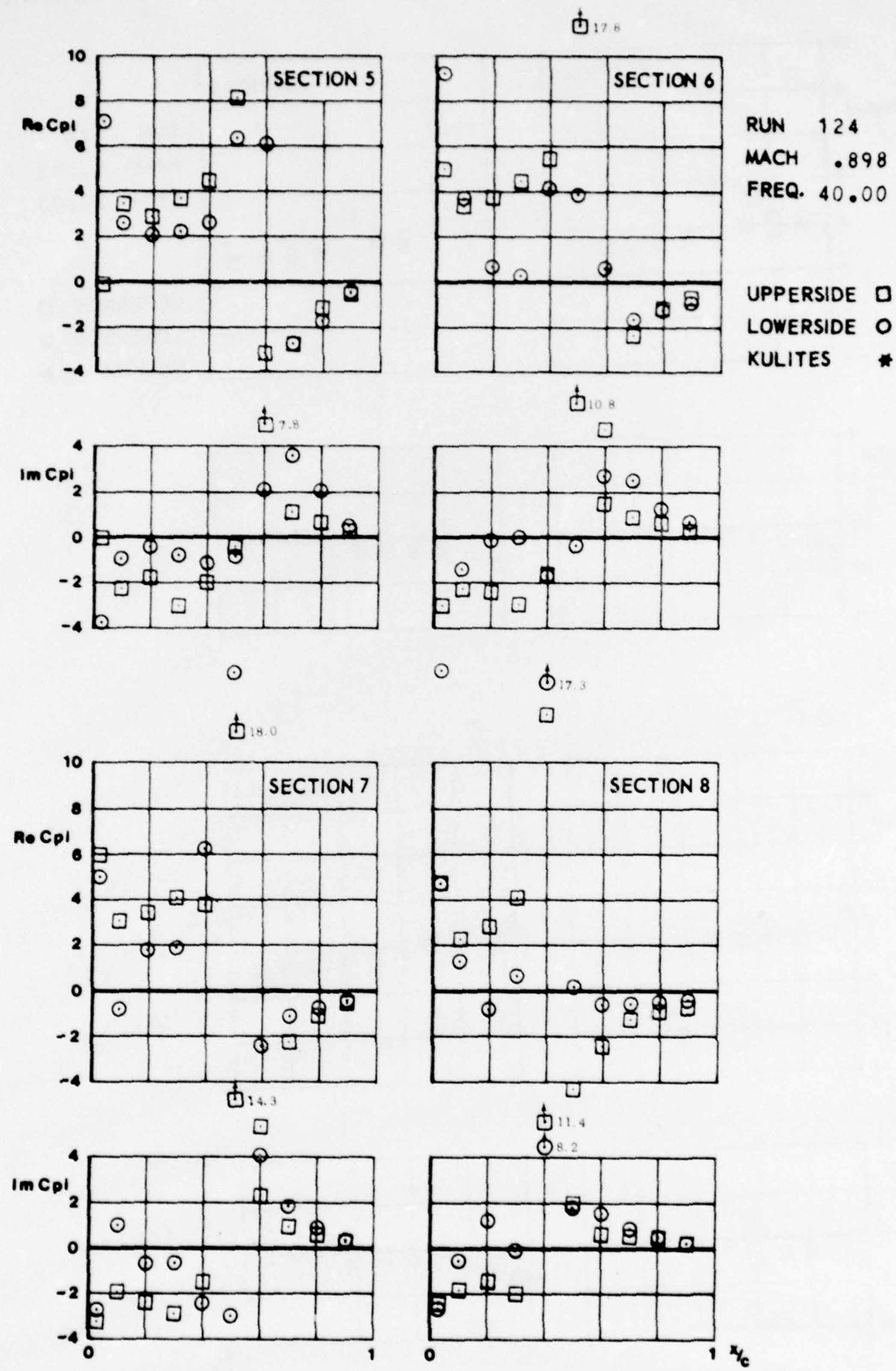

CONF. 10 (WING + PYLON)

FIG.
IV.C.5.a

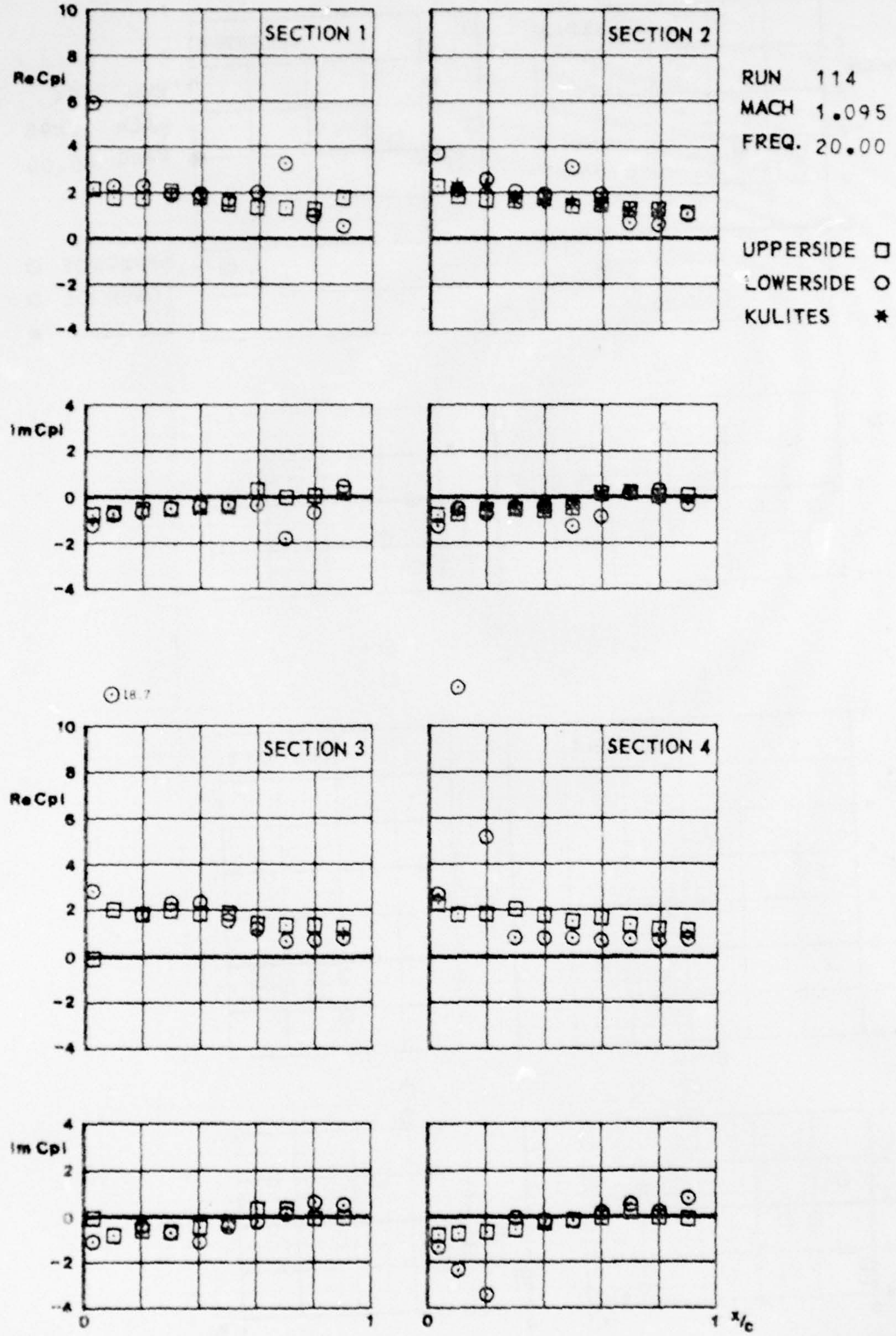

CONF.10 (WING + PYLON)

FIG. IV.C.5.6

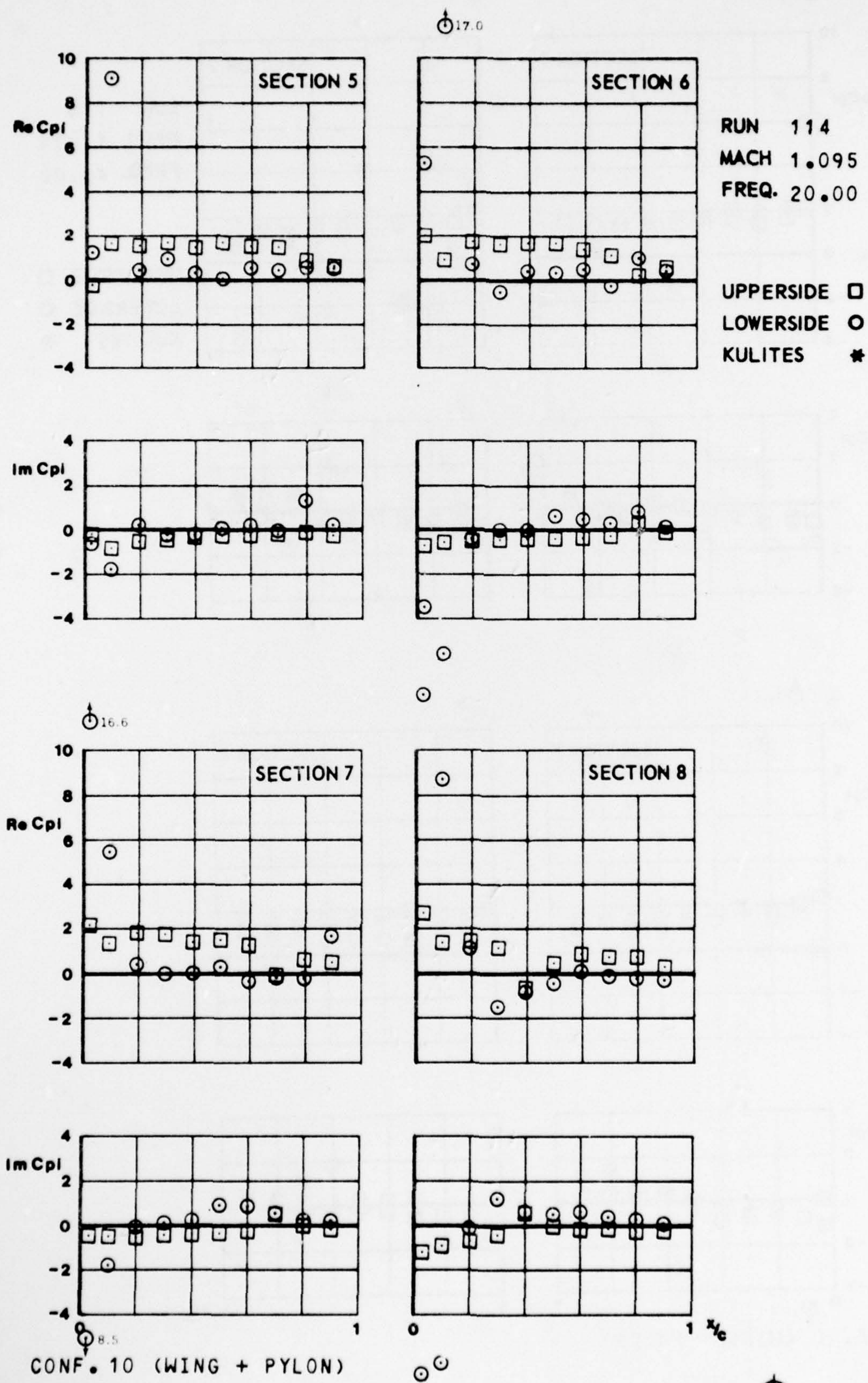

CONF. 10 (WING + PYLON)

FIG.
IV.C.6.a

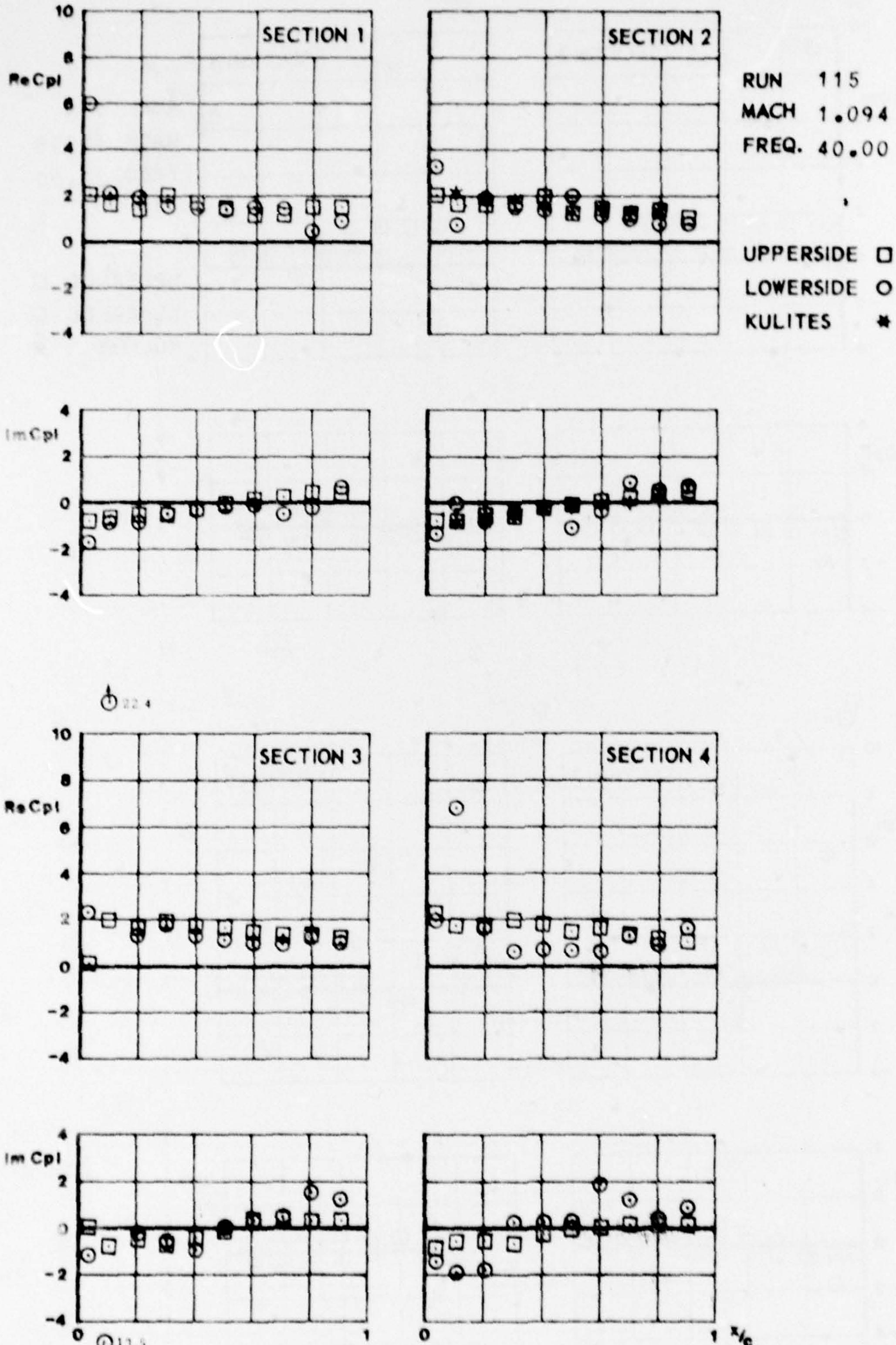

CONF.10 (WING + PYLON)

FIG.
IV.C.6.6

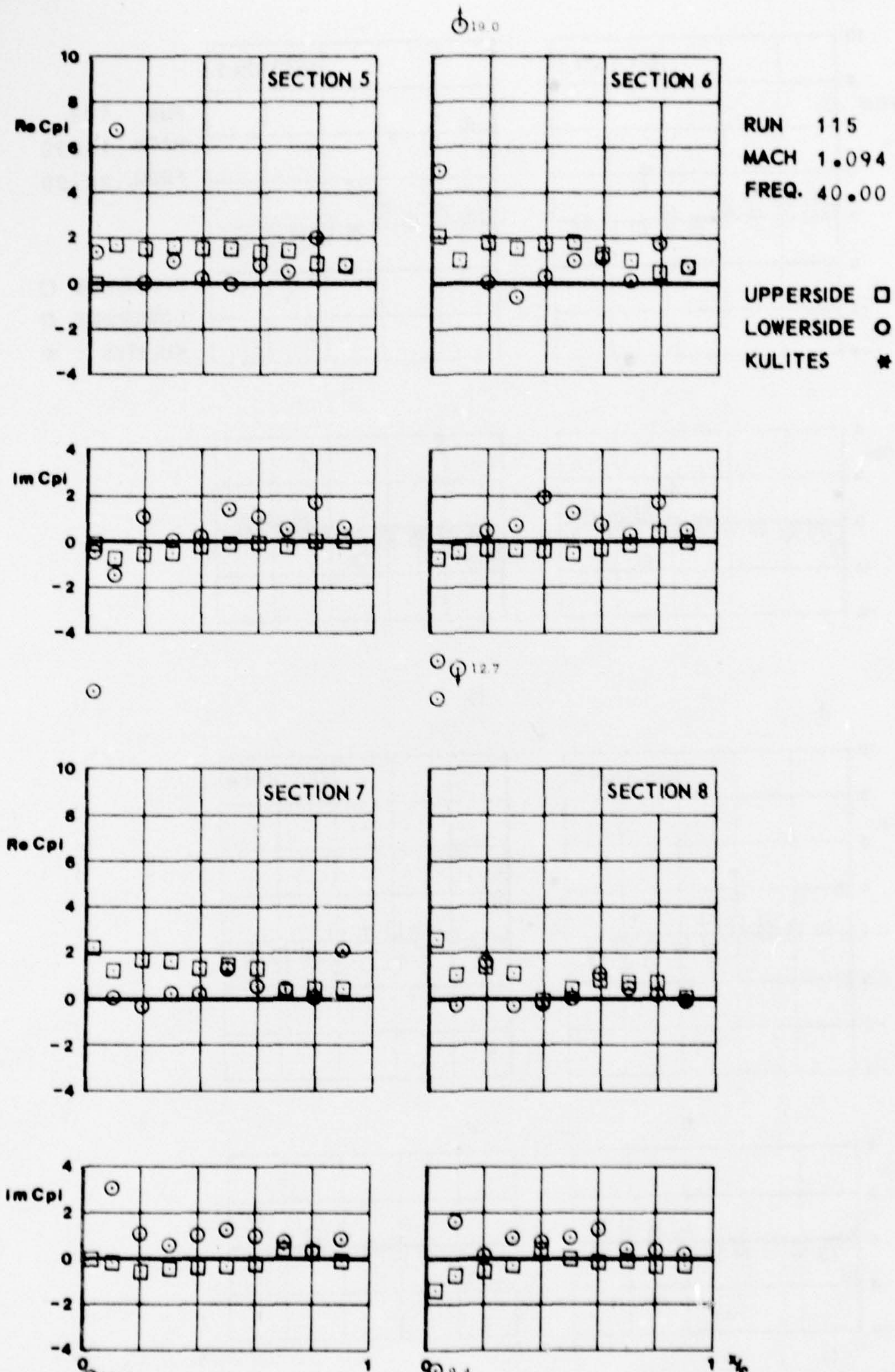

CONF. 10 (WING + PYLON)

FIG.
IV. C. 7. a

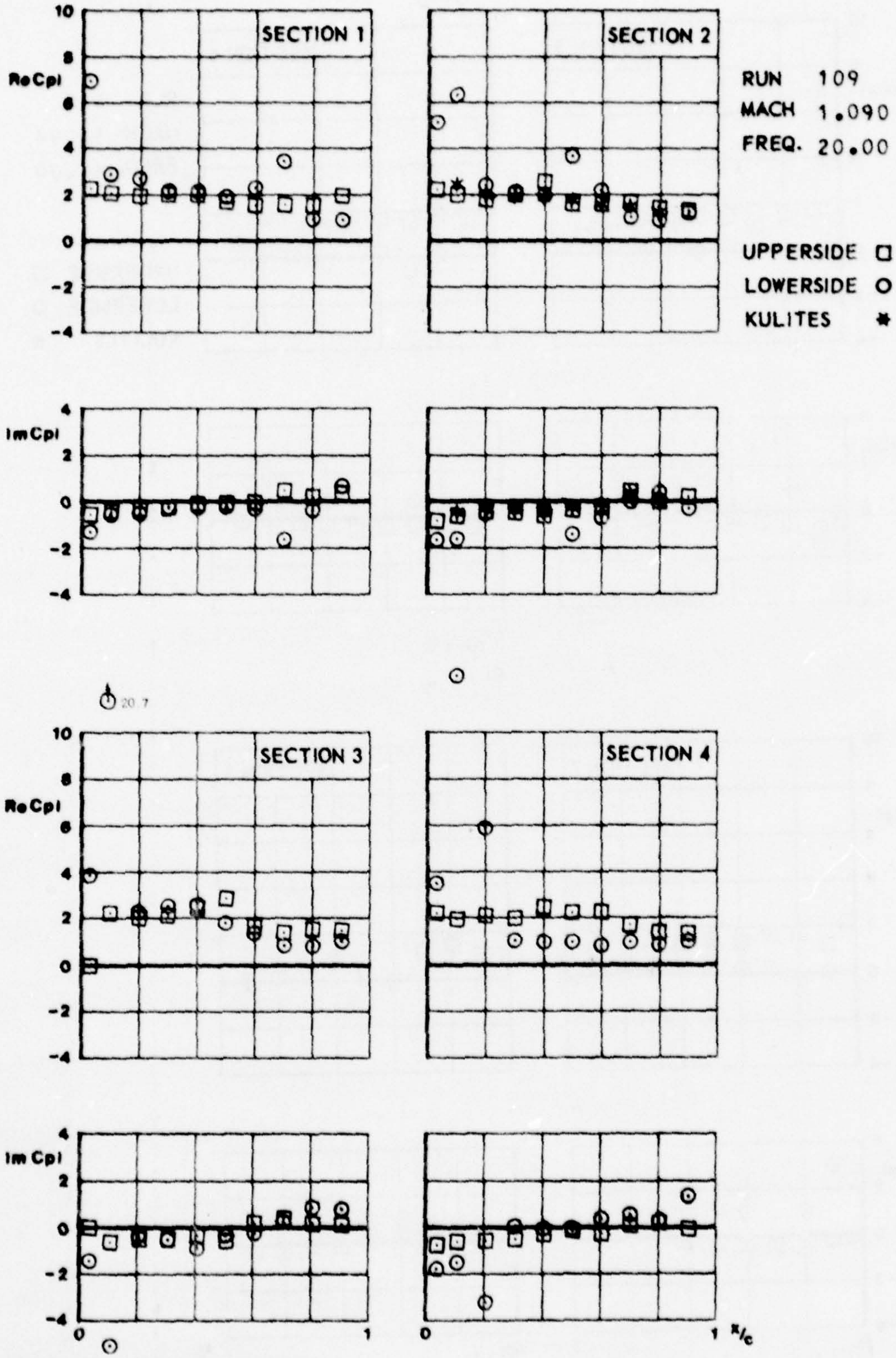

CONF.10 (WING + PYLON)

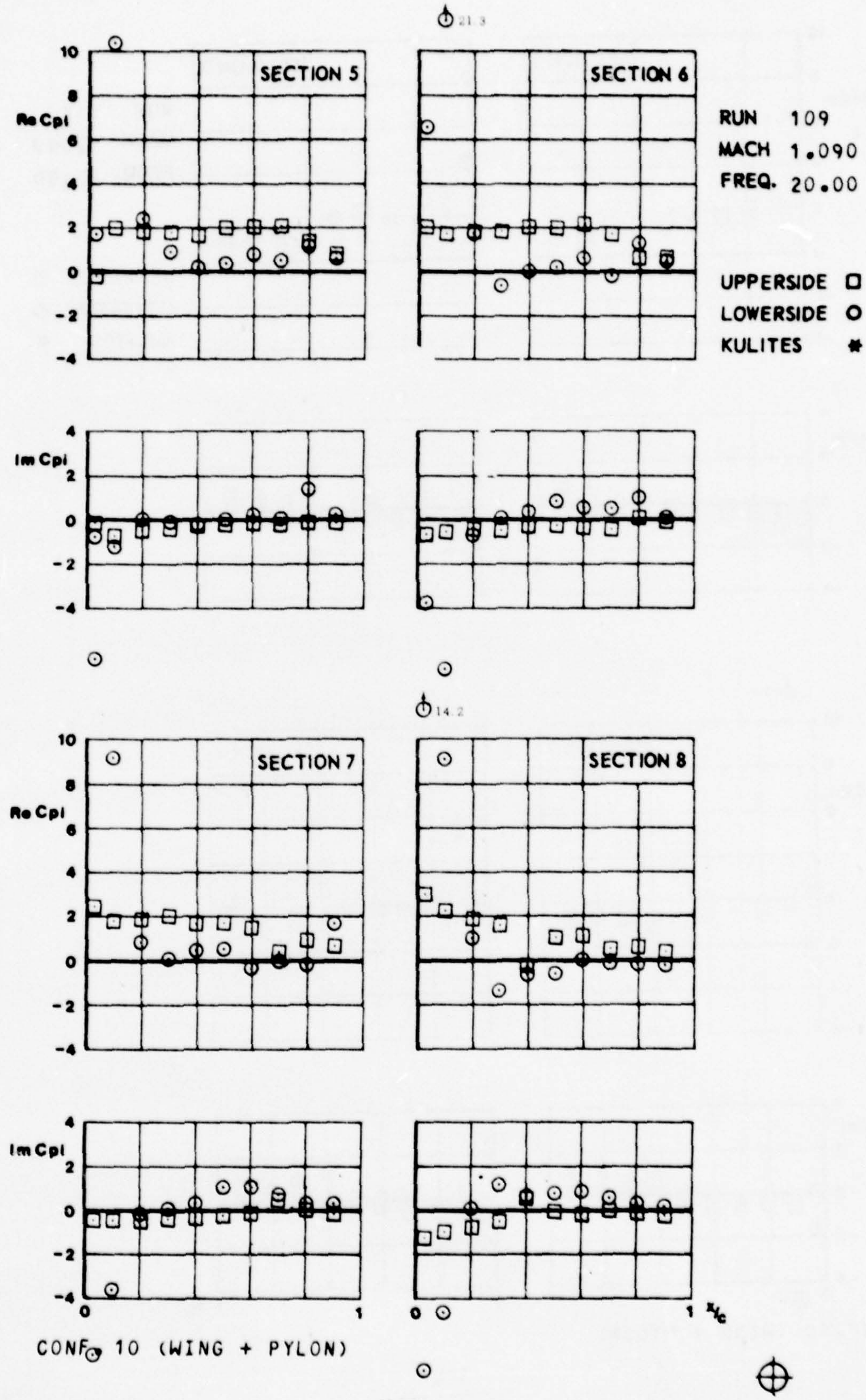
SECTION 5
SECTION 6
SECTION 7
SECTION 8
Re Cpi
Im Cpi
21.3
14.2
RUN 109
MACH 1.090
FREQ. 20.00
UPPERSIDE □
LOWERSIDE O
KULITES *
x/c
CONF. 10 (WING + PYLON)

FIG.
IV.C.8.a

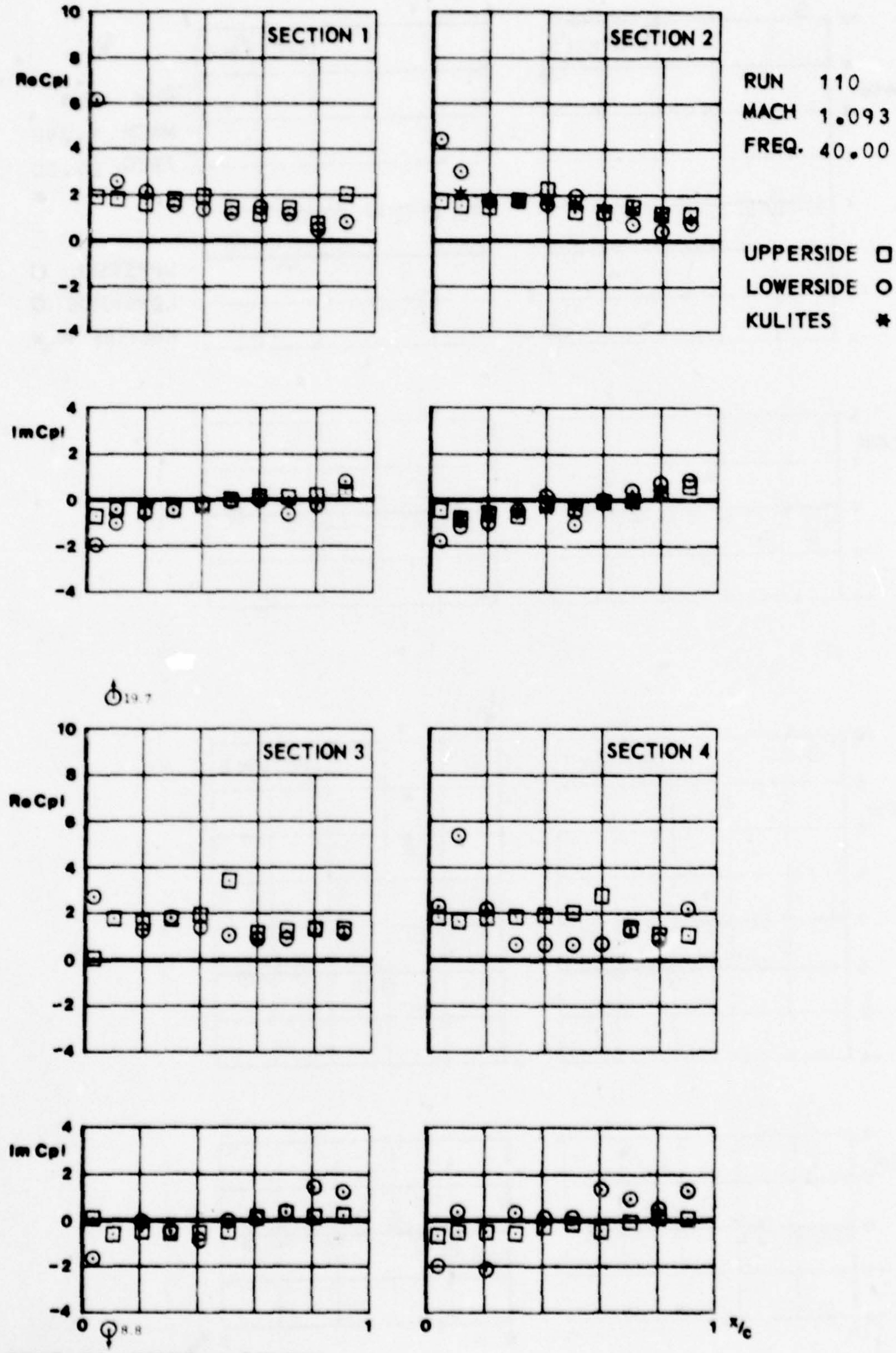

CONF.10 (WING + PYLON)

FIG. IV.C.8.b

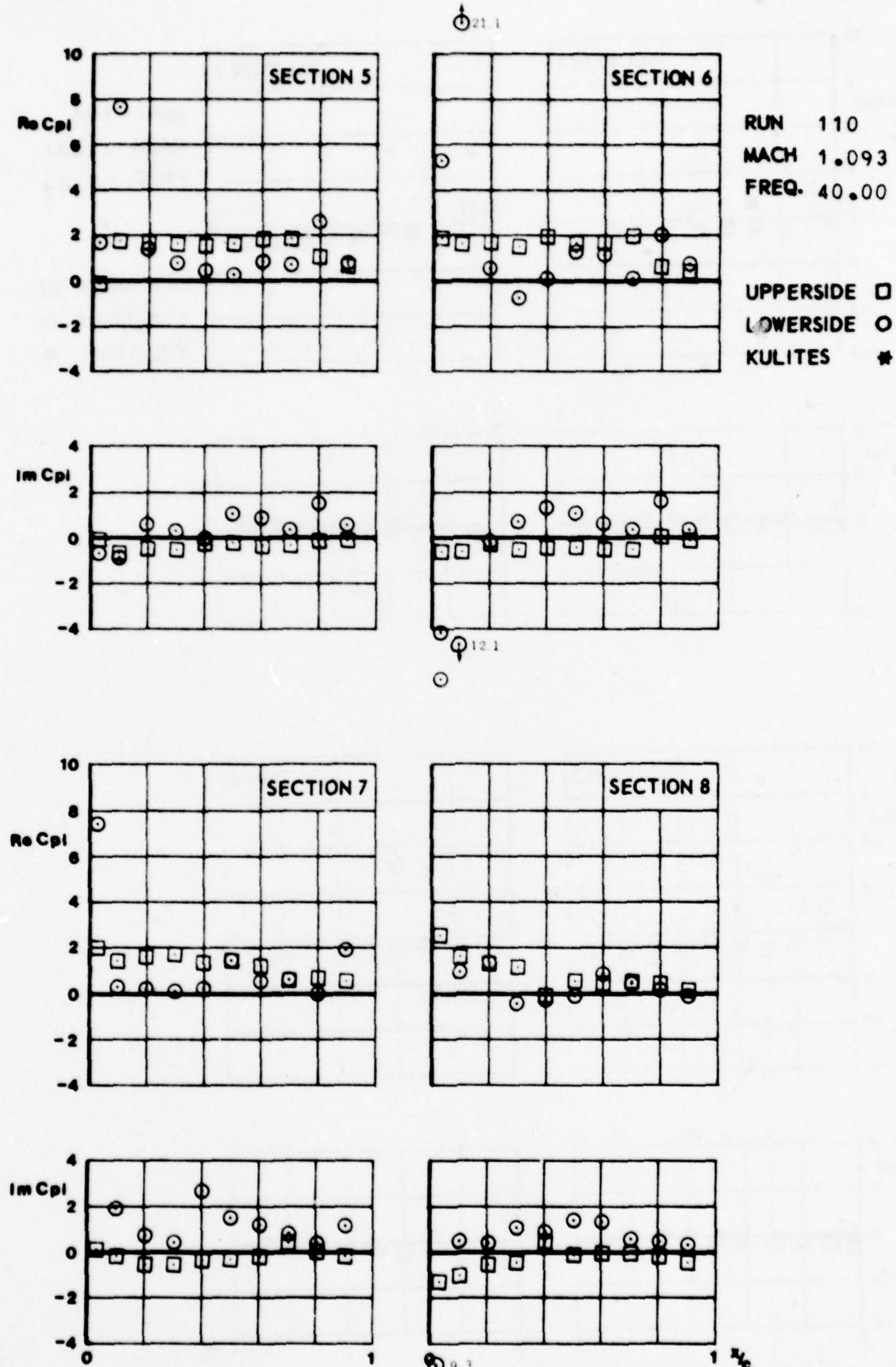

CONF. 10 (WING + PYLON)

FIG.
IV.C.9.a

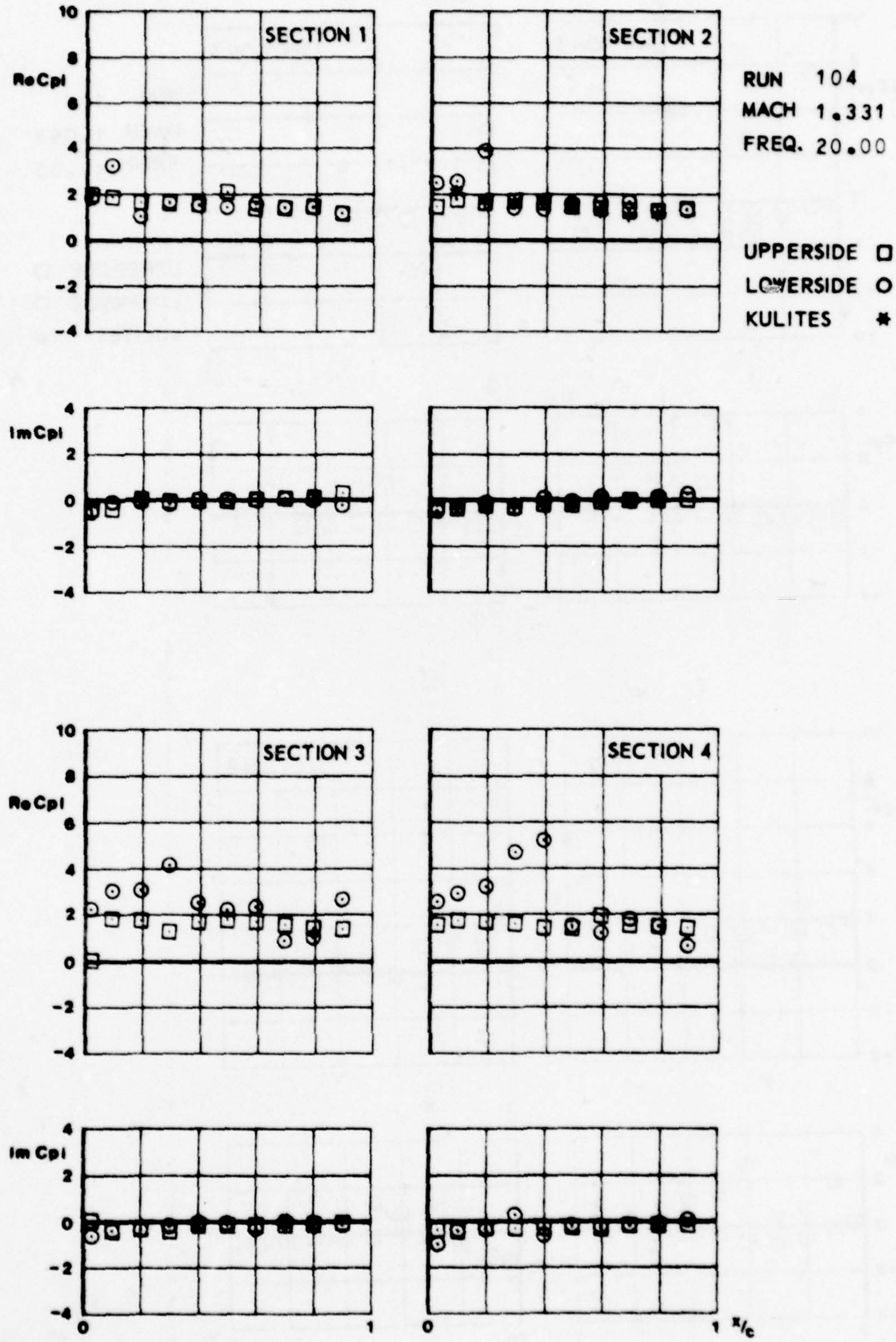

CONF.10 (WING + PYLON)

FIG. IV.C.9.b

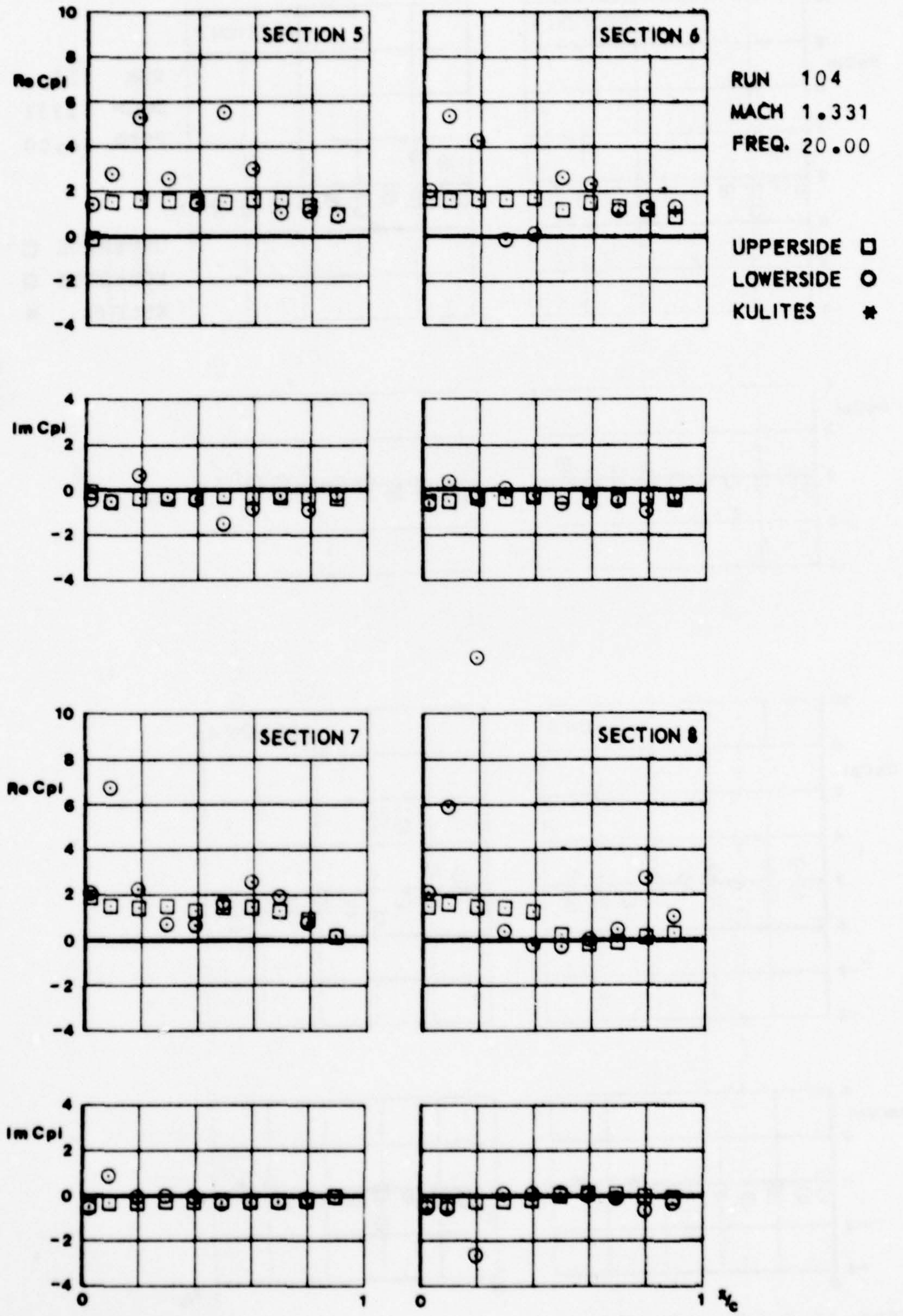

CONF. 10 (WING + PYLON)

FIG.
IV.C.10.a

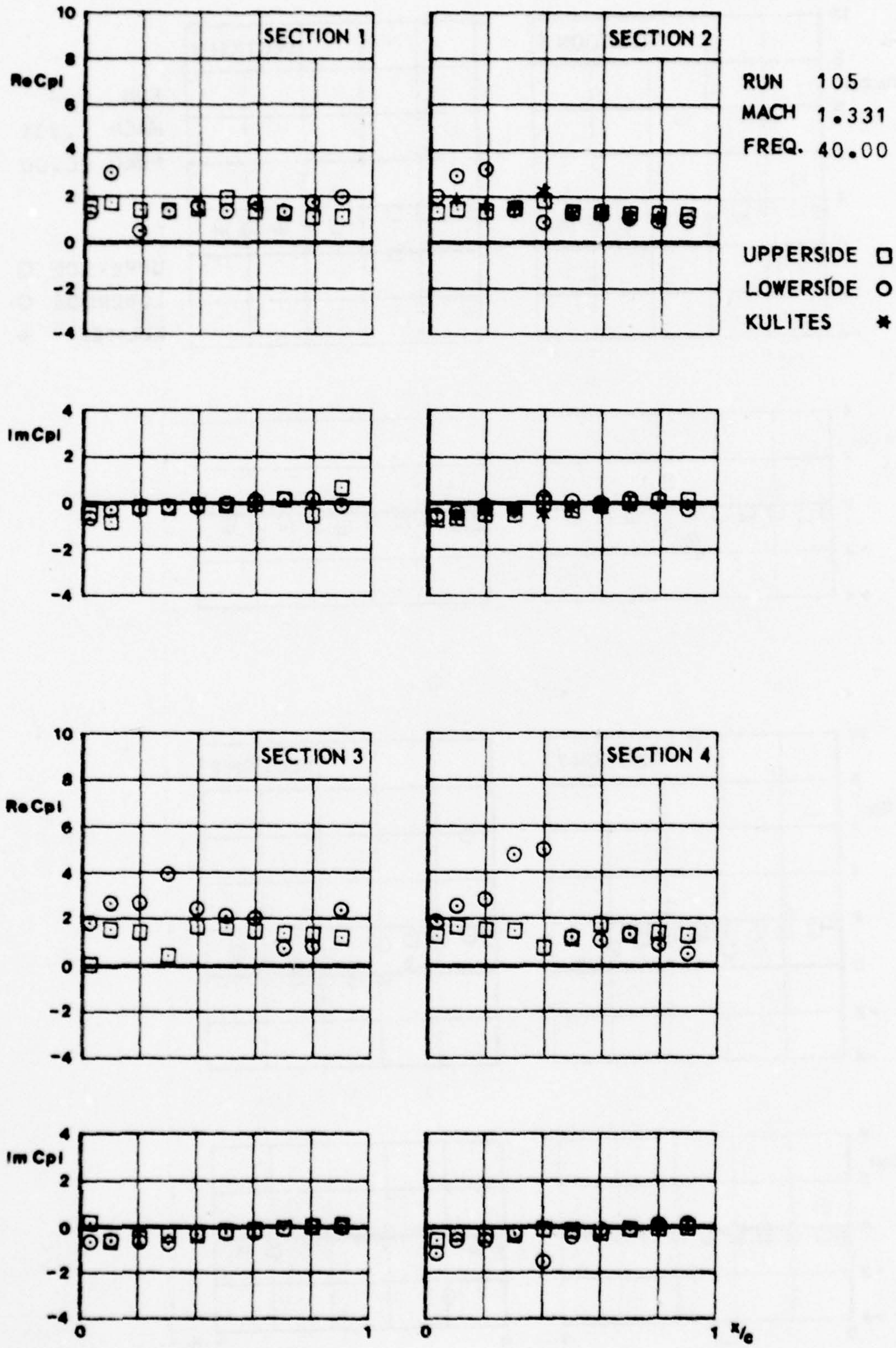

CONF.10 (WING + PYLON)

FIG. IV.C.10.b

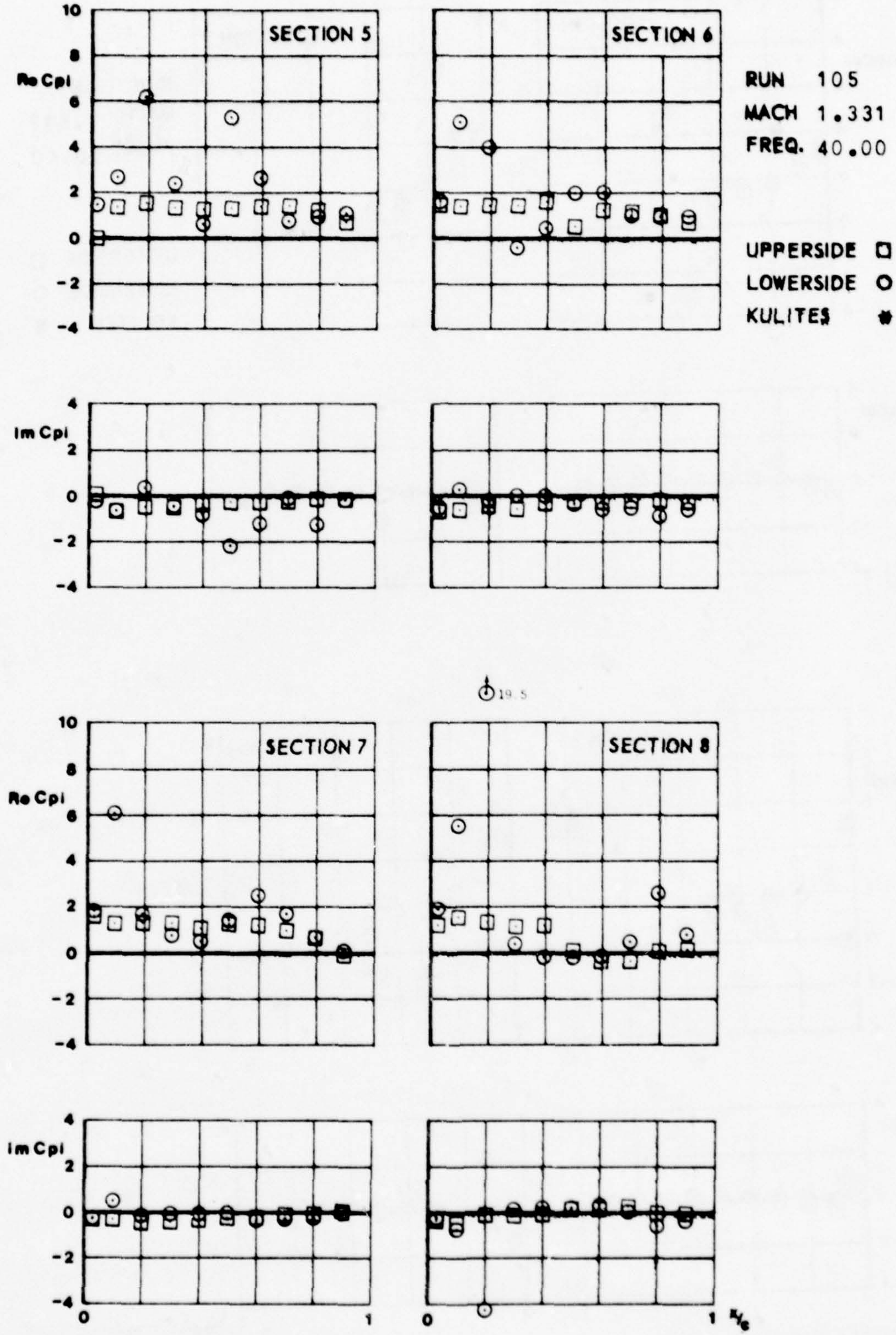

CONF. 10 (WING + PYLON)

FIG.
IV.C.11.a

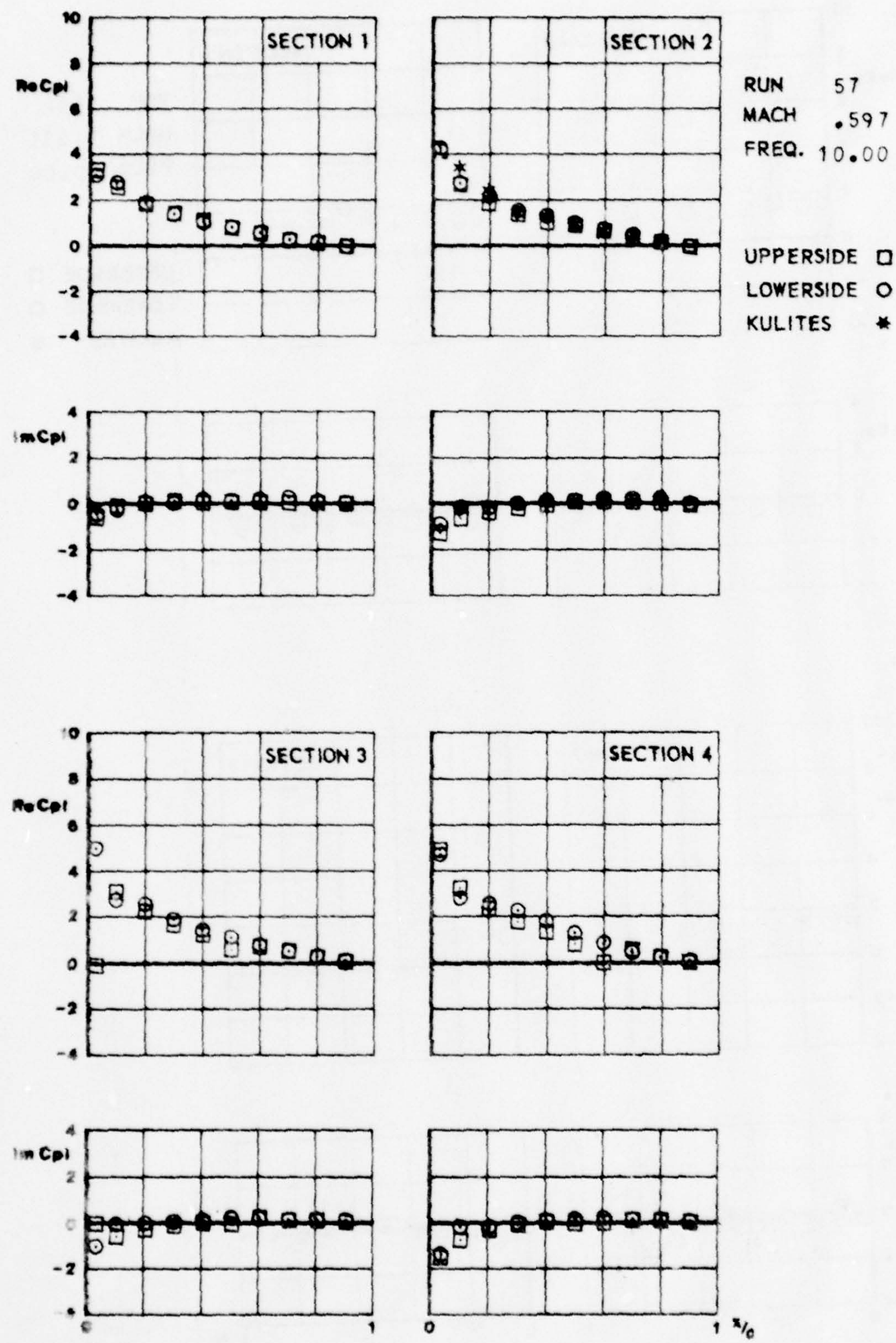

CONF.20 (WING + PYLON + LAUNCHER)

FIG. IV.C.11.b

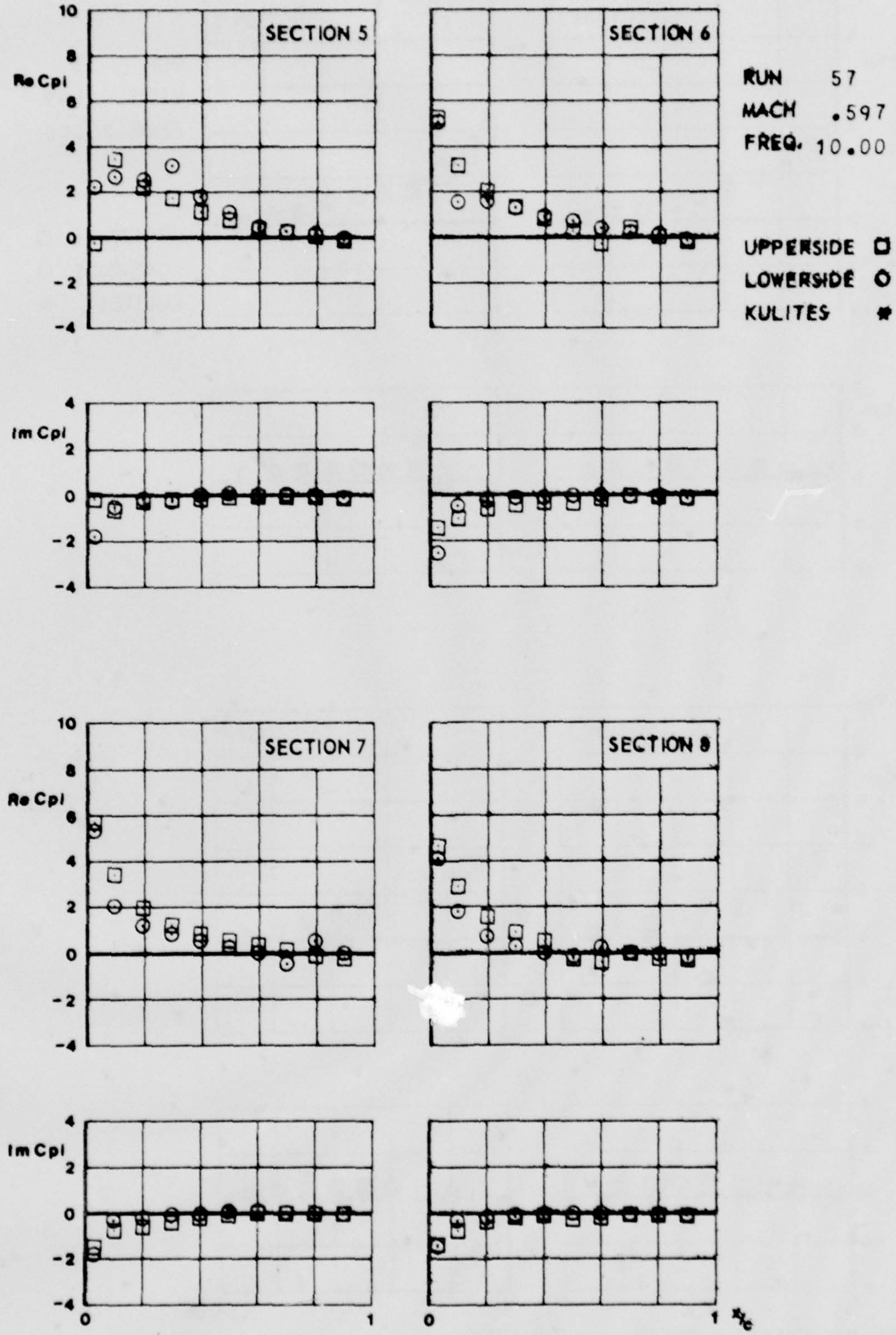

CONF. 20 (WING + PYLON + LAUNCHER)

FIG.
IV.C.12.a

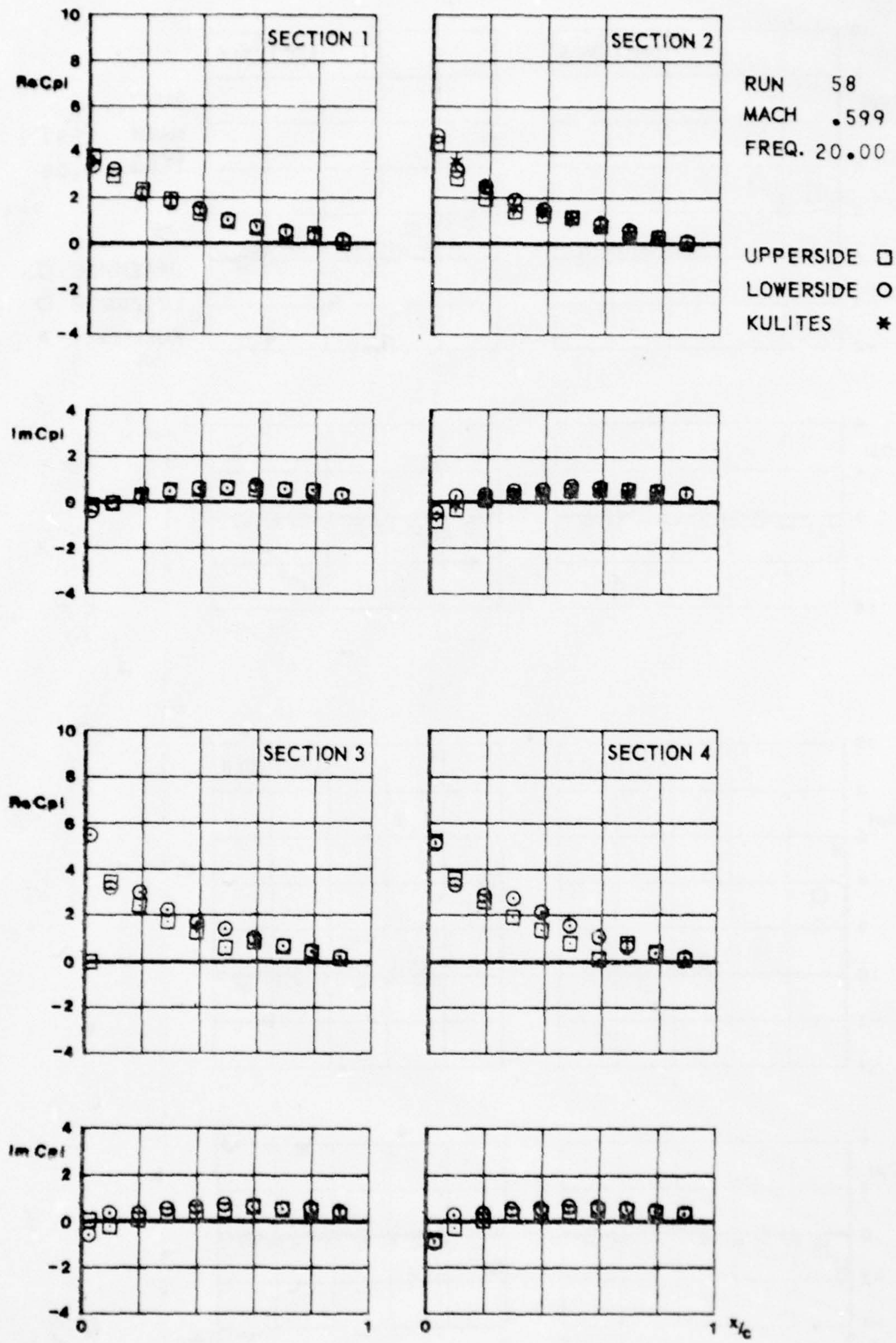

CONF. 20 (WING + PYLON + LAUNCHER)

FIG.
IV.C.12.b

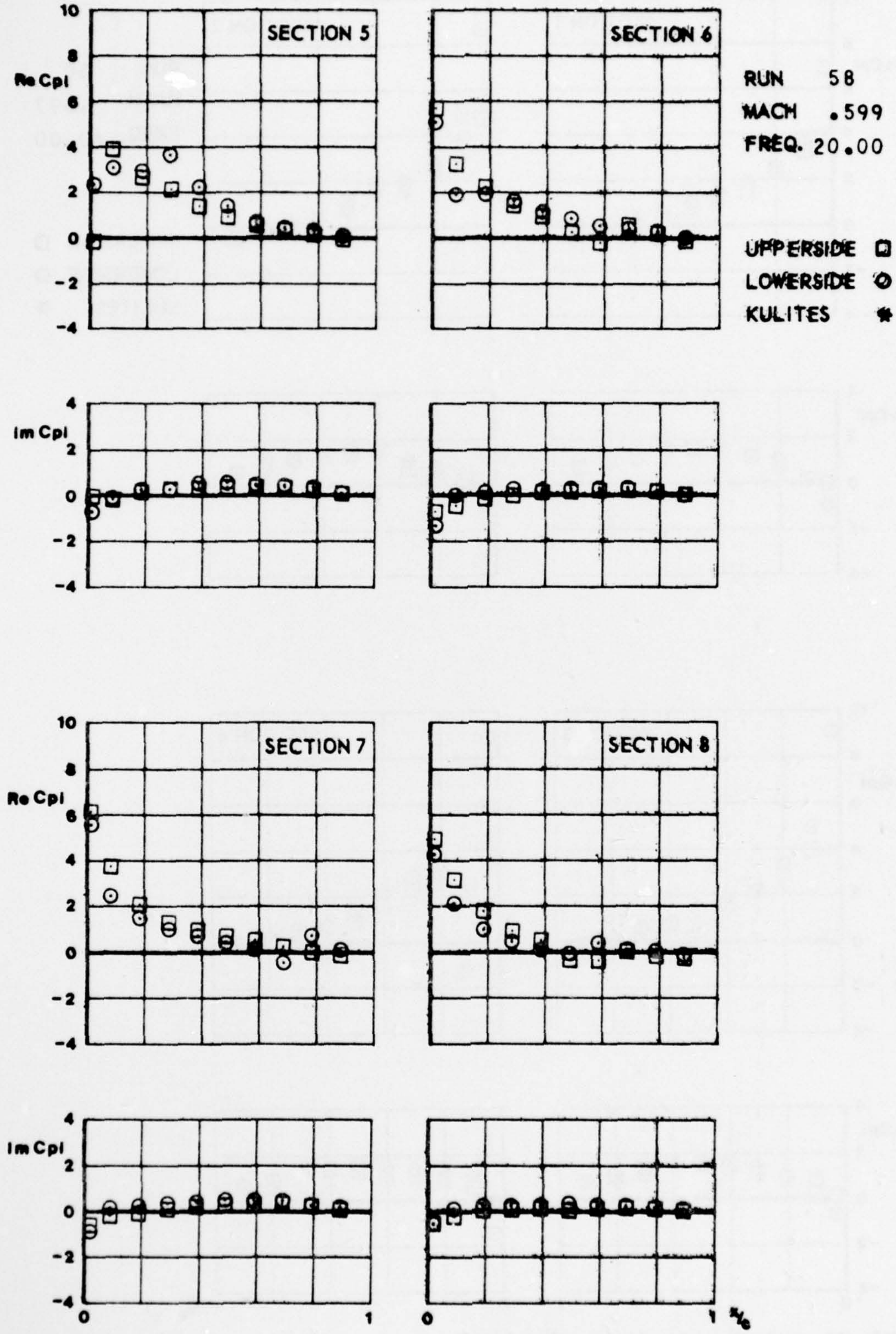

CONF. 20 (WING + PYLON + LAUNCHER)

FIG.
IV.C.13.a

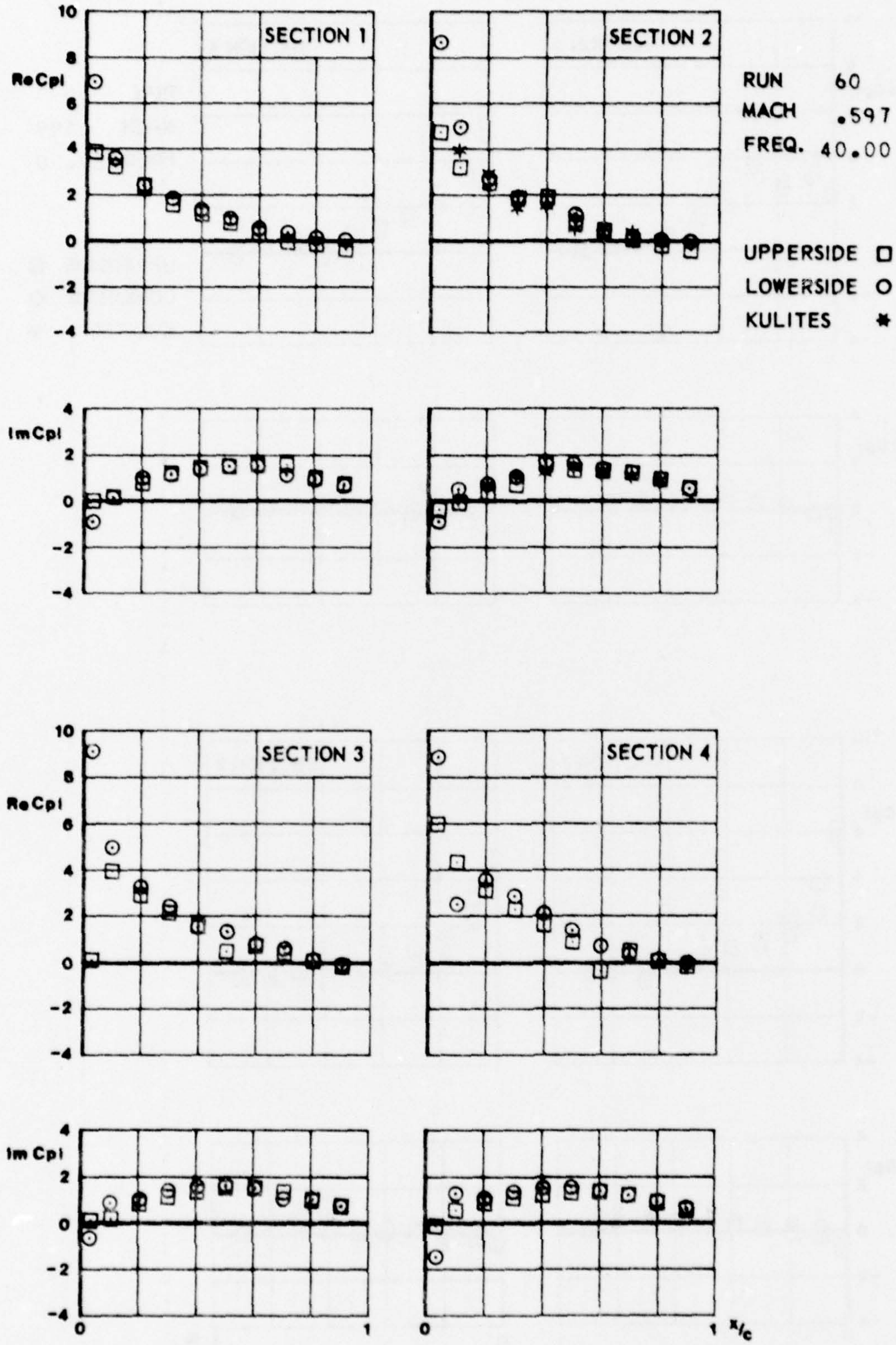

CONF.20 (WING + PYLON + LAUNCHER)

FIG. IV.C.13.6

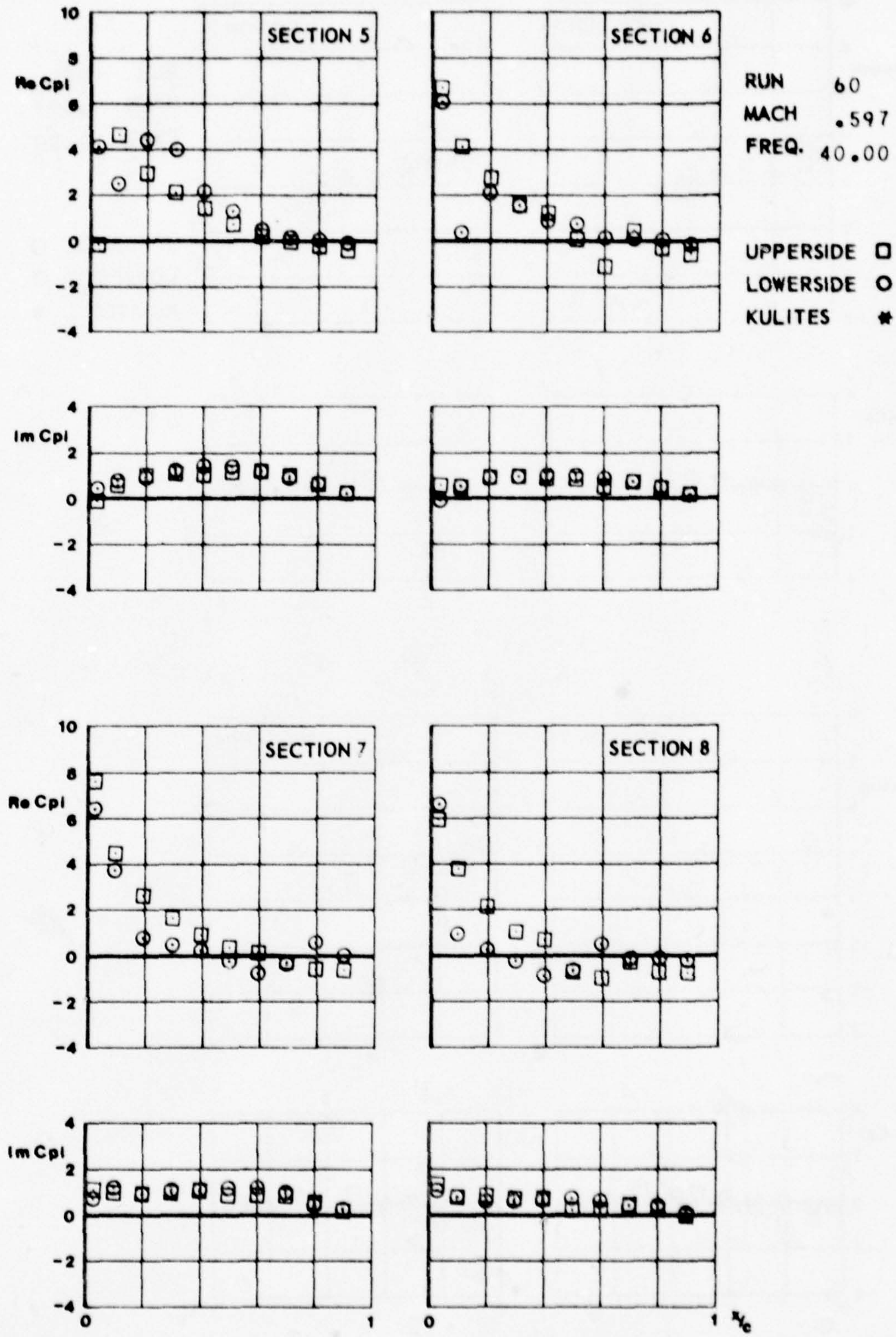

CONF. 20 (WING + PYLON + LAUNCHER)

FIG.
IV.C.14.a

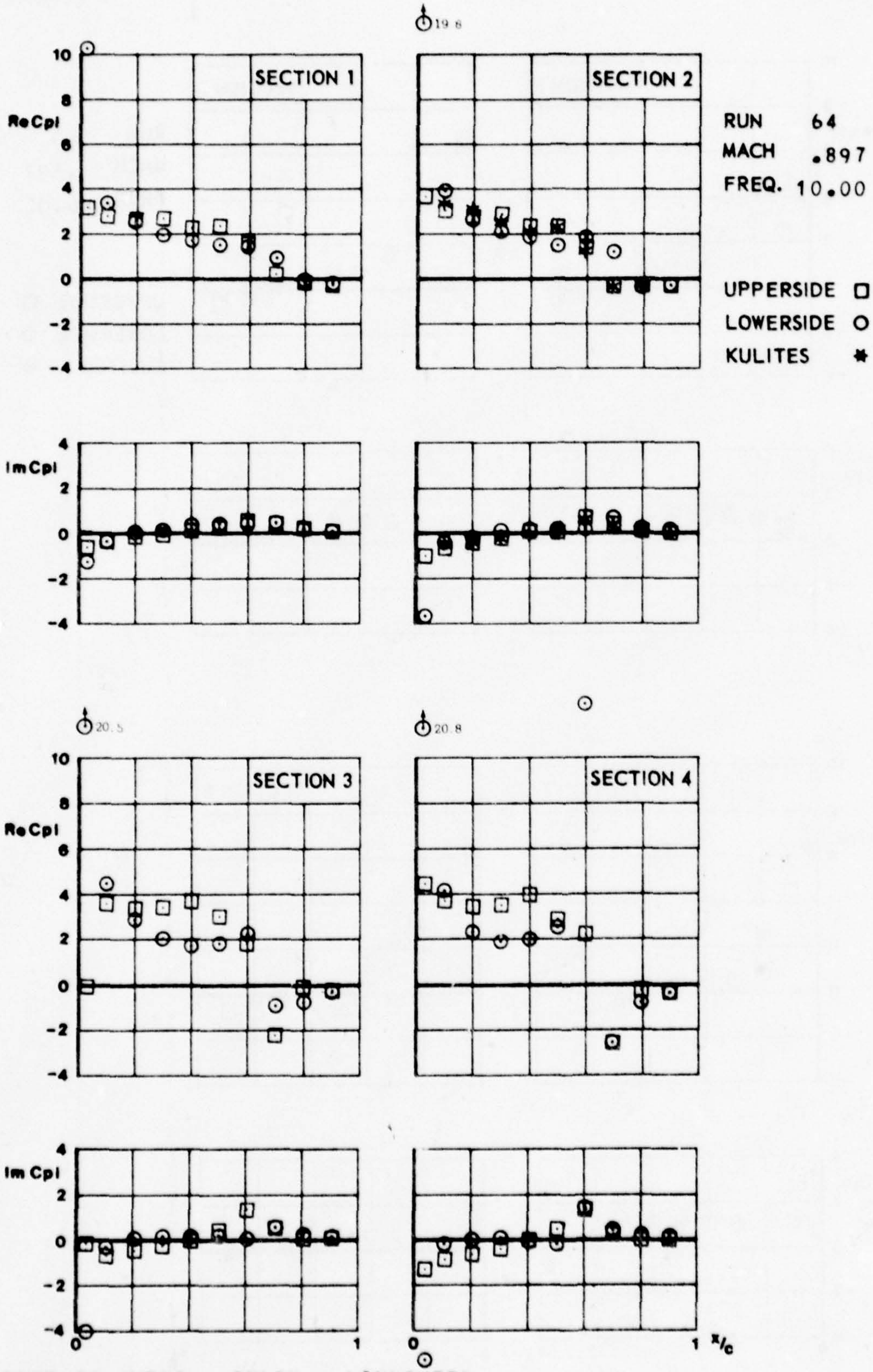

CONF.20 (WING + PYLON + LAUNCHER)

FIG. III.C.14.b

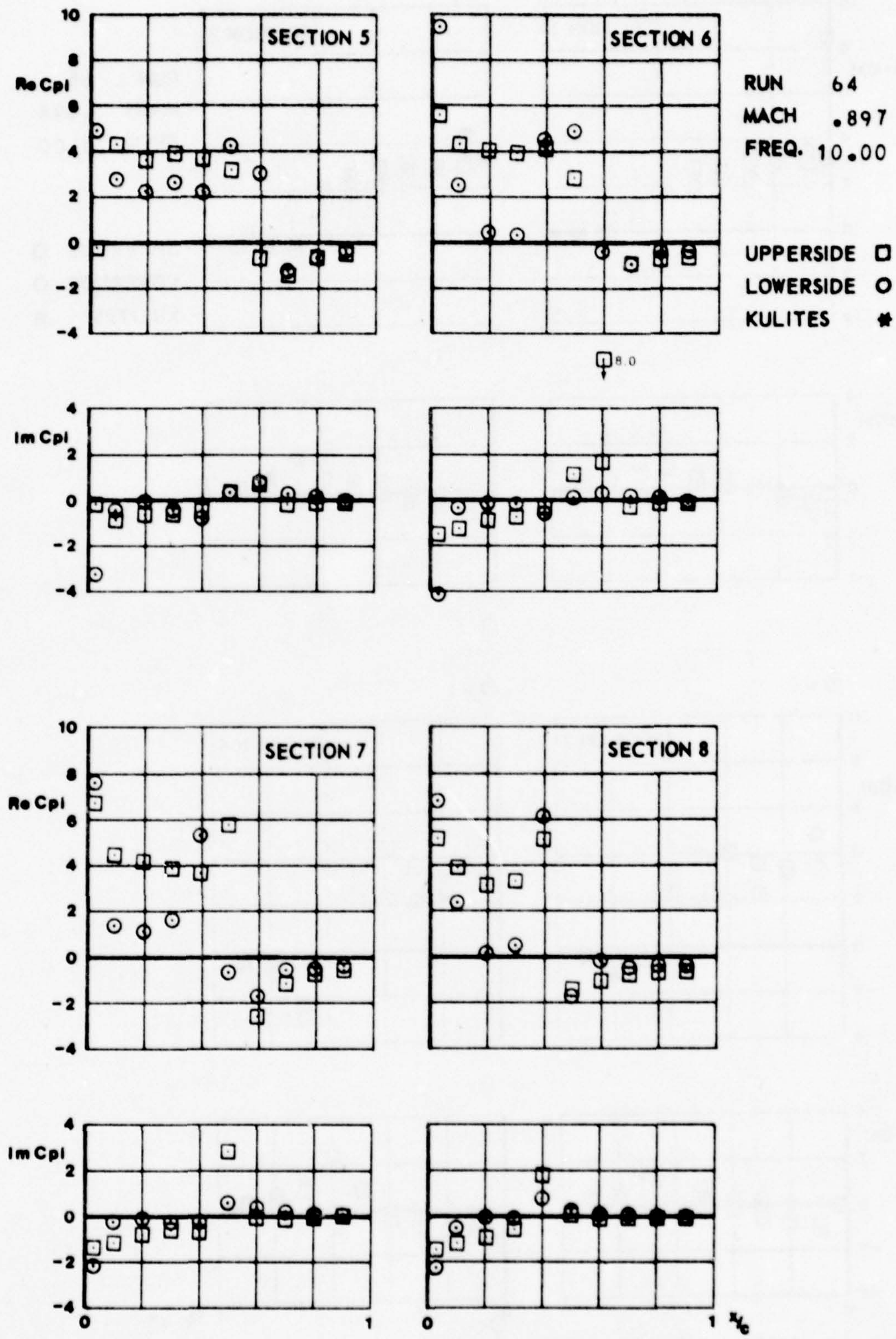

CONF. 20 (WING + PYLON + LAUNCHER)

FIG.
IV.C.15.a

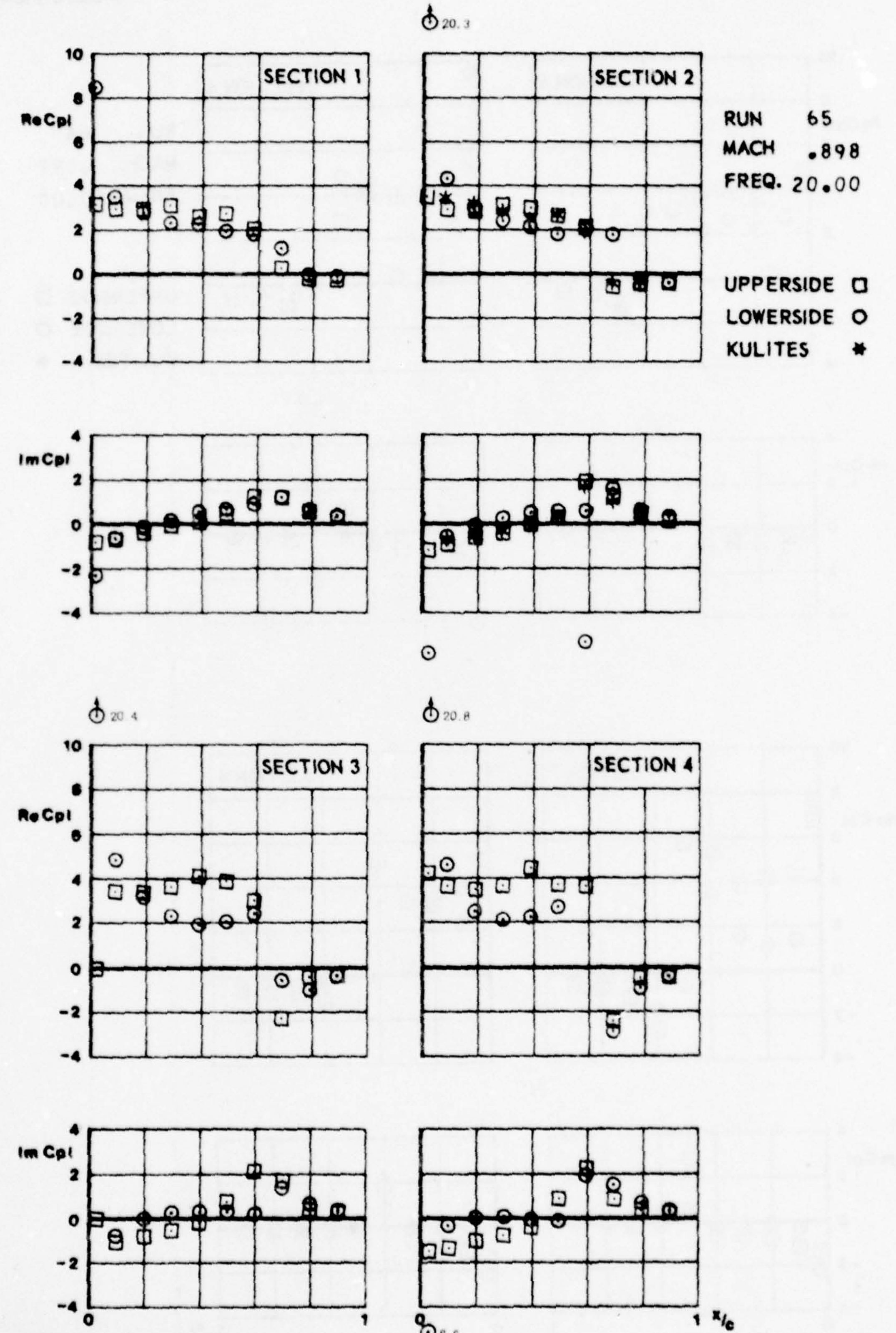

CONF. 20 (WING + PYLON + LAUNCHER)

FIG. III.C.15.b

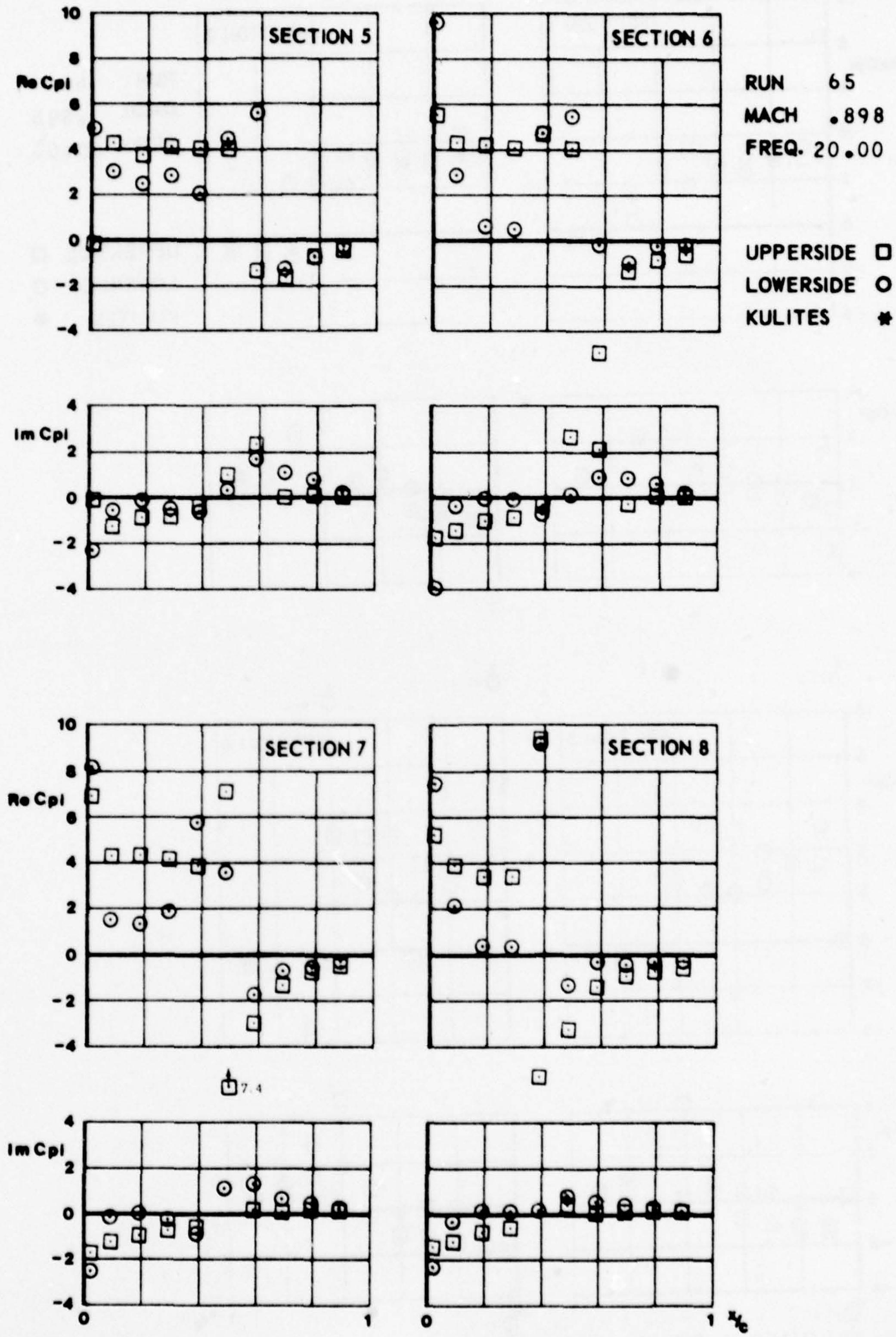

CONF. 20 (WING + PYLON + LAUNCHER)

FIG.
IV.C.16.a

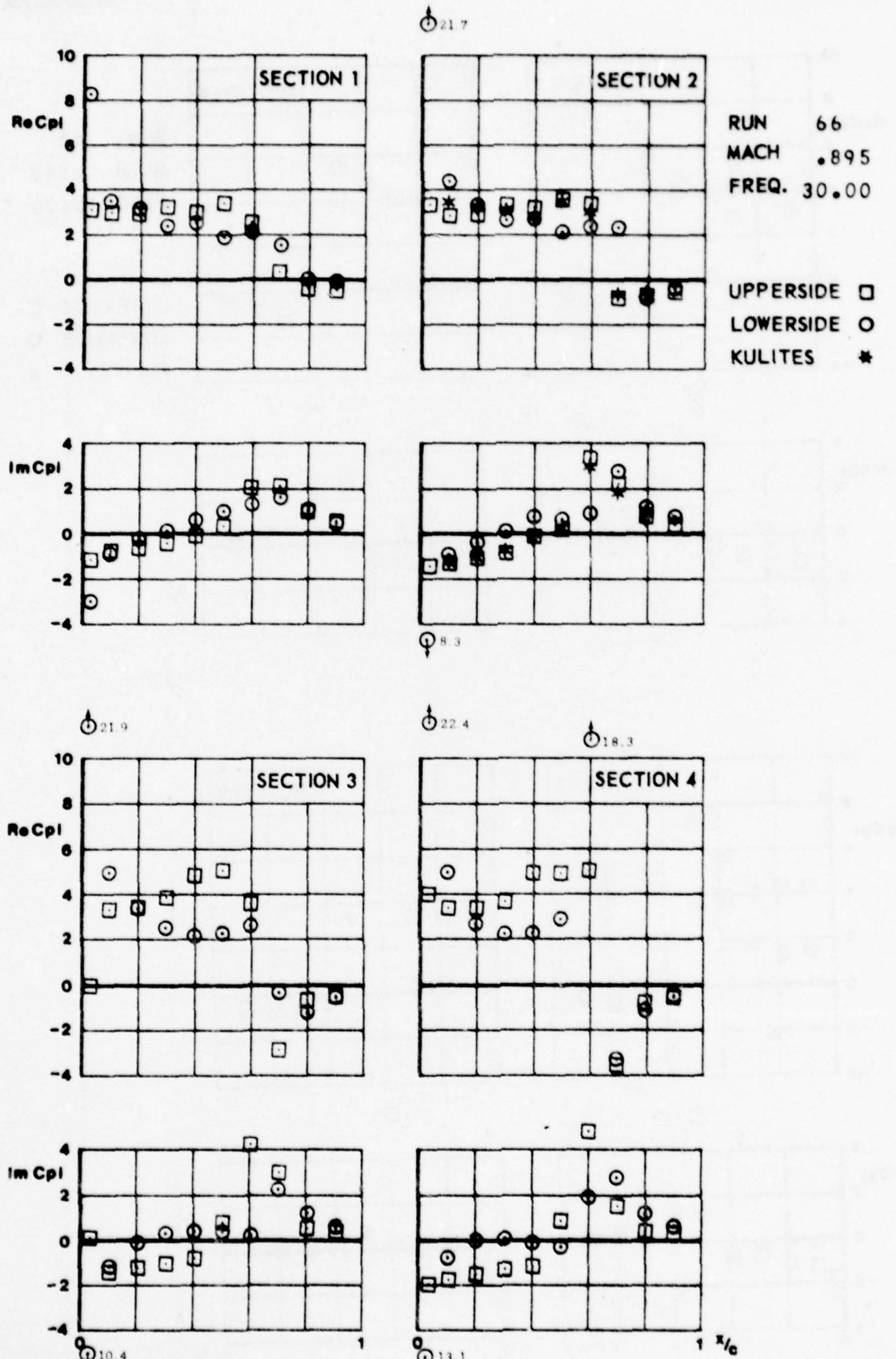

CONF.20 (WING + PYLON + LAUNCHER)

FIG. IV.C.16.b

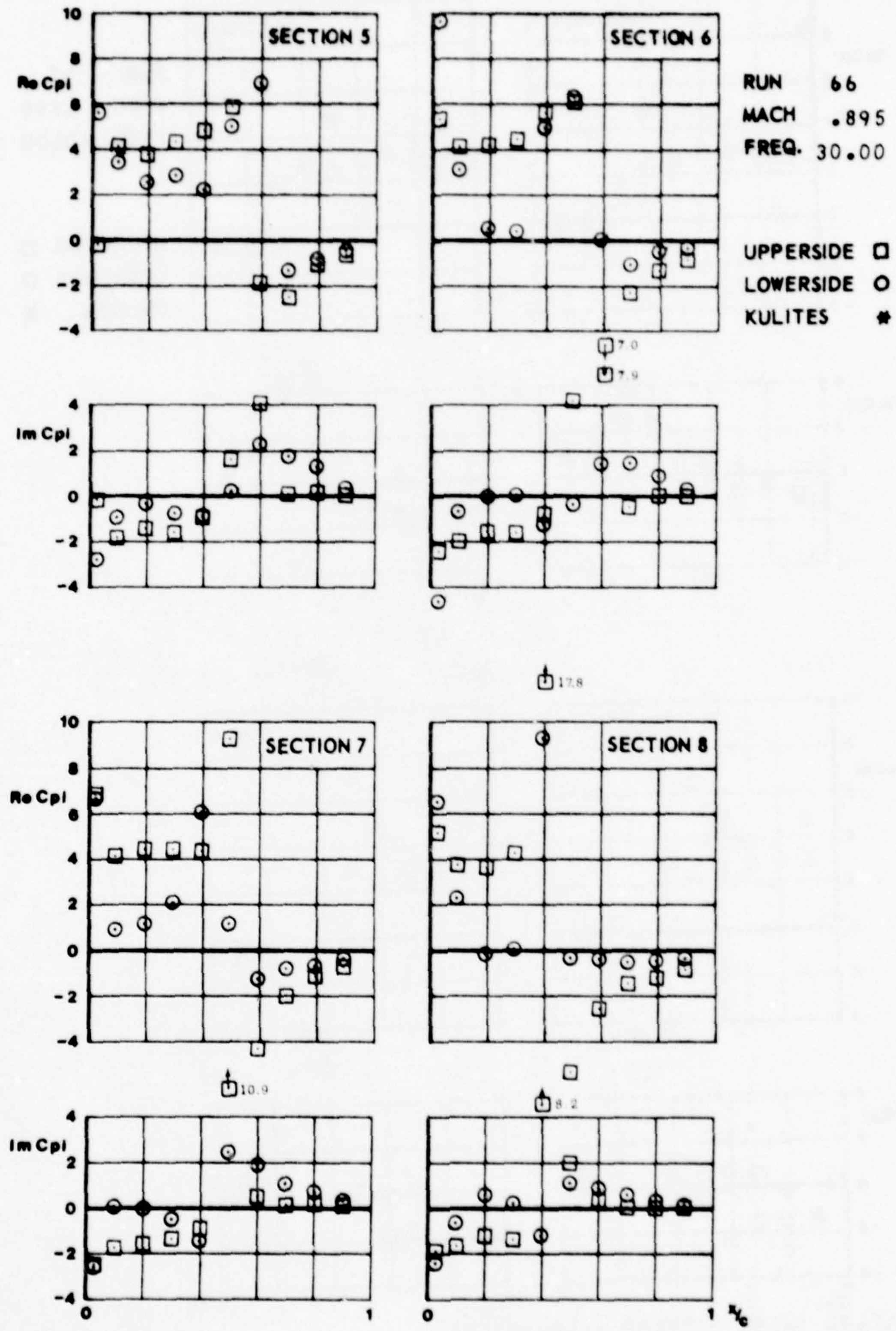

CONF. 20 (WING + PYLON + LAUNCHER)

FIG.
IV.C.17.a

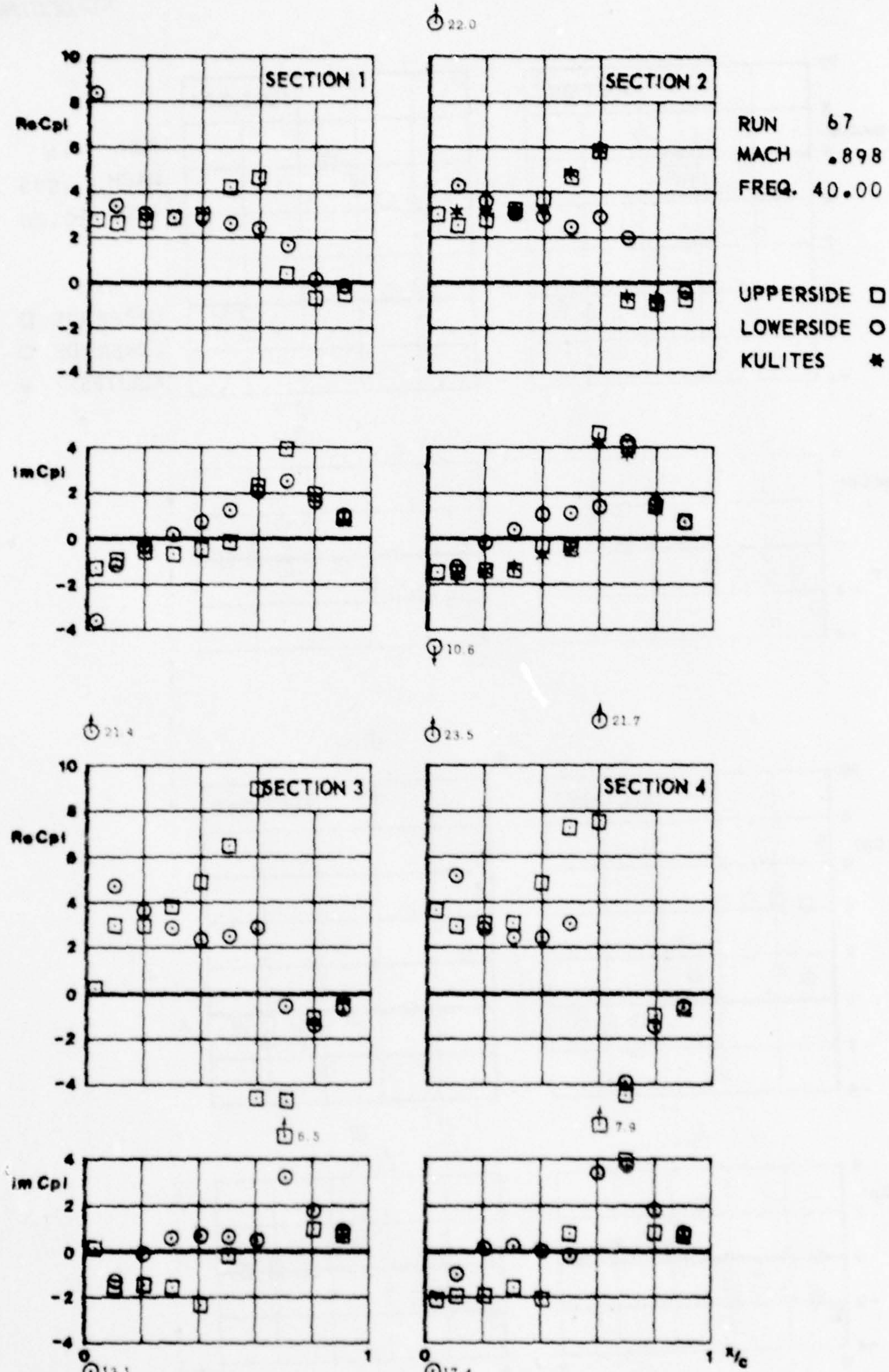

CONF.20 (WING + PYLON + LAUNCHER)

FIG. IV.C.17.b

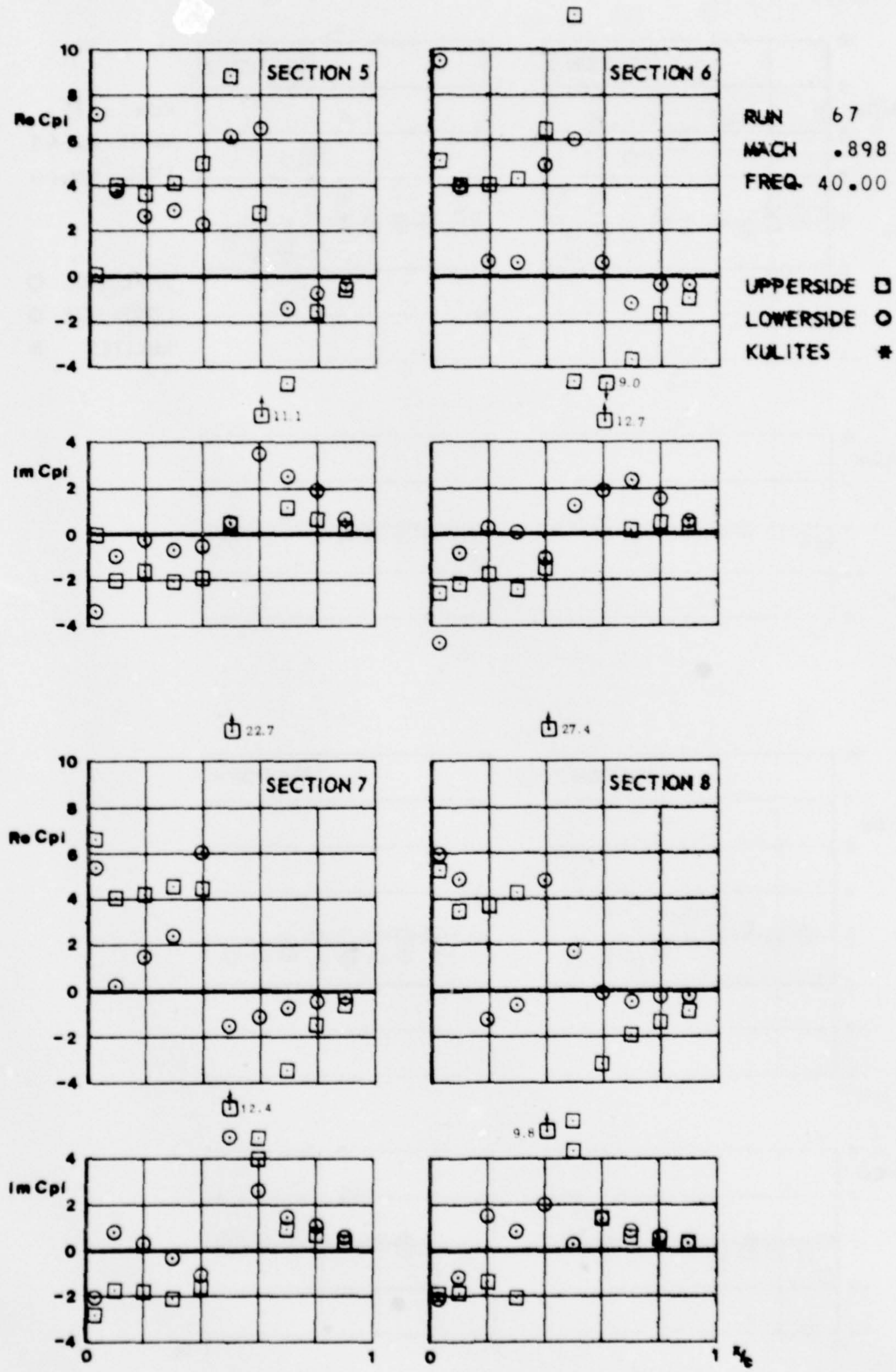

CONF. 20 (WING + PYLON + LAUNCHER)

FIG.
IX.C.18.a

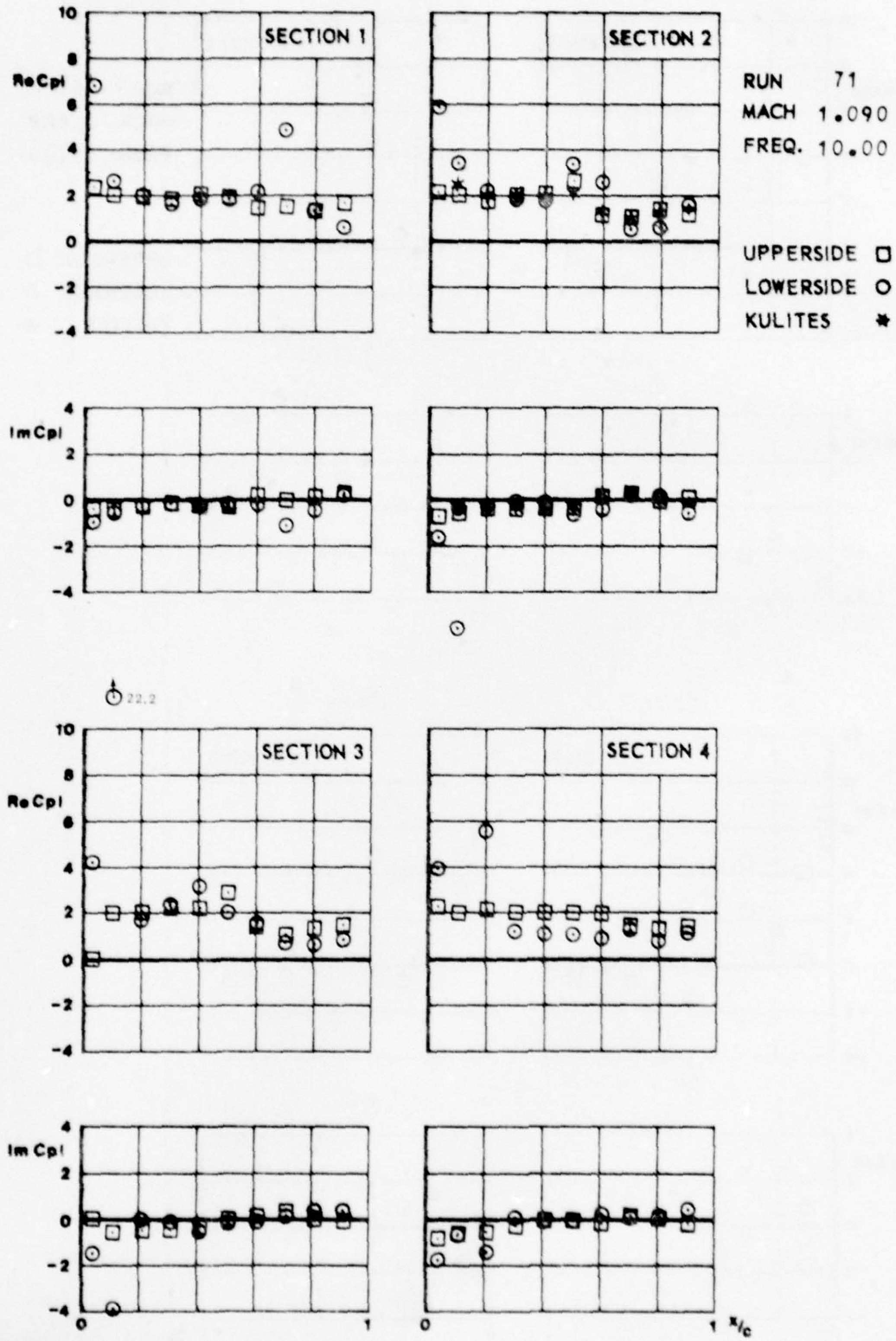

CONF.20 (WING + PYLON + LAUNCHER)

FIG. IV.C.18.b

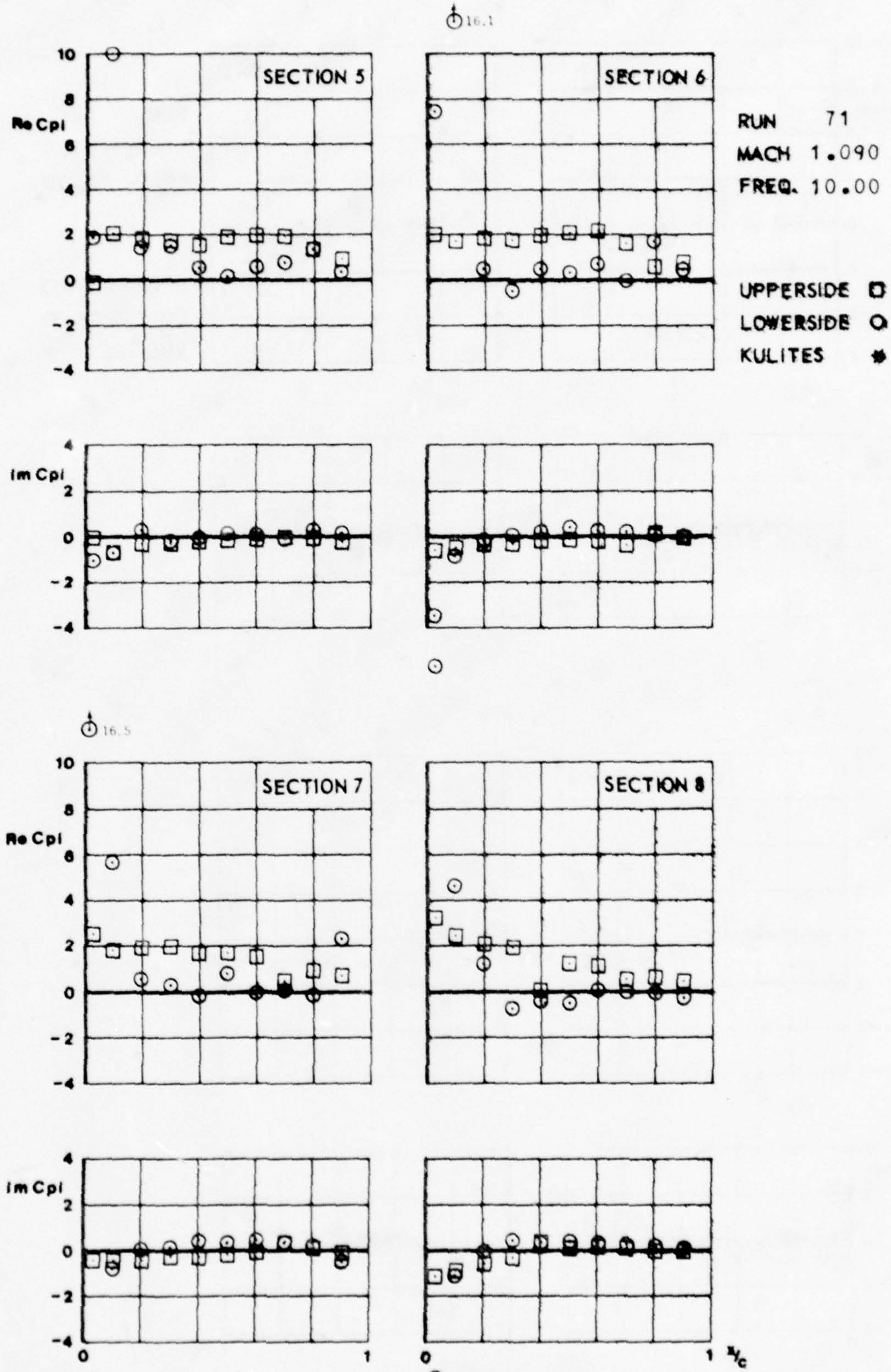

CONF. 20 (WING + PYLON + LAUNCHER)

FIG.
IV.C.19.a

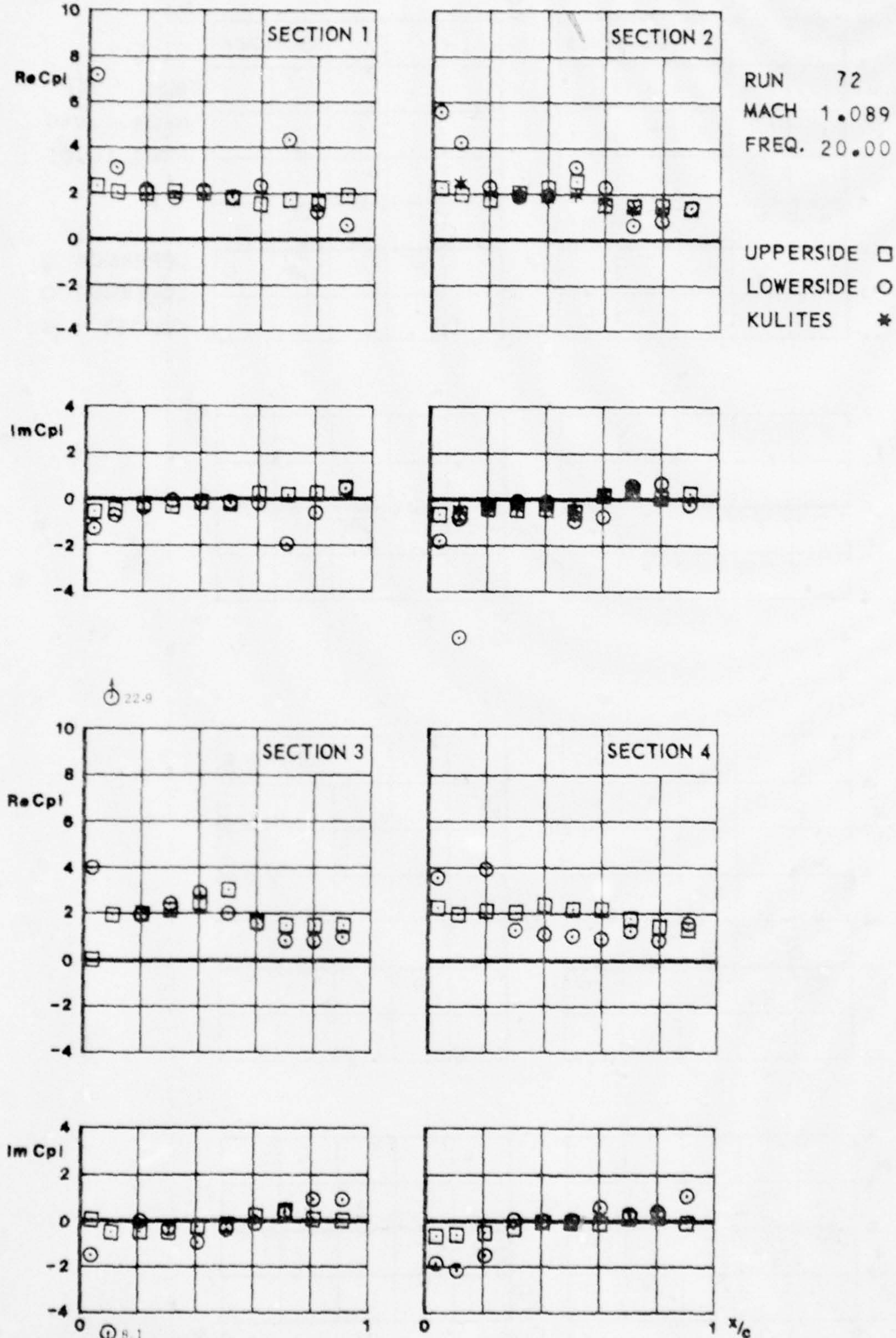

CONF. 20 (WING + PYLON + LAUNCHER)

FIG. IV.C.19.b

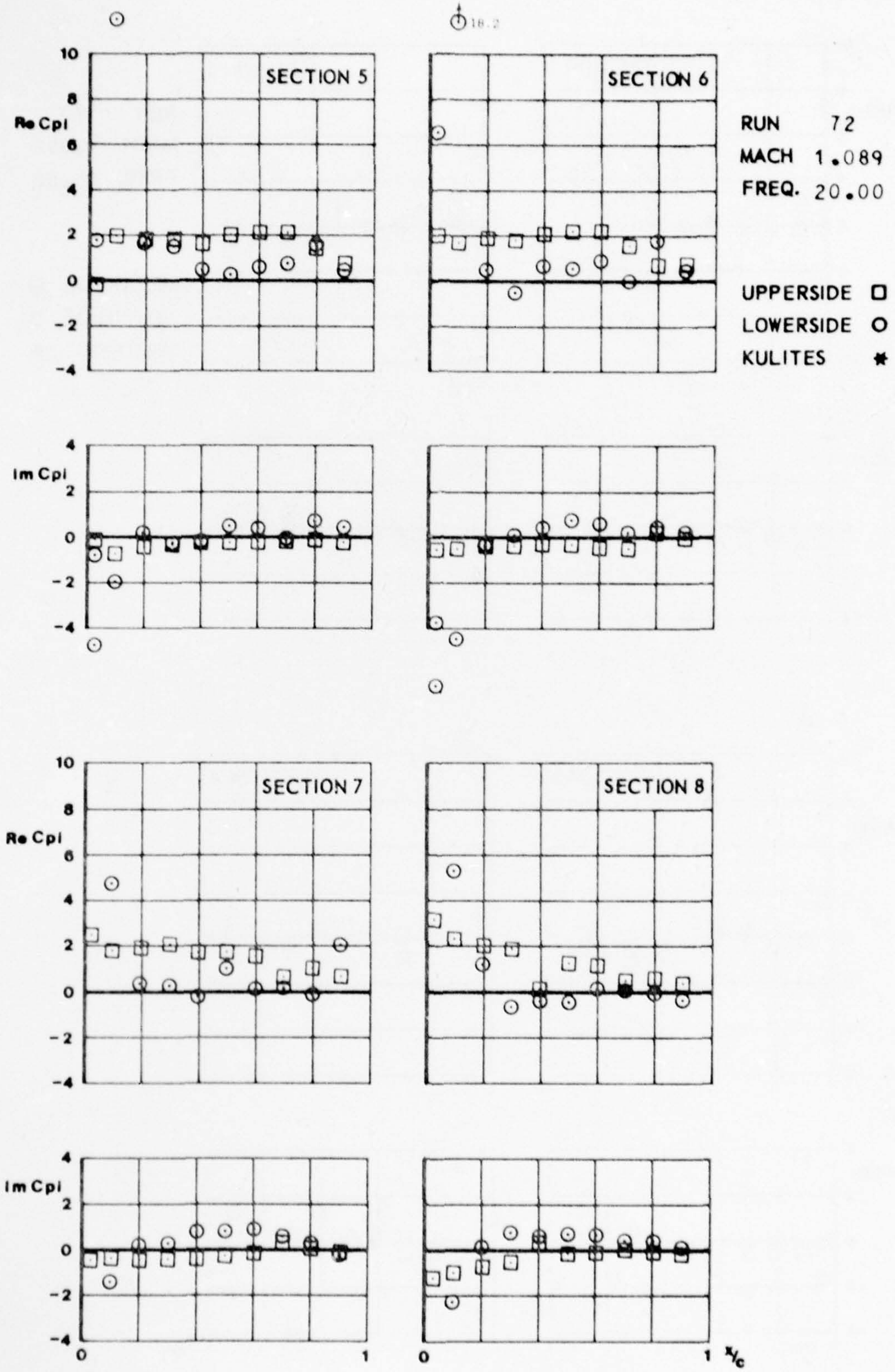

CONF. 20 (WING + PYLON + LAUNCHER)

FIG.
IV.C.20.a

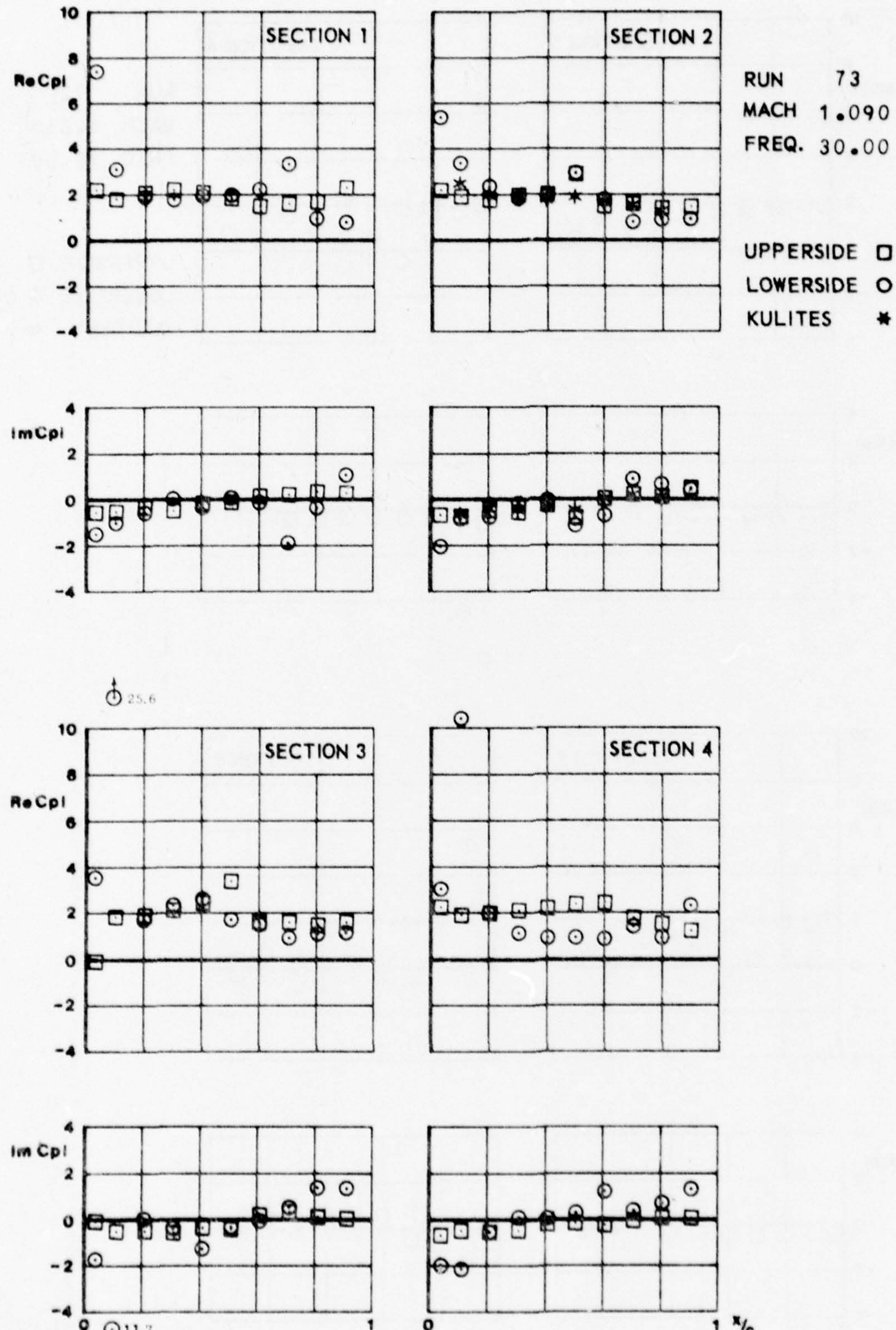

CONF.20 (WING + PYLON + LAUNCHER)

FIG. IV.C.20.b

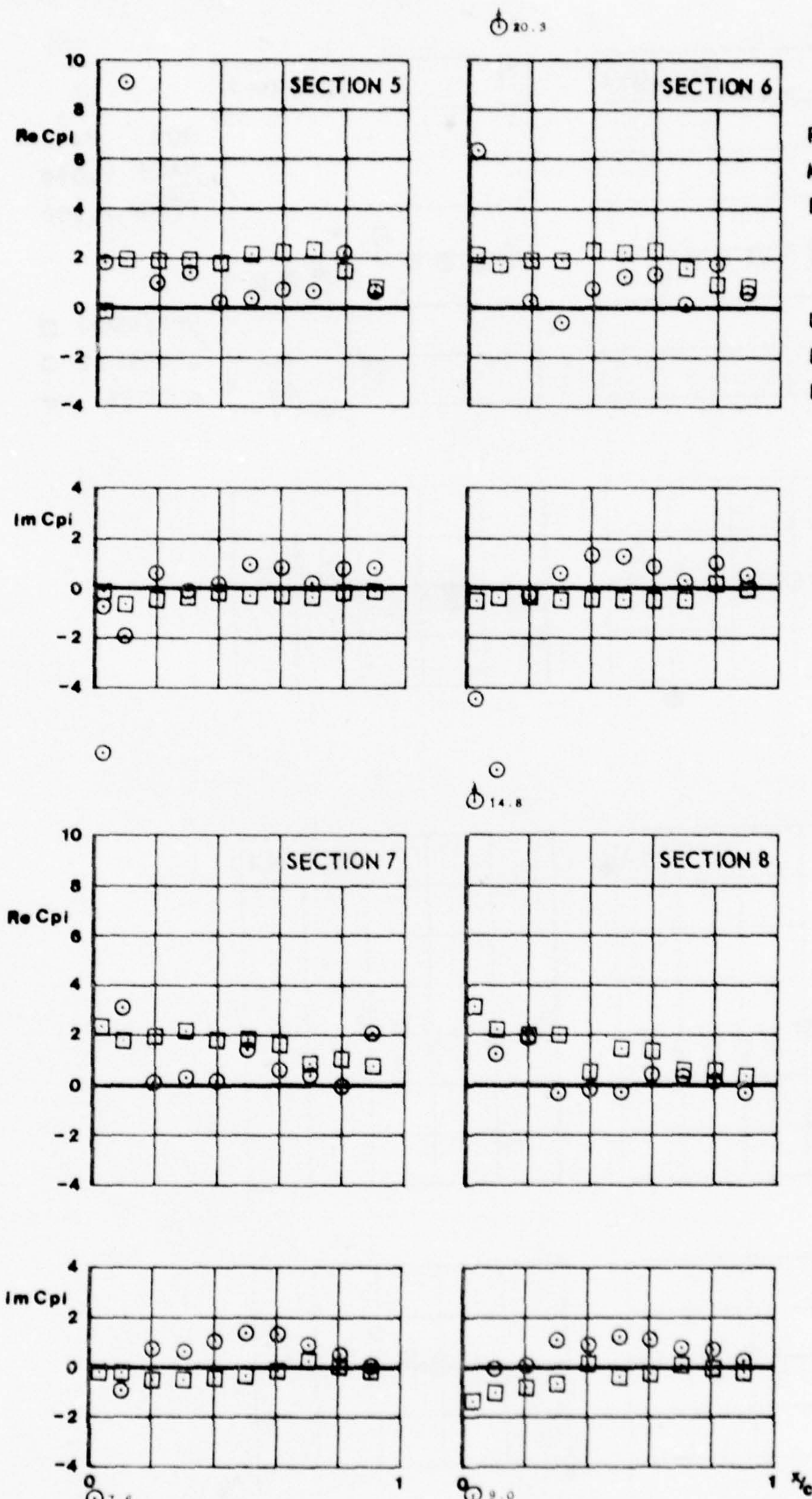

CONF. 20 (WING + PYLON + LAUNCHER)

FIG.
IV.C.21.a

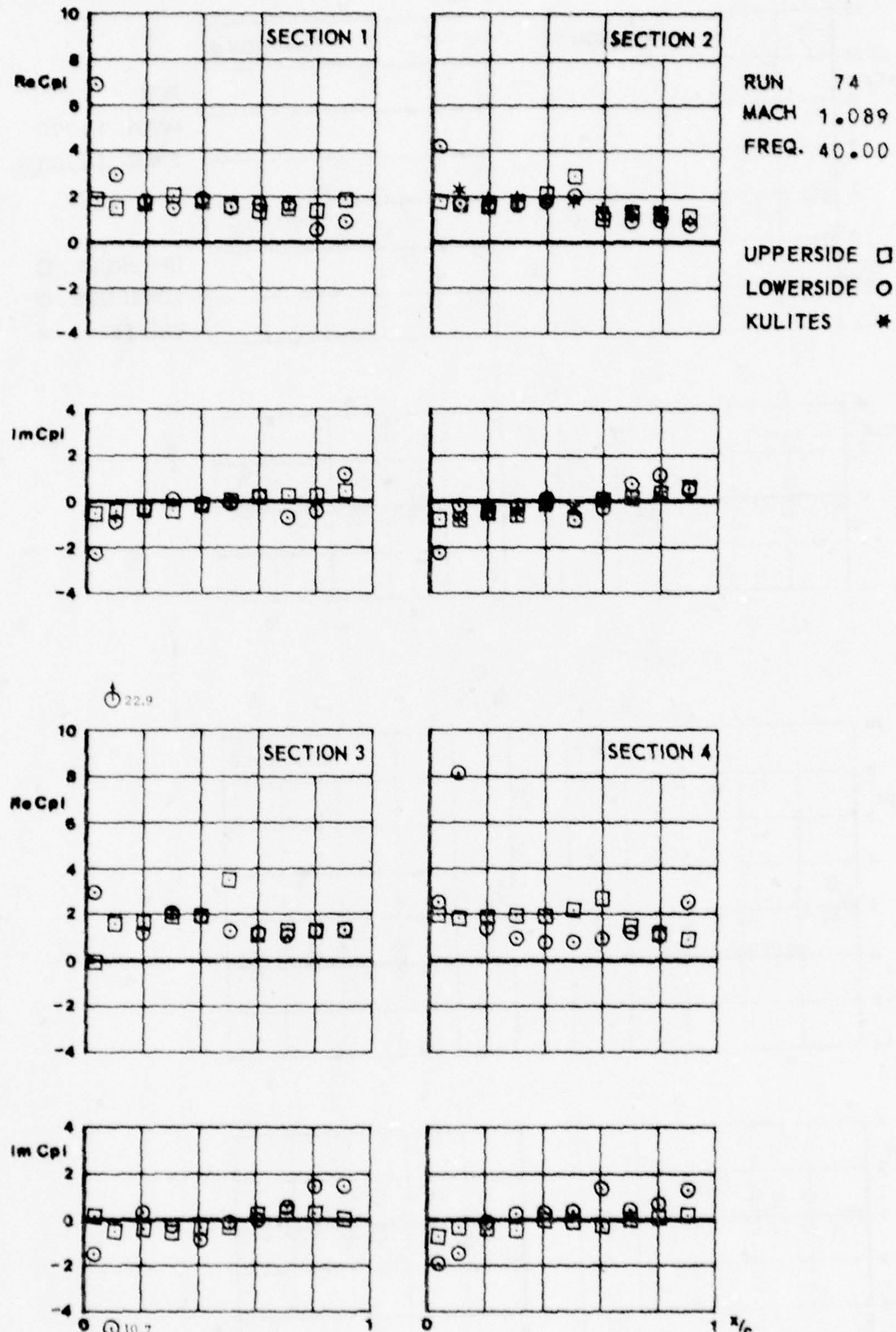

CONF. 20 (WING + PYLON + LAUNCHER)

FIG. IV.C.21.b

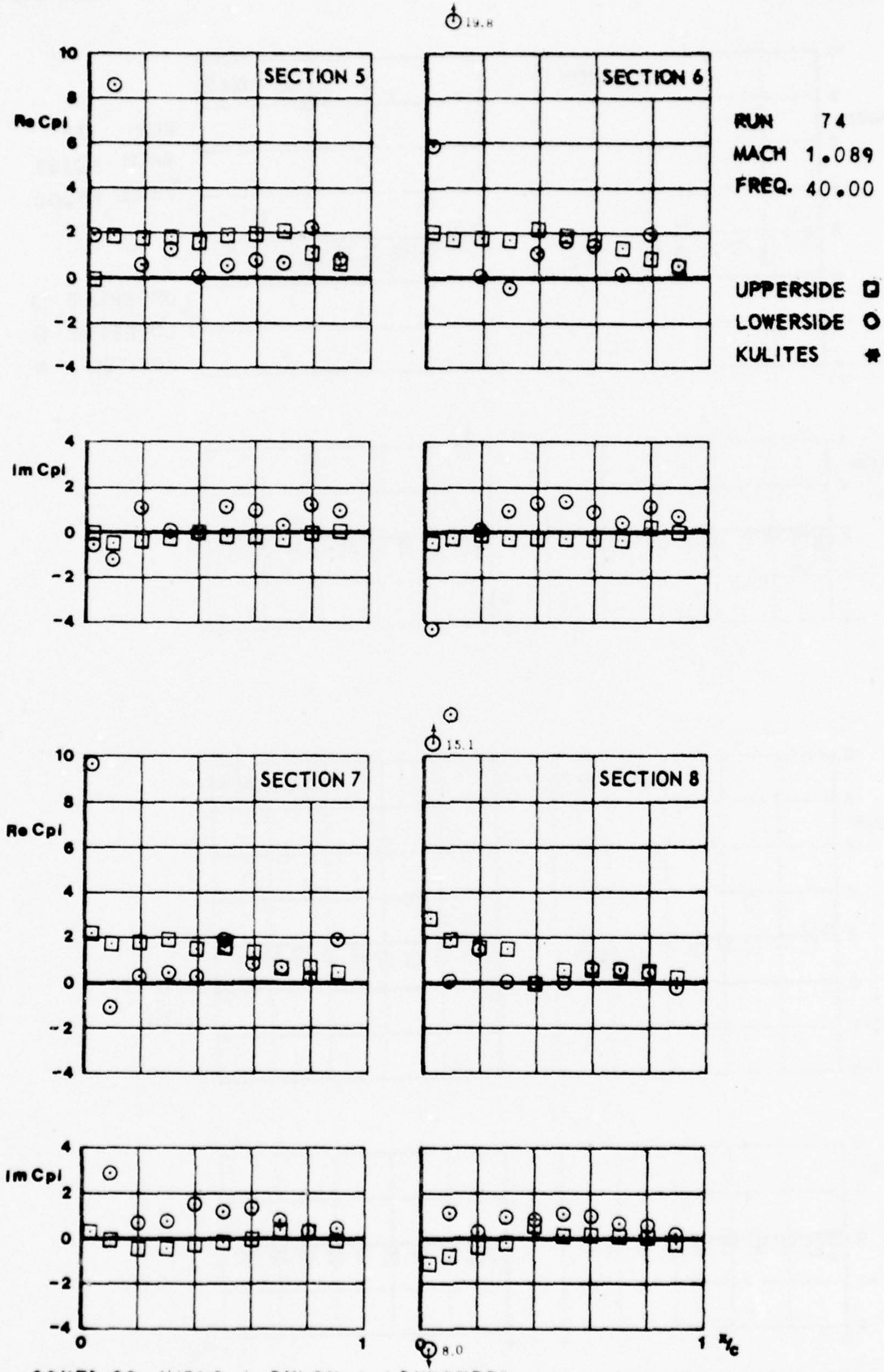

CONFIG 20 (WING + PYLON + LAUNCHER)

FIG.
IV.C.22.a

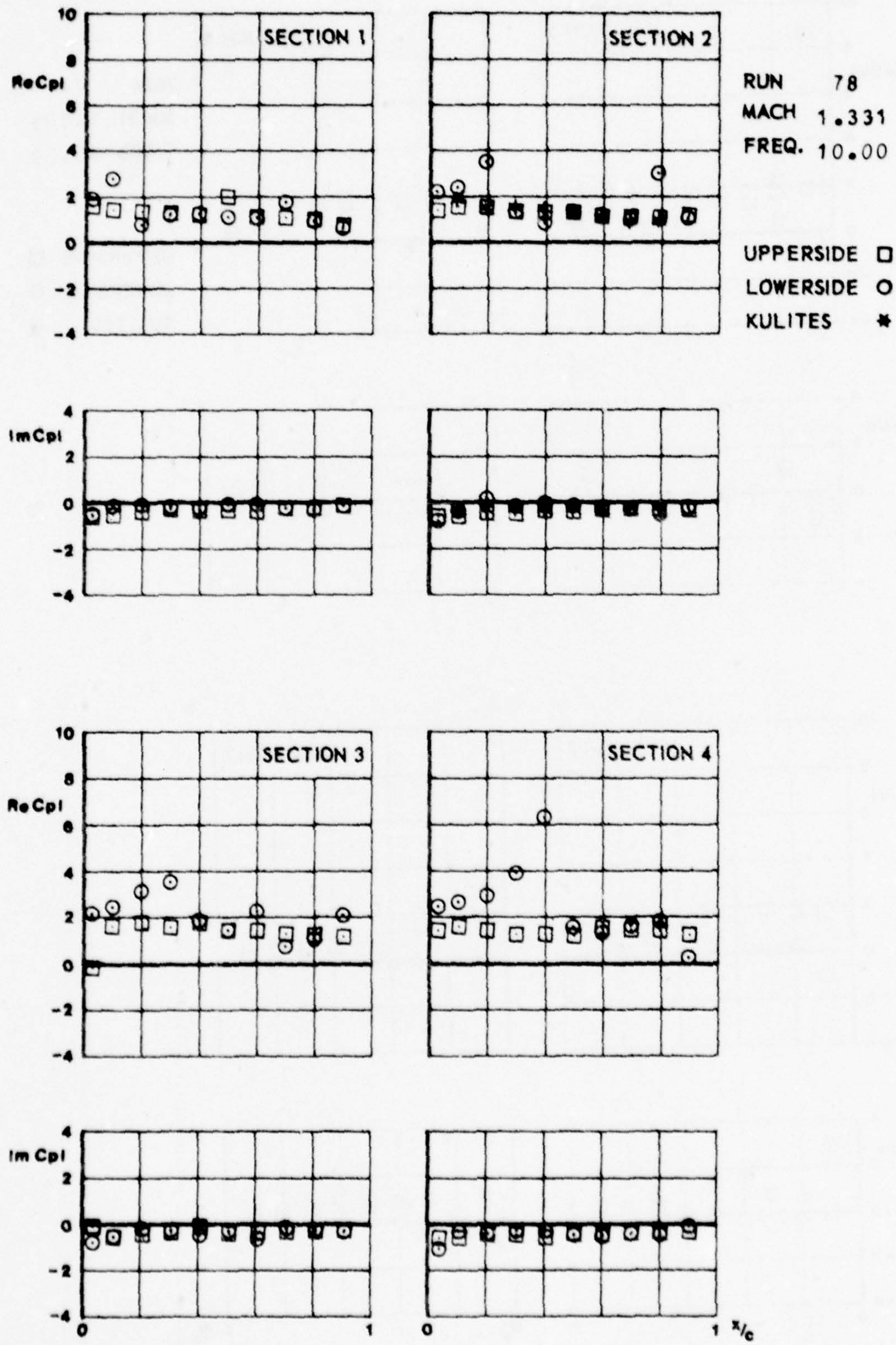

CONF.20 (WING + PYLON + LAUNCHER)

FIG. IV.C.22.b

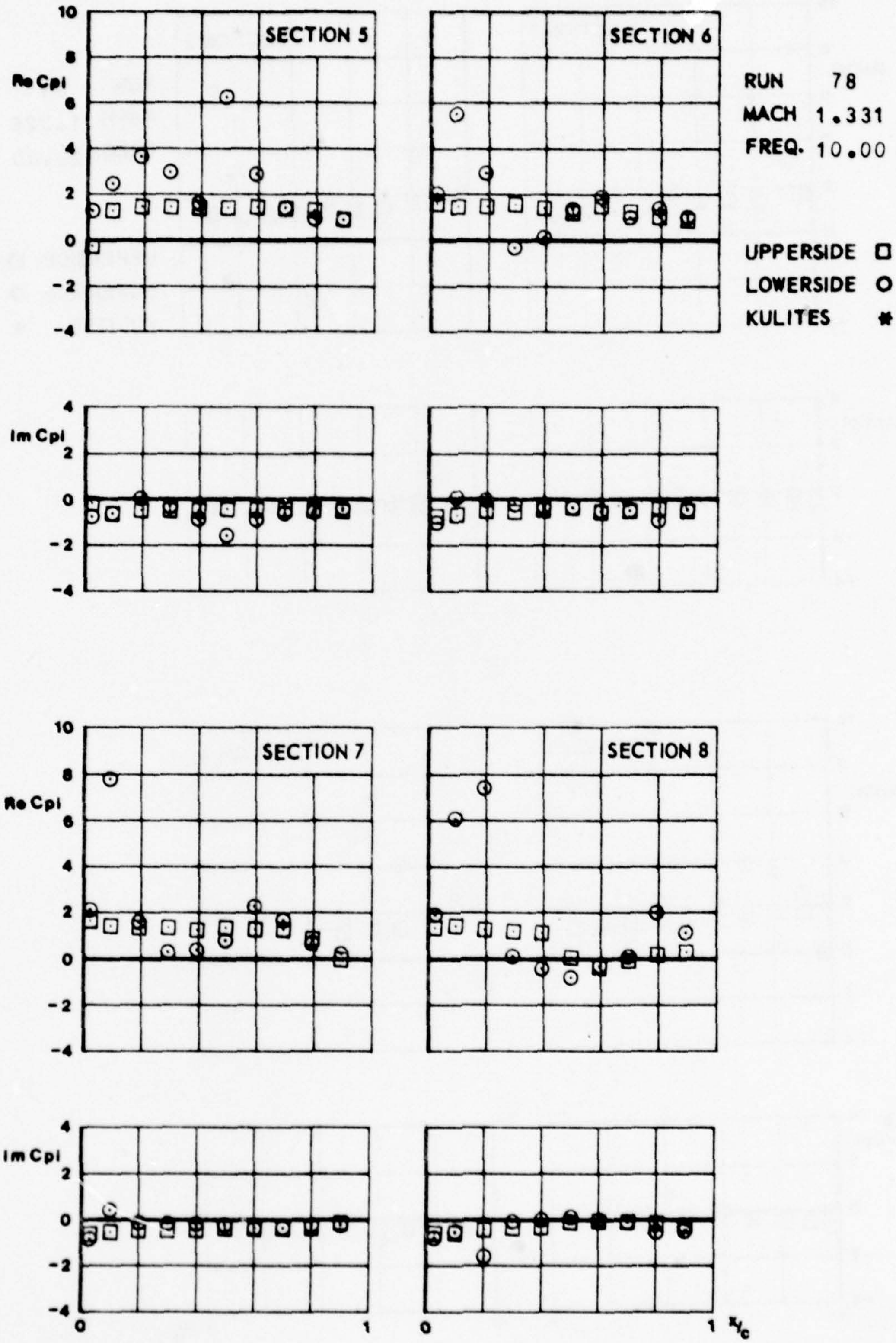

CONF. 20 (WING + PYLON + LAUNCHER)

FIG.
IV.C.23.a

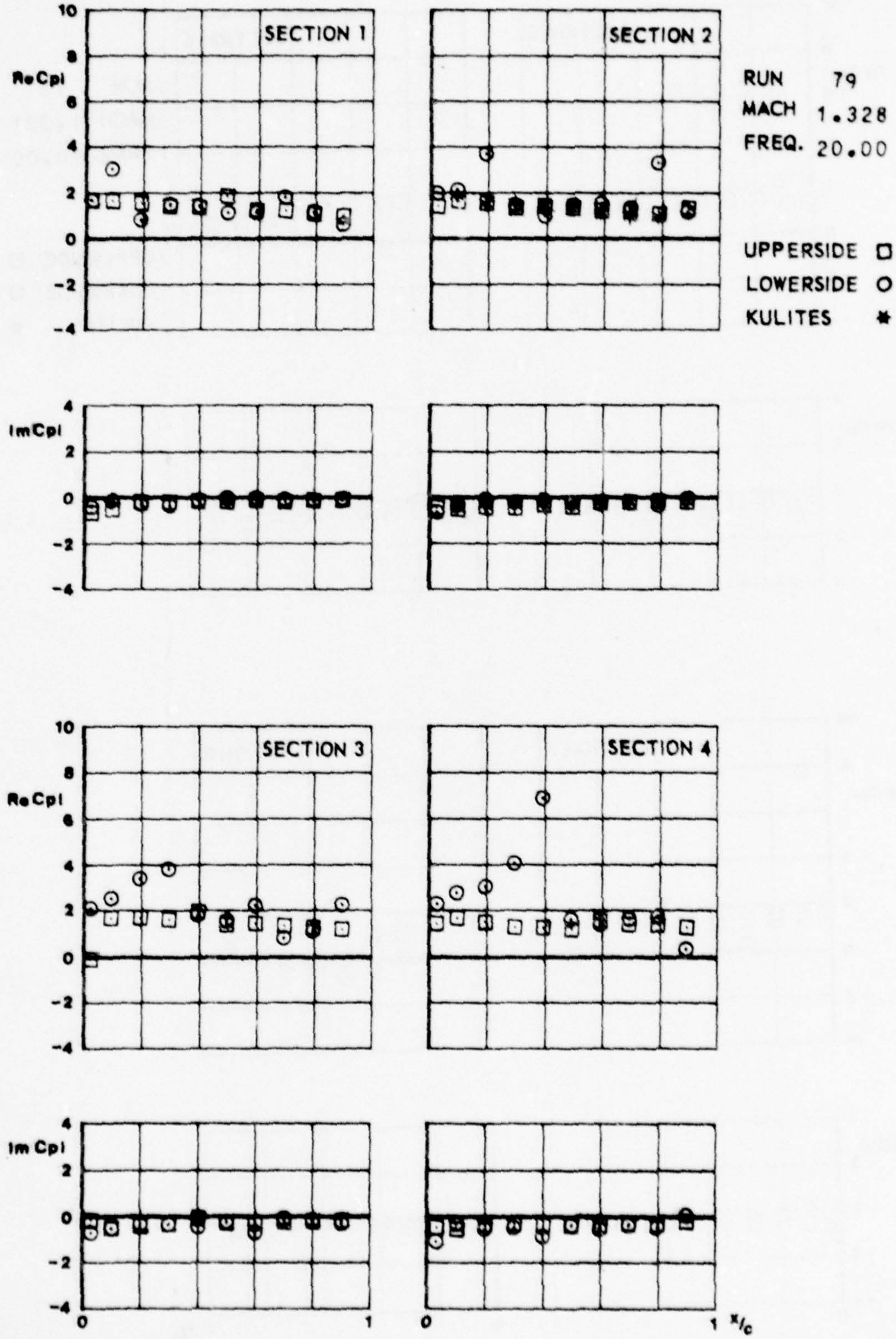

CONF.20 (WING + PYLON + LAUNCHER)

FIG. IV.C.23.6

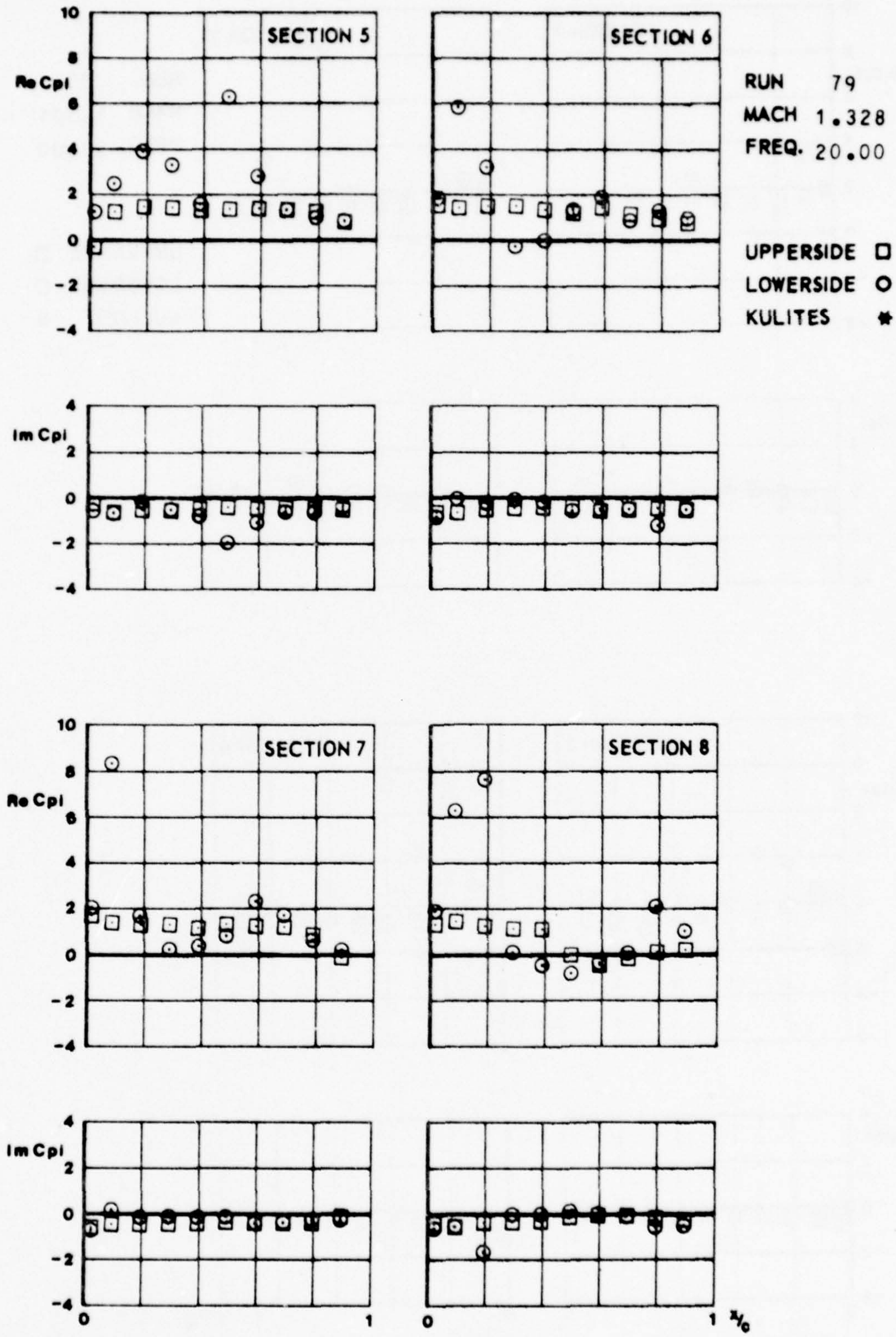

CONF. 20 (WING + PYLON + LAUNCHER)

FIG.
IV.C.24.a

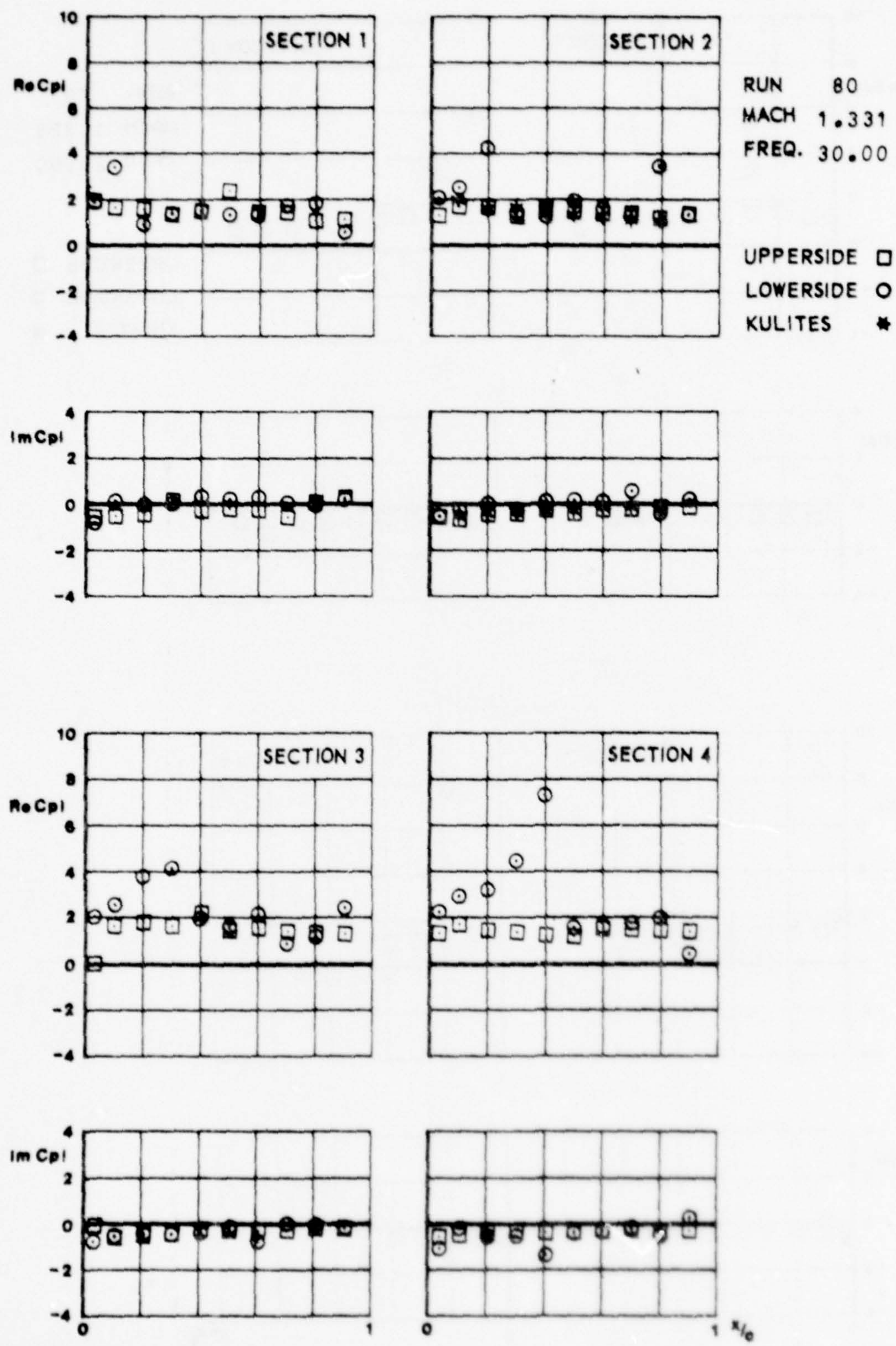

CONF.20 (WING + PYLON + LAUNCHER)

FIG.
IV.C.24.6

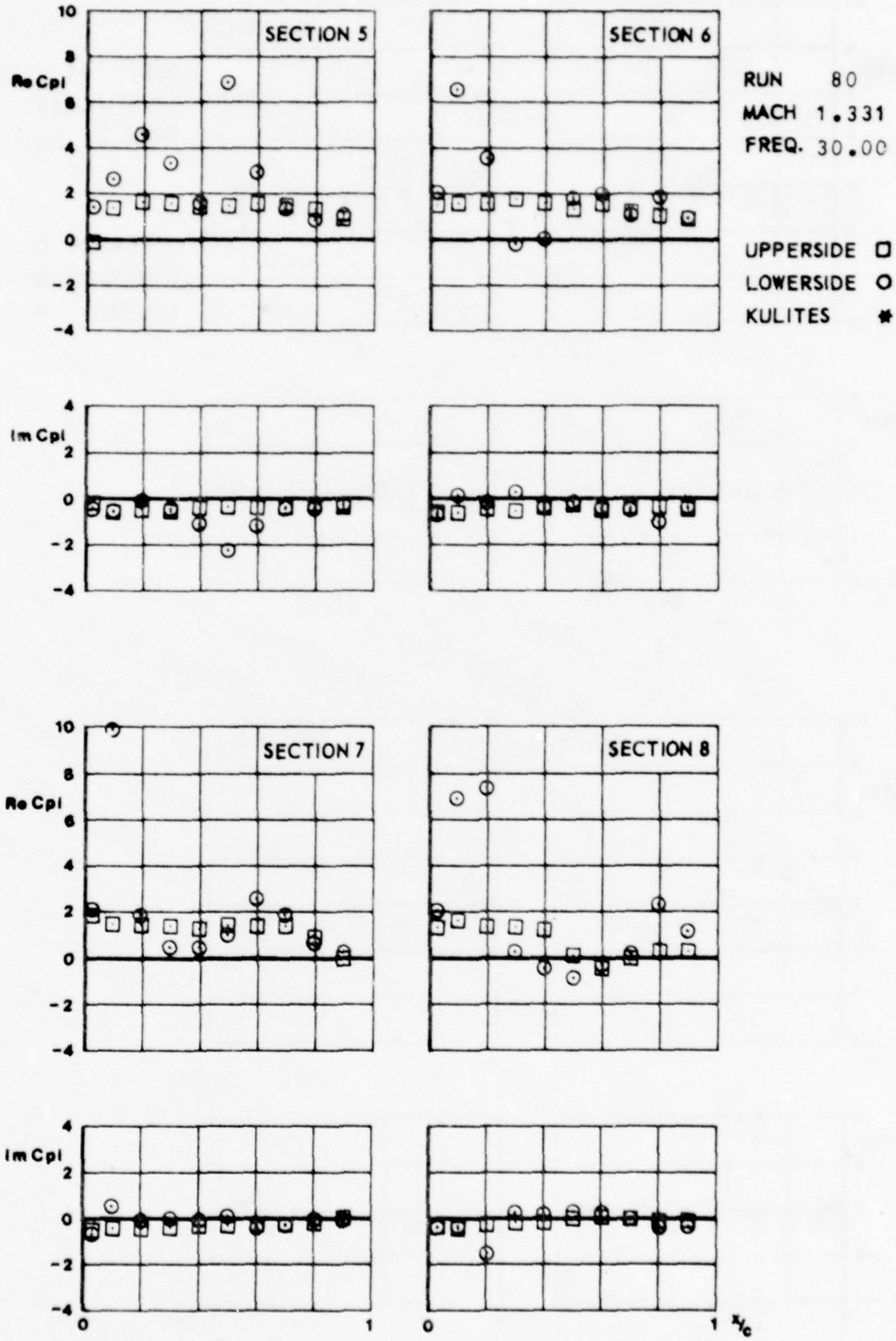

CONF. 20 (WING + PYLON + LAUNCHER)

FIG.
IV.C.25.a

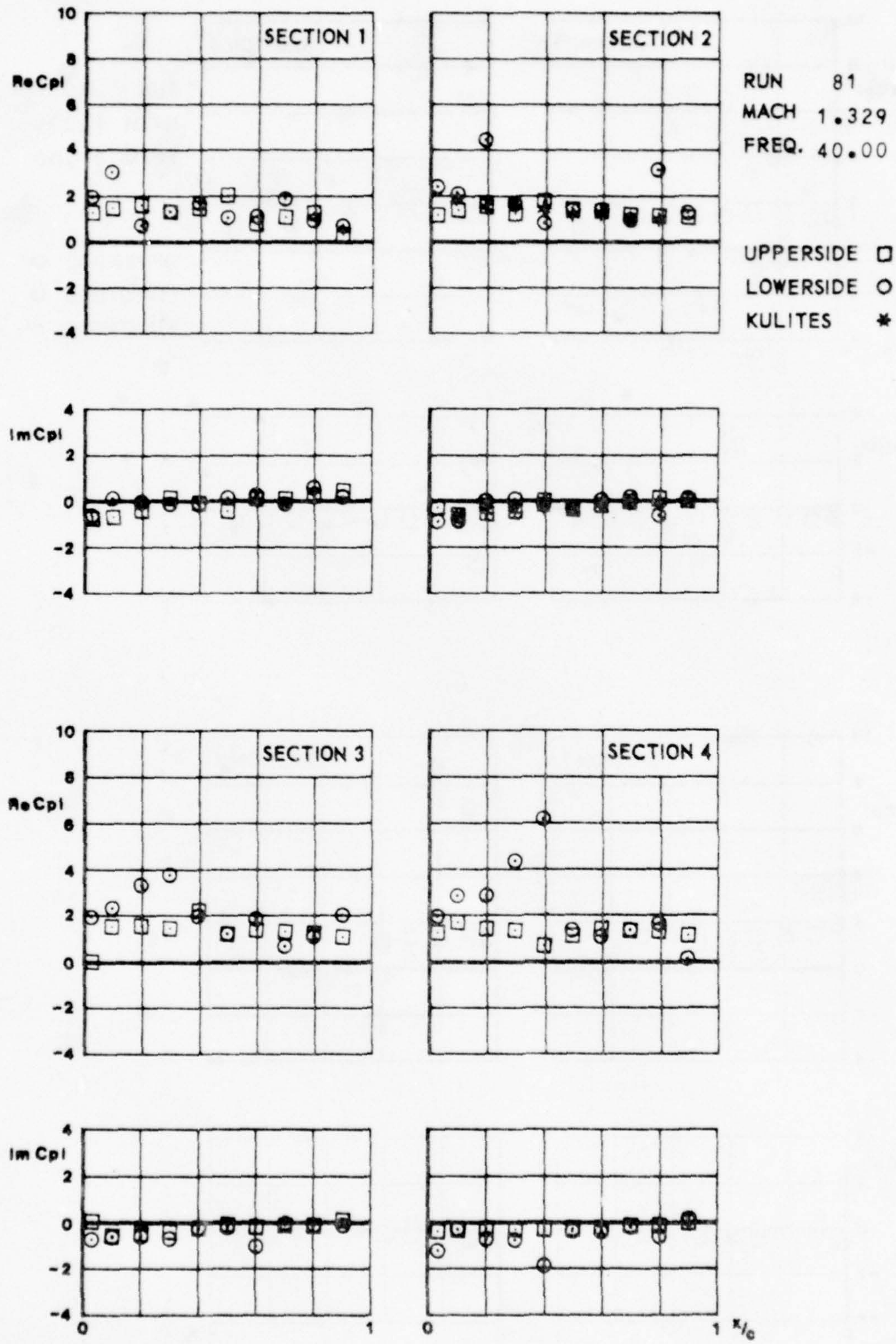

CONF.20 (WING + PYLON + LAUNCHER)

FIG. IV.C.25.b

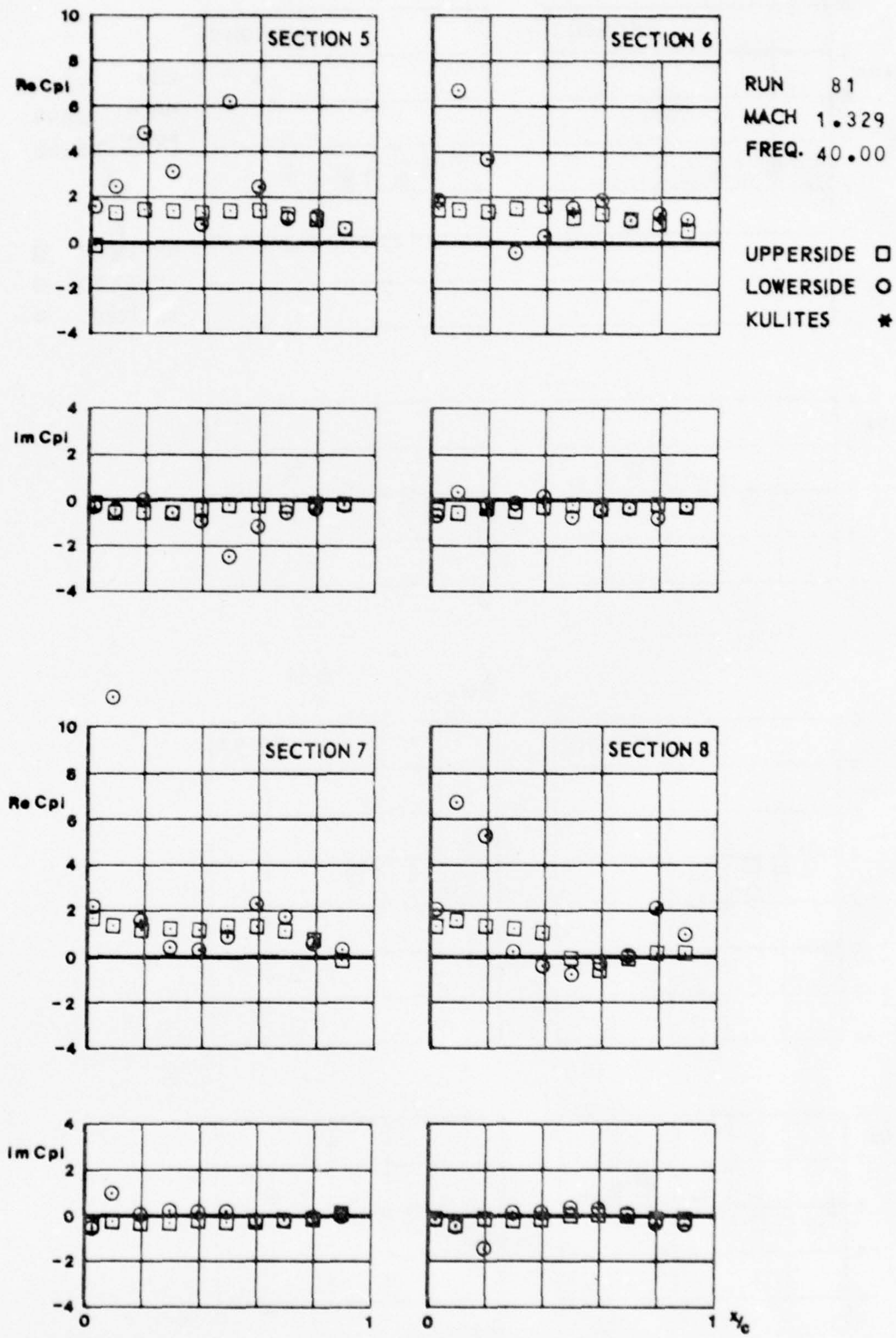

CONF. 20 (WING + PYLON + LAUNCHER)

FIG.
IV.C.26.a

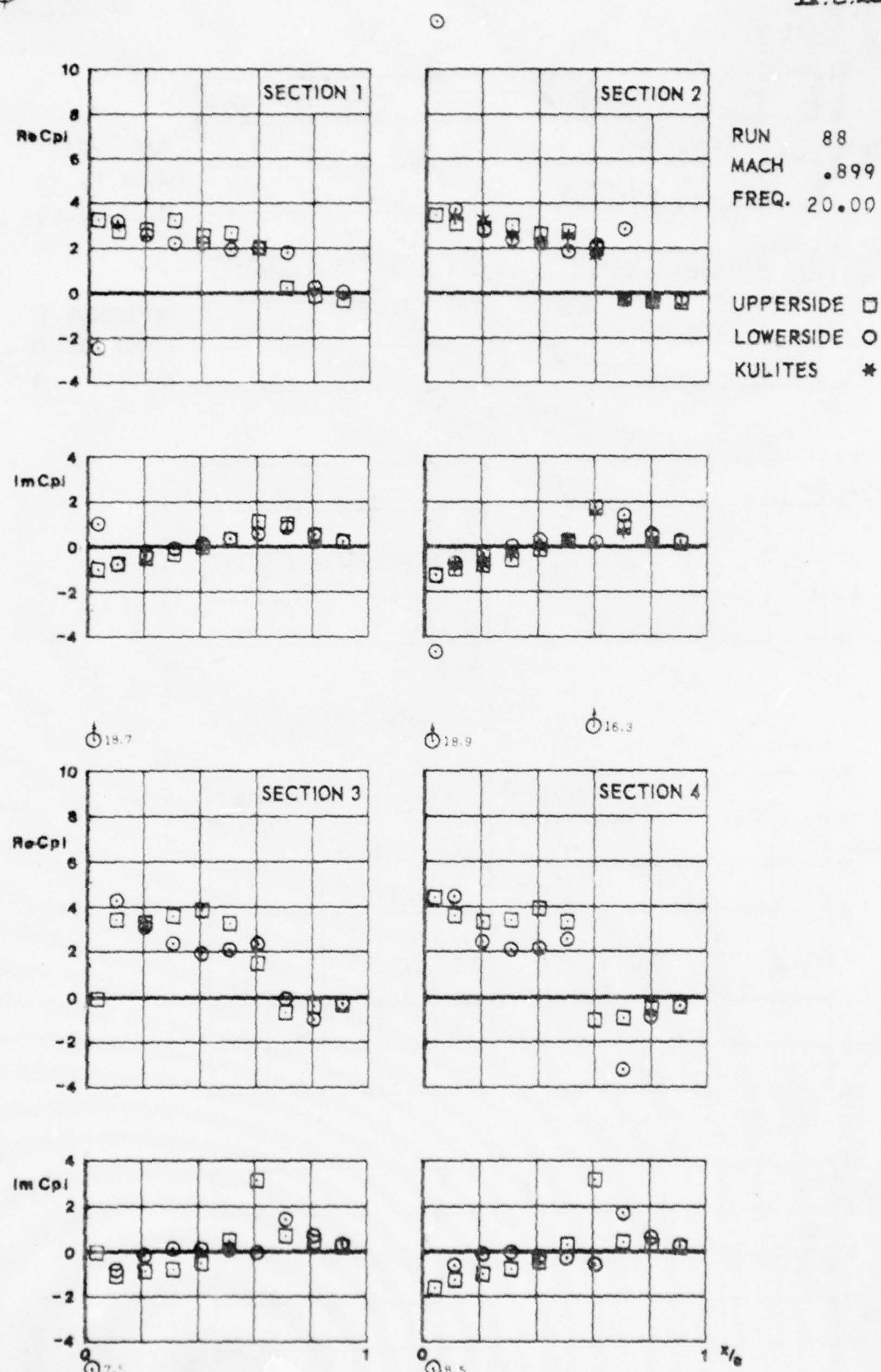

CONF. 31 (WING + PYLON + LAUNCHER + MISSILEBODY WITH AFT WINGS)

FIG. IV.C.26.b

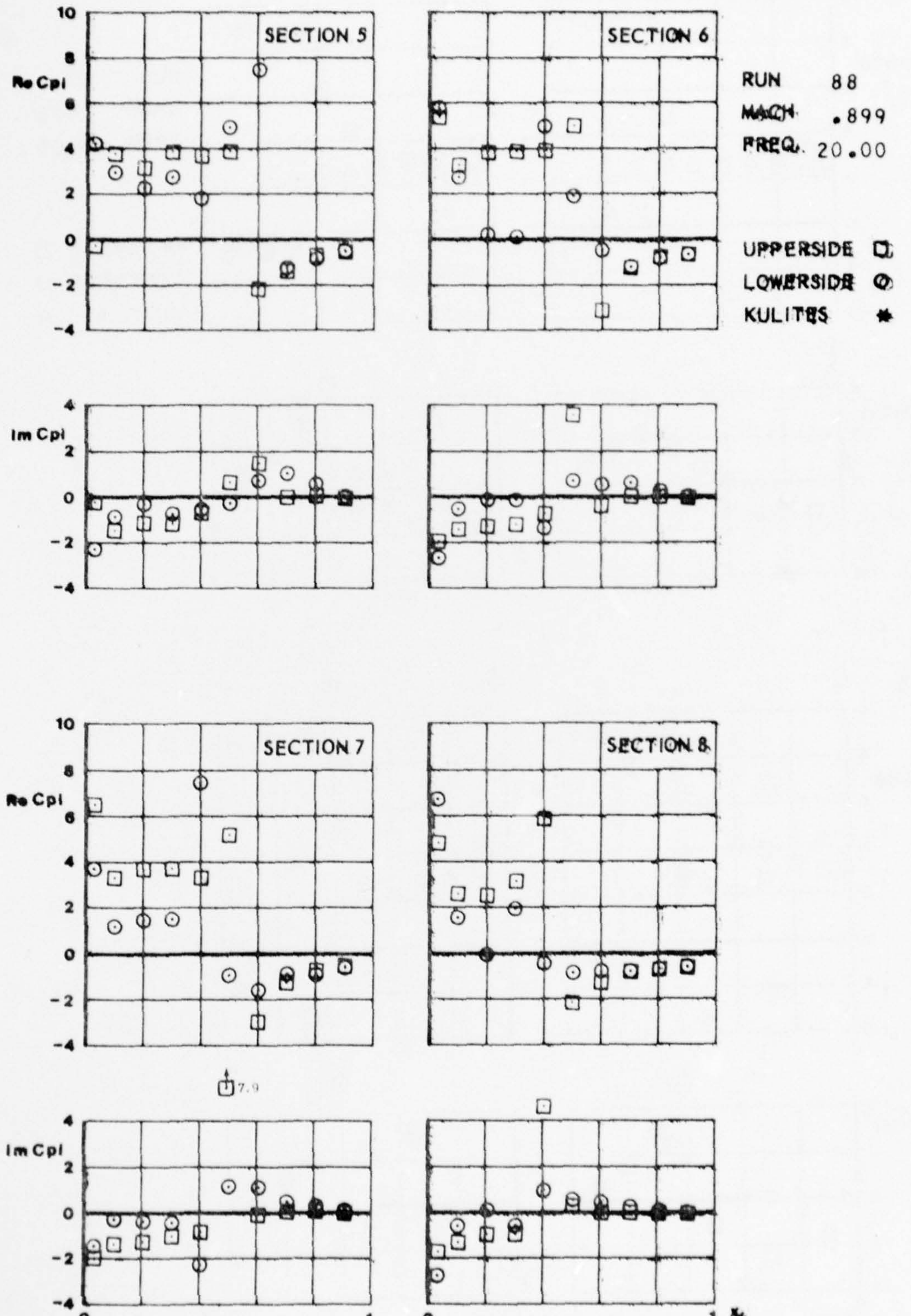

CONF. 31 (WING + PYLON + LAUNCHER + MISSILEBODY WITH AFT WINGS)

FIG.
IV.C.27.a

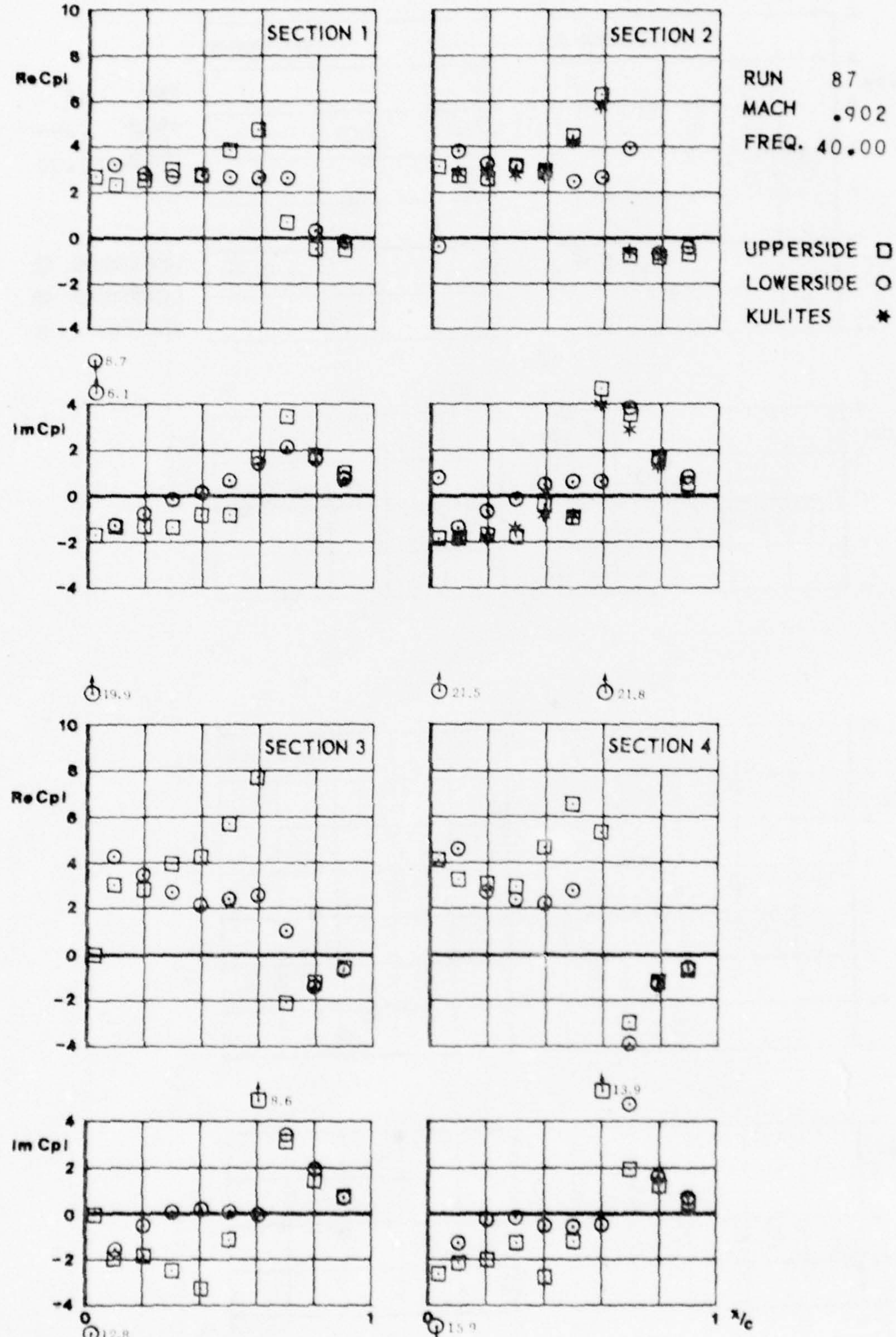

CONF. 31 (WING + PYLON + LAUNCHER + MISSILEBODY WITH AFT WINGS)

FIG.
IV.C.27.b

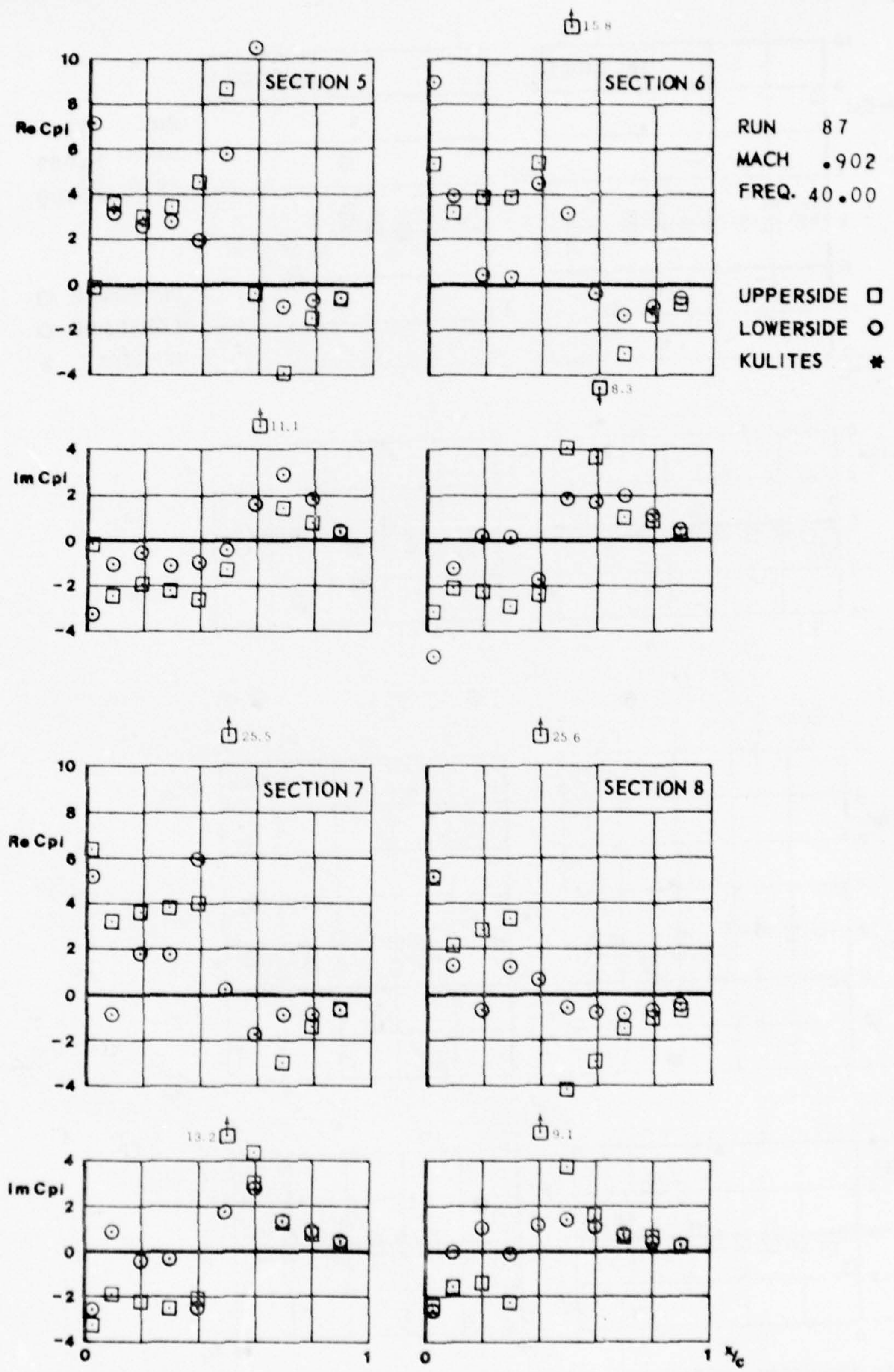

CONF. 31 (WING + PYLON + LAUNCHER + MISSILEBODY WITH AFT WINGS)

FIG.
IV.C.28.a

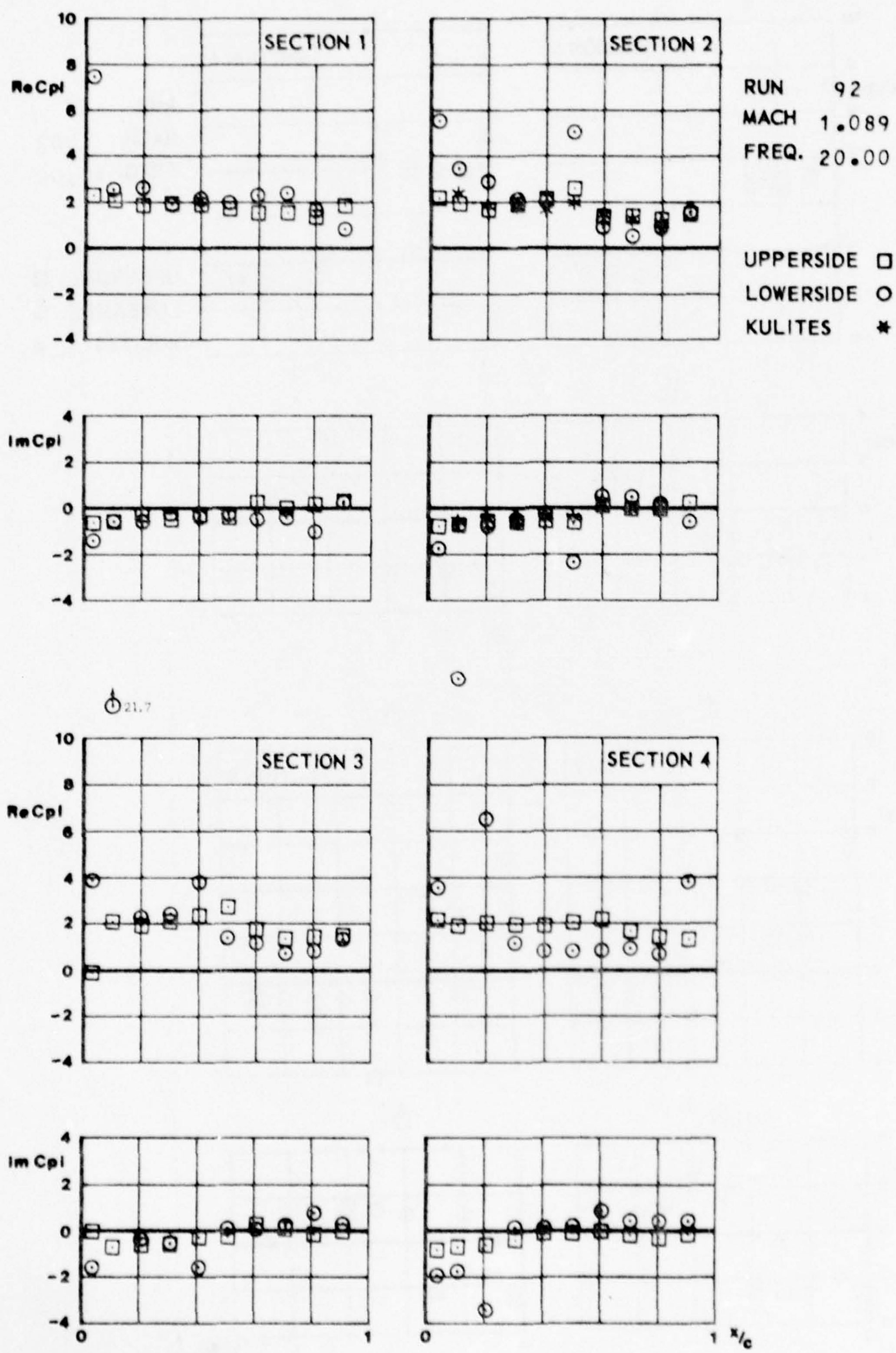

CONF.310 (WING + PYLON + LAUNCHER + MISSILEBODY WITH AFT WINGS)

FIG. IV.C.28.b

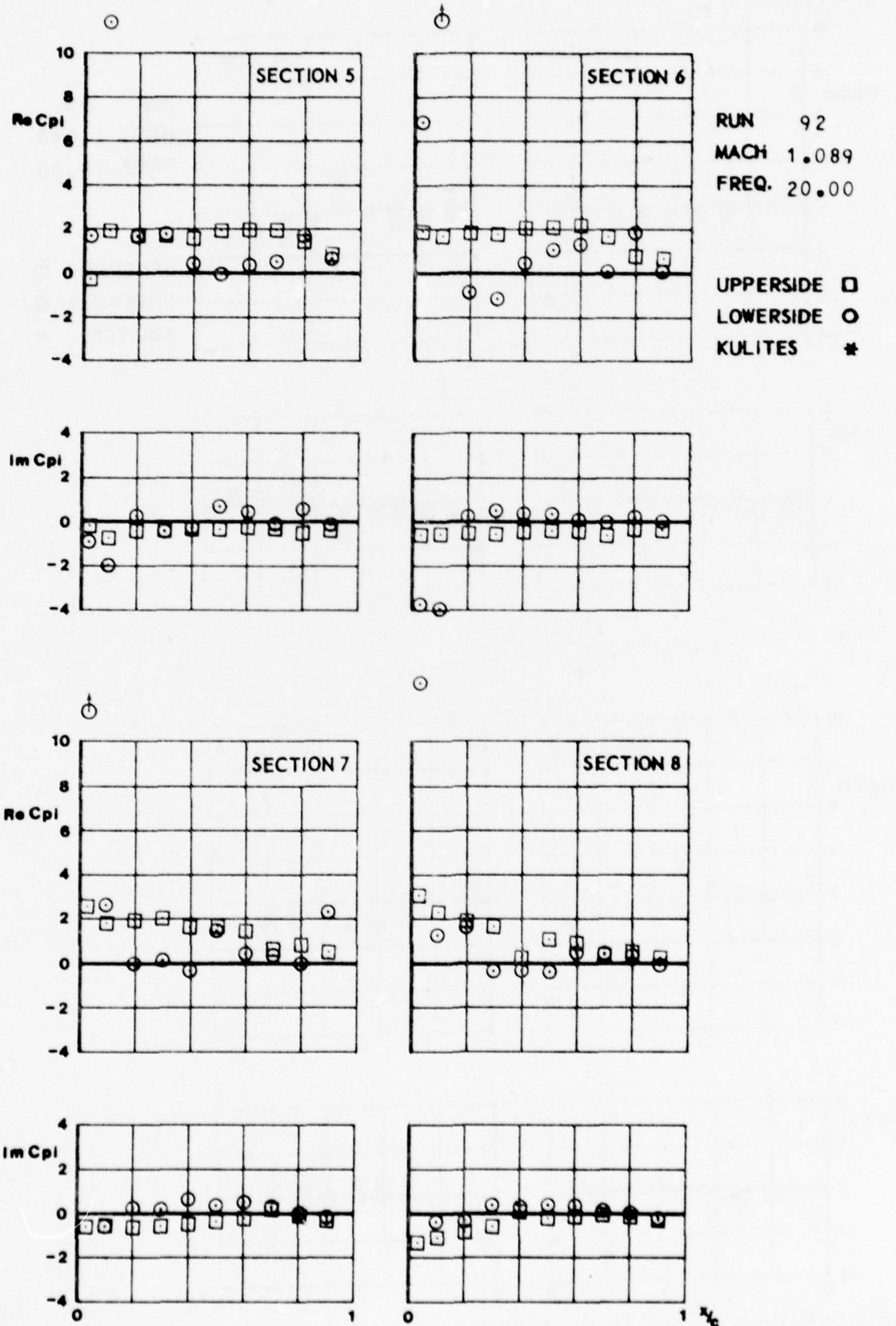

CONF. 31 (WING + PYLON + LAUNCHER + MISSILEBODY WITH AFT WINGS)

FIG. IV.C.29.a

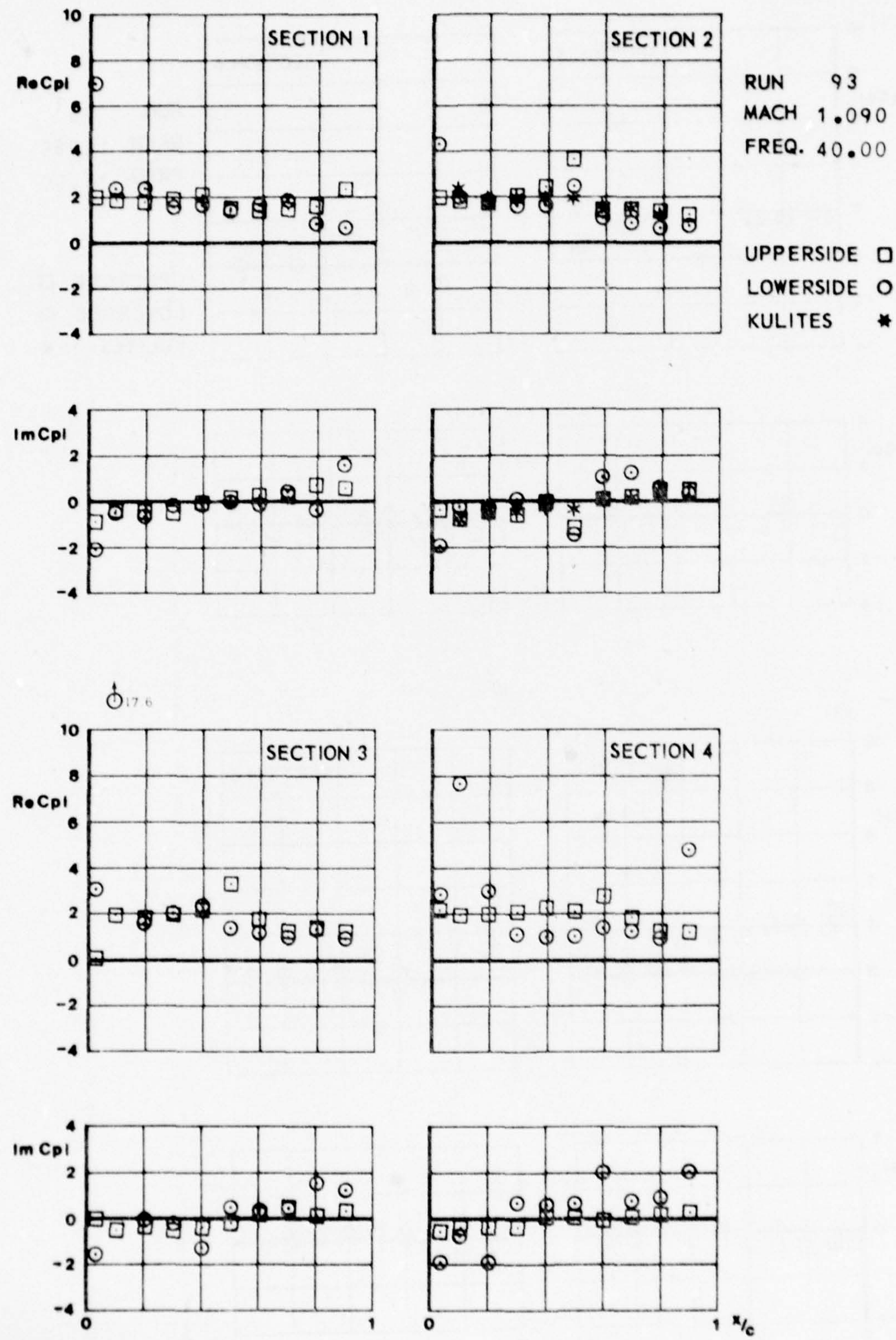

CONF. 31C (WING + PYLON + LAUNCHER + MISSILEBODY WITH AFT WINGS)

FIG. IV.C.29.l

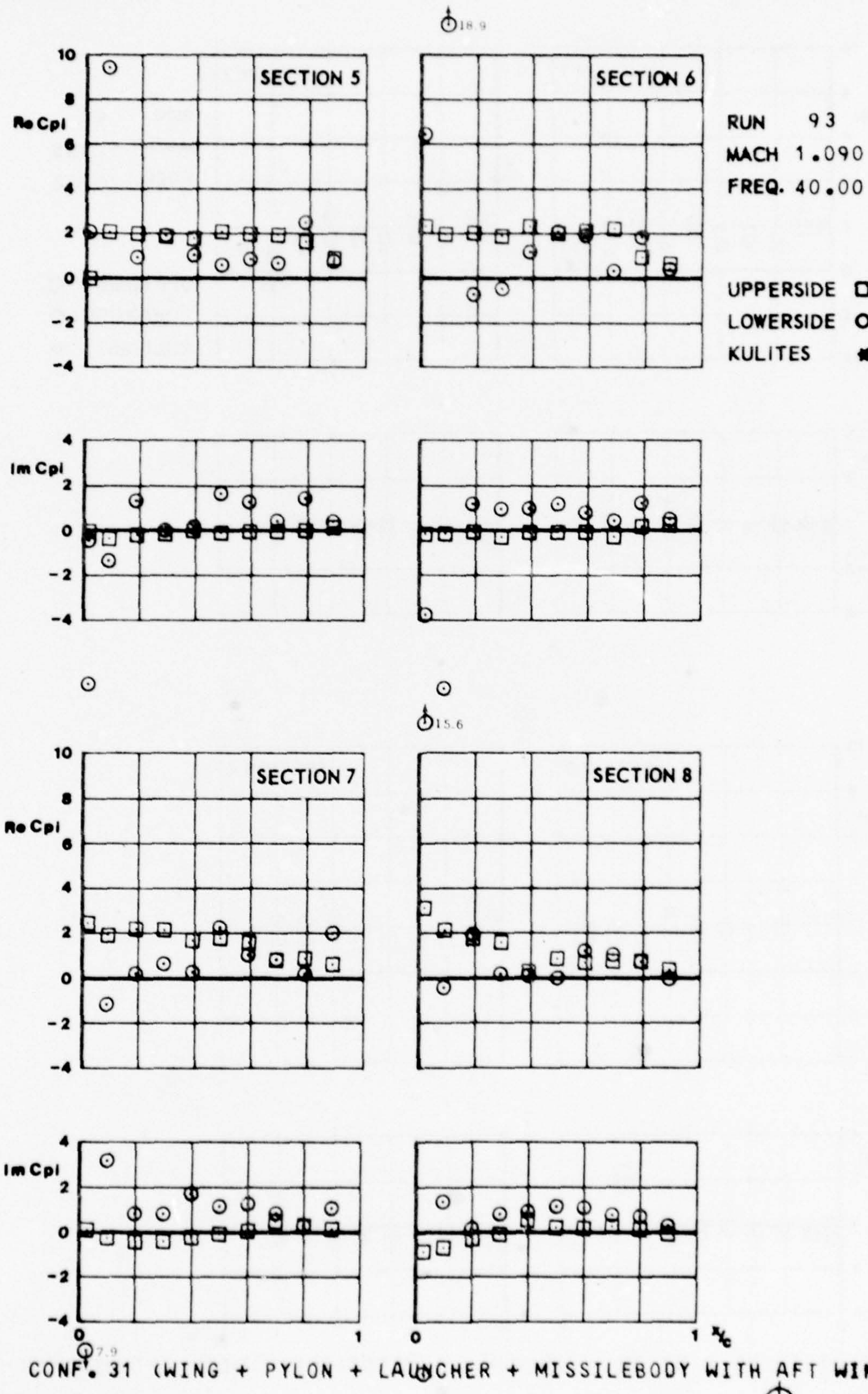

CONF. 31 (WING + PYLON + LAUNCHER + MISSILEBODY WITH AFT WINGS)

FIG.
IV.C.30.a

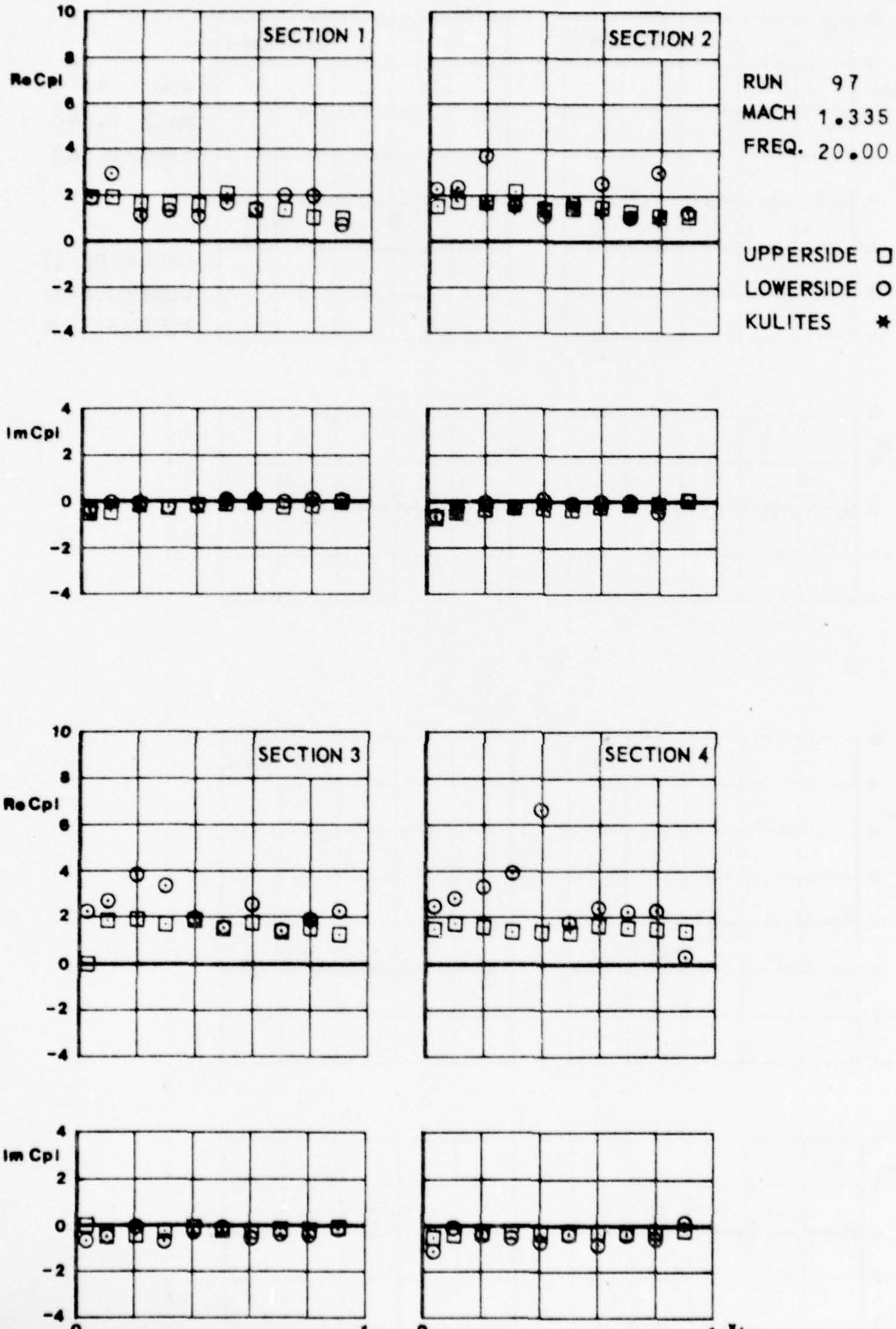

CONF. 31 (WING + PYLON + LAUNCHER + MISSILEBODY WITH AFT WINGS)

FIG. IV.C.30.6

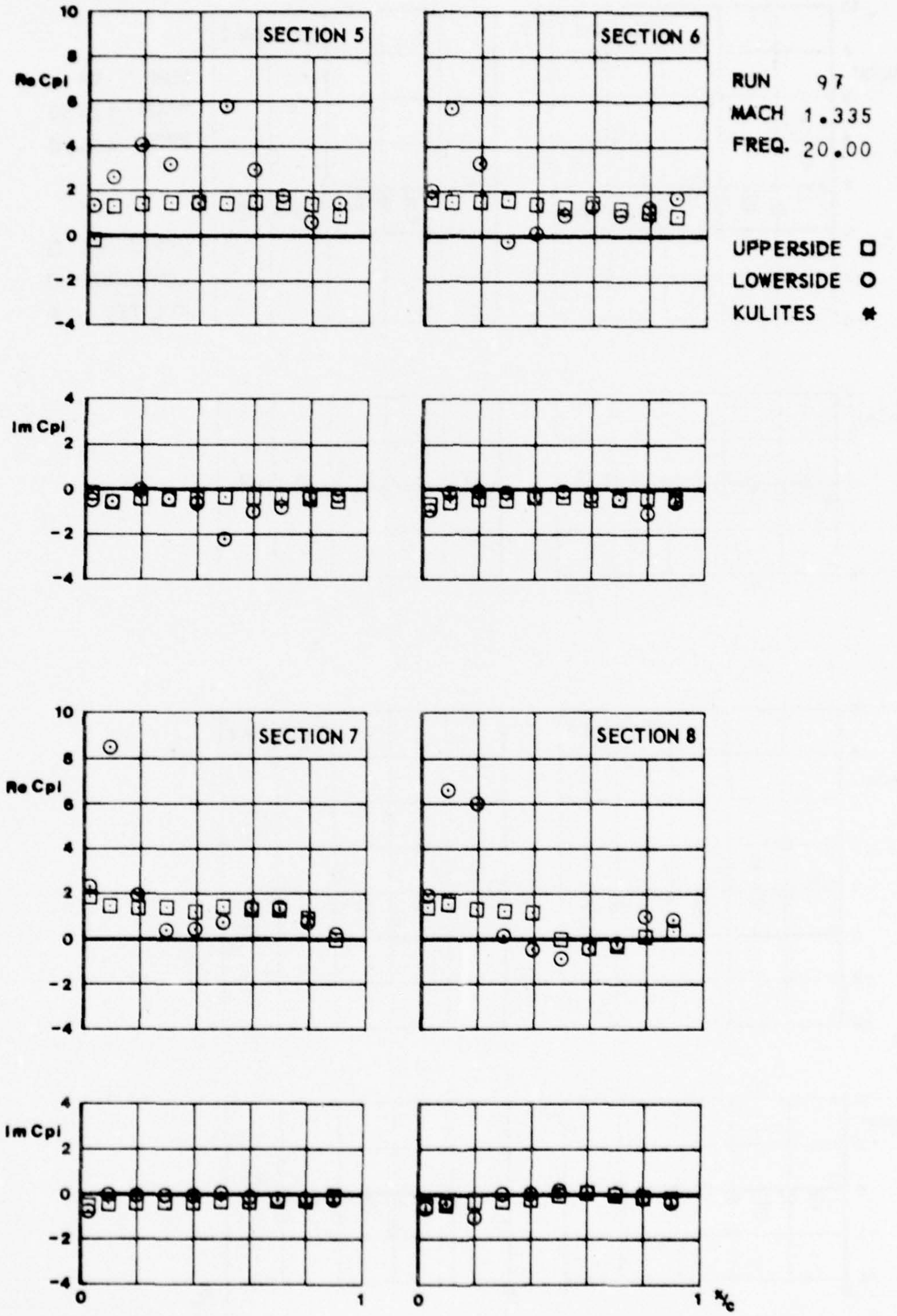

CONF. 31 (WING + PYLON + LAUNCHER + MISSILEBODY WITH AFT WINGS)

FIG.
IV.C.31.a

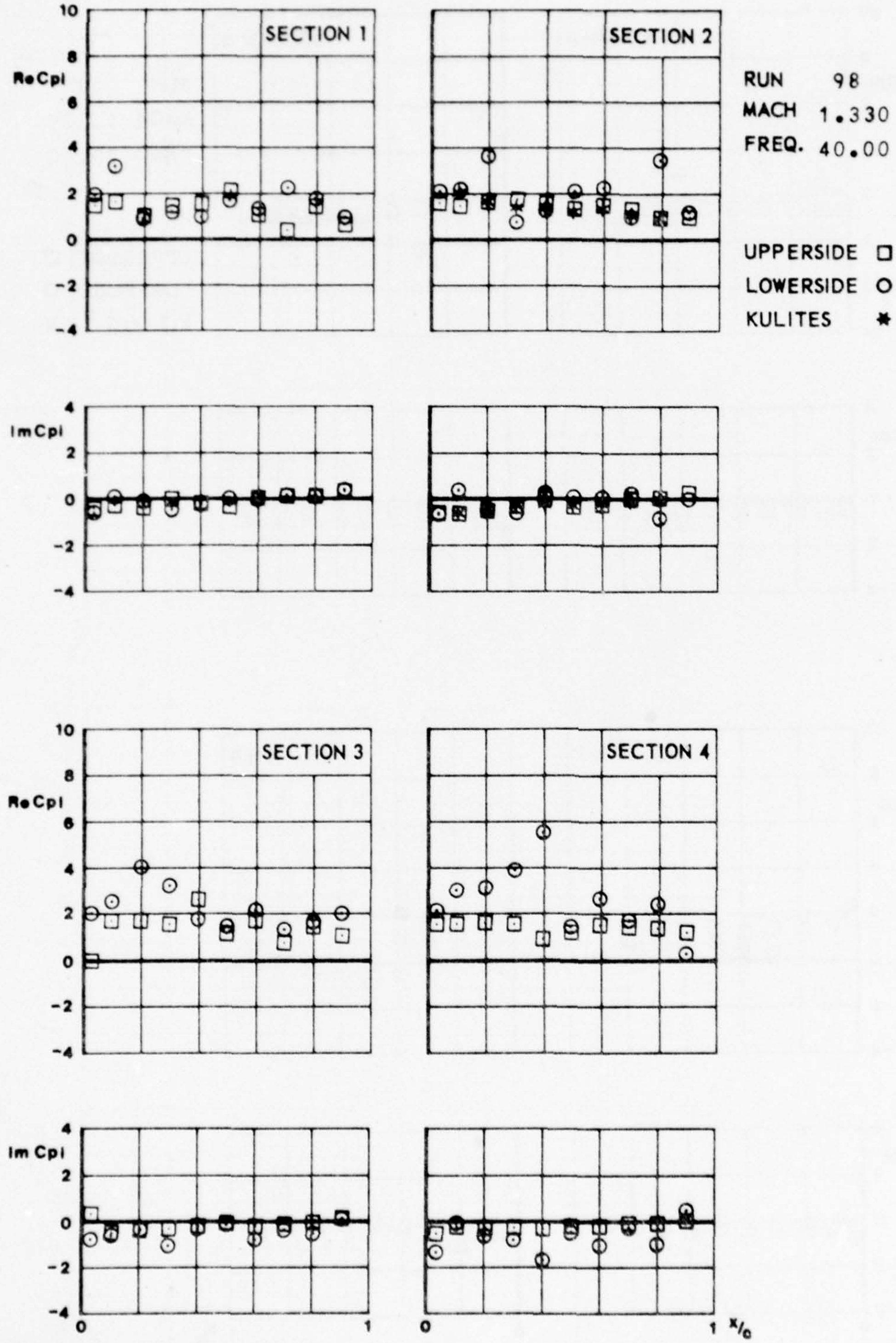

CONF.31 (WING + PYLON + LAUNCHER + MISSILEBODY WITH AFT WINGS)

FIG. IV.C.31.b

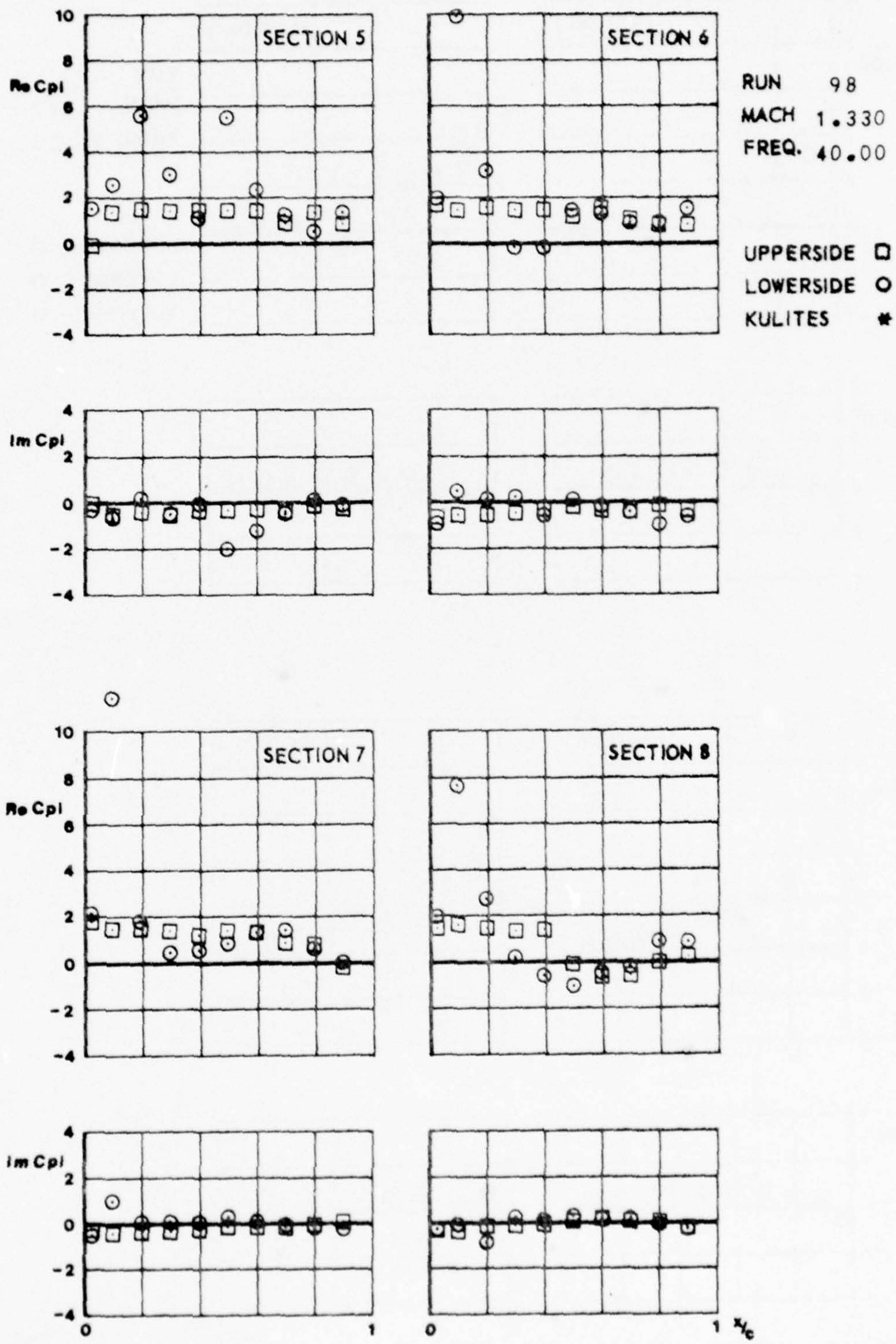

CONF. 31 (WING + PYLON + LAUNCHER + MISSILEBODY WITH AFT WINGS)

FIG.
IV.C.32.a

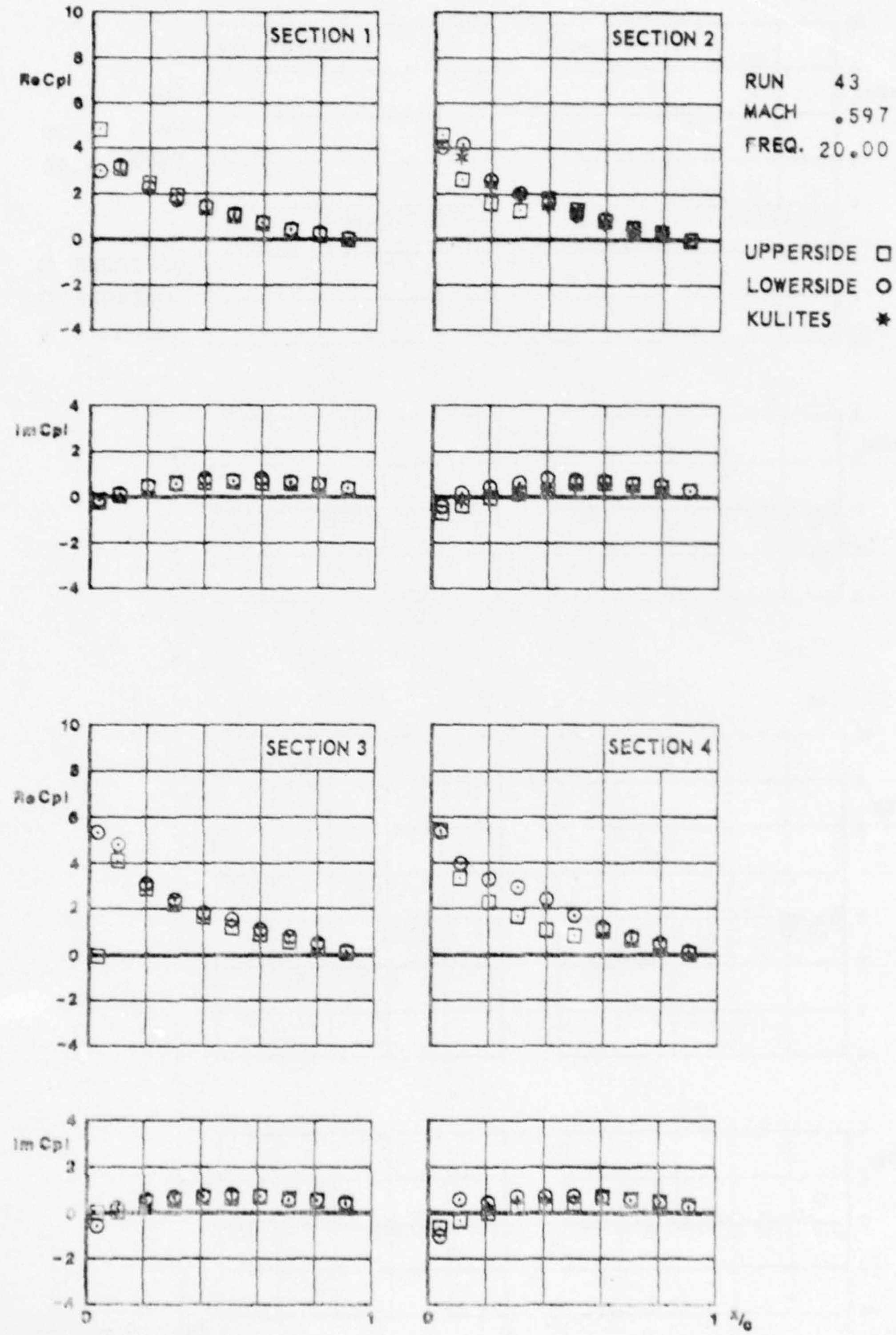

CONF. 301 (WING + PYLON + LAUNCHER + COMPLETE MISSILE)

FIG. IV.C.32.b

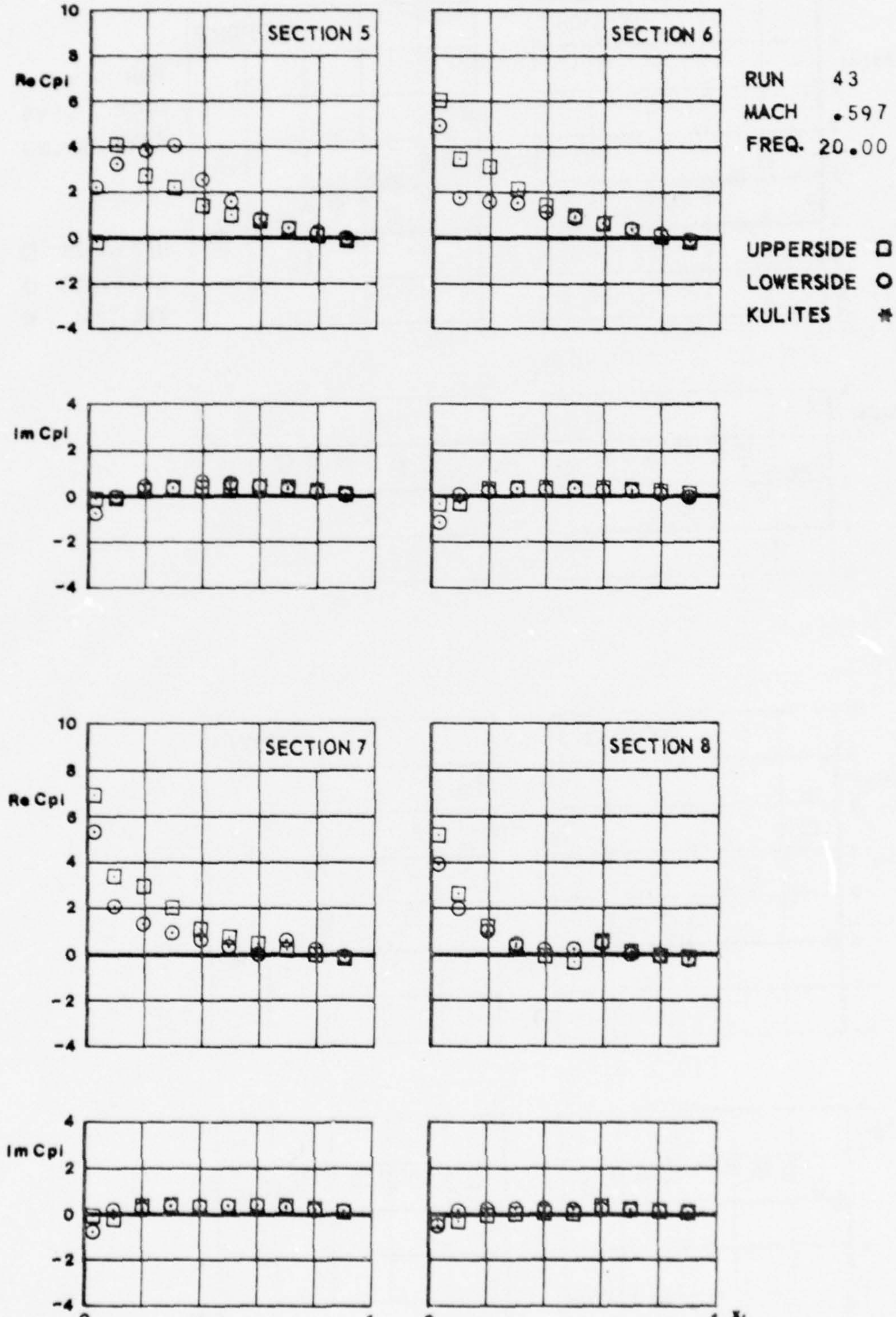

CONF. 301 (WING + PYLON + LAUNCHER + COMPLETE MISSILE)

FIG.
IV.C.33.a

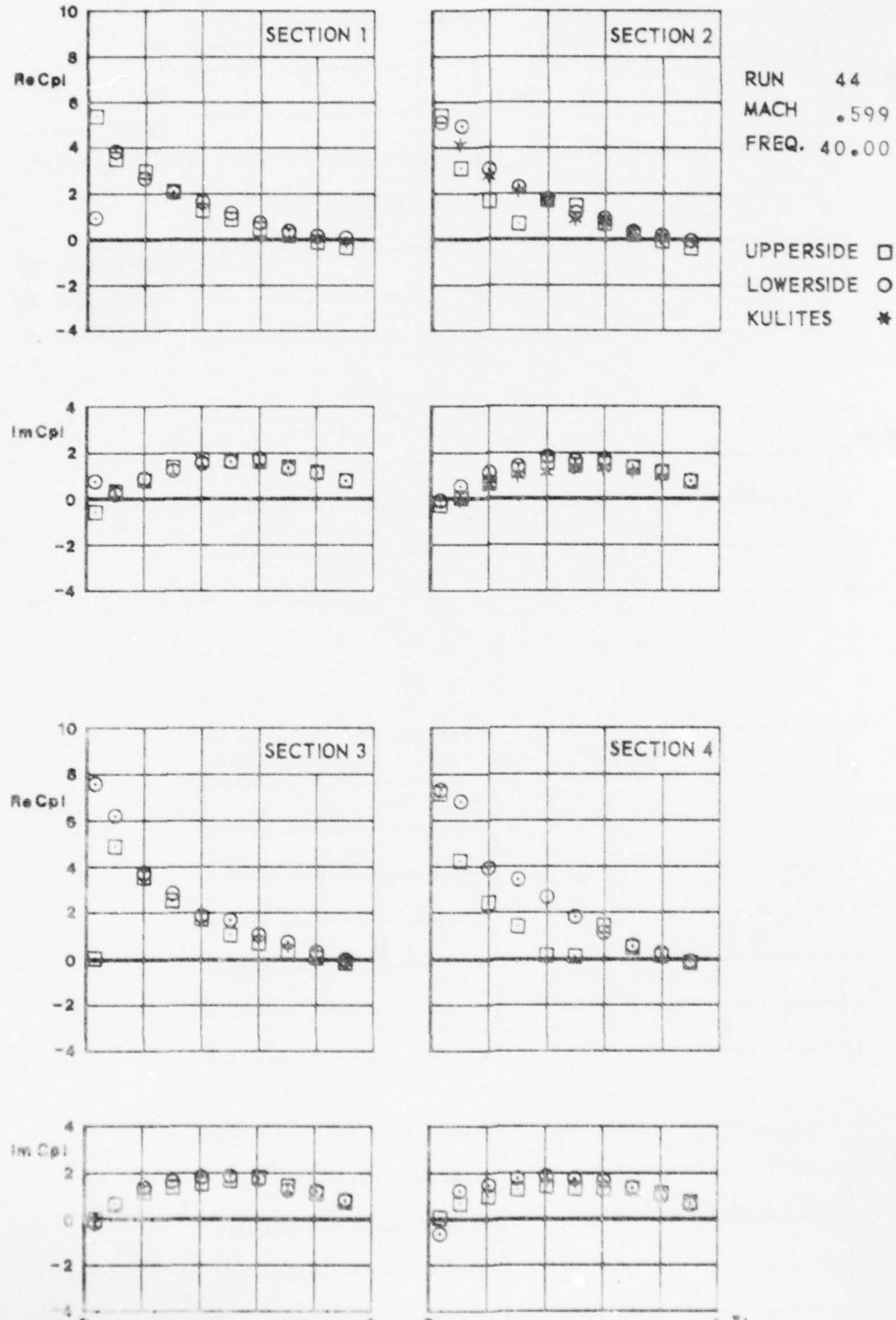

CONF.301 (WING + PYLON + LAUNCHER + COMPLETE MISSILE)

FIG.
IV.C.33.b

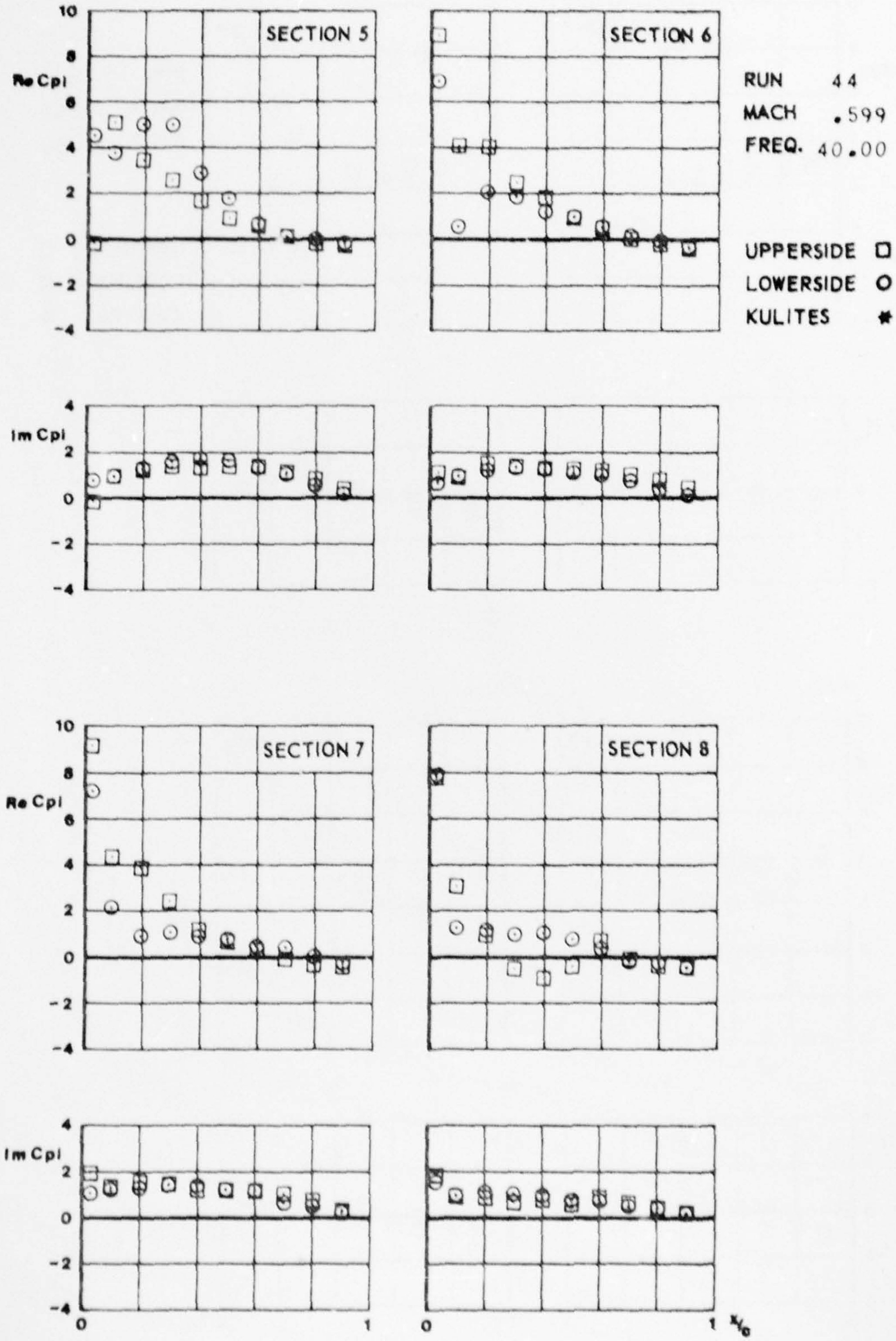

CONF. 301 (WING + PYLON + LAUNCHER + COMPLETE MISSILE)

FIG.
IV.C.34.a

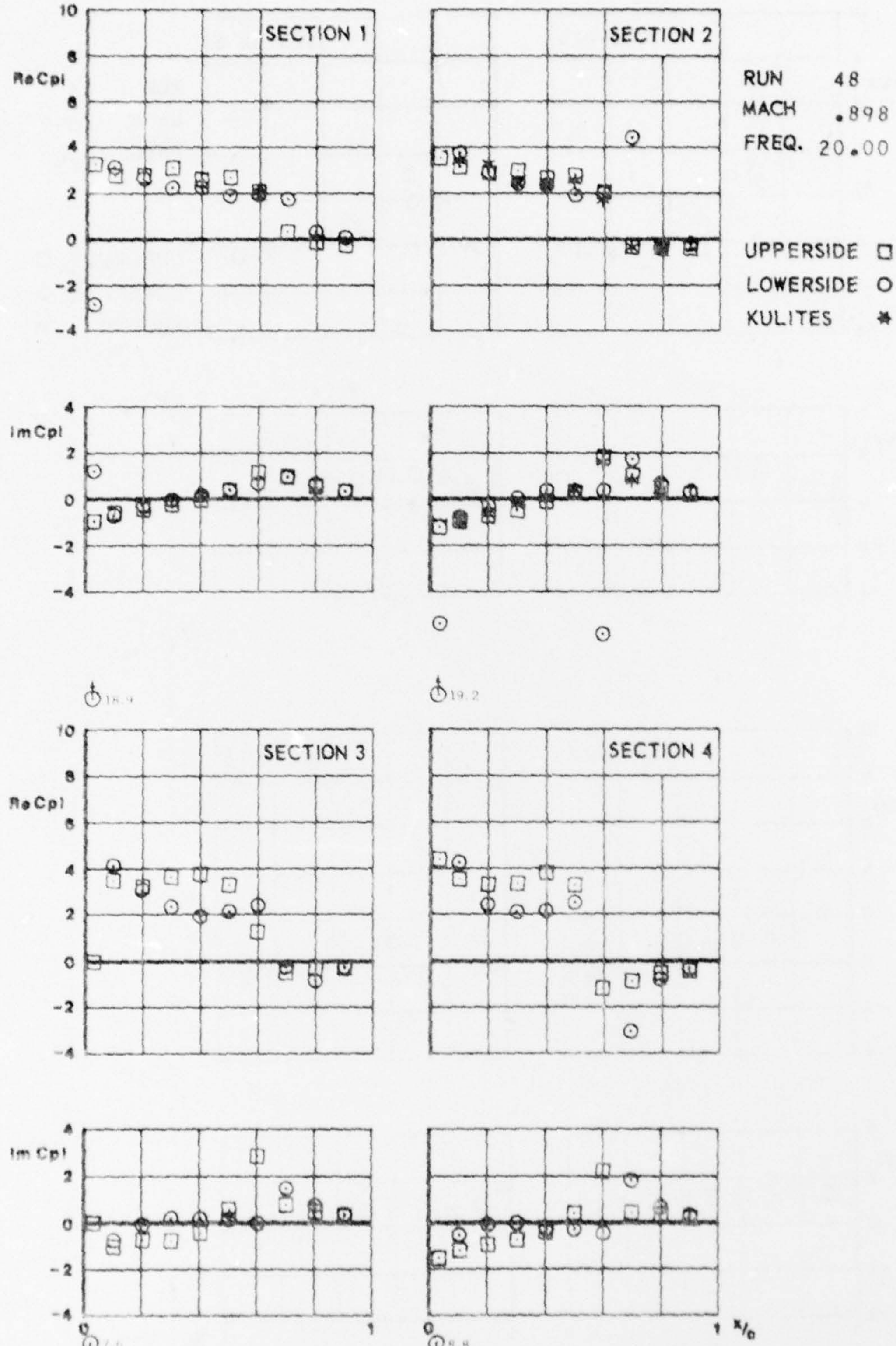

CONF. 301 (WING + PYLON + LAUNCHER + COMPLETE MISSILE)

FIG.
IV.C.34.l

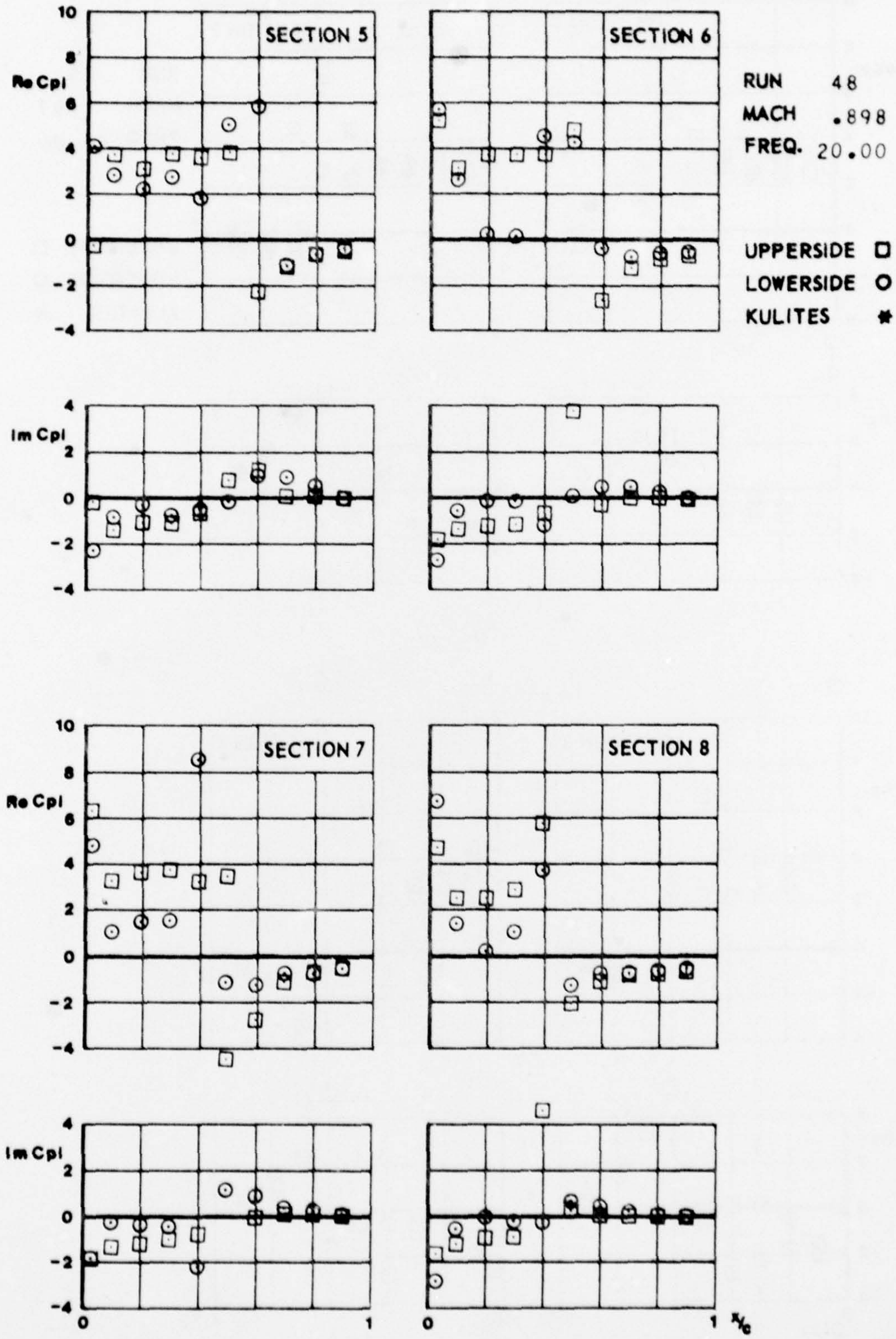

CONF. 301 (WING + PYLON + LAUNCHER + COMPLETE MISSILE)

FIG.
IV.C.35.a

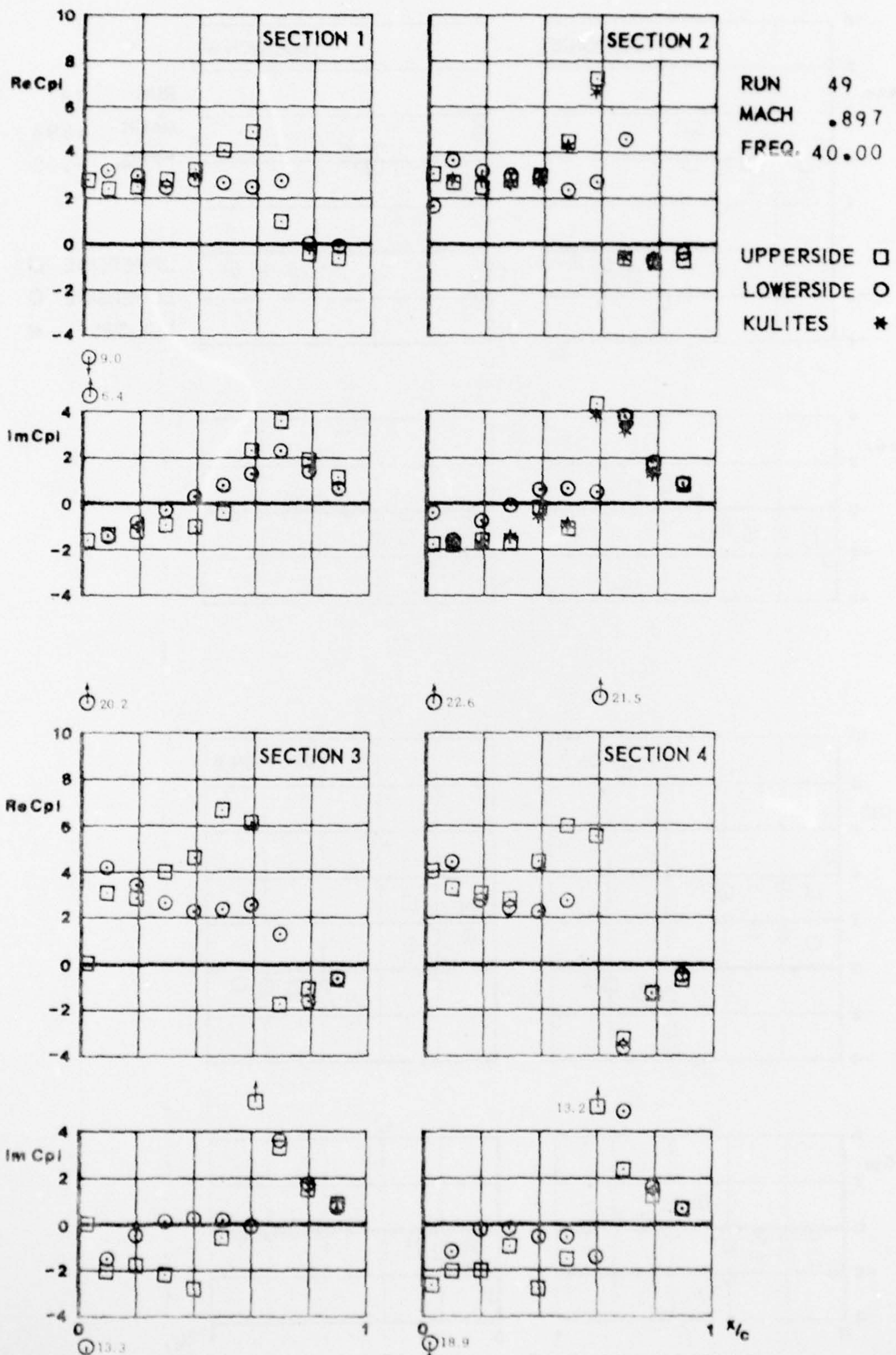

CONF. 301 (WING + PYLON + LAUNCHER + COMPLETE MISSILE)

FIG. IV.C.35.b

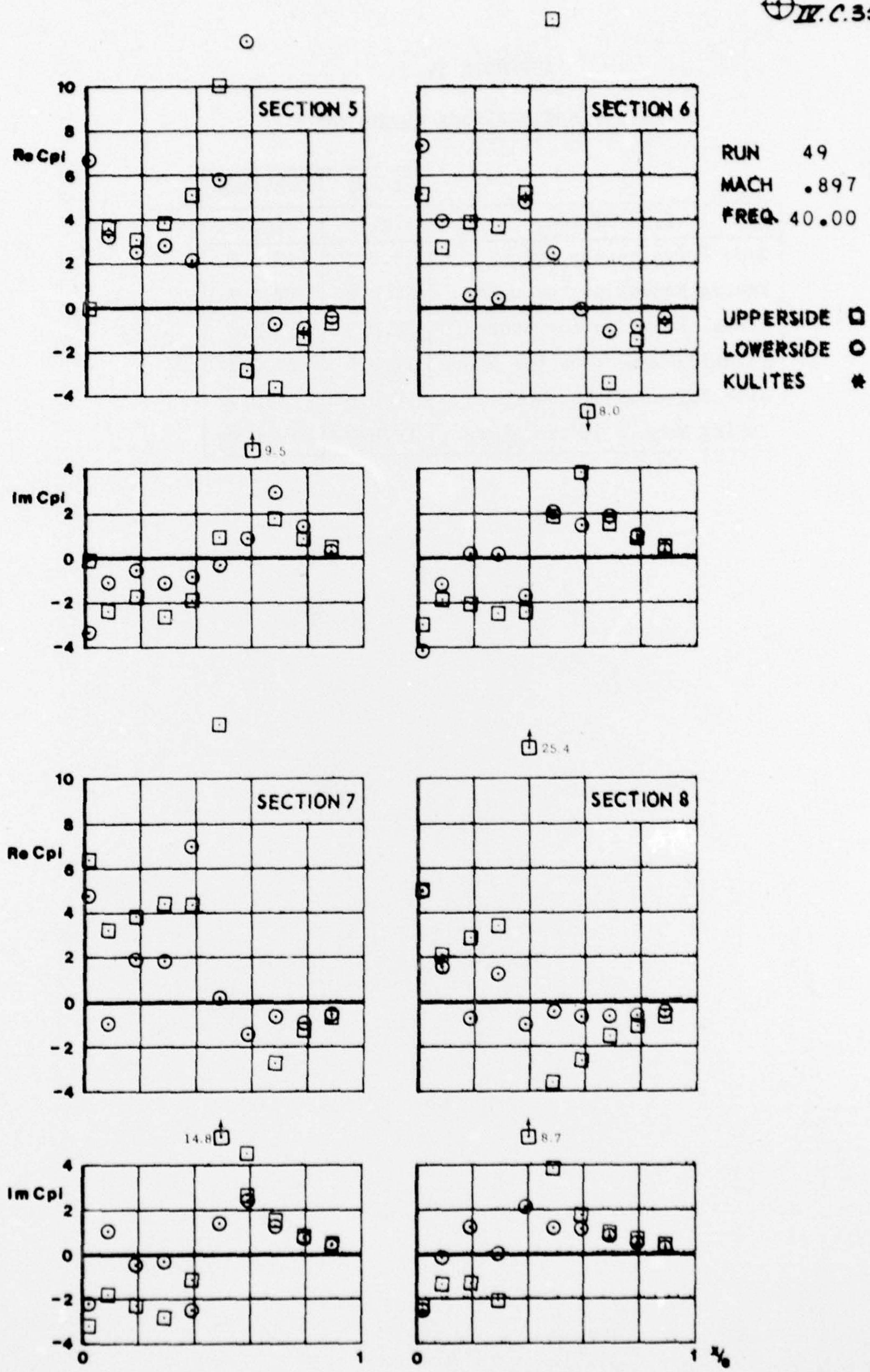

CONF. 301 (WING + PYLON + LAUNCHER + COMPLETE MISSILE)

APPENDIX IV.D

Steady and Unsteady Store Loads

Type of Load	Steady Fig.No.	Unsteady Fig.No.
Side Force on the pylon	IV.D.1	IV.D.7
Yawing Moment on the pylon	IV.D.2	IV.D.7
Normal Force on the store	IV.D.3	IV.D.8
Pitching Moment on the store	IV.D.4	IV.D.8
Side Force on the store	IV.D.5	IV.D.9
Yawing Moment on the store	IV.D.6	IV.D.9

CONF. 31 (WING + PYLON + LAUNCHER + MISSILEBODY WITH AFT WINGS)

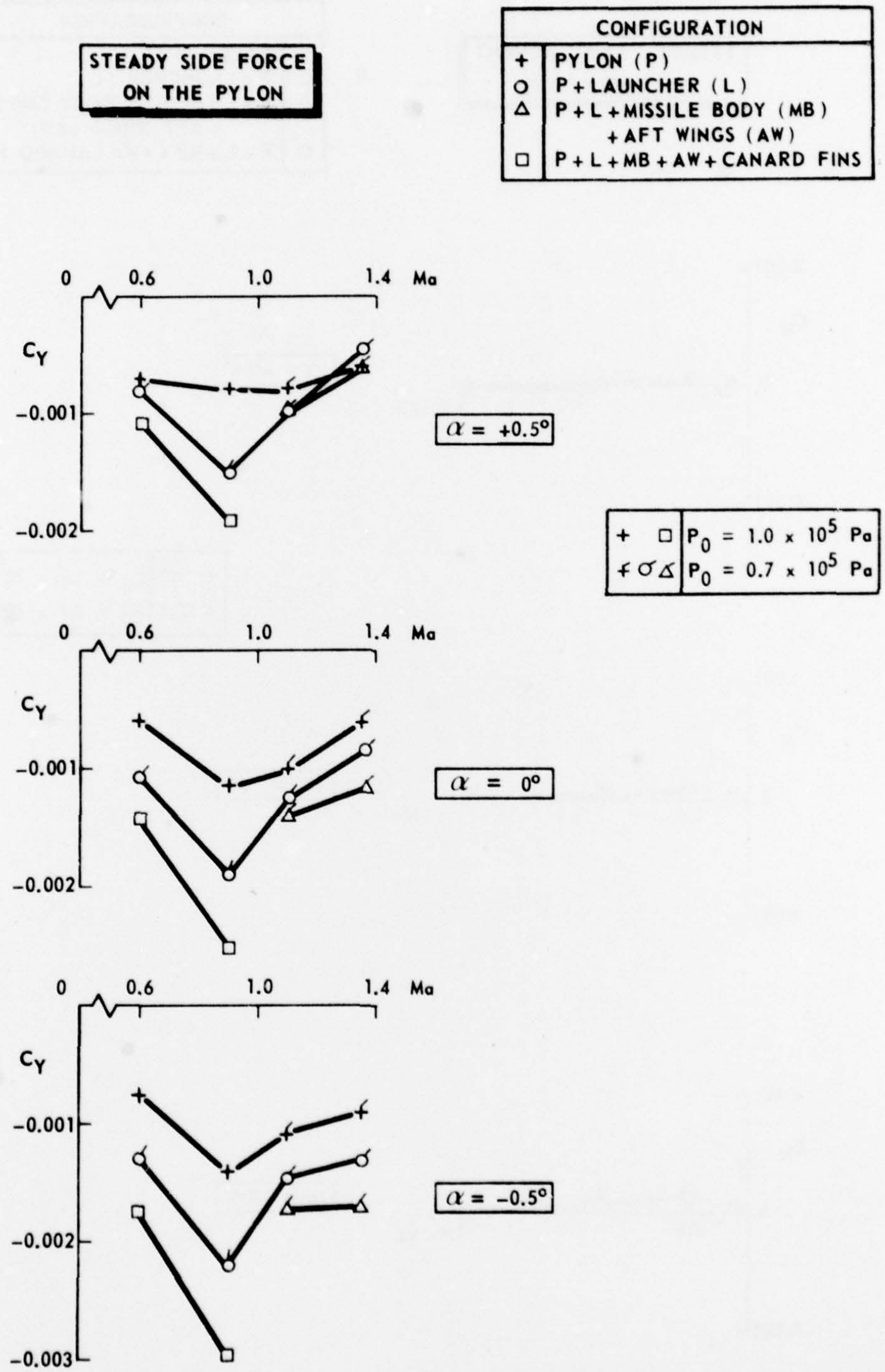

CONF.31 (WING + PYLON + LAUNCHER + MISSILEBODY WITH AFT WINGS)

150

STEADY YAWING MOMENT ON THE PYLON

	CONFIGURATION
+	PYLON (P)
O	P + LAUNCHER (L)
Δ	P + L + MISSILE BODY (MB) + AFT WINGS (AW)
□	P + L + MB + AW + CANARD FINS

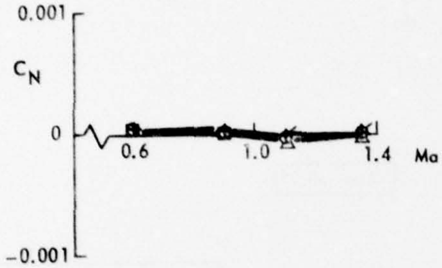

$\alpha = +0.5°$

+ □	$P_0 = 1.0 \times 10^5$ Pa
+ O Δ	$P_0 = 0.7 \times 10^5$ Pa

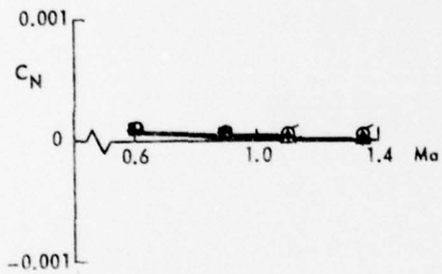

$\alpha = 0°$

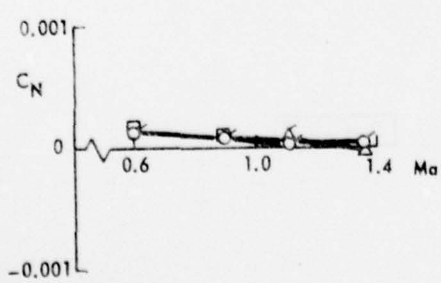

$\alpha = -0.5°$

CONF. 31 (WING + PYLON + LAUNCHER + MISSILEBODY WITH AFT WINGS)

151

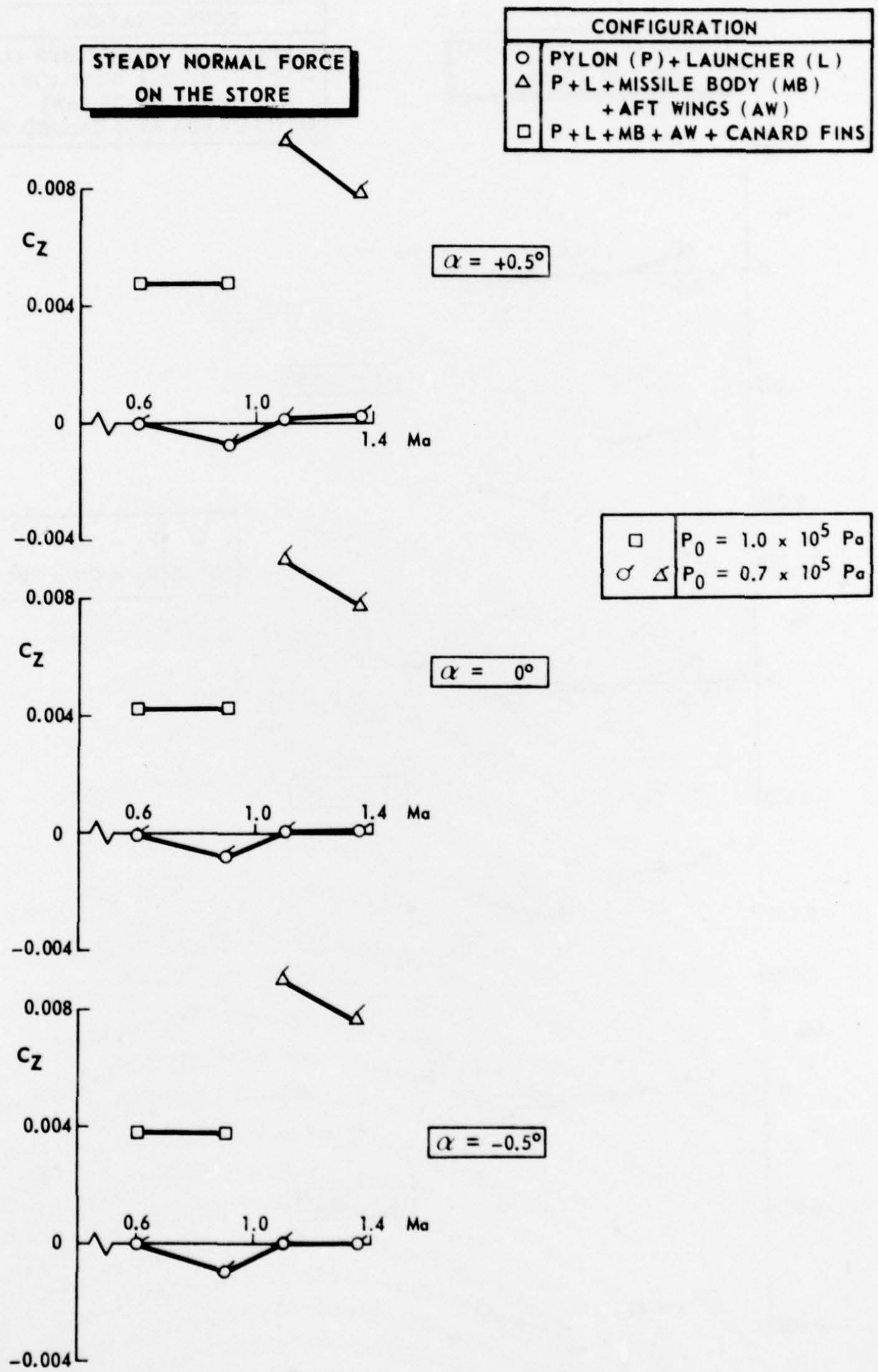

CONF. 31 (WING + PYLON + LAUNCHER + MISSILEBODY WITH AFT WINGS)

152

Fig. IV.D.4

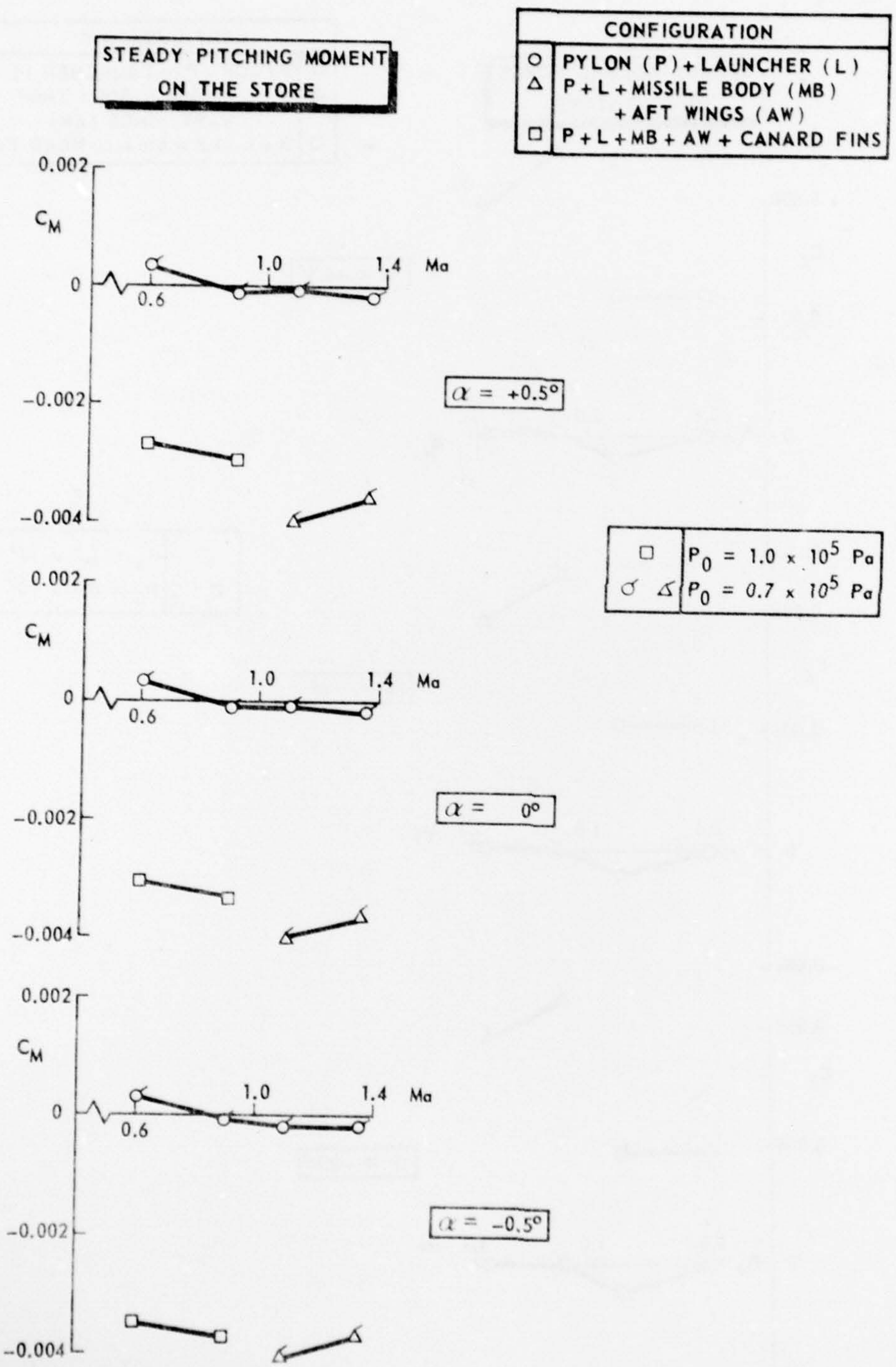

CONF. 31 (WING + PYLON + LAUNCHER + MISSILEBODY WITH AFT WINGS)

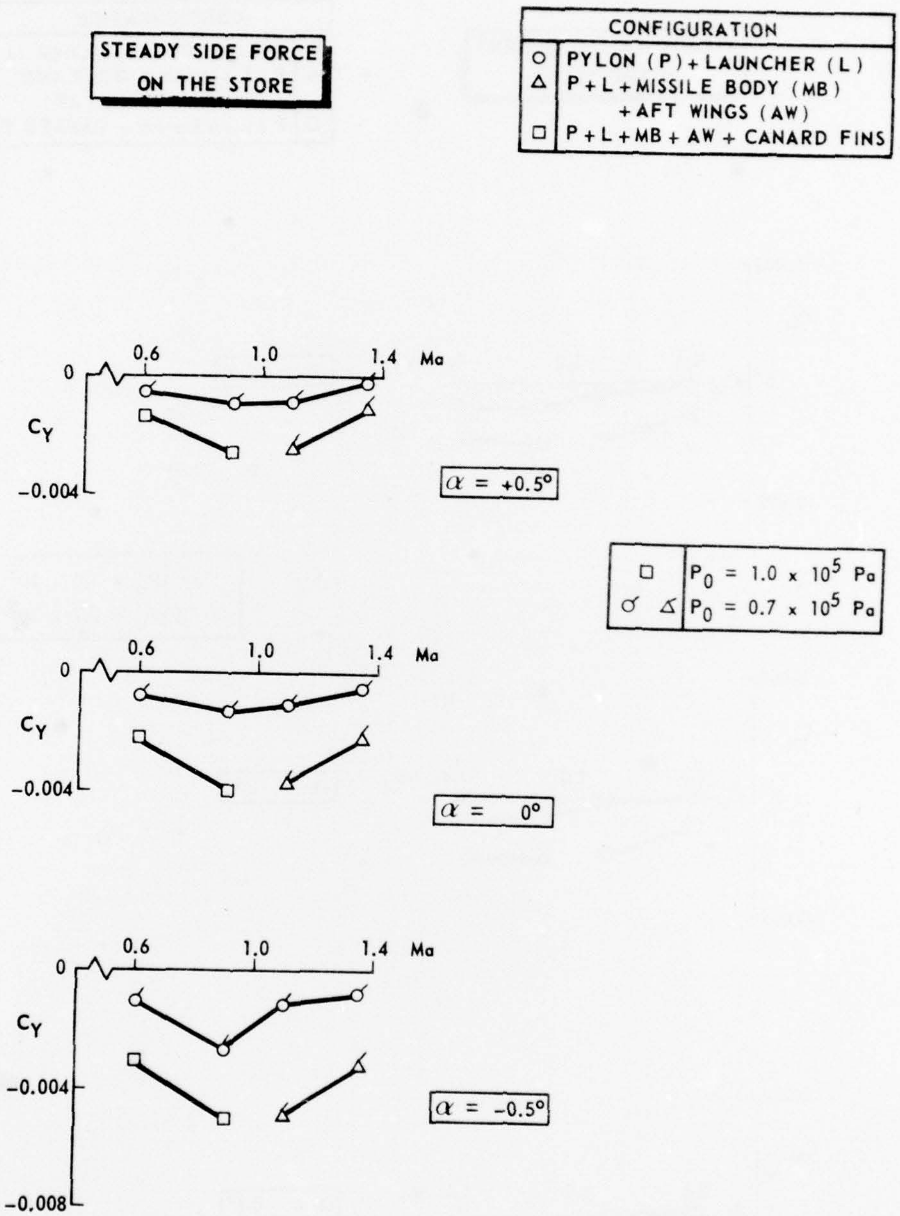

CONF. 301 (WING + PYLON + LAUNCHER + COMPLETE MISSILE)

Fig. IV.D.6

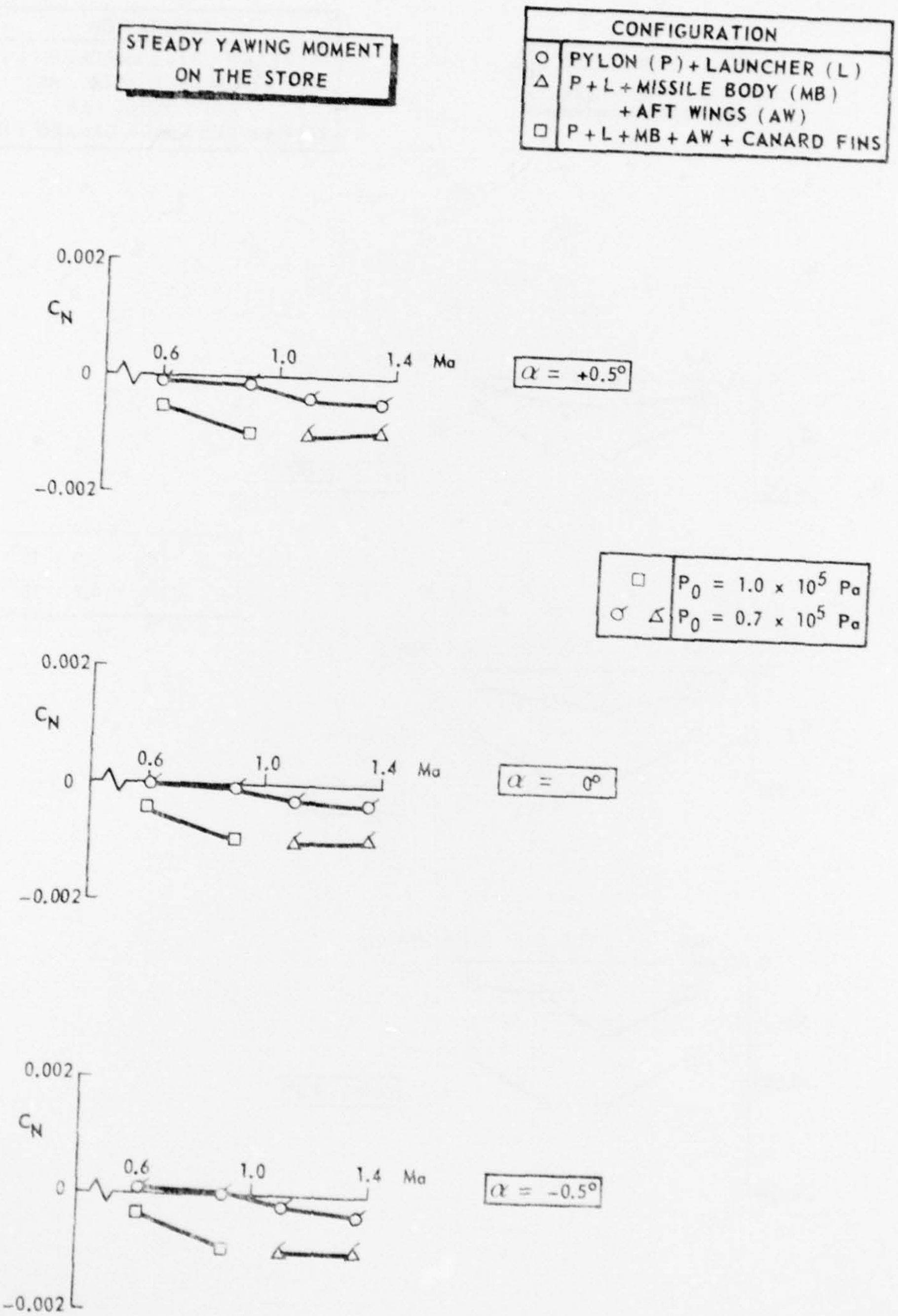

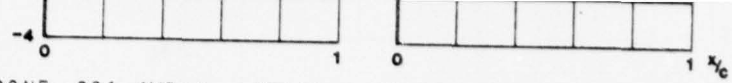

CONF. 301 (WING + PYLON + LAUNCHER + COMPLETE MISSILE)

F = 20 Hz	
CONFIGURATION	
+	PYLON (P)
○	P + LAUNCHER (L)
△	P + L + MISSILE BODY (MB) + AFT WINGS (AW)
□	P + L + MB + AW + CANARD FINS

UNSTEADY SIDE FORCE ON THE PYLON

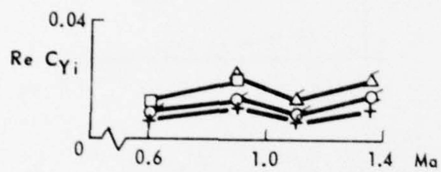

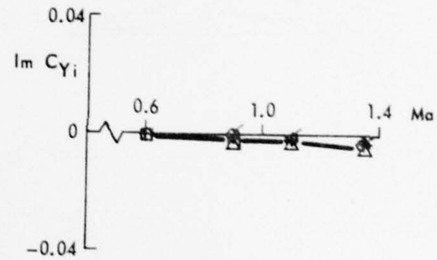

UNSTEADY YAWING MOMENT ON THE PYLON

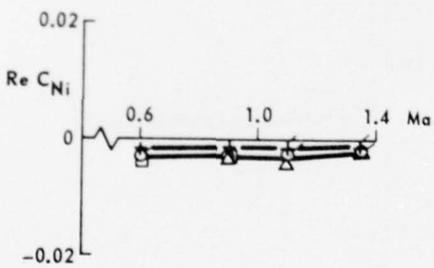

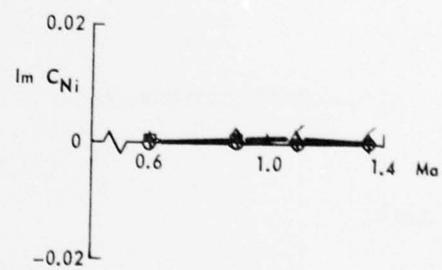

+ □ △	$P_0 = 1.0 \times 10^5$ Pa
+ ○ △ (barred)	$P_0 = 0.7 \times 10^5$ Pa

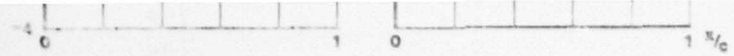

CONF. 301 (WING + PYLON + LAUNCHER + COMPLETE MISSILE)

F = 20 Hz	
CONFIGURATION	
○	PYLON (P) + LAUNCHER (L)
△	P + L + MISSILE BODY (MB) + AFT WINGS (AW)
□	P + L + MB + AW + CANARD FINS

UNSTEADY NORMAL FORCE ON THE STORE

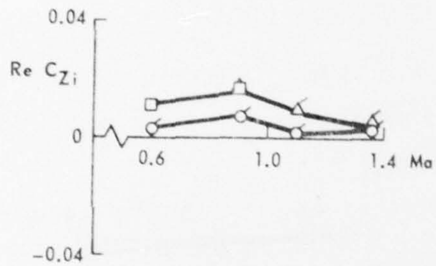

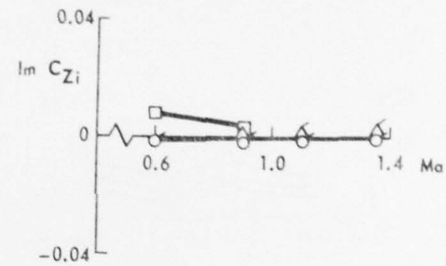

UNSTEADY PITCHING MOMENT ON THE STORE

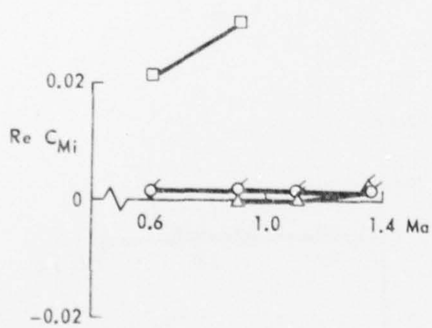

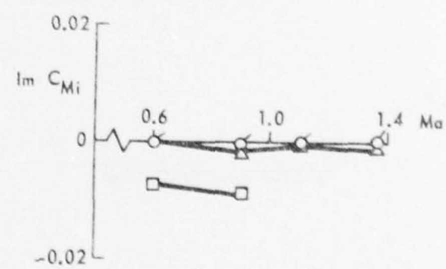

□ △	$P_0 = 1.0 \times 10^5$ Pa
ơ ∆̸	$P_0 = 0.7 \times 10^5$ Pa

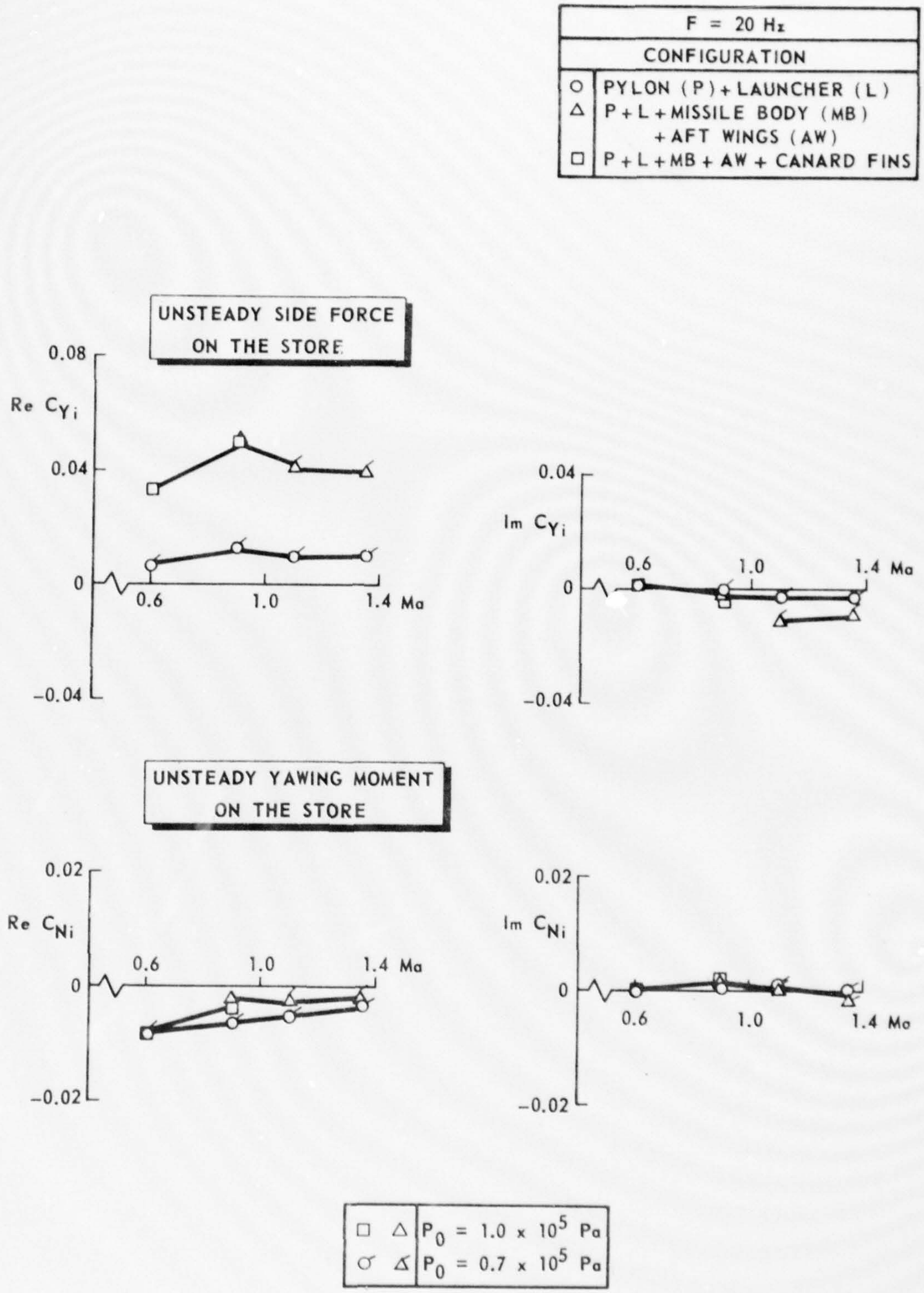
F = 20 Hz
CONFIGURATION
○ PYLON (P) + LAUNCHER (L)
△ P + L + MISSILE BODY (MB) + AFT WINGS (AW)
□ P + L + MB + AW + CANARD FINS
UNSTEADY SIDE FORCE ON THE STORE
Re C_{Y_i}
0.08
0.04
0
−0.04
0.6
1.0
1.4 Ma
Im C_{Y_i}
0.04
0
−0.04
0.6
1.0
1.4 Ma
UNSTEADY YAWING MOMENT ON THE STORE
Re C_{N_i}
0.02
0
−0.02
0.6
1.0
1.4 Ma
Im C_{N_i}
0.02
0
−0.02
0.6
1.0
1.4 Ma
□ △ $P_0 = 1.0 \times 10^5$ Pa
○ △ $P_0 = 0.7 \times 10^5$ Pa

MED

80